EFFECT OF LIGNIN CONTENT AND STRUCTURAL CHANGE DURING TREATMENT ON POPLAR FOR BIOFUEL AND BIOMATERIAL PRODUCTION

A Dissertation
Presented to
The Academic Faculty

By

Qining Sun

In Partial Fulfillment
of the Requirements for the Degree
Doctor of Philosophy in the
School of Chemistry and Biochemistry

Georgia Institute of Technology
May 2015

Copyright © 2015 by Qining Sun

EFFECT OF LIGNIN CONTENT AND STRUCTURAL CHANGE DURING TREATMENT ON POPLAR FOR BIOFUEL AND BIOMATERIAL PRODUCTION

Approved by:

Dr. Arthur J. Ragauskas, Advisor
School of Chemistry and Biochemistry
Georgia Institute of Technology

Dr. Charles L. Liotta
School of Chemistry and Biochemistry
Georgia Institute of Technology

Dr. Adegboyega K. Oyelere
School of Chemistry and Biochemistry
Georgia Institute of Technology

Dr. Jeffery S. Hsieh
School of Chemical and Biomolecular Engineering
Georgia Institute of Technology

Dr. Yulin Deng
School of Chemical and Biomolecular Engineering
Georgia Institute of Technology

Date : March 20 , 2015

ACKNOWLEGMENTS

I would like to express my respectful gratitude to Professor Arthur J. Ragauskas for his guidance and financial support during my doctoral study. Under the direction of Professor Ragauskas, I have learned and accomplished far more than what I could have imagined in the beginning of my study. Furthermore, I also would like to thank my committee members, Professors Charles Liotta, Adegboyega K. Oyelere, Yulin Deng, and Jeffery S. Hsieh, for their patience, encouragement, and advice.

I also appreciate the members of the Professor Ragauskas' group, past and present, for their friendship, helpful discussions, and collaboration. My special sincere thanks go to Drs. Marcus Foston, Yunqiao Pu, Fang Huang, Garima Bali, Fan Hu, Boyi Fu, Hongzhi Wang, Qingqing Li, Feng Jiang, and Kanda Tapily; Coumba Ndoye and my team members Xianzhi Meng, Tyrone Wells, Mikhail Levit and Shaobo Pan. I am also grateful to Dr. Cam Tyson, Dr. Kenyetta Johnson, and Michele Yager from the School of Chemistry and Biochemistry at Georgia Tech for their guidance and support. I would also like to acknowledge the financial support of Paper Science and Engineering fellowships and technical support from Lavon Harper, Bob Davies, Henry (Major) White, Lloyd Williams, and Dr. Norman Marsolan at the Renewable Bioproducts Institute (Institute of Paper Science and Technology).

Most importantly, the love and support of my wife Dr. Chen, my parents, my friends from ACCC and WCF, LSU, Virginia Tech, USDA, and my BASF friends James Godfrey and Sheila Godfrey, who have made my Sino-USA dream possible!

TABLE OF CONTENTS

Page

LIST OF TABLES

Page

LIST OF FIGURES

Page

LIST OF ABBREVATIONS

2D	Two-dimensional
ATR-FTIR	Attenuated total reflectance Fourier transform infrared spectroscopy
C	Cellulose
CBMs	Carbohydrate-binding modules
CP/MAS	Cross polarization/magic angle spinning
CrI	Crystallinity index
CTC	Cellulose tricarbanilate
DAP	Dilute acid pretreatment
DB	Direct blue
DHB	2, 5-Dihydroxybenzoic acid
DI	Deionized
DO	Direct orange
DP	Degree of polymerization
DP_n	Number-average degree of polymerization
DP_w	Weight-average degree of polymerization
EOL	Ethanol organo-solv lignin
G	Guaiacyl or coniferyl alcohol
GPC	Gel permeation chromatography
H	*p*-Hydroxyphenyl unit,or *p*-coumaryl alcohol
HMF	5-Hydroxymethyl furfural
HPAEC-PAD	High-performance anion-exchange chromatography with pulsed amperometric detection
HPLC	High-performance liquid chromatography
HTPH	High throughput pretreatment and enzymatic hydrolysis
HW	Hardwood
IMS	Imaging mass spectrometry

IR	Infrared
LCCs	Lignin-carbohydrate complexes
LFD	Lateral fibril dimension
LFAD	Lateral fibril aggregate dimension
LHW	Liquid hot water
MCC	Microcrystalline cellulose
M_n	Number-average molecular weight
MPa	Mega Pascal pressure unit
M_n	Number average molecular weight
M_w	Weight average molecular weight
MWL	Milled wood lignin
NMR	Nuclear magnetic resonance
S	Syringyl unit or sinapyl alcohol
SEM	Scanning electron microscopy
SW	Softwood
T_g	Glass transition temperature
UV	Ultraviolet
WAXD	Wide-angle X-ray diffraction
WAXS	Wide-angle X-ray scattering
XRD	X-ray diffraction

SUMMARY

Biofuels and biomaterials produced from abundant and renewable lignocellulosic biomass to supplement petroleum chemicals and materials are vital to the global economy and environmental initiatives. However, to fully discover the potential of lignocellulosic biomass, we must improve our understanding of lignocellulosic recalcitrance. Lignin has been considered as one of the most recalcitrant factors inhibiting the release of fermentable sugars during the bioconversion of biomass to biofuels. However, we must address a significant knowledge gap between the content and the structural changes of lignin that occur during treatment and the chemical nature of biomass substrates. Understanding the structural parameters relevant to the recalcitrance of the plant cell wall and the individual and cooperative effects of the parameters on enzymatic saccharification is vital for improving current processing and conversion methods for cellulosic biofuels. Furthermore, to facilitate the manufacturing of biomaterials such as carbon fiber with high performance, the structural parameters relevant to lignin de-polymerization and re-polymerization during thermal treatment are also of high interest because they direct subsequent processes.

The first objective of this thesis aims to establish the effect of several pretreatment technologies on cellulose crystallinity, crystalline allomorph distribution, and the cellulose ultrastructure. To understand biomass recalcitrance, energy crop poplar is taken as a starting material to observe the changes in the cellulose ultrastructure related to changes in enzymatic hydrolysis. This study compares hot-water, organo-solv, lime, lime-oxidant, dilute acid, and dilute acid-oxidant pretreatments with regard to their

changes in enzymatic sugar release and then changes in their cellulose ultrastructure measured by ^{13}C cross-polarization magic-angle spinning nuclear magnetic resonance (^{13}C CP/MAS NMR) and wide-angle X-ray diffraction (WAXD). Then, the study entails the assessment of pretreatment severity and relative chemical de-polymerization/degradation through compositional analysis and high-performance anion-exchange chromatography with pulsed amperometric detection (HPAEC-PAD). Results obtained from this project can be then used in further research such as computational methods applied to the deconstruction of the model cell wall or the generation of new optimized biocatalysts and low-recalcitrant, genetically-engineered plants.

The second objective of this thesis focuses on determining how the presence of lignin influences the efficacy of dilute acid pretreatment and induced changes in the cellulose ultrastructure, both of which may ultimately have large implications for the study of enzymatic deconstruction. The results indicate a strong influence of lignin content on changes in the cellulose ultrastructure occurring during dilute acid pretreatment (DAP). With the reduction of lignin content during DAP, the enlargement of cellulose microfibril dimensions and crystallite size becomes more apparent. Furthermore, this enlargement of cellulose microfibril dimensions is attributed to processes that include the co-crystallization of crystalline cellulose driven by irreversible inter-chain hydrogen bonding (similar to hornification) and/or cellulose annealing that convert amorphous cellulose to *para*-crystalline/crystalline cellulose. Lignin acts as a barrier that prevents the enhancement of cellulose crystallinity and cellulose fibril coalescence during DAP,

which suggests that sugar yield enhancement would benefit most from optimized partial delignification instead of compete lignin removal.

The third objective of this thesis is to obtain a deeper understanding of the structure of lignin, the most recalcitrant component of biomass, during dilute acid pretreatment, which is critical to the continued growth of renewable biofuel production. Our results highlight that lignin is subjected to de-polymerization within a short 2 min of dilute acid pretreatment at 160 ℃, and these changes are accompanied by increasing values for the aliphatic and phenolic hydroxyl groups of lignin. As the reaction residence time is extended beyond 5 min, a competing set of de-polymerization and re-polymerization reactions that lead to a decrease in the content of guaiacyl lignin units and an increase in condensed lignin units. A detailed comparison between the changes in functional groups and those in the molecular weights of cellulolytic enzyme lignins demonstrate different structure-related recalcitrant roles that lignin plays in poplar and switchgrass during pretreatment. These results can aid both in the development of improved enzymes that contain activities that decompose recalcitrant structures and in the design of various processing conditions that efficiently convert specific biomass feedstock into sugars.

The last part of this thesis focuses on identifying the structures of various types of lignin and determining their effects on physicochemical characteristics, including their rheologies and their abilities to form a fiber. Through this study, we will be able to select a type of lignin with superior processing performance characteristics, one that produces high-quality carbon fibers. To determine the type of lignin with superior performance, we

conducted rheology tests. Results showed that lignin with a lower S/G (syringyl/guaiacyl) ratio was more likely to form cross-linkages with higher viscosity values, higher molecular weight, and larger amounts of condensed bonds. This study not only provided a deeper insight into cross-linking and/or scission mechanisms during rheology testing but also established a correlation between the S/G ratio parameters and structural changes of lignin during rheological testing. The findings of this study can help in the design of new chemical modifications of lignin and innovative biosynthesis strategies for producing linear-fiber-forming lignin with controlled monomer ratios and chemical architectures that facilitate both rapid chemical transformation to an infusible mass and the formation of a planar graphitic structure for high-performance lignin carbon fiber manufacturing.

CHAPTER 1

INTRODUCTION

Global concerns have been raised with regard to the need for more sustainable and economic technologies and renewable resources that address environmental issues and meet energy demands.[1] A promising resource that is both renewable and abundant is lignocellulosic biomass, which facilitates the efficient conversion of sunlight into chemical potential energy and displaces or even replaces petroleum feedstocks.[2] These nonfood materials consist of woody crops, agricultural residues, and cellulosic waste composed of up to 75% polysaccharide sugars, which can be utilized in the synthesis of second-generation biofuels based on the lignocellulosic biorefinery techniques applied in the long-term management of greenhouse gas and energy security.[3] By 2022, the required volume of renewable fuels added into the transportation fuel sold in the United States by the Renewable Fuel Standard (RFS) is expected to increase to 36 billion gallons.[4,5]

Currently, the conversion of biomass can be classified into two general processes: thermochemical conversion for the production of biofuels power and heat, by gasification, liquefaction and pyrolysis; and biochemical conversion for the production of fuel and chemicals, including anaerobic digestion, biodiesel conversions, and ethanol synthesis.[6] To date, the generation of bio-ethanol by one biochemical conversion process, enzymatic hydrolysis and fermentation, is one of the most heavily studied conversion processes.[7] The first step of this process from lignocellulosic biomass to biofuels incorporates pretreatment, the purpose of which is to reduce the inherent recalcitrance of plant cell

walls so that the polysaccharide fractions locked in the intricacy of plant cell walls can become more vulnerable to enzyme attack.[8] Several leading pretreatment techniques reduce recalcitrance and enhance the enzymatic sugar yield with high efficiency.[9]

The ultrastructure of cellulose, which is relevant to the enzymatic deconstruction of the biomass, should be monitored for the purpose of deconvoluting factors affecting recalcitrance and developing a more thorough understanding of molecular-level mechanisms that these enzymes employ. However, lack of understanding the relationship between ultrastructures and enzymatic hydrolysis has resulted in several knowledge gaps: such as the relationship between pretreatment severity and cellulose ultrastructures, including crystallinity, allomorphs, cellulose fibril dimension; and another between the lignin content and structural changes during dilute acid pretreatment and cellulose ultrastructure alteration along with downstream enzymatic hydrolysis behavior.

The purpose of this dissertation deals with the impact of lignin content and structural factors on changes in the cellulose ultrastructure taking place during pretreatments for the production of biofuels, and the effect of lignin types and structure during rheology test on physicochemical properties of the precursor material suitable for production of carbon fiber. The primary goal of this thesis (Chapter 4) is to fill in these gaps and investigate the changes in the structural parameters of cellulose during various leading pretreatments and the individual and cooperative effects of these parameters on enzymatic saccharification. A vital component of this study is to generate reliable structural models of cellulose before and after pretreatment which could facilitate the way for optimizing processing

conditions that enhance the production of biofuels and biomaterials. The following section (Chapter 5) aims to assess the influences of the presence of lignin on dilute acid pretreatment-induced changes in the cellulose ultrastructure and to verify the hypothesis stating that, in the absence of intact hemicelluloses and the lignin matrix during pretreatment (elevated hydrothermal conditions), cellulose crystallites have an increased propensity to inhibit enzymatic hydrolysis. Chapter 6 further investigates the structural transformation of the cellulolytic enzyme lignins in poplar and switchgrass during dilute acid pretreatment, thereby drawing a clear picture about the nature of lignin chemistry and the way in which these structural changes limit efficient sugar release in woody and non-woody biomass. In addition, Chapter 7 aims to investigate the physicochemical properties of the carbon precursors from poplar lignin before and after melt rheology so that we can select a lignin with superior processing performance characteristics for fabricating high-quality carbon fibers.

CHAPTER 2

LITERATURE REVIEW: LIGNOCELLULOSIC BIOMASS FOR BIOFUELS AND BIOMATERIALS

2.1 Lignocellulosic Biofuels

The rising global demand for energy and material from unstable and expensive petroleum resources and concerns about the economy and global warming call for the development of renewable energy sources to that replace fossil fuels.[1, 10] Since the first-generation biofuels were produced from sugar, starch, and oil-seed-based feedstocks that have generated serious competition and a debate for food resources. Therefore, second-generation biofuels expanded the feedstocks to lignocellulosic biomass, including agri-residues, agro-industrial wastes, forestry and energy crops, which are abundant, renewable and cost-effective non-food resources.[11] Certain oils produced by plants and algae, which can be used directly as fuel or chemically transesterified to biodiesel. Hydrogen gas can be produced by not only photosynthetic algae and cyanobacteria under certain nutrient- or oxygen-depleted conditions but also bacteria and archaea utilizing organic substrates under anaerobic conditions. Other biofuels such as bioethanol and biobutanol can also be produced as organic substrates fermented by microbes under anaerobic conditions.[10] Energy contents of specific fuel sources are summarized in Figure 1 based on data from the literature. [12]

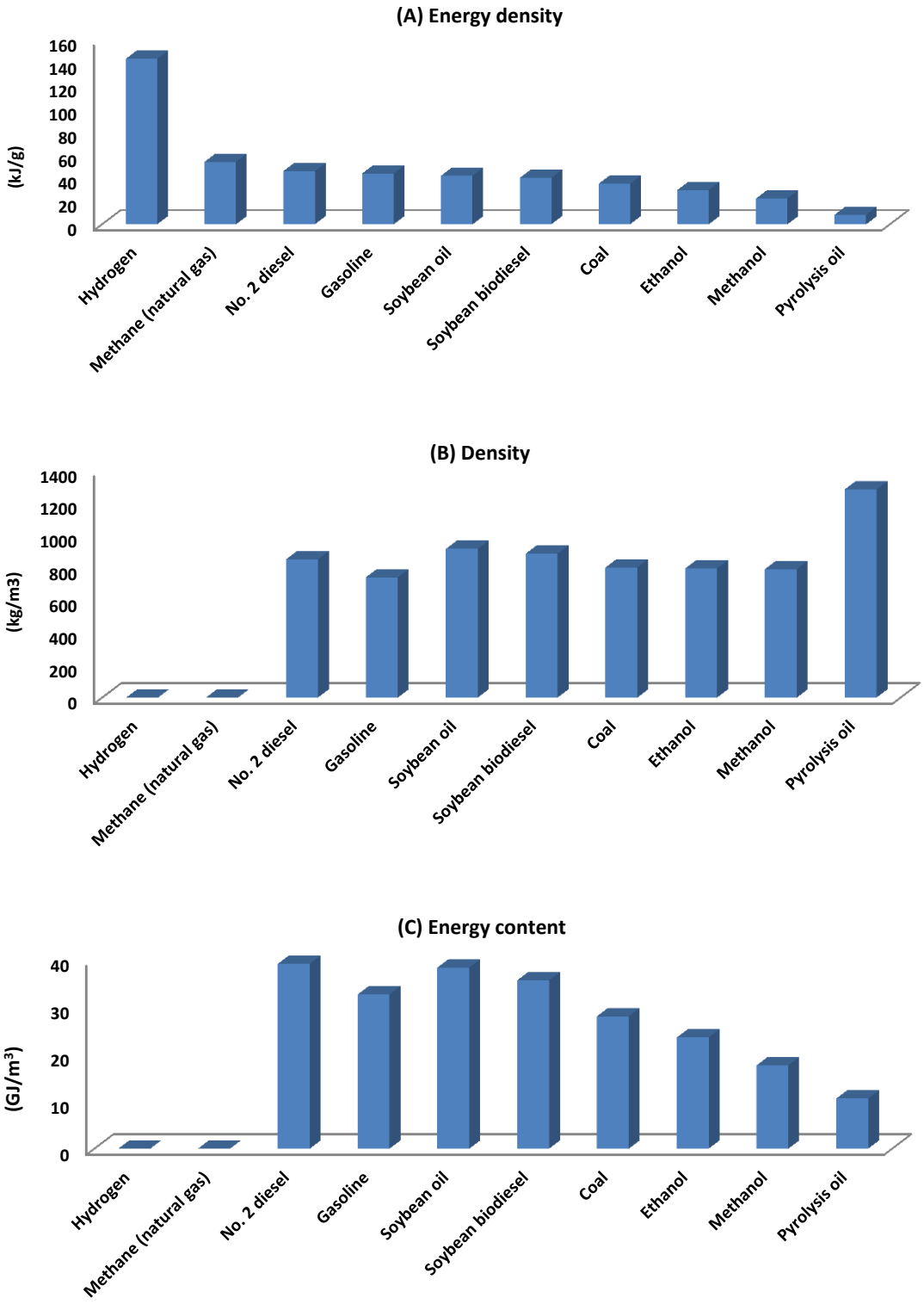

Figure 1 Energy density values for common fuels.[12]

First-generation biofuels can impact the environment, the economy, water overconsumption and pollution, deforestation, biodiversity loss, and social conflict.[13] Most authorities such as the EU-Renewable Energy Directive and Food and Agriculture Organization of the United Nations have become aware of these effects and issued regulations on the production of first-generation biofuels.[13, 14] To date, one of the most important liquid forms of biofuel from carbohydrates is bioethanol, produced in plants or plant-derived materials. In 2005, the United States became the world's largest producer of ethanol fuel, the production of which had increased from 1.63 billion gallons in 2000 to 13.2 billion U.S. liquid gallons (49.2 billion liters) in 2010 and subsequently to 13.9 billion U.S. liquid gallons (52.6 billion liters) in 2011.[15] Moreover, the minimum volumes of various types of renewable fuels that must be included in the United States' supply of fuel for transportation by the Renewable Fuel Standard (RFS) is intended to rise to 36 billion gallons by 2022.[4,5] Recently, technological advances have boosted the production of cellulosic ethanol and ethanol from plant waste (e.g., corn stover) on a commercial scale with the opening of a $275 million, 25-million gallon per year cellulosic ethanol plant in Emmetsburg, Iowa—a joint venture between POET, an American biofuels company, and the Dutch firm Royal DSM.[16] Poet-DSM will produce cellulosic ethanol from corncobs, leaves, husks, and corn stalks harvested by farmers located within a 30- to 40-mile radius of the plant.[17]

Conventional processes for producing lignocellulosic ethanol are typically divided into several steps: size reduction of biomass, pretreatment, enzymatic cellulose hydrolysis (saccharification), fermentation, and distillation.[18] Considering biomass recalcitrance, or

the capability of the natural resistance of the plant cell wall to microbial and enzymatic deconstruction, current cellulosic bioethanol production requires pretreatment prior to enzymatic hydrolysis and fermentation. The purpose of pretreatment is to break down the cell wall structure, alter and redistribute its components, disrupt the lignin-cellulose matrix, and thereby increase cellulose accessibility to enzymes during hydrolysis. Subsequently, bioethanol is derived from simple sugars through fermentation followed by a distillation process for the separation and the purification of final products.[19]

2.2 Lignocellulosic Feedstocks

Lignocellulosic biomass is mostly cell wall material mainly composed of three biopolymers: cellulose (35–50%), hemicellulose (20–32%) and lignin (10–35%), along with smaller amounts of pectin, protein, extractives, and ash.[20] Figure 2 summarizes the composition of lignocelluloses encountered in the most common sources of biomass.[21] The sources can generally be grouped into six categories: energy crops, agricultural residues, logging residues, mill residues, forest resources, and urban waste. Forest-derived resources include forest residues from harvesting or land conversion, unused mills from wood or pulp processing, waste from urban wood, and debris from construction/demolition. The energy crop category includes lignocellulosic crops such as herbaceous switchgrass and woody crop poplar.[22]

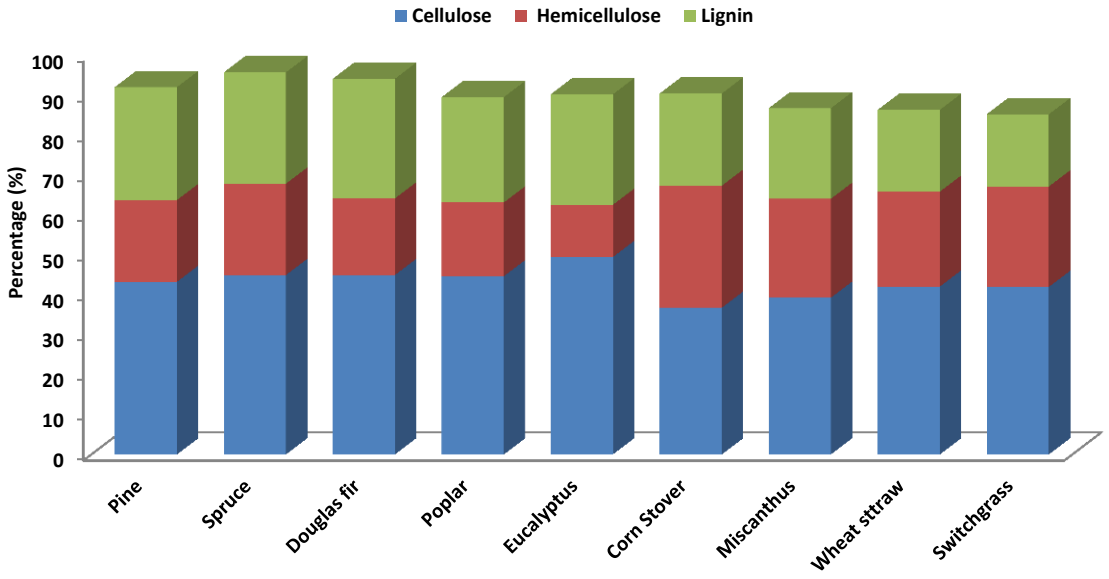

Figure 2 Typical lignocellulosic biomass compositions (% dry basis).[21]

2.2.1 Cellulose

Cellulose is a linear homopolysaccharide composed of β-D-glucopyranosyl units linked by 1→4 glycosidic bonds with cellobiose as the repeating unit (Figure 3).[23]

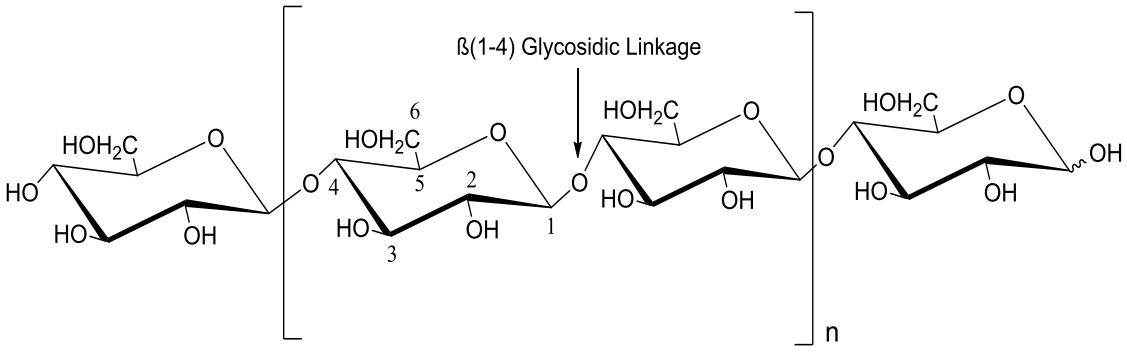

Figure 3 The structure of cellulose.

2.2.1.1 Cellulose Degree of Polymerization

Many properties of cellulose depend on its degree of polymerization (DP), including the effect of pretreatment technologies on the DP and its subsequent influence on the enzymatic hydrolysis of cellulose for the purpose of producing fermentable sugars. DP can be defined in terms of the number-average DP (DP_n), weight-average DP (DP_w) and viscosity-average DP (DP_v) according to the following equations [24]:

$$DP_n = \frac{M_n}{MW_{glu}} = \frac{\Sigma N_i M_i}{\Sigma N_i} / MW_{glu}$$

$$DP_w = \frac{M_w}{MW_{glu}} = \frac{\Sigma N_i M_i^2}{\Sigma N_i} / MW_{glu}$$

$$DP_v = \frac{M_v}{MW_{glu}} = \frac{\frac{\Sigma N_i \eta}{\Sigma N_i}}{MW_{glu}}, where\ \eta = K_m M_i^{\alpha+1},$$

where N_i is the number of moles of a given fraction i with molecular weight M_i, M_n is the number-average molecular weight, M_w is the weight-average molecular weight, M_v is the viscosity-average molecular weight, MW_{glu} is the molecular weight of anhydroglucose (162 g/mol), η is viscosity, K_m is a constant, and the values of α for cellulose and cellulose derivatives range from 0.75 to 1. [24]

Most commonly used techniques of measuring cellulose DP are viscometry and gel-permeation chromatography (GPC) methods.[25] Although the viscometry method provides cellulose DP_v relatively quickly and conveniently, it has several limitations, including non-absolute average M_v values, which depend greatly on solvent and temperature conditions, no clear information concerning the molar mass distribution, and complex metal solutions used with the testing method that can degrade cellulose.[26] In contrast,

GPC can provide more detailed information, including DP_n, DP_w with all three molecular weights (M_n, M_w, M_v), and the polydispersity index ($PDI=M_w/M_n$), which is used to measure the broadness of the molecular weight distribution of a polymer. The relative cellulose molecular weights that GPC provides are based on the molecular weight of well-defined polystyrene standards with varying molecular weights.[26b] A list of the DPs of cellulose determined by the nitration method followed by the measurement of viscosity is summarized in Figure 4.[27] Nitration was carried out in a mixture of HNO_3:H_3PO_4:P_2O_5 (64:26:10, w/w), and the final product was then used for a nitrogen assay and for the viscosity measurement after fractionation. The specific viscosity of each fraction was calculated from the measurement of the efflux times at decreasing concentrations in a viscometer at 25 ℃. The intrinsic viscosity was calculated by extrapolation to zero of a plot of specific viscosity over concentration. The average molecular weight of each fraction was estimated by the Mark-Houwink equation.[28] Thus, the distribution pattern of the DP of the cellulose could be determined. This method does not require pre-isolation of cellulose through holocellulose pulping and the base-catalyzed hydrolysis of the hemicellulose.[26b] However, the nitration method is rarely used because of uncertainty arising from the possible acid hydrolysis of the cellulose chain during derivatization along with the instability of the derivative. Nitric and phosphoric acids are very dramatic, resulting in the over-hydrolysis of cellulose chains, which has been confirmed by several studies that have shown a significant reduction in the DP of cotton and aspen cellulose by the nitration method.[25, 26b]

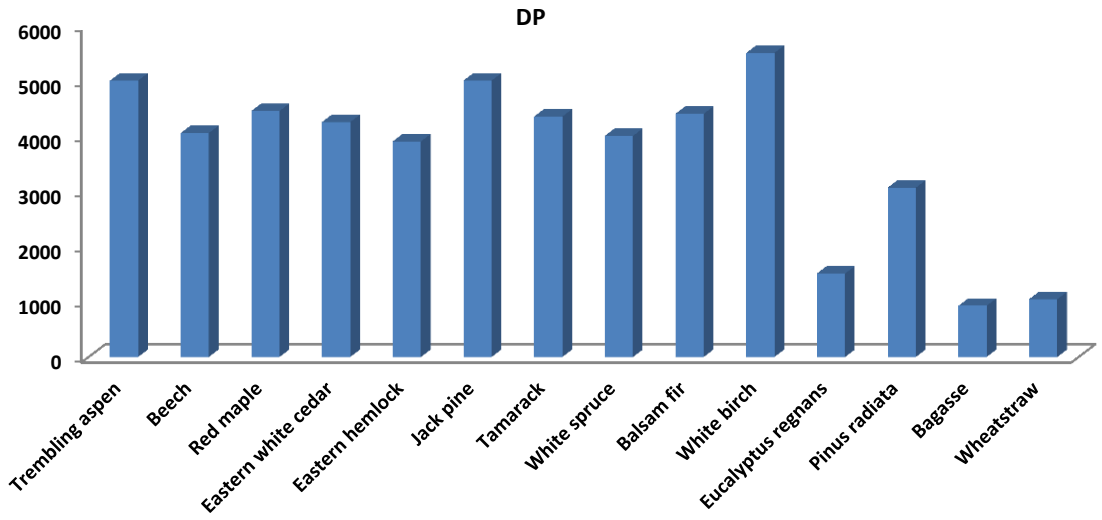

Figure 4 DP of types of cellulose after nitration by the viscometric method. [27]

To date, cellulose tricarbanilate (CTC) has been a commonly used cellulose derivative for DP measurement by GPC.[29] Cellulose tricarbanilation is commonly performed by the reaction of cellulose with phenyl isocyanate in pyridine as the solvent. The unreacted phenyl isocyanate is quenched by methanol that is then added to the mixture. Afterwards, the mixture is poured into a 3:7 water-methanol mixture to precipitate the cellulose tricarbanilate. The derivatized cellulose is finally purified and dissolved in tetrahydrofuran (THF) for GPC measurement.[29a, 30] When CTC facilitates the study of cellulose DP by GPC, it has several advantages, including complete substitution, no de-polymerization during derivatization, the stability of the derivative, and solubility and stability in the THF.[25] However, this testing method is only applied to the pure cellulose isolated from samples that are native biomass and biomass after various treatments. Figure 5 summarizes the DP values of several native cellulose samples based on the viscometry technique,[31] which is more adequate for analyzing cellulose DP because of the complexity of the lignocellulosic biomass.[31a] Cellulose DP ranges from around 1,500

to 4,500, depending on the various origins of biomass such as hardwoods (e.g., poplar and aspen) with a cellulose DP of 3,500 and 4,500, and agricultural residues, which vary within a range of 1,800 to 4,000.

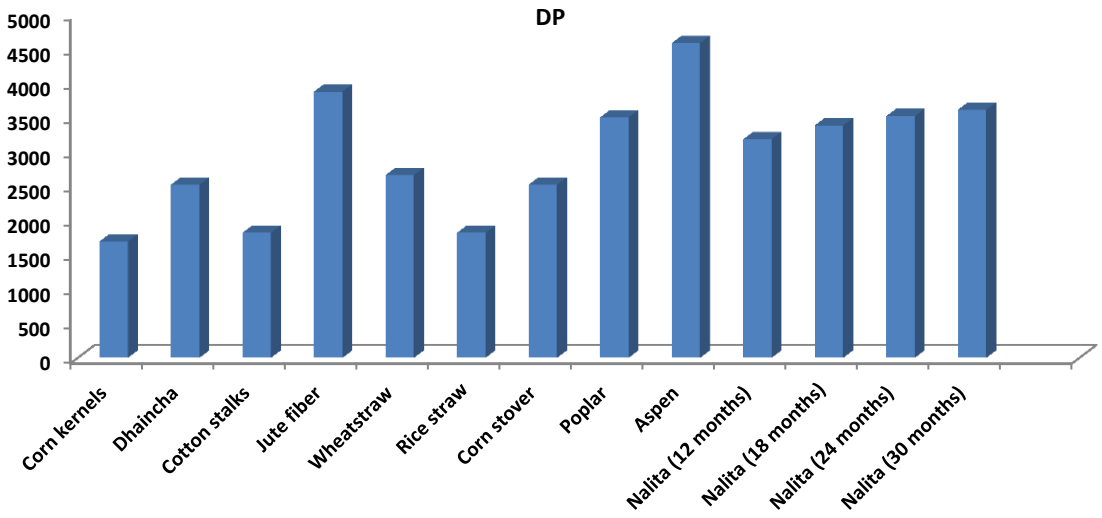

Figure 5 DP of native woody and non-woody cellulose. [31]

2.2.1.2 Cellulose Polymorphs

Cellulose also has a strong tendency to form intra- and intermolecular hydrogen bonds that result in unique ultrastructures of native celluloses in plant. Some of these H-bonds contribute to stiffening the straight chain and promoting aggregation in the crystalline structure (highly ordered regions), the others could form less-ordered (amorphous) regions[23] that result in the change of cellulose crystallinity in lignocellulosic materials according to their origin and acquisition process. Crystalline cellulose displays six various allomorphs (I, II, III_I, III_{II}, $IV_{I,}$ and IV_{II}) with the possibility of conversion from one form to another as summarized in Figure 6.[32]

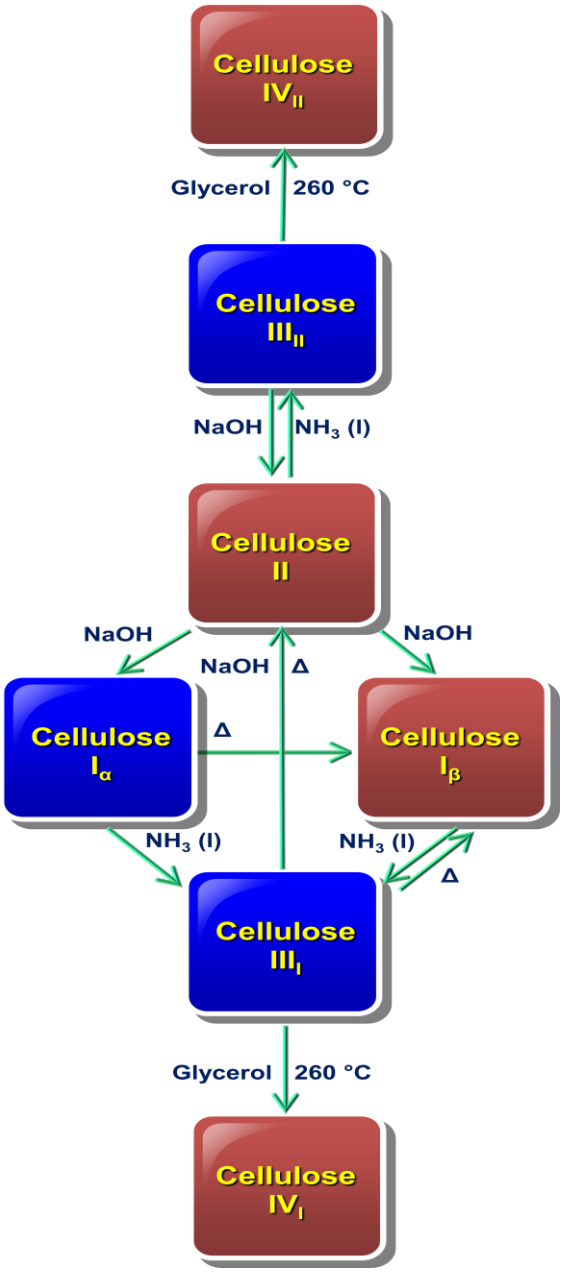

Figure 6 Intercoversion of cellulose into its various polymorphs.[32]

Cellulose I and II are the most predominant among various polymorphs. Cellulose I is the main polymorph found in native form that contains parallel cellulose chains, in which the reducing ends are aligned in same direction.[33] Modern analytical techniques have confirmed that two intra-chain hydrogen bonds exist between O3-H and O5 and between

O2-H and O6, with one inter-chain hydrogen bond between O6-H and O3, which is responsible for the structure of cellulose I.[34] Furthermore, native cellulose is composed of three crystalline allomorphs (I_α, I_β, and para-crystalline cellulose) and amorphous cellulose at accessible and inaccessible fibril surfaces. Para-crystalline cellulose is less ordered than crystalline cellulose I_α and I_β but more ordered than the amorphous region. While accessible fibril surfaces are regions in contact with water, inaccessible fibril surfaces are fibril-fibril contact surfaces and surfaces resulting from distortions in the interior of the fibrils.[35] A structure of cellulose I in which a unit cell of the crystal lattice is a monoclinic unit with the space group $P2_1$ consisting of two anti-parallel cellobiose chain segments has been proposed.[32] Figure 7 summarizes the dimensions of various cellulose allomorphs.[32]

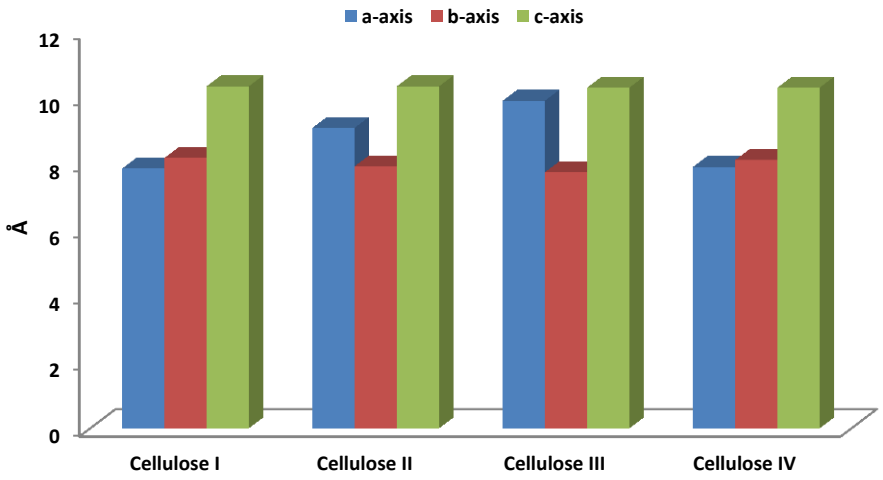

Figure 7 The dimensions of various cellulose allomorphs.[32]

Whereas cellulose I_α, known as a triclinic structure, has one cellulose chain per unit cell, cellulose I_β, known as a monoclinic structure, has two cellulose chains per unit cell. Generally, cellulose I_α is the predominant form in bacteria and algae, and Cellulose I_β

predominantly exists in higher plants. The abundance of I_α or I_β polymorphs in lignocellulosic material may affect the reactivity of cellulose because cellulose I_α is more reactive than cellulose I_β. Cellulose I_α, meta-stable in nature, can be converted to the thermodynamically more stable allmorph I_β by annealing.[36] The basic building unit of the cellulose skeleton is an elementary fibril that contains 36 β–D-glucan chains with a diameter of approximately 3.5 nm (Figure 8).[37]

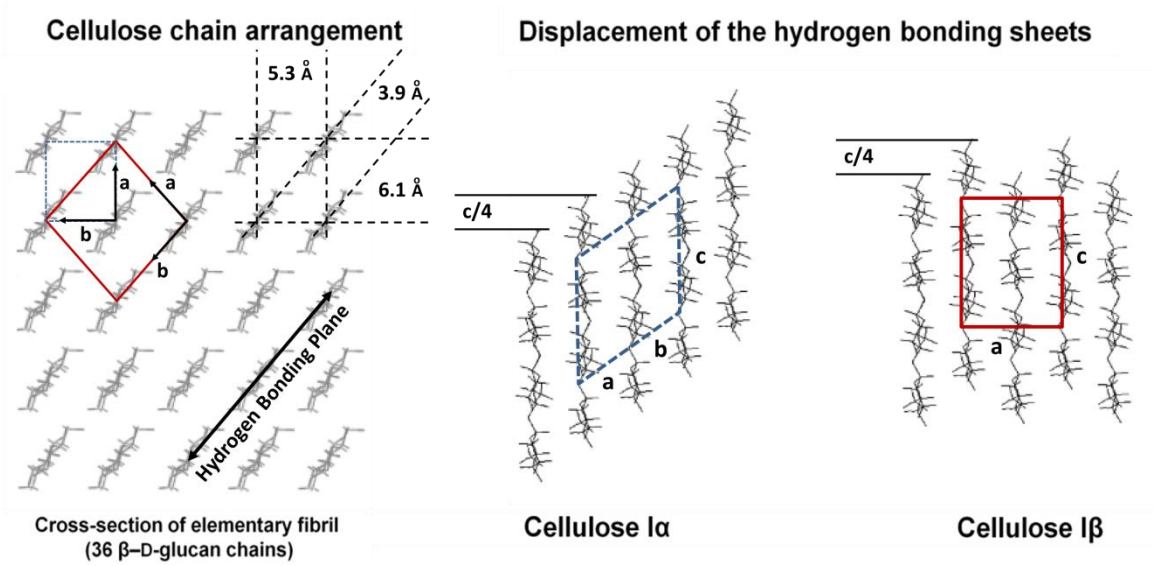

Figure 8 Cross section of the elementary fibril containing 36 glucan chains of the unit cells for cellulose I_α and I_β.[38]

Cellulose II is the second most extensively studied crystalline form with a monoclinic unit cell (i.e., the reducing ends are aligned in an anti-parallel direction). The conversion of cellulose I to cellulose II can be accomplished by mercerization in alkali or by regenerating cellulose I in a suitable solvent such as heavy metal-amine complex solutions, copper with ammonia in water, some inorganic salts above 100 ℃, thiocyanate/amine, LiCl/DMAc mixtures, and NMMO/water systems, among others,

which is generally considered to be irreversible.[39] The nature of hydrogen bonding in cellulose II chains indicates that the outer chains contain intermolecular hydrogen bonding between O2-H and O-6 and intramolecular hydrogen bonding between O3-H and both O5 and O6. The center chains contain intermolecular hydrogen bonding between O6-H and O2, and intramolecular hydrogen bonding is similar to the outer chains. Intermolecular hydrogen bonding occurs not only between O2-H and O2 but also between O6-H and O6 among the outer and center chains.[40]

In addition, cellulose III is usually obtained from cellulose I and II by treating it with liquid ammonia at low temperatures or in ethylene diamine followed by washing with alcohol. Cellulose IV is formed from cellulose II and III upon treatment in a suitable liquid at high temperatures as shown in Figure 6.

2.2.1.3 Cellulose Characterization by NMR

The crystalline structure of cellulose has been studied since its discovery in the 19th century. Crystallinity in cellulose is typically evaluated as the ratio of two phases, defined as either crystalline versus amorphous regions or ordered versus disordered regions. A detailed ultrastructural picture of cellulose, including cellulose crystallinity, crystallite size, and crystalline allomorphs has been provided using several different techniques, including wide-angle X-ray scattering (WAXS) patterns, infrared (IR), Raman, and solid-state CP/MAS ^{13}C NMR spectroscopy.[41] For example, a common X-ray diffraction (XRD) method determining the cellulose crystallinity considers the peak intensity of the 002 diffraction plane compared to the intensity of pure amorphous cellulose on the same

plane.[42] Since some have debated the accuracy of this method, other methods for processing XRD patterns and determining cellulose crystalline are based on the analysis of diffraction spots versus diffraction ring patterns to generate the accurate results.[36b, 41b, 43]

Solid-state ^{13}C CP/MAS NMR spectroscopy provides a high level of detailed chemical and structural information that is especially useful in the ultrastructural analysis of cellulose.[19a] Because solid-state NMR is sensitive to magnetic non-equivalences in an environment of chemically equivalent nuclei, crystalline and amorphous cellulose can be shown to generate chemical shifts. Earlier studies that used ^{13}C CP/MAS NMR to investigate cellulose from Acetobacter, Valonia, kraft pulp, and low-DP acid-hydrolyzed cellulose, not only provided information of crystallinity index but also enabled a thorough investigation of the ultrastructure of cellulose, such as observed variations in chemical shifts for the C_4 and C_6 carbon positions in the anhydro-glucose unit dependent upon the cellulosic source attributed to variations in cellulose crystallinity and the crystal lattice structure.[41a, 44]

Because of the interference with the cellulose amorphous region, hemicelluloses and lignin must be removed from the cellulose samples to ensure the accuracy of this technique.[45] In the ^{13}C CP/MAS NMR spectrum of isolated cellulose, the C_1, C_4, and C_6 signals of cellulose extend over chemical shift ranges of δ=102–108, 80–92, and 57–67 ppm, respectively, along with the first peak in the C-4 region corresponding to the crystalline structure (δ=86–92 ppm) and the amorphous region located in the range of

δ=80–86 ppm, as shown in Figure 9.[46] Therefore, cellulose crystallinity can be determined by a two-peak, non-linear, least-squared fit or the basic peak integration of these two regions. One study developed a novel method that utilized a partial least-squares (PLS) model for not only estimating cellulose I_α and cellulose I_β content[47] but also deconvoluting the contributions of para-crystalline cellulose and accessible and inaccessible fibril surfaces based on the non-linear line-fitting of six or seven resonances to the C_4 peak region of the adjustable shape, width, chemical shift, and relative intensity.[45, 48] Table 1 summarizes the cellulose crystallinity and ultrastructure from typical biomasses characterized by CP/MAS ^{13}C NMR spectroscopy.[48-49] Afterwards, cellulose crystallite or microfibril dimensions can also be estimated using the relative intensity of C_4 amorphous peaks that represents the percentage of chains at fibril surfaces along a square cross-sectional cellulose microfibril model, in which cellulose chains have a width of 0.55 nm, the cellulose microfibril and microfibril bundle dimensions can then be calculated.[50]

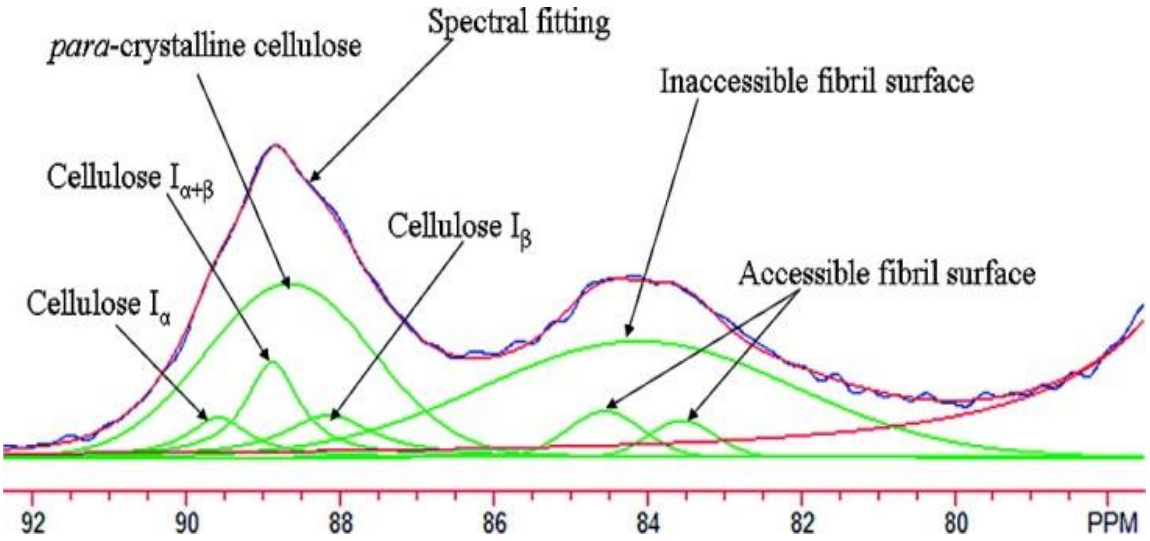

Figure 9 Spectral fitting for the C-4 region of CP/MAS ^{13}C-NMR spectrum of native Buddleja davidii cellulose.[46]

Table 1 The relative contents (%) of crystalline, para-crystalline and amorphous portions of cellulose from poplar, loblolly pine, and switchgrass.[48-49]

Biomass feedstock	Crystallinity	I_α	$I_{\alpha+\beta}$	Para-crystalline	I_β	Accessible fibril surface	Inaccessible fibril surface
Loblolly pine	63	0.1	30.7	24.8	6.9	33.1	15.6
Poplar	63	5.0	14.2	31.1	19.8	10.2	18.3
Switchgrass	44	2.3	8.8	27.3	4.5	5.7	51.3

2.2.2 Hemicellulose

Hemicellulose is a collective term used to present a family of polysaccharides found in the plant cell wall with various compositions and structures. Different from cellulose, hemicelluloses are composed of combinations of pentose and/or hexoses, such as xylose, arobinose, mannose, galactose, and glucose, with acetylated groups, uronic acid and 4-O-methyl ethers.[51] The hemicelluloses are broadly classified into four general classes of polysaccharide types based on structural differences in the cell wall: xylans, mannans, β-glucans with mixed linkages, and xyloglucans. The main hemicelluloses in softwood are galactoglucomannans and arabinoglucuronoxylan while that in hardwood is glucuronoxylan (Figure 10).[51]

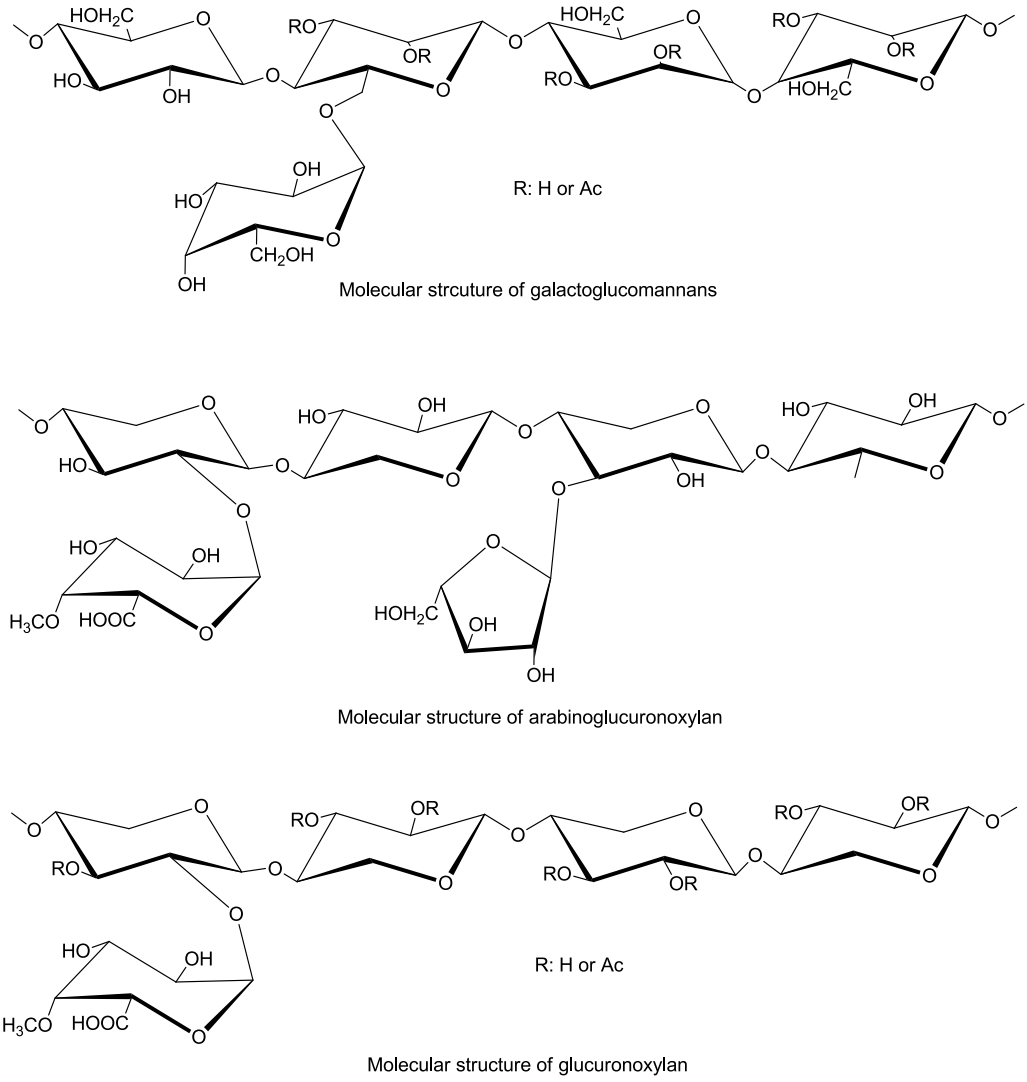

Figure 10 Main molecular structures of woody hemicelluloses.[51a]

Most hemicelluloses have relatively low molecular weight with a DP of 50~300 in wood that could contain 15-30% of hemicellulose in hardwood or softwood, summarized in Table 2.[52] Highly branched structures and acetyl groups on the polymer chain result in a lack of crystalline structure in hemicellulose. The most abundant sugar monomer in the softwood hemicelluloses is mannose; correspondingly, the most abundant sugar monomer in hardwood hemicellulose is xylose. Xylan is a heteropolysaccharide with a

homopolymeric backbone chain of 1,4-linked β-D-xylopyranosyl units. The branches of xylan, which may contain arabinose, glucuronic acid, or the 4-*O*-methyl ether, acetic, ferulic, and *p*-coumaric acids, vary depending on their origins.[53] Poplar normally contains ~20% hemicelluloses in which O-acetylated 4-O-methyl-glucuronic acid xylan or glucuronoxylan is the main component. Numerous studies revealed that xylans (15.9 to 22.4%) are the major hemicellulose in all the poplar species in their study, followed by mannans (0.9 to 3.4%). 4-O-methyl-glucuronic acid (4-O-MeGlcA; 2.2 to 2.8%), galacturonic acid (2.3 to 2.8%) and minor amounts of glucuronic acid (0.1 to 0.3%) have been identified as the uronic acids present in poplar.[52c] Galactoglucomannan is comprised of (1→4)-linked β-D-glucopyranosyl and D-mannopyranosyl units that are partially acetylated at the C2-OH and C3-OH and partly substituted by (1→6)-linked α-D-galactopyranosyl units.[54] Figure 11 summarizes the monosaccharide of several lignocellulosic biomasses from literature.[55]

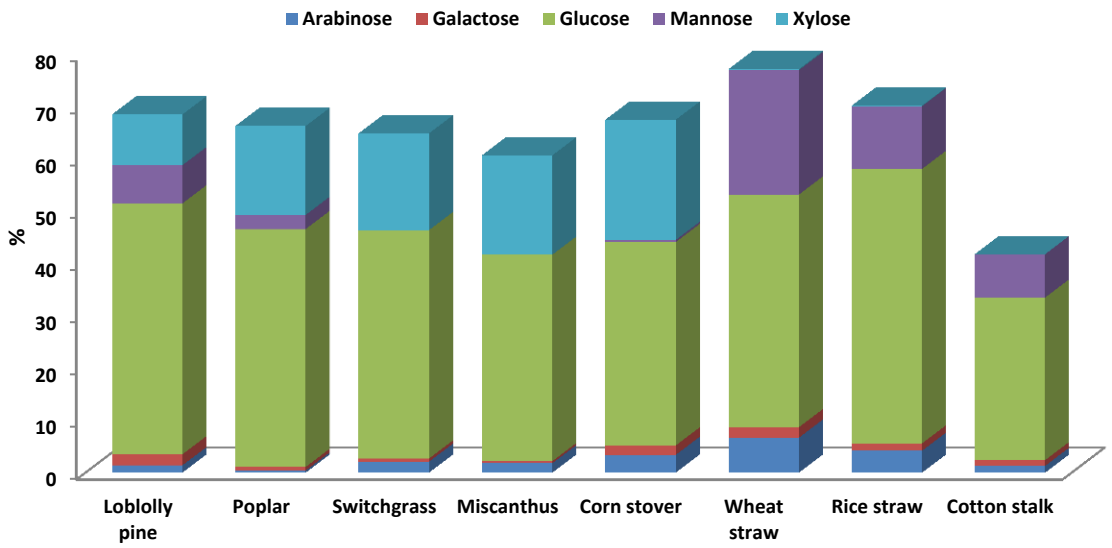

Figure 11 Content of monosaccharides for several lignocellulosic biomasses.[55]

Table 2 Hemicellulose composition and DP in several lignocellulosic feedstocks.[52]

		Carbohydrate composition of the hemicellulose		
Biomass	Hemicellulose	Sugar residues	Molar ratio	DP
Birch	Glucuronoxylan	4-O-MeGlcA:Xyl	5:100	101-122
Aspen	Glucuronoxylan	4-O-MeGlcA:Xyl	9:100	101-122
Poplar	Glucuronoxylan	4-O-MeGlcA:Xyl	12.5~13.8:100*	50 - 300
Spruce	Arabinoglucuronoxylan	Ara: 4-O-MeGlcA:Xyl	6:13:100	107-145
	Galactoglucomannan	Gal:Glu:Man	16:24:100	118-132
Pine	Arabinoglucuronoxylan	Ara: 4-O-MeGlcA:Xyl	10:16:100	107-145
	Galactoglucomannan	Gal:Glu:Man	9:22:100	118-132
Larch	Arabinoglucuronoxylan	Ara: 4-O-MeGlcA:Xyl	10:12:100	107-145
	Galactoglucomannan	Gal:Glu:Man	8:26:100	118-132

*: weight ratio

Table 3 Uronic acid content (%) of various biomasses.[56]

Biomass substrate	Uronic acids content (%)
Poplar hybrid	2.2-2.3
Sweetgum	2.6
Switchgrass	1.5
Weeping lovegrass	1.4
Sericea lespedeza	3.2
Wheat straw	3.8-5.4*

*: percentage of total hemicelluloses in wheat straw.

Moreover, higher plants contain various amounts of different uronic acid-containing hemicelluloses, such as β-D-glucuronic acid, α-D-galacturonic acid, α-D-4-O-methylglucuronic acid. Accurate analysis of the carbohydrate composition in higher plants, particularly uronic acid, is often desired for monitoring process control and product quality parameters in different application areas, such as Kraft pulping, bio-film and bio-foam manufacturing, the fragmentation of hemicelluloses for fermentable sugar,

and biological aspects in food and non-food applications. Table 3 summarizes contents of uronic acid existed in different biomass substrates.[56]

2.2.3 Lignin

Lignin is the second most abundant biomass component and the primary renewable aromatic resource in nature.[57] Lignin fills the spaces between cellulose and hemicelluloses acting as a resin that bonds the lignocelluloses matrix together. Distinctly different from cellulose and hemicelluloses, lignin is one of the most complex natural polymers synthesized by enzymatic dehydrogenative polymerization of 4-hydroxyphenyl propanoid units.[58] Lignin is composed predominantly of three phenylpropane monomers: *p*-hydroxyphenyl (H, from *p*-coumaryl alcohol), guaiacyl (G, from coniferyl alcohol), and syringyl (S, from sinapyl alcohol) units as summarized in Figure 12.[59] The composition of lignin varies depending on its origins, shown in Table 4,[60] softwood (i.e., gymnosperm, Scots pine) lignin is predominantly derived from G-type monolignol, in contrast, hardwood (i.e., angiosperm, *Populus*) lignin is mainly derived from G- and S-type monolignols with trace of H-type monolignol.[61] Softwood generally contains about 25-35% of lignin and hardwood 18-25% of lignin. Grass lignin (e.g., switchgrass) is derived mostly from G- and S-type monolignols with significant amount of H-type monolignol, along with significant levels of *p*-coumaric and ferulic acid (Figure 12) that is involved in cross-linking to lignin and hemicelluloses complex.[61b] Table 5 summarizes the typical G/S/H lignin ratio from several common energy crops.[62]

Table 4 Composition of some lignocellulose sources (% dry weight). [60]

Biomass substrate	Cellulose (%)	Hemicelluloses (%)	Lignin (%)
Bagasse	38	27	20
Wheat straw	30-38	21-50	15-23
Corn stover	38-40	22-28	18-23
Rye grasses	25-40	35-50	10-30
Switchgrass	31-45	20-30	12-18
Pine	44	23	28
Eucalyptus	50	13	28
Poplar	40-50	17-19	18-26

Table 5 The G/S/H lignin ratio from several common energy crops. [62]

Biomass substrate	G lignin (%)	S lignin (%)	H lignin (%)
Wheat straw	49	46	5
Rice straw	45	40	15
Sugarcane bagasse	30	37	33
Switchgrass	51	41	8
Miscanthus	52	44	4
Corn stover	51	3.6	46
Poplar	32-37	63-68	NA

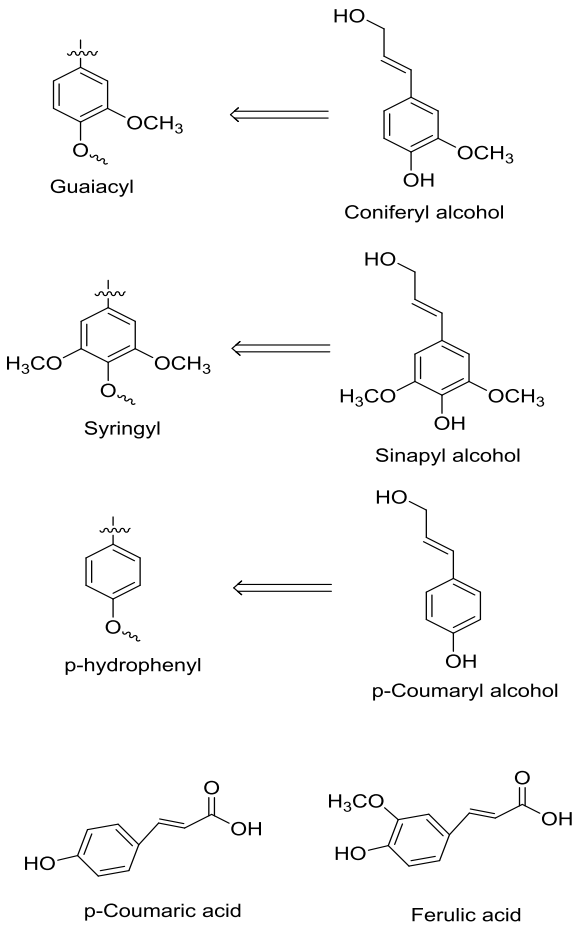

Figure 12 Typical phenylpropanoid precursors employed in the biosynthesis of lignin in plant biomass. [59]

Lignin precursors are polymerized via radical coupling reactions that result in three-dimensional complex, amorphous and phenylpropanoid macromolecules. Figure 13 indicates the phenyl propane precursors of lignin and the enzymatic synthesis pathway from coniferyl unit to the typical linkages in lignin structure — β-O-4 linkage. Some other major types of linkages with reported abundance in lignins from softwood and hardwood have been shown in Table 6.[63] The radical electron occurs at different positions due to resonance which allows the formation of several different inter monomer linkages

via radical polymerization. This polymerization process is normally initiated by an enzyme-catalyzed oxidation of the monolignol phenolic hydroxyl groups to generate free radicals. A monolignol radical can then couple with another one to generate a dilignol. Subsequent nucleophilic attack by water, alcohols, or phenolic hydroxyl groups on the benzyl carbon of the quinone methide intermediate restores the aromaticity of the benzene ring. The generated dilignols then undergo further polymerization to form protolignin. Therefore, various types of inter monomer linkages can be commonly found in biomass, such as resinol (*β-β*), phenylcoumaran (*β*-5), biphenyl (5-5), and 1,2-diaryl propane (*β*-1), shown in Figure 14.[62f]

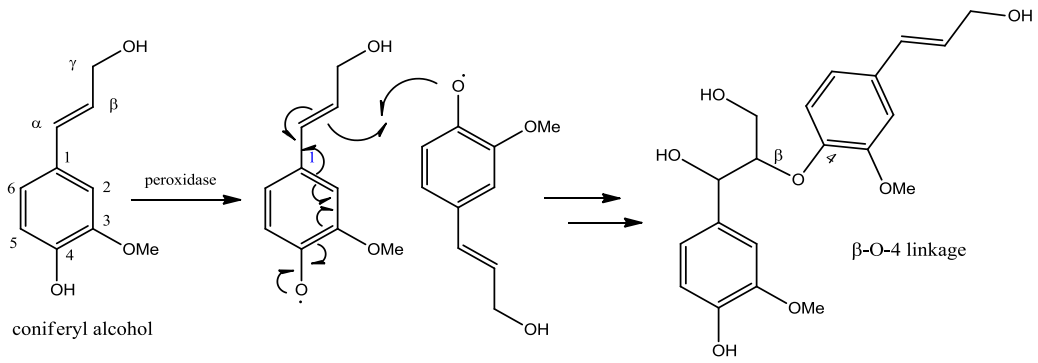

Figure 13 Possible radical coupling pathway to form β-O-4 linkage from coniferyl unit.

Table 6 Major linkages in lignins from softwood and hardwood (number of linkages per 100 C_9 units).[63]

Linkage	β-O-4	4-O-5	Dibenzodioxocin	β-5	5-5	β-1	β-β
Softwood	45-50	4-7	5-7	9-12	19-22	7-9	2-4
Hardwood	60-62	7-9	0-2	3-11	3-9	1-7	3-12

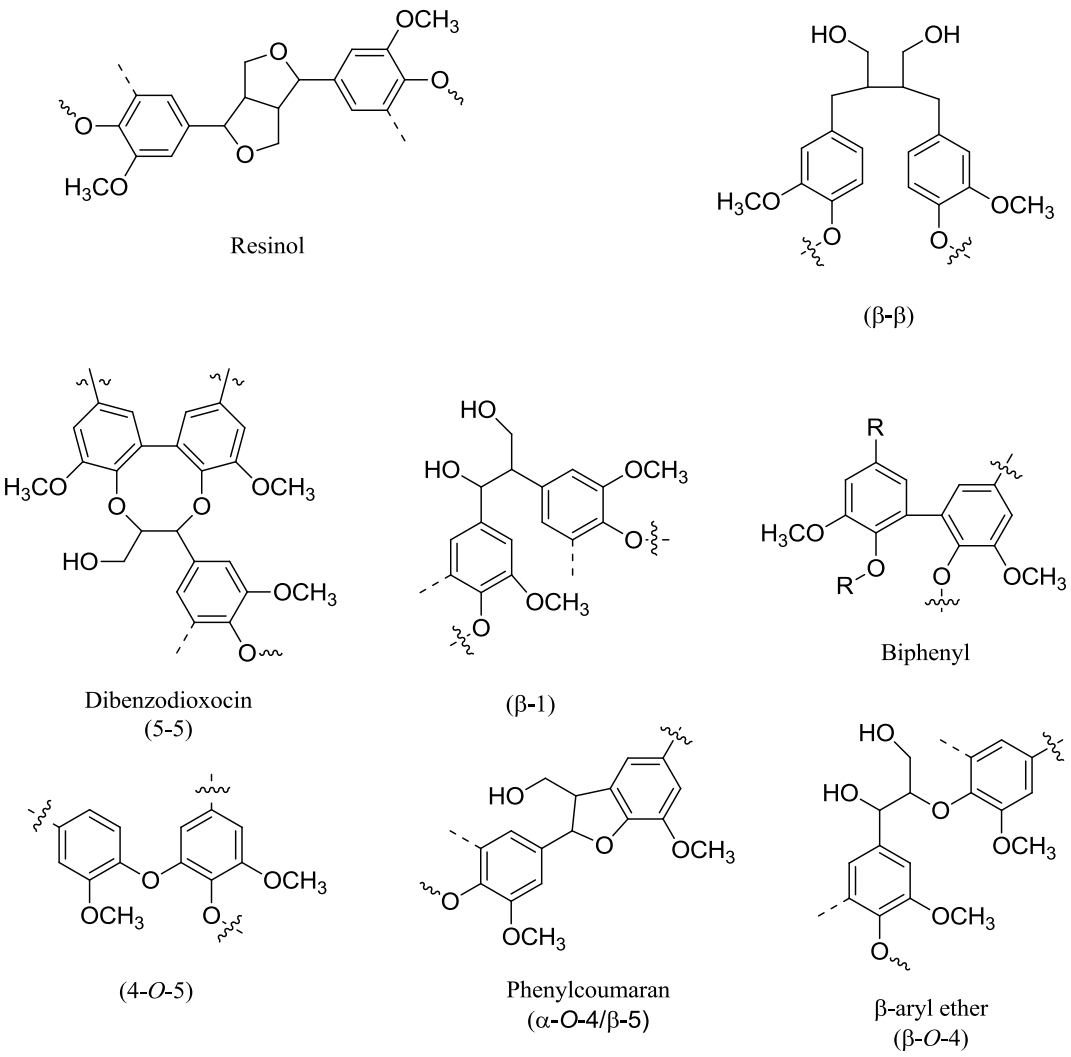

Figure 14 Typical inter-unit linkages found in lignin.[62f]

Various types of lignin polymerization pathways result in a highly branched macromolecule with weight average of molecular weight (M_w) ~20,000 in softwood and slightly low molar mass in hardwood, along with polydispersity of 2.5 and 3.5, respectively.[64] The molecular weights of various lignins isolated using enzymatic mild acidolysis from different resources are summarized in Figure 15.[65]

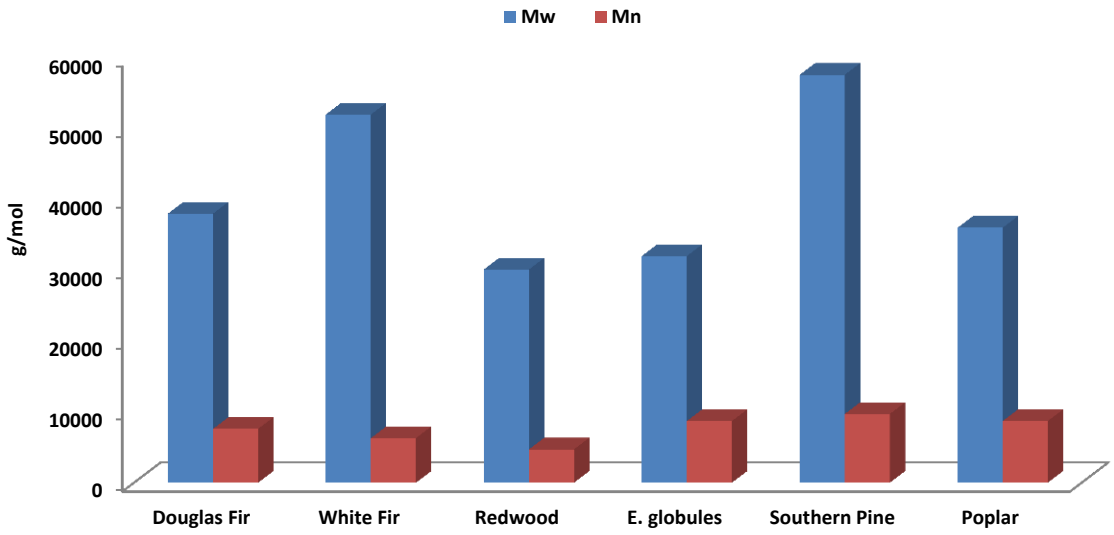

Figure 15 Weight-average molecular weight (M_w) and number-average molecular weight (M_n) of various lignins isolated using enzymatic mild acidolysis from various biomasses.[65]

2.2.3.1 Lignin Characterization by NMR

The chemical structure of lignin depends on multiple conditions, such as environmental effects during growth and various separation processes. Nuclear magnetic resonance spectroscopy is a powerful tool for detailed structure elucidation. Lignin analytical techniques by NMR are briefly reviewed in this section, especially focusing on the application of solution and solid state NMR (^{1}H, ^{13}C, ^{31}P and heteronuclear single quantum coherence (HSQC)) measurement to gain detailed insights into lignin structural changes during various treatments.

^{1}H NMR enables the differentiation between at least carboxylic, carbonyl, phenolic, aromatic, methoxy and aliphatic functionalities of lignin (Figure 16), because one

advantage is the most abundant ^{1}H nucleus among the nuclei. Although several signal overlaps resulting from the short chemical shift ranges cannot be avoided easily,[66] ^{1}H NMR of acetylated and un-derivatized lignin can still provide useful information for those key lignin functional groups.

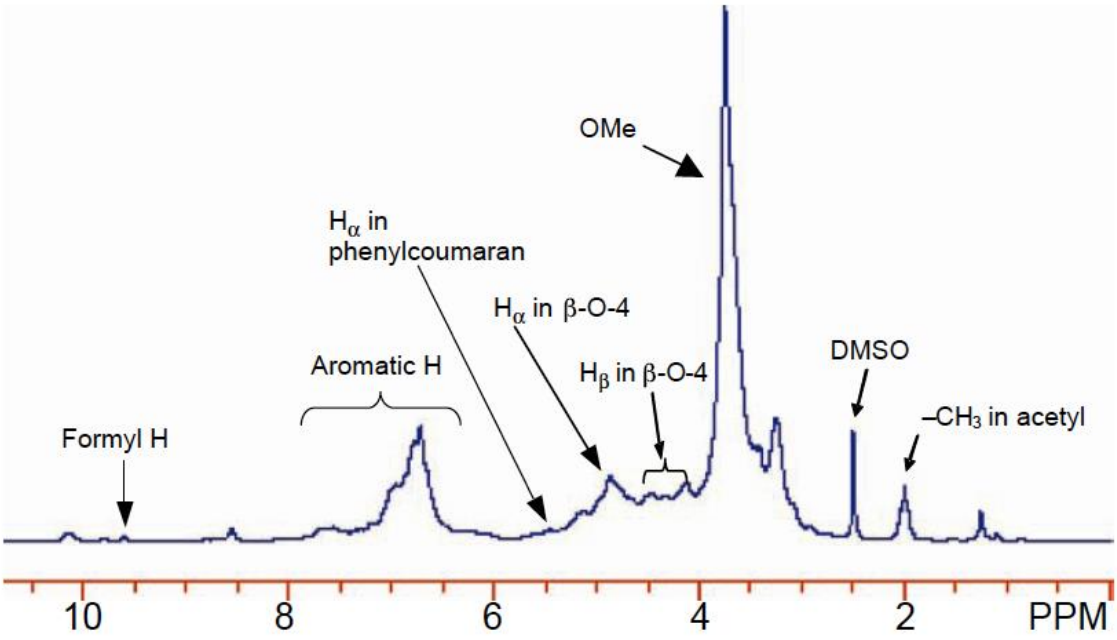

Figure 16 An example of ^{1}H NMR spectrum of poplar mill-wood lignin using dimethyl sulfoxide (DMSO) as solvent.[46a]

^{13}C NMR provides comprehensive information of the structures of all carbons in lignin with multiple advantages compared to proton NMR, such as better resolution, better reliability, less overlap of signals, and broader spectral window (i.e. δ 240-0 ppm). Earlier study of carbon NMR on Kraft lignin employed DEPT (distortionless enhancement by polarization transfer) to separately evaluate CH, CH_2, CH_3 and aromatic ring from their combination quaternary spectra.[67] Acetylation of lignin not only overcame signal overlap but also enabled to calculate the amounts of given inter-unit linkages by

differentiation between integrals. Quantitative analysis of lignin is based on the phenylpropane (C_9) by calculating the ratio of the integral value of a given carbon signals to 1/6 the integral of the aromatic carbons (signal located at δ 162-102 ppm).[68] Figure 17 represents a quantitative ^{13}C NMR spectrum for a milled wood lignin (MWL) isolated from a hardwood Buddleja davidii.[46]

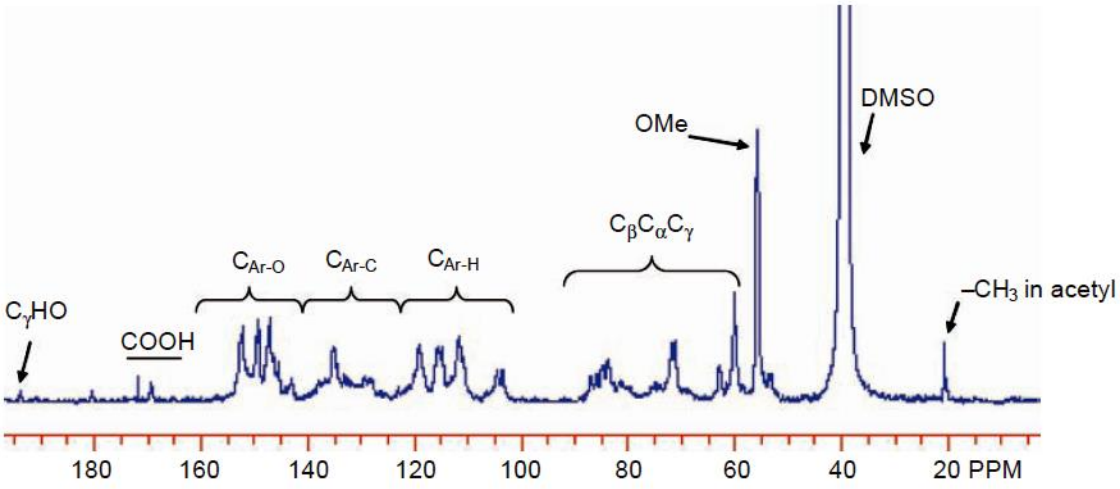

Figure 17 Quantitative ^{13}C NMR spectrum of a MWL isolated from a hardwood Buddleja davidii.[46] Ar: aromatic; OMe: methoxyl; DMSO: dimethyl sulfoxide.

Multidimensional NMR techniques, such as HSQC, in the structural analysis of lignin have a significant advantage that allows the resolution of otherwise overlapping resonances in either ^1H or ^{13}C spectra axis. In HSQC, two polarization transfer delay periods are used to transfer magnetization between ^1H and ^{13}C nuclei, and the spectrum is obtained with the optimized $^1J_{CH}$-coupling of 145 Hz.[69] This advanced two-dimension (2D) NMR technique not only enables the separation of signals heavily overlapped in 1D spectrum but also provides increasing sensitivity of ^{13}C nuclei by polarization transfer,

which make this correlation method a high resolution tool for analyzing lignin. Compared to overlapping 1D spectrum, it can show functionalities and inter-unit linkages well separated.[70] Although the limitation including the semi-quantitative analysis and spectral overlap of lignin functionality still exists, HSQC is widely used for structural identification and estimation of the relative abundance of inter-unit linkages in lignin, such as S/G ratios.[71]

Furthermore, ^{31}P NMR is a rapid analysis tool to quantify the hydroxyl functionalities in lignin with its "selective tag", through phosphitylation with ^{31}P containing TMDP (2-chloro-4,4,5,5-tetramethyl-1,3,2-dioxaphospholane), as shown in Figure 18.[46a] This method demonstrates a unique advantage in measuring lignin hydroxyls within a single spectrum, providing quantitative information for various types of major hydroxyl groups in a relatively short experimental time with small amounts of sample (Figure 19).[72] Hydroxyl groups in lignin, including aliphatic, carboxylic, guaiacyl, syringyl, C_5-substituted phenolic hydroxyls, and p–hydroxyphenyls are among the most important functionalities that influence lignin physical and chemical properties. These functional groups exhibit a prominent role in defining reactivity of lignin, such as the cleavage of inter-unit linkages, oxidative degradation, and re-polymerization (condensation) reactions during various treatment processes.[35b, 46b, 73] The ^{31}P NMR method has been shown to be very effective for determining the presence of hydroxyl groups to provide the precious information about the structural change occurred in lignin.

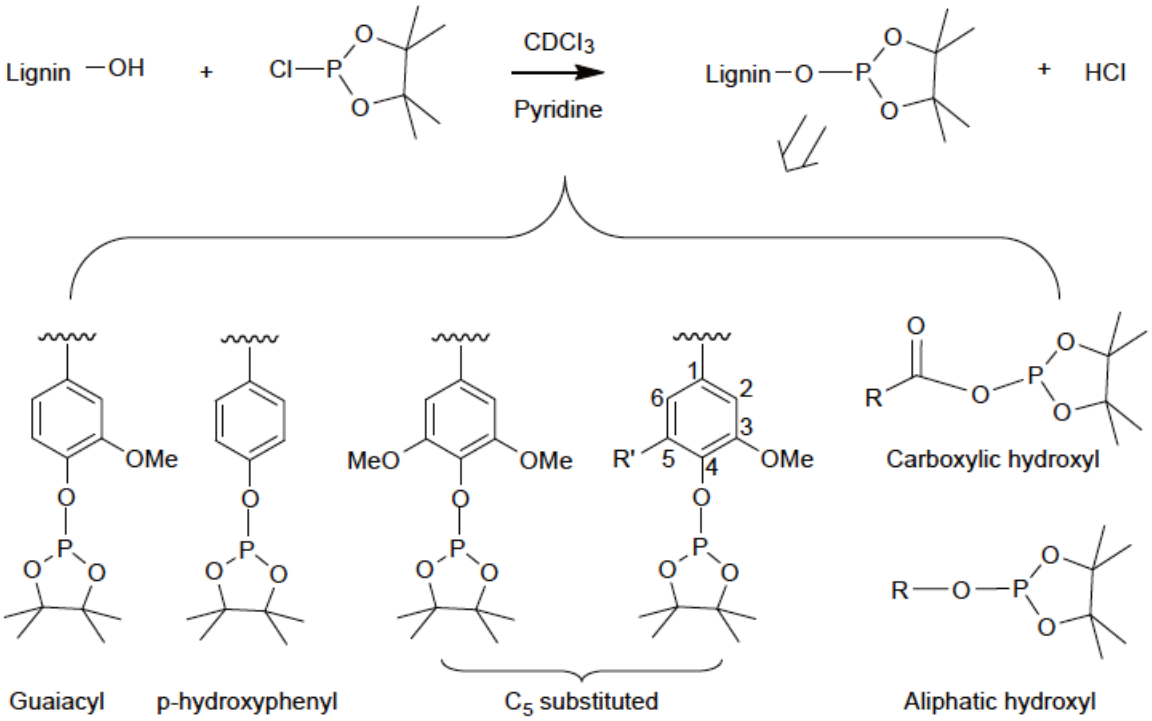

Figure 18 Reaction of labile hydroxyls present in lignins with 2-chloro-4,4,5,5 tetramethyl-1,3,2-dioxaphospholane.[46a] R: Lignin side-chain; R': lignin unit.

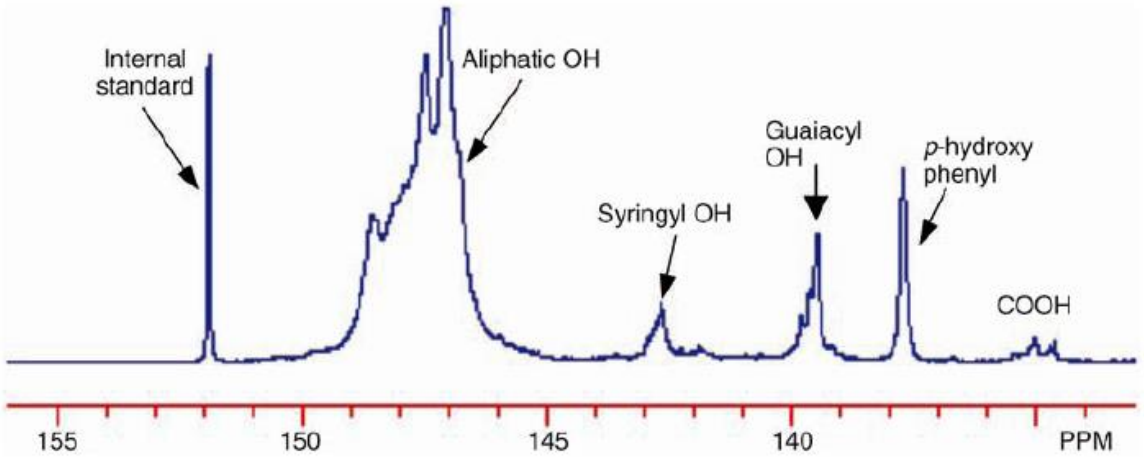

Figure 19 Quantitative ^{31}P NMR spectrum of a softwood lignin derivatized with TMDP using N-hydroxy-5-norbornene-2,3-dicarboximide as internal standard.[46a]

2.2.4 Lignin-carbohydrate Complex

Hemicelluloses are covalently linked by relative hydrophobic lignin and thereby form those cross-links that are also called lignin-carbohydrate complexes (LCCs) with heterogeneous structures. LCCs are presumed to exist in higher molecular weight lignin fractions which are water insoluble. LCCs in hardwood and grass are composed in part from 4-O-methylglucuronoxylan and arabino-4-O-methylglucuronoxylan, respectively.[74] In contrast, carbohydrate portions are mainly composed of galactomannan, arabino-4-*O*-methylglucuronoxylan, and arabinogalactan, all of which linked to lignin at benzyl positions for LCCs in softwood.[75] Those LCCs consist of phenyl glycoside bonds, esters, and benzyl ethers as summarized in Figure 20.[76]

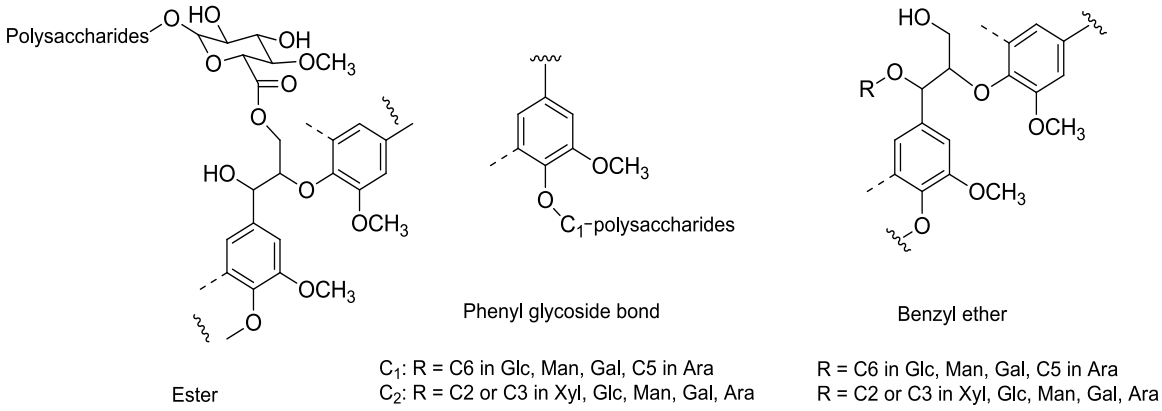

Figure 20 Proposed types of lignin carbohydrate linkages.[76]

2.3 Biomass Recalcitrant Factors

Structural sugars are stored as cell wall polysaccharides as a common energy source. Millions of years of evolution have honed the chemical and molecular features of plant

cell wall to protect those sugars. This inherent capability of lignocellulosic biomass to resist enzymatic and microbial deconstruction referred to biomass recalcitrance.[77] Improving the understanding of the origins and mechanisms of biomass recalcitrance is important to advance the conversion of large-scale lignocellulosic biomass. Enzymatic hydrolysis is influenced by both structural features of substrate and the mode of enzyme action. Several substrate related factors are believed to contribute to this recalcitrance, such as the structure and content of lignin, acetylated hemicelluloses, LCCs, cellulose crystallinity , degree of polymerization, pore size/volume, and specific surface area of cellulose.[18]

2.3.1 Cellulose Related Factors

The main purpose of enzymatic hydrolysis is to deconstruct cellulose and related carbohydrate polymers to fermentable sugars that can be further converted to valuable biofuels and biochemicals such as bioethanol and/or biobutanol, through biological or chemical approaches. Although bioconversion of cellulose is complicated by existence of other components and derivatives after pretreatment, it is essential to understand the effects of key features of cellulose itself on the effectiveness of enzymatic hydrolysis.

2.3.1.1 <u>Cellulose Crystalline Allomorphs Factor</u>

Cellulose can be taken as a composite material that is built from nano-scale microfibrils due to inter/intra molecular hydrogen bonding. These hydrogen bonds hold the network flat and allow stacking of cellulose chains. Those microfibrils are insoluble cable-like structures that are typically composted of about 36-chain model of cellulose elementary

fibril, each of which contains between 500 and 14000 β-1,4-linked glucose molecules.[19b, 78] Cellulose contains crystalline and amorphous regions (as shown in Figure 9 and Table 1), the latter have been reported to be subjected to a faster decrease as a function of enzymatic hydrolysis time.[36a] Although there is debate in considering cellulose crystallinity as a key inhibitory factor affecting efficient hydrolysis, cellulose crystallinity played a role in enzyme adsorption that can be correlated with hydrolysis rates and yields. It has been reported that enzyme adoption, including complete glycosyl hydrolase system, cellulose binding module and individual enzyme components, declined as cellulose crystallinity increase. Increased hydrolysis rates and yields were shown to be related to the higher capacity of amorphous cellulose than crystalline part for enzymes.[79] Furthermore, it has been recognized that various crystalline allomorphs of cellulose have different effects on enzymatic hydrolysis.[80] Comparison of the digestibility of amorphous cellulose and all four crystalline allomorphs (I, II, III and IV) indicated that the initial digestion rates were followed interesting order: amorphous > III_I > IV_I > III_{II} > I > II. Some interesting study also indicated that hydrolysis rate of cellulose II hydrate form was much faster than I and II because of its slightly (8.5%) expanded structure.[81] The amorphous cellulose obtained 10-fold hydrolysis rate as that of cellulose I due to the 4-fold higher gross specific surface area compared to the cellulose I.[82] Study also found the enzymatic hydrolysis rate of alga cellulose and derived forms was in an order of III_I >> I_α > I_β, which was attributed to the reduced crystallinity, lower packing density, and greater distances between hydrophobic surfaces of cellulose III_I than cellulose I. Moreover, 0.02 Å shorter in the distance of hydrophobic surface along with smaller 4 $Å^3$ in the volume of cellobiose unit of I_β than I_α were found to result in the lower hydrolysis behavior of

cellulose I_{β}.[83] An additional source of confusion is related to the measurement of cellulose crystallinity and structural alteration with various techniques, such as XRD, solid state ^{13}C NMR, IR and Raman spectroscopy, based on different operating principles and different physical characteristics that generate various crystalline indices. These technique related variation in crystallinity can be further compounded by the necessity of sample preparation, the effect sample preparation has on crystallinity and new analysis methods such as using sum-frequency-generation vibration spectroscopy that selectively detects crystalline cellulose in lignocellulosic biomass.[84]

2.3.1.2 Cellulose DP Factor

The degree of polymerization (DP) and molecular weight refer to the number of monomeric units in the cellulose chain. Although several studies have investigated the change in DP as a function of enzymatic hydrolysis with cellulose, its role is still under debate. However, the recognition required for the binding of cellulose components to cellulose chains is highly connected to the chain length. It has been found the greater the number of reducing ends in cellulose, the higher the rate of hydrolysis by exoglucanase is.[85] When the focus is concentrated on the changes in cellulose DP before and after pretreatment and the effect of DP on enzymatic deconstruction of cellulose, it can be found shorter chains enable cellulose to be more amenable to enzymatic digestion due to the weaker hydrogen bonding network formation.[86] Research focused on the enzymatic hydrolysis of organo-solv-pretreated softwood shows that similar to cellulose crystallinity, any single observed substrate characteristics including cellulose DP and fiber length have

little effect on cellulase adsorption and the following behavior of enzymatic hydrolysis, because synergistic effects must also be considered.

2.3.1.3 Cellulose Accessibility Factor

Cellulose accessibility to cellulase is limited by the structure of cellulose microfibrils. Crosslinking among chains of cellulose fibers that are further embedded in a matrix of hemicelluloses and lignin, provide extra rigidity in native plant cell walls but complexity for enzymatic digestion. The combination of cellulase size and shape with respect to the cell wall three-dimensional structure determines if the bonds in cellulose are accessible to enzymatic attack.[19b, 77] Enzymatic hydrolysis of cellulose is believed to be a surface reaction, accessible surface area of cellulose for cellulase attack should be one of the most influential structural features of biomass that affect cellulase adsorption on the cellulose surface and subsequent enzymatic breakdown.[87] Enzymatic available surface area is greatly related to biomass particle size, porosity, pore volume, cellulose de-polymerization, and the relative amount of exposed hydrophilic crystalline cellulose faces. However, debate still exists in making the critical distinction among those factors. Particle size did little to account for the interior surface area in highly porous of biomass.[88] The internal surface area of biomass has been estimated as much as 1 to 2 orders of magnitude greater than the external surface area. External surface area is mainly described by particle size or diameter; however, specific surface area is also governed by the size of the lumen and capillaries as well as voids and cracks that are localized in the lignocellulosic matrix, existing on a wide length-scale from nano to millimeter.[24, 89] Moreover, the relative amount of exposed hydrophilic crystalline cellulose faces also

limit the enzyme accessible surface area that can be interpreted by the binding mechanisms of cellulase binding modules, which are driven by both chemical and structural recognition to cellulose crystallite surfaces, consistently attaching to the two "hydrophobic" planar faces of the cellulose crystal.[90]

There are several methods which can be used to determine the accessible surface area. The classic techniques to measure the specific surface area is the Brunauer–Emmett–Teller (BET) method using nitrogen adsorption, but it requires prior drying of the substrate that makes it less effective due to water removal from non-rigid porous materials could produce partial irreversible collapse of pores.[91] One direct method to measure the accessibility is monitoring the adsorption of fluorescently tagged carbohydrate-binding modules (CBMs); however, the presence of lignin can skew results due to non-specific binding. An alternative approach to examining pore size employs direct dyes, such as Simons' stain as a potentially useful semi-quantitative method for estimating the total available surface area of lignocellulosic substrates.[92] In addition, cellulose accessibility can be assessed by solute exclusion based on the accessibility of different sized solute molecules, such as differential scanning calorimetry (DSC) based on the principle that water contained inside pores has a lower freezing point than that of bulk water, NMR relaxometry, water or gas adsorption, small angle X-ray scattering, and mercury porosimetry.[19a, 93]

2.3.2 Hemicellulose Related Factors

The enzymatic digestion of cellulose has been shown to significantly improve with hemicellulose removal, since hemicellulose is known to coat the cellulose microfibrils in the plant cell wall and form a physical barrier to access by enzymes.[94] Removal of hemicellulose is also associated with the breakdown of the cross-linked polysaccharides and LCCs. It has been found the addition of hemicellulase during enzymatic digestion of pretreated biomass has been proved to substantially increase cellulose hydrolysis, because the hydrolysis of hemicelluloses consequently improved the access of cellulase to cellulose.[95] Although it is still debatable if hemicellulose removal or the breakdown of the crosslinked network of polysaccharides and bonds among them is responsible for enhanced digestion of cellulose in pretreated substrates, it is much easier to remove from the cell wall and its removal seems to have less effect on the accessibility of cellulose than lignin removal.

Acetyl group in hemicellulose has been considered as one of the inhibitory components to resist the enzyme hydrolysis. Hemicelluloses backbone is extensively acetylated with acetyl groups amounting to about 1 to 6 % of the biomass substrate depending on various plant species and origins.[96] There is not much evidence as to if selective hemicellulose removal or deacetylation impact cellulase adsorption. However, research indeed found acetic acid pulp obtained by acetosolv delignification showed much poor enzymatic digestibility than organo-solv ethanol pulp because of the acetylation of cellulose during acetic acid delignification. In contrast, the remove of acetyl groups by saponification recovered the enzymatic hydrolysis of the pulp.[97] Acetyl groups in pulp might restrict

cellulase accessibility to cellulose by inhibiting productive binding, which might be caused not only by increased diameter of cellulose that increases the steric hinderance of enzymes but also by increased changed hydrophobicity.[97] Although cellulose digestion has been a major consideration for pretreatment design and optimization, significant portion of sugars from hemicellulose is also essential to maintain the hemicellulose in either a solid or soluble form during pretreatment to maximize sugar recovery for fermentation.

2.3.3 Lignin Related Factors

Lignin is one of the most important factor that limits the rate and extent of enzymatic hydrolysis of biomass due to its phenolic chemical structure and physical distribution.[98] Lignin not only reduces the accessibility of cellulose to enzymes by covering cellulose fibrils and restricting fiber swelling[99] but also causes recalcitrance through chemical means by irreversibly binding cellulase enzymes and preventing further enzymatic activity on cellulose.[100]

Direct physical contact between enzyme and substrate is essential during enzymatic hydrolysis. Diffusion of enzymes from the bulk aqueous solution to the substrate surface could be inhibited by irreversibly entrapping enzymes within the three dimensional matrix of lignin that significantly reduced the enzyme-cellulose interactions.[101] Further, the removal of lignin increases the porosity of pretreated pulps and consequently improved enzymatic hydrolysis. Those pores created by removal of lignin and/or hemicellulose leave cellulose substrates more accessible and open for enzymes.[98, 102] This

lignin barrier depends on the content of lignin, distribution, and macromolecular structure of lignin. Microscopic techniques reveal a range of lignin droplet morphologies as the temperature of a thermochemical pretreatment reaches above the range for lignin phase transition. This is because lignin was caused to coalesce into larger molten bodies that migrate within and out of plant cell wall, and can redeposit on the surface of cell wall.[103] Higher S/G (syringyl:guaiacyl) lignin ratios was found to result in higher sugar release after investigating the correlation between S/G ratio and the enzymatic hydrolysis efficiency among 47 extreme phenotypes of *Populus trichocarpa* trees.[104] It is believed S-rich lignin features predominantly linear chains with less cross-links than G-rich lignin, because the latter have no C-5 occupied methoxyl groups. Therefore, more branched guaiacyl units in lignin are prone to distribute as a surface barrier restricting the swelling of the cellulosic substrate and reducing the accessible surface area to enzymes.[105] Besides, LCCs has been shown to inhibit the availability of enzymatic hydrolysis of carbohydrates by limiting the action of CBH II, which attacked the cellulose chain from the non-reducing ends that was occupied by LCCs linkages.[106] The steric hindrance of various cross-links between lignin and polysaccharides is a non-negligible obstacle for the adsorption of enzymes.

Decline of hydrolysis efficiency results also from the nonproductive adsorption of enzymes onto lignin preventing their access to carbohydrates. This adsorption is attributed to the hydrophobic interaction and/or ionic-type interaction.[107] Hydrophobic interaction aggregates non-polar molecules together to reduce the surface area exposed to water and minimize the disruption of hydrogen bonds in solution. Furthermore, presence

of charged functional groups (e.g. COOH, OH) in both lignin and enzyme surfaces can build ionic-type lignin-enzyme interactions.[107b] However, those negative charges formed under hydrolysis conditions might decrease enzyme binding by electrostatic repulsion.[108]

In addition, soluble lignins were found to negatively affect microorganisms and enzymes due to phenolic compounds such as vanillin, syringaldehyde, trans-cinnamic acid and hydroxybensoic acid.[19b] Study has found the mixture of Spezyme CP and Novozyme 188 is largely inhibited by vanillin along with hydroxybenzoic acid.[109] Acid containing soluble lignins p-coumaric acid and gallic acid exhibit 38 and 47 % degree of inhibition on the original activity of xylanase XynA, respectively.[110] The formation of phenolic radicals due to the oxidation generates polymerization between enzyme and lignin which may deactivate enzymes.[111]

2.4 Pretreatments

Pretreatment process in lignocellulosic biomass involves the structural breakdown of the cross-linked matrix of hemicelluloses and lignin, disrupting hydrogen bonds in crystalline cellulose, altering and redistributing structural components, increasing cellulose accessibility, and thereby resulting in the reduction of biomass recalcitrance for subsequent enzymatic hydrolysis. Although the pretreatment process is considered as one solution for producing lignocellulosic bioethanol with low costs and high productivity, there is no universal pretreatment process to date because of the complexity of various biomass feedstocks. A large number of pretreatment techniques have been investigated on a wide variety of feedstock types, which are typically divided into physical (grinding

and milling, microwave and extrusion), chemical (alkali, acid, organo-solv, ozonolysis and ionic liquid), physicochemical (steam explosion, liquid hot water, ammonia fiber explosion, wet oxidation and CO_2 explosion) and biological applications (using microorganisms such as fungi can selectively degrade lignin and/or hemicellulose).[2, 112] Pretreatment methods have to be selected based on the substrate and the desired end-product balancing with economic value. In this review, the selected cost-effective and leading pretreatment techniques are briefly discussed: dilute acid pretreatment, hydrothermal pretreatment, lime, and organo-solv pretreatment.

2.4.1 Dilute Acid Pretreatment

Dilute acid pretreatment (DAP) typically employs 0.4−2 % H_2SO_4 (or hydrochloric acid, nitric acid, phosphoric acid and peracetic acid) at temperature ranging from 160 to 220 ℃ to significantly reduce lignocellulosic recalcitrance. DAP is one of the most important chemical pretreatment techniques because of its high sugar yields in enzymatic hydrolysis of cellulose along with hemicellulose solubilization and recovery. It has been successfully applied to a wide range of feedstocks, including softwoods, hardwoods, herbaceous crops, and agricultural residues.[113] There are general two types of DAP processes, including a high-temp (T > 160 °C) continuous-flow process for low solids loadings (5−10 wt. %) and a low-temp (T < 160°C) batch process for high solids loadings (10−40 wt. %).[20a] The advantage of DAP is the solubilization of hemicelluloses and disruption of lignin structure, making the cellulose more easily accessible for the enzymes. There is however a risk on the formation of volatile degradation products [114] and the pseudo-lignin that is generated from carbohydrates without significant

contribution from lignin during dilute acid pretreatment, especially under high severity pretreatment conditions.[115] Table 7 summarizes DAP results for different lignocellulosic substrates.[55f, 116]

Table 7 Summary of DAP conditions for different substrates. [55f, 116]

Substrate	Acid	Temperature (℃)	Time (min)	Cellulose conversion yield after cellulase treatment (%)
Corn stover	2.0% H_2SO_4	121	120	75.6
	2.0% H_3PO_4	121	120	56.0
Sugarcane bagasse	50.0% Peracetic acid	80	120	80.0
Cotton stalk	2.0% H_2SO_4	121	60	23.9
Aspen	0.25% H_2SO_4	175	30	42.3
	1.10% H_2SO_4	170	30	88.0
Switchgrass	0.50% H_2SO_4	175	40	26.3
Sweet sorghum bagasse	1.0% H_2SO_4	180	20	55

In order to yield low inhibition compounds and hemicelluloses recovery, it is necessary to optimize the pretreatment condition which is mathematically represented as the combined severity factor [94a] (CS) calculated as:

$$R_0 = t \bullet \exp[(T_H - T_R)/14.75]$$

$$\log CS = \log R_0 - pH ,$$

where R_0 is the severity factor, t is the reaction time in minutes, T_H is the hydrolysis temperature in ℃, and T_R is a reference temperature. Xylan-rich hemicelluloses could be hydrolyzed to fermentable sugars; in contrast, glucomannan is relatively stable under the

acidic conditions.[114] It has been demonstrated that lower combined severity accumulates released xylan in the liquors in the form of xylose, whereas at higher combined severity the releases xylan is partially converted to furfural.[117] Although DAP achieves high xylose conversion yields from xylan, undesired by-products such as furfural, formic acid, acetic acid, and uronic acid are inevitably formed from hemicelluloses under high severity conditions (Figure 21).[112a] Besides, the re-polymerization (condensation) of lignin under DAP becomes more pronounced at higher combined severity factor. It has been observed that the formation of spherical droplets on the surface of residual plant cell wall during DAP at high temperature.[118] Further studies also revealed that lignin becomes fluid and then coalesce to form droplets within the cell wall matrix when the lignin phase transition temperature is reached. The hydrostatic pressures within the cell wall layers force a fraction of this lignin to the outer face, which in turn contacts with the pretreatment bulk and deposits back onto the plant cell wall surface during DAP.[115, 119] Recently, Hu et al. found further rearrangements of furfural and/or HMF can produce aromatic compounds, and further polymerization and/or polycondensation reactions converted those aromatic compounds to pseudo-lignin. Therefore, the formation of pseudo-lignin during pretreatment is unfavorable because it comes from carbohydrate degradation and more importantly it could be detrimental to enzymatic hydrolysis of cellulose just like native lignin.[120] Therefore, the following research strategy needs to be tailed to facilitate the hemicelluloses recovery and suppression of pseudo-lignin formation along with the largest enhancement of glucose sugar yields.

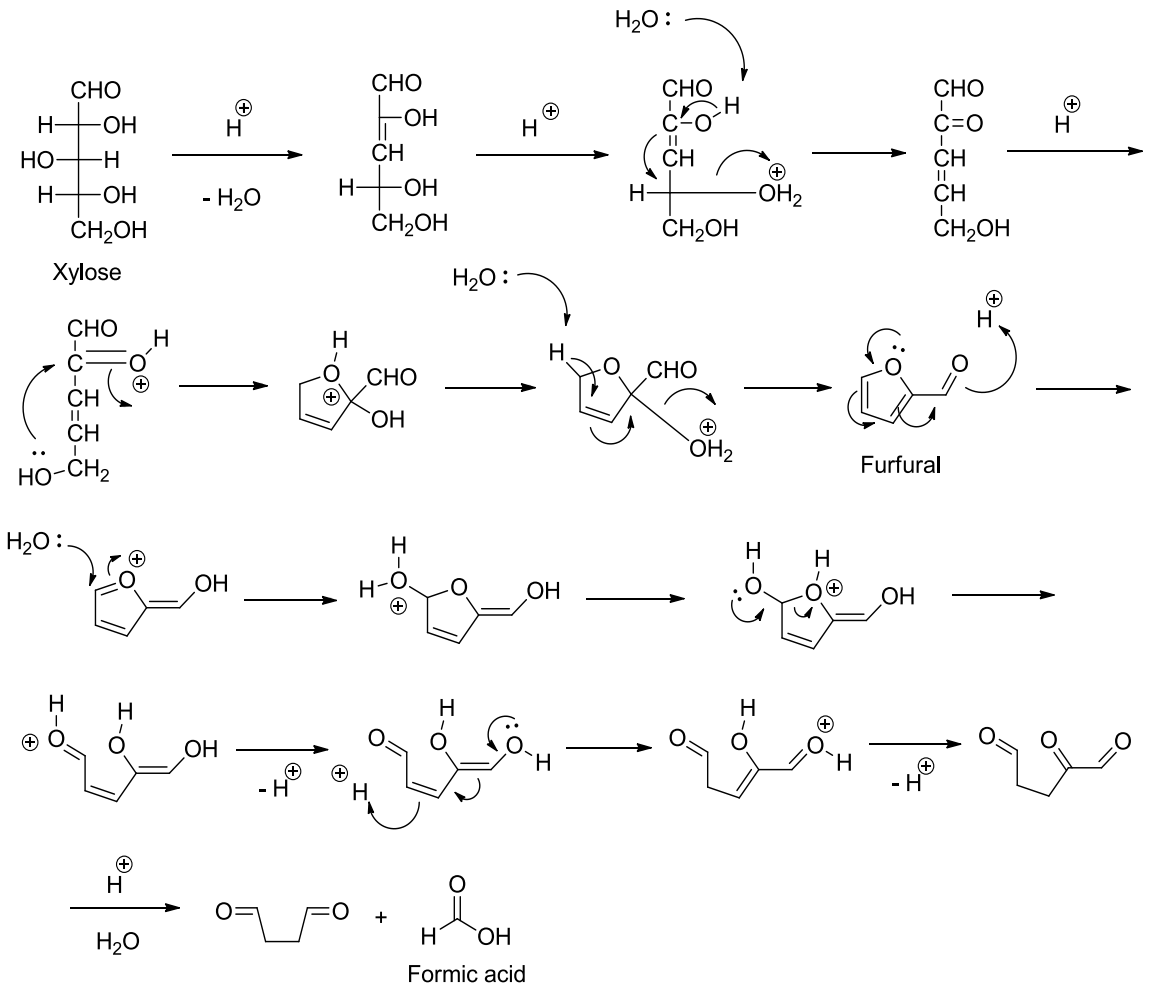

Figure 21 Proposed mechanisms of the formation of furfural and formic acid from xylose under hydrothermal condition.[112a]

Effect of DAP on cellulose feature changes has been investigated in order to discover the chemistry of cellulose before and after DAP. The reduction of molecular weight of cellulose caused by DAP is an acid-catalyzed and thermally accelerated chain scission mechanism.[30] Study reveals that the reaction occurs within the fibril structure from within either a crystalline or amorphous region of cellulose. This process consists of two major stages, including an initial rapid hydrolysis of the more solvent accessible amorphous region, and a latter much slower hydrolytic attack of the crystalline portion.[121] In terms of

crystallinity, many researchers have found that DAP caused an increase in crystallinity index (CrI), which could result from hydrolyzation of cellulose and subsequent solubilization of glucose. In general, the crystallinity of cellulose increases throughout the process of DAP as summarized in Table 8.[30-31, 35b, 49b, 116f, 122] Para-crystalline content of cellulose from poplar and switchgrass was observed to increase during DAP by solid-state ^{13}C CP/MAS NMR studies, which suggests that the increase in crystallinity and para-crystalline percentage could be primarily attributed to localized hydrolyzation and removal of amorphous cellulose. The more solvent accessible amorphous regions are more prone to degradation during pretreatment at higher temperature because cellulose hydrolysis is thermally accelerated.[30] In addition, hydrothermal conditions in DAP could promote cellulose annealing of cellulose I_α into cellulose I_β crystal, which is due to the metastable properties of the triclinic one-chain crystal structure of cellulose I_α.[123] Sannigrahi et al. have observed a large increase in the relative proportion of cellulose I_β accompanied by a decrease in the relative proportions of both cellulose I_α and para-crystalline region during DAP. This suggests that cellulose crystalline allomorphs could also be affected by the types of lignocellulosic biomass and specific pretreatment conditions during DAP.[35b]

Table 8 Crystallinity index (CrI) before and after DAP for various substrates.[30-31, 35b, 49b, 116f, 122]

Biomass	CrI (%) before DAP	CrI (%) after DAP
Poplar	49.9	70.5
Corn stover	50.3	52.5
Loblolly pine	62.5	69.9
Sugarcane bagasse	42.6	63.0
Rice Straw	57.0	65.0
Switchgrass	44.0	52.0

2.4.2 Hydrothermal Pretreatment

Hydrothermal pretreatment also called auto-hydrolysis or hot water pretreatment (e.g., 160-260 ℃ corresponding pressure 0.69-4.83 MPa for several seconds to a few minutes) is another promising pretreatment process due to several potential advantages including no requirement for catalysts, no corrosion of the equipment and low yield of the inhibition compounds.[8] Under hydrothermal condition water acts as a weak acid and releases the hydronium ion that further depolymerizes hemicelluloses by selective hydrolysis of glycosidic linkages, liberating *O*-acetyl group and other acid moieties from hemicellulose to form acetic and uronic acids. Further hydrolysis reaction occurs by those organic acids generated from functional groups associated with hemicelluloses at high temperature, and thereby results in the breakdown of more glycosidic linkages in hemicelluloses and the β-O-4 ether bonds in lignin, solubilizing in liquid fraction. Hydrothermal pretreatment can be performed in co-current, countercurrent or flow-through reactors, of which co-current process heats the water-lignocellulosics slurry to pretreatment conditions during the required residence time, the countercurrent process

allows the water and lignocellulosics flow in the opposite directions, and the flow-through process allows hot water flows through a stationary bed of lignocellulosics.[124] This alternative processes offer some additional advantages such as higher ethanol yields with lower enzyme dosages during subsequent enzymatic cellulose hydrolysis. Table 9 summarizes hydrothermal pretreatment results for different substrates from literature.[125]

Table 9 Hydrothermal pretreatment results for different substrates.[125]

Substrate	Cellulose conversion yield (%)	Pretreatment conditions	Enzymes loadings	
			Cellulase from Celluclast 1.5 L (FPU/g)	β-glucosidase from Novozyme 188 (IU/g)
Wheat straw	95.8 in 72 h	200 ℃, 40 min	15	15
	87.5 in 72 h	195 ℃, 20 min	15	15
	81.2 in 72 h	195 ℃, 40 min	15	15
Switch-grass	77.4 in 48 h	200 ℃, 10 min	49	40

2.4.3 Lime Pretreatment

Alkaline pretreatments have drawn much attention as another major chemical pretreatment technique besides DAP, because the whole process is normally a delignification process and more effective on hardwoods, herbaceous crops and agricultural residues with relatively lower lignin content.[126] The efficiencies heavily depend on the reaction temperature, pretreatment time, and alkali loading. In addition to its limitations such as the conversion of alkali into slats and capital cost of recycling alkali, there are multiple process advantages including lower action temperatures and pressures, reuse of residual alkali, and no need for complicated reactors along. [20a, 126]

Lime is one of the major chemicals applied to alkaline pretreatment of lignocellulosics because it is inexpensive and easier recovery by using carbonated wash water.[127] The general process of lime pretreatment involves slurrying the lime with water, spraying it into the biomass material and storing the material in a pile for a period of hours to weeks based on various temperatures applied. Lime has been proven to successfully increase cellulose conversion yield of lignocellulosics and it works remarkably better than sodium hydroxide as summarized in Table 10.[128] The enzymatic hydrolysis of lime-pretreated biomass is affected by structural features resulting from the treatment,[129] including the extents of acetylation, lignifications and crystallization as summarized in Table 11.[31a, 116e] Chang et al. have investigated the correlations between enzymatic hydrolysis and structural factors and reported that high digestibility can be obtained by extensive delignification as a result of lime pretreatment; initial hydrolysis rates can be affected by crystallinity but with less effect on ultimate sugar yields; delignification and deacetylation can remove parallel barriers to enzymatic hydrolysis.[130] This indicates lime pretreatment can play a significant role in increasing access to the remaining polysaccharides and eliminating the nonproductive adsorption of cellulases by removing all of the acetyl groups with reduction of lignin content.

Table 10 Summarized lime pretreatment results for different substrates.[128]

Biomass substrates	Pretreatment conditions	Cellulose conversion yield after cellulase treatment (%)
Corn stover	55 ℃, 0.073g $Ca(OH)_2$/g raw biomass, 4 weeks	98 in 96h
Corn stover	120 ℃, 0.075g $Ca(OH)_2$/g dry biomass, 4h	88.0 in 7 days
Switchgrass	120 ℃ 0.1g $Ca(OH)_2$/g dry biomass, 2h	60 in 72 h
Jatropha curcas	100 C, 0.1g $Ca(OH)_2$/g raw biomass	68.9 in 48h

Table 11 Cellulose crystallinity changes before and after lime pretreatment. [31a, 116e]

Biomass substrates	Pretreatment conditions	CrI (%) before pretreatment	CrI (%) after pretreatment
Sweet sorghum bagasse	121 ℃, 1.5% lime, 1 hr	71.4	62.3
Poplar	65 ℃, 0.5:1 $Ca(OH)_2$ to biomass, 4 weeks	49.9	54.5
Corn stover	55 ℃, 0.5:1 $Ca(OH)_2$ to biomass, 4 weeks	50.3	56.2

2.4.4 Organo-solv Pretreatment

Organo-solv pretreatment refers to the process to treat lignocellulosic feedstocks in organic solvents (e.g. methanol, ethanol, acetone, ethylene glycol, triethylene glycol and tetrahydrofurfuryl alcohol) with/without added catalysts (e.g. HCl, H_2SO_4, oxalic acid, acetylsalicylic acid and salicylic acid) in temperature ranging from 100 to 250 ℃.[131] The organo-solv process involves simultaneous prehydrolysis and delignification of lignocellulosic biomass with the help of organic solvents and acidic solutions. It removes extensive lignin and hemicelluloses, and thereby increases accessible surface area and pore volume. The main reaction involved in lignin degradation and dissolution is the hydrolysis of the internal bonds in lignins as well as lignin-carbohydrates bonds, such as 4-O-methyglucuronic acid ester bonds to the α-carbons of the lignin unites.[132] The disruption of cellulose along with the de-polymerization and change in cellulose crystallinity strongly depends on the species of organic solvents, concentration and temperature.[86b, 133] However, organic solvent need to be separated due to its inhibition role at downstream enzymatic cellulose hydrolysis and can be reused due to the high

commercial price of solvents. Table 12 summarizes cellulose conversion of various lignocellulosic substrates after organo-solv pretreatment.[133-134]

Table 12 Organo-solv pretreatment results for different substrates.[133-134]

Substrate	Pretreatment conditions	Enzymes loadings		Cellulose conversion after cellulase treatment (%)
		Cellulase (FPU/g)	β-glucosidase from Novozyme 188 (IU/g)	
Poplar	180 ℃, 1.25% H_2SO_4, 50% ethanol, 60min	20	40	93 in 24 h 97 in 48 h
Switchgrass	180 ℃, 3:1 (v/v) ethanol/water ratio, 0.99% (w/w) H_2SO_4, 60min	20	40	~70 in 8 h ~98 in 72 h
Miscanthus	170 ℃, 0.8 ethanol/water ratio, 0.5% (w/w) H_2SO_4, 60min	20	40	98 in 48 h
Loblolly pine	170 ℃, 65% ethanol, 1.1% H_2SO_4, 60min	8	16	70 in 80 h
Olive tree	180 ℃, 43% ethanol, 15min	15	15	89.6 in 72 h

2.5 Lignocellulosic Biomass for Biomaterials

In addition to the biofuel production from plant cellulose and hemicellulose, manufacture of biomaterials from lignocellulosic biomass is also essential to the functioning of industrial societies and critical to the development of a sustainable global economy. Although wood and paper products have already played an important role in the evolution of civilization, there is increasing interest in the improvement of the quality and manufacturing efficiency of high performance lignocellulosic composites. As main

biopolymers in plant cell wall, cellulose and hemicellulose along with their derivatives such as cellulose esters, silyl celluloses, cellulose sulfonates, aminocelluloses, cellulose nanowhiskers, have been widely and successfully applied to the practical products including novel film, foam, coating systems membranes, pharmaceuticals, cosmetics, and food.[135] However, lignin as the second most abundant biopolymer on earth after cellulose is still underutilized in related fuel and material projects.[57] Although lignin combustion helps the papermaking chemical recovery process, as a fuel it is very inefficient, processing less than ¼ as much energy per pound as middle distillate fuels.[136] Therefore, new processes are needed to generate value-added products from lignin. In this review, the lignin will be briefly discussed in the manufacturing of high performance carbon fiber.

2.5.1 Practical Lignin Isolation from Lignocellulosic Biomass

There are several practical methods for isolating lignin from biomass for large-scale utilization. Chemical pulping processes (sulfite and Kraft processes) produce lignosulfonate and Kraft lignin in the cooking liquor as residue in order to obtain the polysaccharide component and/or produce plant fiber with uniform characteristics. Furthermore, ethanol organo-solv lignin (EOL) acquired during pretreatment is also one of the most promising future lignin resources.[21a] The lignin isolated by known methods (physical, chemical or enzymatic treatments) is a mixture of degraded or solubilized lignin from various morphological regions, which inevitably altered the chemical structure of lignin to different extents compared with native lignin.

2.5.1.1 Lignin from Kraft Pulping

The purpose of wood pulping is to remove lignin from woody and/or non-woody biomass with plant fiber left for paper production. The pulp and paper industry has probably the highest quantity of underutilized lignin in the form of black liquor (BL) with worldwide production reaching 50 million tons.[63b, 137] As the most dominant chemical pulping technique, Kraft pulping employs high pH and considerable amounts of aqueous sodium hydroxide and sodium sulfide to treat biomass (mostly wood chips) at an elevated temperature around 170 ℃ for about 2 h.[138] Afterwards, Kraft lignin is precipitated and isolated from the black liquor by acidification process, including initial precipitation as a sodium salt by reducing pH of liquor to 9-10 with carbon dioxide followed by a second purification step (e.g. suspending lignin in water and acidifying with H_2SO_4 to a pH lower than 3).[139] Alkaline pulping chemicals (OH^-, SH^-) could act as Bronsted bases initiating internal rearrangements that result in quinone methides and epoxides by internal nucleophilic reactions from neighboring hydroxyls, which are in turn prone to external nucleophilic attack. β-5 and β-O-4 structures can undergo reverse aldol reaction during Kraft pulping in case γ-OH is present, resulting in the formation of stilbene and enol-ether structures respectively that are recalcitrant to pulping.[63a, 64, 137, 140] As a result, the extensive cleavage of β-O-4 structures in Kraft pulping process yields a large number of phenolic end-groups in the dissolved lignin with the concomitant formation of partially degraded and partially modified side chains accompanied with a small amount of oxygenated carbons compared with native lignin as shown in Figure 22.[63a, 137, 140-141] As a dark-colored and water- and solvent-insoluble product, Kraft lignin can dissolve in alkali due to its high concentration of phenolic hydroxyl groups with a small number of

aliphatic thiol groups that give the isolated lignin a characteristic odor. Study on Kraft pine lignin reveals that its initial degradation occurs at temperature above 120 ℃, involving bond fragmentation in the phenyl propane side chains as evidenced by the formation of formic acid, formaldehyde, carbon dioxide, water. [142]

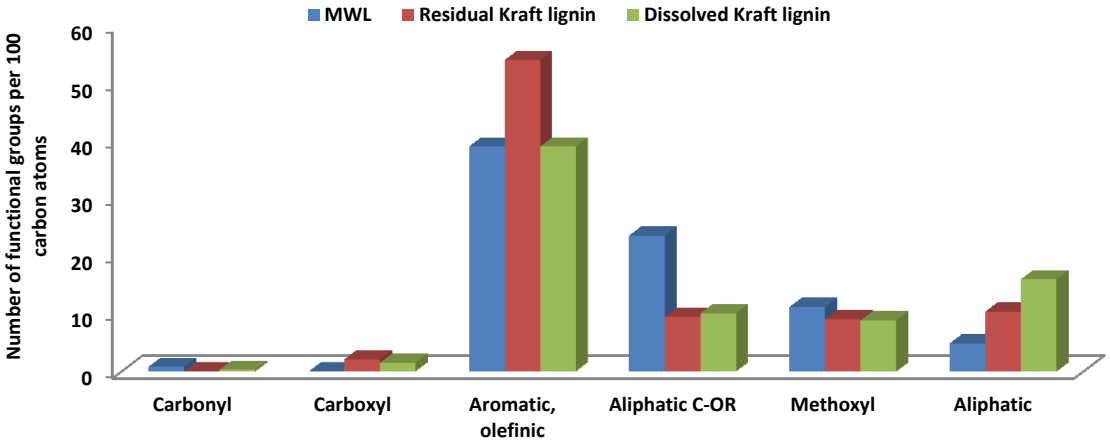

Figure 22 Functional groups in spruce MWL and in the residual and dissolved Kraft lignins. [54a, 119, 122-123]

2.5.1.2 Lignin from Organo-solv Pretreatment

As discussed in pretreatments part above, one role of organo-solv pretreatment in the conversion of biomass to biofuels (e.g. bioethanol) is to decrease hemicellulose and lignin content leaving cellulose more accessible. During pretreatment the hydrolyzed lignin is extracted into the organophilic phase then recovered as the filtrate, leaving the cellulose recovered as the solid residue and the hemicellulose in the water-soluble fraction as monomeric and oligomeric sugars.[143] The predominant substructures in lignin after organo-solv pretreatment are still β-O-4 linkages but with different levels of acid-

catalyzed cleavage of those ether linkages that is less than starting material.[62d, 73a] In-depth NMR analysis of ethanol organo-solv lignin (EOL) from loblolly pine showed that aromatic C-C bonds increase significantly, while the number of aromatic C-H bonds all decrease (C-6, C-5 and C-2), suggesting a more substituted lignin than native lignin as summarized in Figure 23.[73a] Moreover, comparing to other isolation methods, EOL is usually a high-purity, low molecular weight, narrow polydispersity, less condensed, sulfur free, and low ash content product with relatively narrow molecular weight distributions and low glass transition temperature, as summarized in Table 13.[64-65, 143-144]

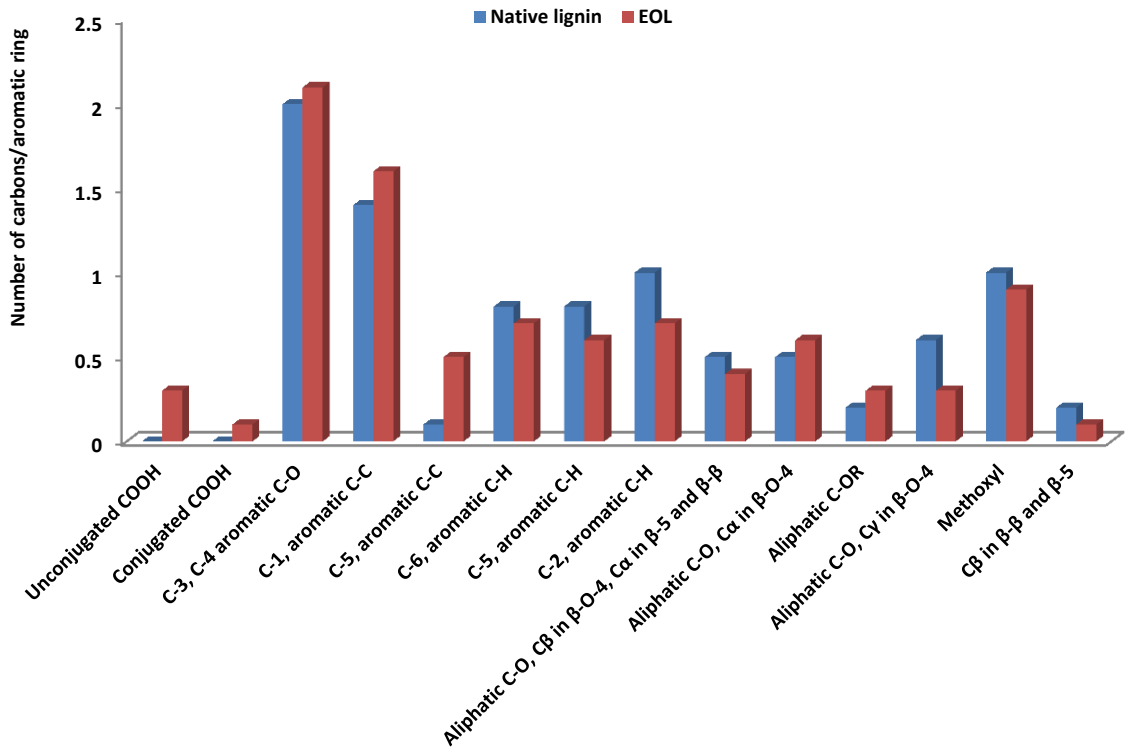

Figure 23 Effect of ethanol organo-solv pretreatment on loblolly pine lignin by ^{13}C NMR.[73a]

Table 13 Molecular weight properties and glass transition temperature of selected lignins. [56, 125, 127]

Isolation method	Substrates	M_w (g/mol)	polydispersity	T_g (℃)
Milled wood	Pine	11400	8.8	160
Kraft	Pine	4300	3.3	169
Organo-solv	Pine	1400	2.8	91
Acid Hydrolysis	Pine	40000	50	96
Organo-solv	Aspen	2100	3.5	97
Acid Hydrolysis	Aspen	10100	15.3	95
Steam Explosion	Aspen	2300	2.9	139
Milled wood and enzyme	Poplar	36000	4.1	171
Organo-solv	Poplar	1093	1.93	119-141

2.5.2 Lignin for Carbon Fibers

Lignin is the only large-volume renewable feedstock that is composed of aromatics.[145] Although very little of the effort focusing on converting lignin to commercial chemicals, materials, and fuels, the global development of energy-efficient light-weight vehicles as a promising lignin product platform draws more attention due to lignin's advantages over other precursors (e.g. polyacrylonitrile, pitches), including inexpensive and renewable sources, oxidative thermostabilization at potentially much higher rates than polyacrylonitrile.[57, 146] In the process of manufacturing carbon fiber from lignin, key steps contain preparation of a suitable lignin that is melt-spun into fiber under an inert atmosphere, fiber spinning and extrusion, thermostabilization and carbonization. The integrity of lignin during thermostabilization depends on its crosslinking capability in order to maintain the glass transition temperature T_g above the process temperature to thereby keep lignin fiber infusible. In the melt-spinning step lignin needs to be prepared

with a proper low-melt-flow temperature for melting spun without polymerization during extrusion, but a higher T_g for fiber stabilization to process at an acceptable rate.

Earlier study starting from 1960s developed several methods of forming fiber from lignin, including hardwood kraft, softwood kraft, and alkali softwood lignins, by both melt-spinning and dry spinning to produce carbon fiber, graphite fiber, and activated carbon fibers with tensile strength less than 1.0 GPa and diameter in the range of 10-40 μm.[147] Recently, there are several studies investigating the production of carbon fibers from lignin directed towards improving the melt-spinning of fiber and their conversion to carbon fiber at low cost, such as production of lignin carbon fiber without additives or chemical modifications before extrusion, co-extrusion and/or chemical modification of lignin carbon fiber before extrusion, manufacture of submicron carbon fibers from lignin. Kadla et al. carried out preparation of carbon fiber from three types of lignin (e.g. organo-solv kraft lignin, softwood kraft lignin and hardwood kraft lignin) under desalting process prior to extrusion, and found hardwood lignins were readily melt spun into fiber, but softwood lignin had low thermal stability and therefore crosslinked during extrusion. Alcell lignin gave fibers with strength of 0.388 GPa, 40 GPa modulus, 1.00% extensibility and 41.8% yield, and hardwood kraft lignin gave fiber with 0.422 GPa strength, 40 GPa modulus, 1.12% extensibility and 48.1% yield.[136] Although carbon fiber from subsequent lignin-polymer blends were not suitable for high-performance application, this research provided a straightforward access to activated carbon fibers.[148] Later studies focused on addressing the quality of lignin precursor and its purification, giving lignin-PET (polyethylene terephthalate) blend fibers up to 1.03 GPa tensile

strength with a Young's modulus 109 GPa.[149] More recently, a growing interest in preparing carbon fiber derives from lignin nanocomposite fibers with better mechanical properties compared to pure lignin fibers. Baker et al. explored the possibility of using carbon nanotubes to enhance the strength, modulus, electrical conductivity and thermal conductivity, of various lignins used to manufacture carbon fiber and revealed that the carbon nanotubes (multiwall) could be added in quantities as high as 15 wt % before fibers could not be melt-spun.[150] Eberle also reported a tensile strength of 1.2 GPa and a Young's modulus of 83 GPa for a carbon fiber prepared from softwood lignin.[151] Further studies have examined the possibility of lignocellulosic and liquid wood precursors, and suggested a novel process to polymerize liquid wood with addition of hexamethylenetetramine by soaking the extruded fibers in a solution containing formaldehyde and hydrochloric acid, giving the carbon fiber tensile strength of 1.7 GPa and modulus of 176 GPa.[152] The electrospinning of lignin to manufacture carbon nanofibers caused much interest, since they have great potential for use in separation, energy storage, and structural composite application because of their relatively high strengths, high specific areas and the ease of imparting morphological and chemical functionality.[153] For example, Hosseinaei and Baker used purified softwood kraft lignin by solvent extraction prior to electrospinning that gave a high T_g lignin (185 ℃) facilitating the electrospinning, oxidative thermostabilization and carbonization for manufacturing carbon nanofiber mats without additives, giving the fibers smooth surfaces without defects.[154]

The nature of lignin as well as the isolation method applied largely defines the properties of carbon fiber. In order to obtain high quality carbon fiber, lignin needs to be improved in several aspects, such as higher purity, lower softening temperature (T_s) at which liquid flow is observed under low shear, higher T_g to allow lignin fibers to undergo oxidative thermostabilization, and narrow molecular weight distribution to facilitate the uniform growth in molecular weight during oxidative thermostabilization that pave the way for uniform structure during carbonization. Structural analysis on the lignin carbon fiber has been carried out to understand the alternation of lignin biopolymer during various processes. The formation of rigid oxidized segments during thermal treatment of lignin was accompanied by an ordered structure formed at low temperatures (from 600 ℃) as a result of the better mobility of the smaller molecules.[155] Study also revealed more details about the structural changes in thermostabilization, including the increased oxygen content and the formation of carbonyl and carboxyl groups at heating rates of 0.11 to 1.0 K min^{-1}, which was followed by the formation of more C-C bonds at higher temperatures with decrease in the number of aromatic protons. An optimum heating rate could be predicted for the investigated lignin from a continuous heating transformation diagram.[155b] Foston et al. used NMR spectroscopy to monitor the structural changes occurring to hardwood Alcell lignin as a result of fiber devolatilization/extrusion, oxidative thermo-stabilization and carbonization, and found that demethoxylation and the appearance of carbonyl and carboxyl structures during stabilization, which were presumed to be formed by the generation of ester and anhydride groups through crosslinking reactions. A lower number of carbonyl and carboxyl structures were also observed at higher temperatures, but with the increase in the fractions of uncondensed

and condensed aryl carbon atoms.[156] This structural information can be used to not only improve processing conditions but also understand how the resulting structures in the carbon fiber may enhance the mechanical properties of lignin based composites. New chemical modifications of lignin and/or innovative biosynthesis strategies are needed to produce linear-fiber-forming lignin with controlled monomer ratios and chemical architectures that facilitate rapid chemical transformation to infusible mass and formation of planar graphitic structure during pyrolysis.[57]

CHAPTER 3

EXPERIMENTAL MATERIALS AND PROCEDURES

3.1 Materials

3.1.1 Chemicals and Materials

All chemicals were purchased either from Sigma-Aldrich (St. Louis, MO) or VWR (West Chester, PA), and used as received. All gases were purchased from Airgas (Radnor Township, PA). G8 glass fiber filter for carbohydrate analysis was purchased from Thermo Fisher Scientific (Madison, WI). Plastic pouch for holocellulose pulping was purchased from Kapak Corporation (Minneapolis, MN). Cellulase (Accellerase™ 1500, Lot number: 1681198062) and xylanase (Accellerase XY, Lot number: 4901131618) were generously provided by DuPont Industrial Biosciences (Palo Alto, California, United States).

3.1.2 Biomass Substrate

Hybrid poplar (*Populus trichocarpa x deltoides*) for biofuels research was obtained from Oakridge National Laboratory, TN. Logs were debarked, split with an axe, chipped (Yard Machines 10HP, MTD Products Inc., Cleveland, OH), and knife milled (Model 4 Wiley Mill, Thomas Scientific, Swedesboro, NJ) through a 1 mm screen size; all of these operations were performed at NREL. After one month of air-drying at NREL, the chips had a moisture content of approximately 5 wt%. The material was further milled through a 0.841- 0.177 mm screen to produce particles with diameters of 0.18 mm to 0.85 mm

(Thomas-Wiley Laboratory Mill Model 4, Arthur H. Thomas Company, Philadelphia, PA) before being shipped to Georgia Tech. Alamo switchgrass for biofuel research was provided as a courtesy by University of Georgia.[125c] Fresh poplar stem was pre-dried in vacuum oven at 40 ℃ overnight prior to milling. Dried poplar stem was milled using Thomas-Wiley Laboratory Mill machine and was simultaneously sieved through a 20-80 mesh screen. Milled poplar sample was stored at -20 ℃ for further treatments. The switchgrass samples were air-dried until the moisture content was less than 10% of dry weight, and ground in a Wiley mill to pass through a 0.841 mm screen. Samples were then additionally sieved to achieve a final particle size between 0.297 mm and 0.707 mm screened and stored at room temperature.

For the study on lignin carbon fiber, three-year-old black cottonwood (*Populus trichocarpa*) clones harvested from a Genome-wide Association Study at Clatskanie, OR were harvested in December, 2012, cut into ~50 cm logs and shipped to ORNL, where they were dried for 2 weeks at 70 ℃. Logs were then debarked with an axe and an angle grinder, with logs then chipped to ~1-3 cm pieces in a commercial chipper.

3.2 Experimental Procedures

3.2.1 Soxhlet Extraction

Extractive-free poplar and switchgrass were prepared with sequential 5 h Soxhlet extractions according to TAPPI method T 204 cm-07. Extractives for both the cross sectioned and milled samples were removed by placing the samples (5.00 g of dry weight) into an extraction thimble in a Soxhlet apparatus. The extraction flask was filled with 1:2

ethanol/benzene mixture (~300 mL), dichloromethane, and then refluxed with boiling rate of five solvent cycles per hour. The extractive-free solids were air dried overnight.

3.2.2 Poplar Samples under Partial Delignification and Dilute Acid Pretreatment

Poplar samples were size-reduced in a Wiley mill (Thomas Scientific, Swedesboro, NJ, United States) using a 0.250 to 0.177 mm screen. Extractives were subsequently removed by placing the biomass into an extraction thimble in a Soxhlet extraction apparatus (VWR, West Chester, PA, United States). The extraction flask was filled with 1:2 ethanol:benzene mixture (Sigma-Aldrich (St. Louis, MO, United States) (approximately 150 mL in total) and then refluxed at a boiling rate which cycled the biomass for at least 24 extractions over a 4 hour period (PL23-t0). Modified acid-chlorite delignification was used to reduce lignin content. Samples were generated by exposure of extracted baseline poplar to $NaClO_2$ (0.6 g/1.00 g lignocellulosic dry solids) in acetic acid (375 mL of 0.14 M) (Sigma-Aldrich (St. Louis, MO, United States) at 70 ℃ for about 15 minutes, followed by a further 30 minutes to generate solids with 19.2 and 14.3% Klason lignin content (sample labeled as PL19-t0 and PL14-t0, respectively, shown in Table 14). The native sample without any lignin removal and delignified samples with Klason lignin content 19.2 and 14.3 % were subjected to DAP under the same conditions. Poplar samples were transferred to a 4560 mini-Parr 300 ml pressure reactor (Parr Instrument Company, Moline, IL, United States) with 0.1 M H_2SO_4 solutions at 5% dry solids and were then sealed. The impeller speed was set to about 100 rpm, and the vessel was heated to 160 ℃ for 25 to 30 minutes (at approximately 6 ℃/min). The reactor was held at the pretreatment temperature ± 2 ℃ (approximately 0.65 to 0.69 MPa) for the specified

residence time ± 30 seconds (15 or 35 minutes). The reactor was then quenched in an ice bath for approximately 5 minutes. The pretreated slurry was filtered to remove the solid material and washed with an excess of deionized filtered water. The pretreated lignocellulosic samples were dried in the fume hood overnight. All yields for biomass recovered after pretreatment ranged between 75 and 85% by mass. Poplar samples under delignification and DAP at various conditions are summarized in Table 14.

Table 14 Pretreatment methods and conditions of poplar.

Sample Code	Poplar Sample	Starting% Klason Lignin	Pretreatment Conditions
PL23-t0	Native	23.2	-
PL23-t15	Dilute acid pretreated	23.2	0.1 M H_2SO_4,160 ℃, 15 min
PL23-t35	Dilute acid pretreated	23.2	0.1 M H_2SO_4,160 ℃, 35 min
PL19-t0	Delignified	19.2	-
PL19-t15	Delignified then dilute acid pretreated	19.2	0.1 M H_2SO_4,160 ℃, 15 min
PL19-t35	Delignified then dilute acid pretreated	19.2	0.1 M H_2SO_4,160 ℃, 35 min
PL14-t0	Delignified	14.3	-
PL14-t15	Delignified then dilute acid pretreated	14.3	0.1 M H_2SO_4,160 ℃, 15 min
PL14-t35	Delignified then dilute acid pretreated	14.3	0.1 M H_2SO_4,160 ℃, 35 min

3.2.3 Various Pretreatments

The same poplar material used in section 3.2.2 was transferred to a 4560 mini-Parr 300 ml pressure reactor with a pretreating solution prepared as described in Table 15 at 5.0 % dry solids and then sealed. The impeller speed was set to about 100 rpm, and the vessel was heated to a temperature as described in Table 15 over ~ 25 – 30 min (at ~ 6 ℃/min). The reactor was held at the pretreatment temperature ± 2 ℃ (120 – 160 ℃; ~ 0.65 – 0.69

MPa) for the specified residence time ± 30 s. The reactor was then quenched in an ice bath (~ 5 min). Pretreatment conditions were adapted from literature which investigated optimal pretreatment conditions.[31a, 113a, 128a] The pretreated slurry was filtered to remove the solid material and washed with an excess of deionized (DI) filtered water. Paramagnetic impurities were removed by washing the solids with a 2 % aqueous solution of ethylenediaminetetraacetic acid (EDTA) and DI water. The pretreated lignocellulosic samples were then dried in the fume hood overnight. All gravimetric yields for biomass recovered after pretreatment ranged between 75–85 %.

Table 15 Various pretreatments conducted on hybrid poplar.

Pretreatment	Reagents	Residence time (min)	Temp (℃)	% dry solids
Hot Water	H_2O	5, 10, 60	160	5
Dilute Acid	0.1 M H_2SO_4	5, 10, 60	160	5
Dilute Acid/Ox	0.1 M H_2SO_4, 0.55 MPa of O_2	5, 10, 60	160	5
Organo-Solv	0.02 M H_2SO_4, 65 % Ethanol / Water	5, 10, 60	160	5
Lime	0.1 M $Ca(OH)_2$	5, 10, 60	120	5
Lime/Ox	0.1 M $Ca(OH)_2$, 0.55 MPa of O_2	5, 10, 60	120	5

3.2.4 Cellulose Preparation for GPC

Isolated α-cellulose was generated by first isolating holocellulose from milled biomass pulp using the method described above. Isolated cellulose was prepared from the holocellulose sample (1.00 g) by extraction with a 17.5% NaOH solution (50 mL) at 25 ℃ for 30 minutes. A total of 50 mL of deionized filtered water was then added to the NaOH solution. The extraction was continued with the 8.75% NaOH solution (100 mL) at 25°C for an additional 30 minutes. The isolated α-cellulose samples were then

collected by filtration and rinsed with 50 mL of 1% acetic acid, an excess of deionized filtered water, and dried in fume hood.

3.2.5 Cellulose Preparation for CP/MAS ^{13}C NMR

In order to compare cellulose ultrastructural changes during various pretreatments, cellulose from various pretreated poplar samples was isolated and purified for solid state CP/MAS ^{13}C NMR analysis. Holocellulose was first isolated from pretreated poplar samples by treatment with $NaClO_2$ (1.30 g/1.00 g lignocellulosic dry solids) in acetic acid (375.00 mL of 0.14 M) at 70 ℃ for 2 h. The samples were then collected by filtration and rinsed with an excess of DI water. Isolated cellulose was prepared from the holocellulose sample (1.00 g) by refluxing with HCl (100.0 mL of 2.50 M) as reported by Foston.[30] The isolated cellulose samples were then collected by filtration and rinsed with an excess of DI filtered water, and air dried. Illustration of the procedure is shown in Figure 24.

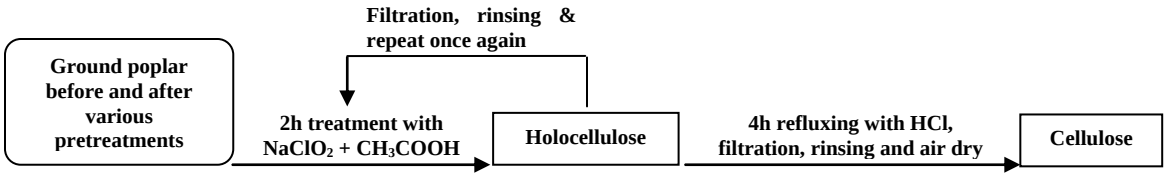

Figure 24 Illustration of cellulose sample preparation for NMR test.

3.2.6 Enzymatic Isolation of Lignin

Poplar used in this study was provided by Oak Ridge National Laboratory, TN. Alamo switchgrass was provided as a courtesy by University of Georgia.[125c] Cellulolytic enzyme lignins of poplar and switchgrass were isolated by modifying the procedures described in

literatures.[74c, 157] Poplar and switchgrass biomass was ball-milled for 7 days after Soxhlet extraction with dichloromethane, those extractives-free ball-milled materials were then subjected to two consecutive rounds of enzymatic hydrolysis. Biomass (15g/L) was suspended in 20 mM, pH 5.0 sodium acetate buffer solution containing 2 mg/mL CELLULYSIN® cellulase (Calbiochem, *Trichoderma viride*, activity : > 10000.0 U/g) for 48 h at 50 ℃ shaken at a frequency of 150 rpm. Following hydrolysis, the residue was collected by centrifugation, washed with distilled water, centrifuged and freeze-dried. The freeze-dried residue was then subjected to two rounds of extraction with dioxane/water (96:4, v/v, 10 ml/g biomass) under a nitrogen atmosphere for 24 h. After extraction, the supernatant was collected, combined, concentrated, precipitated in water and freeze-dried.

3.2.7 Dilute Acid Pretreatment of Cellulolytic Enzyme Lignins

Poplar and switchgrass cellulolytic enzyme lignins were transferred to a 4560 mini-Parr 300 ml pressure reactor at 5.0 % dry solids in 0.1 M H_2SO_4 solution and then sealed. The impeller speed was set to about 100 rpm, and the vessel was heated to the temperature 160 ℃ over 25–30 min (at 6 ℃/min). The reactor was held at the pretreatment temperature ±2 ℃ (160 ℃; 0.65–0.69 MPa) for the specified residence time ± 30 s. The reactor was then quenched in an ice bath (5 min).[158] Following DAP, aqueous phase was extracted with ethyl acetate, dried with anhydrous $MgSO_4$, concentrated with rotary evaporator and combined with solid lignin residues.

3.2.8 Lignin Isolation for Carbon Fiber Study

A small amount of the poplar chips (as described in 3.1.2) were ground to 0.420 mm and the powder samples were analyzed by pyrolysis molecular-beam mass spectrometry (py-MBMS) to determine the S/G ratio. Five trees with S/G ratio ranging from 1.43 to 2.27 were selected to perform organo-solv fractionation process. Poplar clone identification codes for selected samples are shown in Table 16. The chemical compositions of the samples were analyzed by following procedures developed by National Renewable Energy Laboratory (NREL/TP-510-4268 and NREL/TP-510-42622). The ash, extractives, cellulose, hemicellulose, and lignin content are summarized in Table 16. The selected hybrid poplar wood chips were sieved and particles with size larger than 2.36 mm were placed in a flow through reactor and heated with a mixture of methyl isobutyl ketone/ ethanol/water (16/34/50 wt%) in presence of sulfuric acid (0.05 M).[159] The organo-solv fractionation process was carried out at 140 ℃ for 120 min or 160 ℃ for 60 min. The combined severity factor (R_o') of the fractionation, which combines the effects of reaction time, temperature, and acid concentration into a single value, was calculated as following:[160]

$$R_o' = \text{Log } R_o - \text{pH}$$

$$R_o = (t)\,(\exp\,(T_r - T_b)/14.75)$$

Where *t* represents fractionation time in minutes; T_r is the fractionation temperature in ^oC; T_b is the baseline temperature, mostly at 100 ^oC. After organo-solv process, lignin was isolated from the resulting cooking liquor by a reported salting-out method.[159, 161]

Table 16 The S/G (syringyl/guaiacyl) ratio and chemical composition of hybrid poplar wood.

Biomass ID	S/G	FC	Se	Ce	Hm	L	A	E
TAG750	2.275	140 ℃ 120min	1.91	43.69 ±0.01	21.24 ±0.06	21.61 ±0.21	0.96 ±0.03	8.35 ±0.28
TAG896	2.26	160 ℃ 60min	2.19	42.89 ±0.56	22.1 ±0.22	22.22 ±0.28	0.72 ±0.01	6.28 ±0.22
TAG1672	2.245	140 ℃ 120min	1.91	42.14 ±0.23	21.26 ±0.08	22.63 ±0.15	0.62 ±0.00	7.92 ±0.11
TAG562	1.549	140 ℃ 120min	1.91	43.55 ±0.20	21.91 ±0.07	22.4 ±0.15	0.72 ±0.02	6.17 ±0.17
TAG99	1.432	160 ℃ 60min	2.19	43.79 ±0.44	20.48 ±0.12	22.98 ±0.09	0.79 ±0.01	8.01 ±0.20

S/G: S/G by MBMS, FC: Fractionation conditions, Se: Severity, Ce: Cellulose, Hm : Hemicellulose, L: Lignin, A: Ash, E: Extractives.

3.3 Analytical Procedures

3.3.1 Carbohydrate and Acid-insoluble Lignin (Klason Lignin) Analysis

In order to monitor biomass composition change as a result of pretreatments and calculate the sugar conversion from enzymatic hydrolysis, carbohydrate and Klason lignin analysis were carried out based on methods described in Tappi T-249.[162] The first stage utilizes a severe pH and a low reaction temperature (72 vol. % H_2SO_4 at 30 ℃ for 1 h). The second stage is performed at much lower acid concentration and higher temperature (3 vol. % H_2SO_4 at 121 ℃ for 1 h) in an autoclave. The resulting solution was cooled to room temperature and filtered using G8 glass fiber filter (Fisher Scientific, USA). The remaining residue is considered as Klason lignin which was oven-dried and weighed to

obtain the Klason lignin content. The filtered solution was analyzed for carbohydrate constituents of the hydrolyzed poplar samples determined by high-performance anion-exchange chromatography with pulsed amperometric detection (HPAEC-PAD) using Dionex ICS-3000 (Dionex Corp., USA). Error analysis was conducted by performing carbohydrate and Klason lignin analysis three times on the untreated and pretreated biomass samples.

3.3.2 Attenuated Total Reflectance Fourier Transform Infrared (ATR-FTIR) Spectroscopy Analysis

PerkinElmer Spectrum 100 FTIR spectrometer with a universal attenuated total reflectance (ATR) sampling accessory (Perkin-Elmer Inc., Wellesley, MA, United States) was used to monitor the structural changes in biomass. Samples were pressed uniformly against the crystal surface via a spring-anvil, and spectra were obtained by 64 scans accumulation from 4,000 to 500 cm^{-1} at 4 cm^{-1} resolution. The ATR correction and the baseline correction were carried out orderly by PerkinElmer Spectrum software (Perkin-Elmer Inc., Norwalk, CT, United States) with the equipment.

3.3.3 WAXD Analysis of Untreated and Pretreated Poplar

Wide-angle X-ray diffraction (WAXD) measurements were performed using a theta-theta goniometer PANalytical X'Pert PRO diffractometer (PANalytical in Almelo, Netherlands) with Cu $K\alpha$ radiation (λ = 1.542 Å) operating at 45 kV and 40 mA. Beam divergence on the incident and diffracted beam paths are controlled by the programmable divergence and programmable anti-scatter slits to maintain a constant illuminated spot of

10 mm on the sample. A fixed 2 °anti-scatter slit and a 10 mm width limiting beam mask on the incident beam path; soller slits of 0.04 rad divergence on both beam paths; Nickel as a beta-filter and X'Celerator scientific detector on the diffracted beam path were the other optic components. The pretreated poplar samples, covered with a kapton film to maintain its humidity during measurements, were mounted onto the Spinner PW3064 stage and rotated at 7.5 rpm. Data was collected in the continuous scan mode from 5 °to 90 °2θ. The width of the diffraction peaks associated with specific reflecting planes (*hkl*) having a repeat spacing of d_{hkl} was used to estimate the crystallite size, L_{hkl} using the Scherrer equation. The crystallite size (or dimension) L_{hkl} is calculated by the relation[41b, 163]:

$$L_{hkl} = \frac{0.9\lambda}{\beta_{hkl}\cos\theta}$$

Where λ is the X-ray wavelength in Å; β_{hkl} is the angular full-width at half maximum intensity (FWHM) in radians of the (*hkl*) line profile; and θ is the scattering angle. The calculated values of crystallite size, L_{200} were obtained from diffraction peak widths according to the Scherrer method for all samples.

3.3.4 Gel Permeation Chromatography Analysis of Cellulose and Lignin

The number-average molecular weight (M_n) and weight-average molecular weight (M_w) were determined by GPC after tricarbanilation of cellulose. Lignin-free cellulose (15 mg) from each sample was placed in separate test tubes equipped with micro stir bars and dried overnight under vacuum at 40 ℃. The test tubes were then capped with rubber septa. Anhydrous pyridine (4.00 mL) and phenyl isocyanate (0.50 mL) were added

sequentially via syringe. The test tubes were placed in an oil bath at 70 ℃ and allowed to stir for 48 hours. Methanol (1.00 mL) was added to quench any remaining phenyl isocyanate. The contents of each test tube were then added drop-wise to a 7:3 methanol:water mixture (100 mL) to promote precipitation of the cellulose derivative. The solids were collected by filtration and then washed with the methanol:water mixture (1 × 50 mL), followed by water (2 × 50 mL). The cellulose derivative was then dried overnight under vacuum at 40 ℃. Prior to GPC analysis the cellulose derivative was dissolved in tetrahydrofuran (1.0 mg/mL), filtered through a 0.45 μm filter, and placed in a 2 mL auto-sampler vial. DP_n and DP_w were obtained by dividing M_n and M_w by 519 g/mol, the molecular weight of the tricarbanilated cellulose repeat unit. All reported values for molecular weight and DP were the mean average of duplicate samples, except in the case of the untreated material which was the average of six samples for each type of cellulose.

The lignin samples (dried under vacuum at 40 ℃ overnight) were acetylated with acetic anhydride/pyridine (1/1, v/v) at RT for 24 h in a sealed flask under an inert atmosphere. The concentration of the lignin in this solution was approximately 20 mg/ml. After 24 h, the solution was diluted with ~20 ml of ethanol and stirred for an additional 30 min, after which the solvents were removed with a rotary evaporator followed by drying in a vacuum oven at 40 ℃. The number-average molecular weight (M_n) and weight-average molecular weight (M_w) were determined by GPC after acetylation of lignin. Prior to GPC analysis the acetylated lignin sample was dissolved in tetrahydrofuran (1.0 mg/mL), filtered through a 0.45 μm filter, and placed in a 2 mL auto-sampler vial.

The molecular weight distributions of those samples were then analyzed on an Agilent GPC SEC 1200 system equipped with four Waters Styragel columns (HR1, HR2, HR4, HR6), Agilent refractive index (RI) detector and Agilent ultraviolet detector (Waters, Inc., Milford, MA, United States) (270 nm) using tetrahydrofuran (THF) as the mobile phase (1.0 mL/min) with injection volumes of 20.0 μL. A calibration curve was constructed based on eight narrow polystyrene standards ranging in molecular weight from 1.5×10^3 to 3.6×10^6 g/mol. Data collection and processing were performed using Polymer Standards Service WinGPC Unity software (version 7.2.1, Polymer Standards Service USA, Inc., Warwick, RI, United States). Error analysis was conducted by performing three individual isolations and GPC peak integrations.

3.3.5 Simons' Staining

DB 1 (Pontamine Fast Sky Blue 6BX) and DO 15 (Pontamine Fast Orange 6RN) dyes were obtained from Pylam Products Co. Inc. (Garden City, New York United States). DB 1 was used as received. Although the original staining method developed by Simons utilized both dyes as received,[164] later studies suggested that only the high molecular weight fraction of the DO 15 dye was responsible for the increased affinity for cellulose, whereas the low molecular weight part had a very similar affinity for cellulose as DB 1.[165] Therefore, an ultrafiltration of DO 15 to remove the low molecular weight part was necessary, and was done by filtering a 1% (wt/wt) solution of DO 15 through a 100 K membrane using an Amicon ultrafiltration apparatus (Amicon Inc., Beverly, Massachusetts, United States) under approximately 200 kPa nitrogen gas pressure.[166] To calculate the concentration of the DO 15 after ultrafiltration, 1.00 mL of the solution was

dried in a 50 °C oven for a week and the weight of the solid residue was measured. Simons' stain was performed according to the modified procedure by Chandra et al.[92b] The amount of dye adsorbed by the biomass sample was determined using the difference between the concentration of the initial added dye and the concentration of the dye in the supernatant calculated by solving two Lambert-Beer law equations simultaneously.

3.3.6 Down-scaled Enzymatic Sugar Release Assay

The high throughput enzymatic hydrolysis method is based on the High Throughput Pretreatment and Enzymatic hydrolysis (HTPH) design at University of California, Riverside (UCR, California, United States).[167] In this particular study, 4.5 mg dry biomass was loaded into individual wells of a custom-built metal well plate by an automation robotics platform (Symyx Technologies, Sunnyvale, California, United States). Then, 446 μL deionized water was pipetted into all wells (8-channel pipette, 30 to 300 μL, Eppendorf, Hamburg, Germany) to achieve a solid loading of 1 wt%. Next, 39 μL of a mixture of 1 M citrate buffer (pH 4.8), sodium azide solution and enzymes was pipetted into each well (8 channel pipette, 10-100 μL, Eppendorf, Hamburg, Germany). The final hydrolysates contained 0.05 M citrate buffer (pH 4.95), and 0.2 g/L sodium azide. The resulting enzyme loading corresponded to a high 112.5 mg protein of Accellerase 1500 and 37.5 mg protein of Accellerase® XY (DuPont Industrial Biosciences, Palo Alto, CA, United States), respectively, per gram of glucan plus xylan in tested biomass. The high protein loading was applied to ensure that the substrate reactivity is not masked by the enzymes ineffectiveness as they can be strongly inhibited by the compounds (such as xylooligomers and phenols) present in the enzymatic

hydrolysates. After enzyme addition, the well plate was then clamped between two stainless steel plates with a flat silicone gasket in between. The plate was then placed on its side in an incubation shaker (Multitron Infors-HT, ATR Biotech, Laurel, Maryland, United States) at 50 ℃ for 72 hours at 150 rpm. Following enzymatic hydrolysis, the well-plate block was allowed to cool to room temperature and then opened. A sealing tape (Nunc, Rochester, New York, United States) was secured to the top of all vials and the entire well plate was centrifuged (CS-6R Centrifuge, Beckman, Fullerton, California, United States) for 20 minutes at 2650 rpm. Then, 260 μL of the clear hydrolysates solution was transferred to a polypropylene 96-well plate (Agilent, Santa Clara, California, United States) for HPLC analysis. In this part, sugar concentrations were quantified using Agilent 1200 HPLC (Agilent, Santa Clara, California, United States) equipped with an Aminex™ HPX-87H column (BioRad, Hercules, California, United States) and a refractive index detector. The column heater was set at 65 ℃ and the detector was set at 50 ℃. The eluent (5 mM sulfuric acid) was used at a flow rate of 0.6 ml min^{-1}.

3.3.7 Characterization and Thermal Analysis of Lignin for Carbon Fiber Study

The S/G ratio of the lignin fractions was determined by Pyrolysis-Gas Chromatography/Mass Spectrometry (Py-GC/MS). Briefly, 200 μg of lignin were pyrolyzed in a Frontier multi-shot pyrolyzer (PY3030D) at 450 ℃ for 12s. The interface temperature was 280 ℃. A Perkin Elmer Clarus 680 GC with a split ratio of 80:1 was used for compound separation. The sample was injected into a 30m × 0.25 i.d. × 0.25 μm Elite 1701 (Perkin Elmer) capillary column with 1mL/min helium gas. A Perkin Elmer

Clarus SQ8C mass spectrometer with scanning range of 35-550 Da was used to detect the eluting component. The S, G, H % of lignin fractions were calculated following the method developed by Sykes et al.[168] The chemical composition of the lignin samples was determined by following the procedures developed by National Renewable Energy Laboratory (NREL/TP-510-42618 and NREL/TP-510-42622).

Thermal analysis of the lignin samples was conducted in a TA Q500 thermogravimetric analyzer (TGA) heated from room temperature (30 ℃) to 1000 ℃, at 10 ℃/min under nitrogen atmosphere. Differential scanning calorimetry (DSC) was carried out on lignin samples using a TA Instruments DSC Q2000 in standard mode. Second heating scans ran at 10 ℃/min was used to determine glass transition temperature of the lignin samples.

3.3.8 Rheological Measurement of Lignin Samples

Melt viscosity values of the lignin samples (~ 400 mg) were measured using a strain-controlled ARES rheometer (TA Instruments). Isothermal transient rheological analysis was conducted using parallel plate geometry (25-mm diameter plate) at three temperatures (170, 180, and 190 ℃) at 1 mm gap and a shear rate of 10 rad/s. Parallel aluminum plates were first heated to desired temperature at ramp rate 5 ℃/min. Once the desired temperature was reached, the nitrogen gas was purged through the oven. The lignin pellet was loaded after the reset of the gap and force between the upper and lower plate. The upper plate was gradually lowered to contact the lignin sample and finally to reach 1 mm gap. The lignin sample was isothermally sheared at constant shear rate (10 rad/s) and viscosity data were monitored at 170, 180 and 190 ℃ under nitrogen, and then

cooled down to room temperature under air and nitrogen environments, separately. Codes of various sheared samples are shown in Table 17. The recorded data show a short duration of steady viscosity after a hump at the beginning of measurement of transient data; then the viscosity increases due to thermally-induced reactions. The gradual increase in viscosity data was analyzed by fitting equations (I)-(III).

$$\ln \eta(t) = \ln \eta_\gamma + kt \quad \text{(I)}$$

$$\eta_\gamma = \eta_\infty \exp\left(\frac{\Delta E_\eta}{RT}\right) \quad \text{(II)}$$

$$k = k_\infty \exp\left(\frac{\Delta E_k}{RT}\right) \quad \text{(III)}$$

Equation (III) shows k as the temperature dependent reaction rate constant and η_γ as the steady viscosity value at the onset of viscosity rise. Chemorheological activation energies associated with temperature dependence of viscosity (ΔE_η) and rate constants (ΔE_k) were studied using isothermal viscosity data and fitting equations (II) and (III).[169]

Table 17 Rheological measurement temperature and cooling conditions of poplar lignin samples with their codes.

Sample Code	Lignin Sample	Temp.(℃)	Cooling condition
TAG562	Controlled lignin TAG562	--	--
TAG562-170A	After rheology test	170	Air
TAG562-180A	After rheology test	180	Air
TAG562-190A	After rheology test	190	Air
TAG562-190N	After rheology test	190	Nitrogen
TAG99	Controlled lignin TAG99	--	--
TAG99-170A	After rheology test	170	Air
TAG99-180A	After rheology test	180	Air
TAG99-190A	After rheology test	190	Air
TAG896	Controlled lignin TAG896	--	--

TAG896-170A	After rheology test	170	Air
TAG896-180A	After rheology test	180	Air
TAG896-190A	After rheology test	190	Air
TAG896-190N	After rheology test	190	Nitrogen
TAG1672	Controlled lignin TAG1672	--	--
TAG1672-170A	After rheology test	170	Air
TAG1672-180A	After rheology test	180	Air
TAG1672-190A	After rheology test	190	Air
TAG1672-190N	After rheology test	190	Nitrogen
TAG750	Controlled lignin TAG750	--	--
TAG750-170A	After rheology test	170	Air
TAG750-180A	After rheology test	180	Air
TAG750-190A	After rheology test	190	Air

3.3.9 Nuclear Magnetic Resonance (NMR) Spectroscopy

3.3.9.1 Solid-state CP/MAS ^{13}C NMR Analysis of Cellulose

The cellulose samples with ~ 55 % water content were prepared with isolated cellulose packed into a 4-mm cylindrical ceramic MAS rotor. Repetitive steps of packing sample into the rotor were performed to fully compress and load the maximum amount of sample. Solid-state NMR measurements were carried out on a Bruker DSX-400 spectrometer operating at frequencies of 100.55 MHz for ^{13}C in a Bruker double-resonance MAS probehead at spinning speeds of 10 kHz. CP/MAS experiments utilized a 5 μs (90°) proton pulse, 1.5 ms contact pulse, 4 s recycle delay and 4-8 K scans. All spectra were recorded on wet samples, and the line-fitting analysis of spectra was performed using NUTS NMR Data Processing software (Acorn NMR, Inc) as reported by Foston et al.[30, 49a] Error analysis was conducted by performing three individual isolations, NMR acquisitions and line-fit data processing (5-6 times).

3.3.9.2 ^{13}C-^{1}H 2D Heteronuclear Single Quantum Coherence (HSQC) NMR Characterization of lignin

HSQC experiments were carried out in a Bruker Avance/DMX 400 MHz NMR spectrometer. NMR samples were prepared as follows: 50 mg of lignin sample (for carbon fiber study in Chapter 7) was added to 0.5 ml deuterated hexamethylphosphoramide (HMPA-d_{18}) solution (During biofuel study in Chapter 6, enzymatic isolated lignin was dissolved in 0.5 ml deuterated dimethyl sulfoxide DMSO-d_6) and stirred at 45 ℃ for 4 hours, employing a standard Bruker pulse sequence with 13-ppm spectra width in F2 (^{1}H) dimension with 1024 data points (95.9-ms acquisition time), 210-ppm spectra width in F1 (^{13}C) dimension with 256 data points (6.1-ms acquisition time), a 90 ° pulse, 0.11s acquisition time, 1.5-s pulse delay, $^{1}J_{C\text{-}H}$ of 145 Hz and 48 scans. NMR data were processed using the TopSpin 2.1 software (Bruker BioSpin) and MestreNova (Mestre Labs) software packages.

3.3.9.3 Quantitative ^{31}P-NMR

Phosphitylation and ^{31}P-NMR have been exploited to quantitatively determine hydroxyl functional groups in isolated lignin. Quantitative ^{31}P-NMR were acquired after in situ derivatization of the lignin sample using about 15.0 mg of lignin sample with 2-chloro-4,4,5,5-tetramethyl-1,3,2-dioxaphospholane (TMDP) in a solution of (1.6:1, v/v) pyridine/$CDCl_3$, chromium acetylacetonate (relaxation agent) and endo-N-hydroxy-5-norbornene-2,3-dicarboximide (NHND, internal standard). ^{31}P NMR analysis of lignin samples were carried out using a Bruker Avance-400 spectrometer operating at

frequencies of 161.93 MHz for ^{31}P at 25℃ in a magnetic field of 9.4 Tesla. The quantitative ^{31}P NMR spectra were acquired at a frequency of 161.93 MHz over 32 K data points with acquisition time of 1.29 s, using an inverse gated decoupling pulse sequence with a 25-s pulse delay and 128 scans. Average data of lignin functional groups were presented based on three repeated rheology tests on each poplar lignin sample at various temperatures.

3.4 Error Analysis

The experiments of the carbohydrate analysis, acid-insoluble Klason lignin analysis, and molecular weight measurement of cellulose and lignin were performed in triplet, and the results represented the mean values of three independent experiments. The standard deviation associated with the carbohydrate, acid-insoluble lignin and molecular weight measurements were ± 0.3-3.5%, ± 0.2-0.5%, and ± 5.5-10.0%, respectively. All enzymatic hydrolysis experiments were performed in twice, and the results represented the mean values of two independent experiments. The standard deviation associated with the glucose yield at each time interval was in the range of ± 1.0-8.0%. For solid-state NMR analysis, error analysis was conducted by three to five individual line-fit data processing analyses. The standard deviation associated with the proportion of each cellulose allomorph was in the range of ± 0.3-1.6%.

CHAPTER 4

COMPARISON OF CHANGES IN CELLULOSE ULTRASTRUCTURE DURING DIFFERENT PRETREATMENTS OF POPLAR[1]

4.1 Introduction

Several *Populus* species are presently being developed as high potential energy crops because they exhibit drought tolerance, pests and insects resistance, and high biomass yields on a range of lands.[52b] More importantly, through genetic modification, the extensive sequencing of the *Populus* genome has made it possible to enhance many of these characteristics unlike ever before.[170] Potential applications for poplar include biofuels, pulp and paper, a variety of wood-based products, and the next generation of commodity and fine chemicals. Among the most promising utilization of poplar feedstocks is the production of bioethanol.[52b] Considering the inherent resistant of lignocellulosic cell walls to deconstruction by microbes and enzymes (i.e., biomass recalcitrance), current cellulosic bioethanol production requires pretreatment prior to enzymatic hydrolysis and fermentation. The goal of this pretreatment has commonly been cited as a process to (1) open the lignin-hemicellulose matrix, (2) alter and re-distribute

[1] This manuscript was accepted for publication in Cellulose, 2014. It is entitled as — Comparison of changes in cellulose ultrastructure during different pretreatments of poplar. The other authors are Marcus Foston, Daisuke Sawada, Sai Venkatesh Pingali, Hugh M. O'Neill, Hongjia Li, Charles E. Wyman, Paul Langan, Yunqiao Pu, Art J. Ragauskas.

structural components in the cell wall, (3) lower the degree of polymerization of cellulose, and (4) disrupt the ultrastructure of the cellulose, ultimately aimed at enhancing substrate accessibility and digestibility for enzymatic hydrolysis .[127]

Pretreatment of lignocellulosic materials can include physical, physicochemical, chemical, and biological processes, of which chemical pretreatments typically utilize acid or base with controlled time, temperature, and pH profiles and/or organic solvents to facilitate cell wall component removal.[112a, 134b, 171] One of the most promising options because of cost effectiveness and ease of scalability employs dilute sulfuric acid (0.5 – 1.0 %) at moderate temperatures (140 – 190 ℃) to hydrolyze hemicelluloses, disrupt lignin and enhance sugar yield in subsequent enzymatic deconstruction of cellulose.[30, 172]

Kumar et al. conducted a comprehensive study applying some of the leading pretreatment technologies including ammonia fiber expansion, aqueous ammonia recycle, dilute sulfuric acid, lime, neutral pH, and sulfur dioxide to poplar, evaluating each technology based on enzymatic release following a common sugar assay procedure.[31a, 173] This particular study indicated that one of the most notable changes in the composition of dilute acid pretreated solids is a significant reduction in the relative hemicellulose content. In a separate publication by Wyman et al. dilute acid pretreatments of poplar facilitated ethanol yields of approximately 85% when using simultaneous saccharification and fermentation (SSF), and produced glucose yields around 64 % when using separate hydrolysis and fermentation (SHF).[113a]

Another very common treatment is hot water pretreatment (i.e., without adding acid or base) referred to as auto-hydrolysis because the hot water cleaves acetyl and hemiacetal linkages, liberating acids along with the natural acidity of water catalyzes the hydrolysis of linkages in the cell wall. This pretreatment is associated with lower capital and production costs and reduced formation of degradation products.[174]

An alternative to acidic pretreatments are alkali pretreatments which are processes that typically utilize lower temperatures and pressures when compared to other pretreatment technologies. The commercial application of alkaline bases is often not preferred because sodium hydroxide and other bases are costly and difficult to recover and to reuse in a cost-effective manner.[127] Lime pretreatment with proven effectiveness and low cost has been used to pretreat a variety of substrates including poplar.[175] Wyman et al. demonstrated lime pretreatment of poplar exhibited a reduction in relative lignin content rather than hemicelluloses with SHF glucose yields of ~ 71%.[113a] Chang et al. conducted a systematic study of lime pretreatment conditions on switchgrass and found a residence time of 2.0 h at 100 – 120 ℃ with a 0.1 g $Ca(OH)_2$/g dry biomass lime loading and water loading of 9 mL/g of dry biomass as optimal to enhance enzymatic digestibility. [128a]

An additional interesting class of pretreatment technologies includes wet oxidant methods.[176] For example, lime and oxygen were used to enhance the enzymatic digestibility of poplar in a study by Chang et al. indicating a partial pressure of 1.4 MPa of absolute oxygen gave the optimal condition to enhance the enzymatic digestibility, with a three day total enzymatic sugar conversion of ~ 97%.[171]

Understanding the structural parameters relevant to plant cell wall recalcitrance and how those parameters individually and cooperatively affect enzymatic saccharification are vital for improving current processing and conversion methods for cellulosic biofuels. Though, in more recent work, research has started to indicate that increases in accessibility maybe one of the major first order rate determining factors in enzymatic hydrolysis.[92a, 127] However, among various substrate characteristics cellulose morphology and crystallinity index are inherently connected with cellulase enzyme activity and therefore efficient enzymatic hydrolysis of lignocelluloses.[19a, 177] A study by Pu et al. examined the enzymatic hydrolysis of bleached softwood Kraft pulps in which they reported a faster decrease in the relative amount of amorphous cellulose as a function of enzymatic hydrolysis time.[36a] Recent research studies on the structural reorganization of cellulose fibrils during hydrothermal deconstruction and their relationship with enzymatic digestion indicated that cellulose morphological changes occurred within the lignocellulosic cell wall as a result of pretreatment deconstruction and that these changes are very important for maximizing enzyme digestibility and minimizing energy consumption.[178] This suggests cellulose ultrastructure is a substrate characteristic relevant to the enzymatic deconstruction of biomass and must be monitored to not only deconvolute the factors affecting recalcitrance but also to help develop a deeper understanding of the molecular-level mechanisms that these enzymes employ. A vital component of this is to generate reliable structural models of cellulose before and after pretreatment. These results can be then used in further research such as computational

methods applied model to cell wall deconstruction or the generation of new optimized biocatalysts and low-recalcitrant genetically engineered plants.

In this study, a *Populus trichocarpa x deltoides* hybrid was subjected to hot-water, organo-solv, lime, lime-oxidant (lime/Ox), dilute acid and dilute acid-oxidant (dilute acid/Ox) pretreatments. These samples were then examined for changes in cellulose ultrastructure during pretreatment by ^{13}C cross polarization magic angle spinning (CP/MAS) nuclear magnetic resonance (NMR) and wide-angle X-ray diffraction (WAXD). An enzymatic recalcitrance screen was performed to evaluate and compare the changes in glucose sugar release with respect to different types of pretreatment. Moreover, in this study we intended to investigate transformations occurring in cellulose ultrastructure during various pretreatments, and examine possible links between changes in sugar release (i.e., biomass recalcitrance) and alterations in cellulose crystallinity and crystalline allomorph distribution.

4.2 Experimental Section

4.2.1 Materials

Poplar samples were prepared as described in Chapter 3 section 3.1.2. Hybrid poplar (*Populus trichocarpa x deltoides*) for biofuel research was obtained from Oakridge National Laboratory, TN. The biomass was size-reduced in a Wiley mill using a 0.250 – 0.177 mm screen. Extractives were subsequently removed by placing the biomass into an extraction thimble in a Soxhlet extraction apparatus. The extraction flask was filled with

1:2 ethanol/benzene mixture (~ 150 mL) and then refluxed at a boiling rate which cycled the biomass for at least 24 extractions over a 4 h period.

4.2.2 Pretreatments

Pretreatment process was described in Chapter 3 section 3.2.3.

4.2.3 Carbohydrates and Klason Lignin Analysis

Chemical composition analysis of native and pretreated poplar samples was carried out based on the procedure described in Chapter 3 section 3.3.1.

4.2.4 Cellulose Sample Preparation for ^{13}C NMR

Preparation of cellulose from native and pretreated poplar samples was described in Chapter 3 section 3.2.5.

4.2.5 CP/MAS ^{13}C NMR Analysis of Cellulose

Characterization procedure was described in Chapter 3 section 3.3.9.1.

4.2.6 WAXD Analysis of Untreated and Pretreated Poplar

Characterization procedure was described in Chapter 3 section 3.3.3.

4.2.7 Down-scaled Enzymatic Sugar Release Assay

Sugar analysis procedure was described in Chapter 3 section 3.3.6.

4.3 Results and Discussion

4.3.1 Cell Wall Composition

Carbohydrate and Klason lignin values for the different pretreatments as described in Table 15 are reported in Figure 25 for untreated and pretreated solids. Alkaline pretreatments, lime and lime/Ox, did not significantly alter the relative carbohydrate and Klason lignin distributions, which is in agreement with previous studies under the similar experimental conditions.[179] These studies suggested little alteration in the compositional analysis of alkaline pretreated biomass occurred, in part, due to the relatively lower pretreatment temperatures utilized. In this case compositional analysis indicated lime and lime/Ox pretreatment were much less severe than the other pretreatments conducted and would consequently cause less alterations and degradation to the remaining cellulosic components. On the other hand, dilute acid and dilute acid/Ox pretreatments removed the most significant fraction of xylan, increasing the relative Klason lignin content by almost 50 %. This accompanying increase in the relative Klason lignin content observed for acid pretreatments could be attributed to not only the hydrolysis of hemicellulose and maybe cellulose but also the formation of 'pseudo-lignin', a polysaccharide degradation product resulting from the re-polymerization of dehydrated sugars forming lignin-like polyphenolic structures.[115] The fact cellulosic components may have been degraded/removed during acid pretreatments that could have large implication on concurrent changes in cellulose ultrastructure. Organo-solv pretreatment reduced the relative Klason lignin content significantly (by ~33 %) while removed most of the xylan and yielded a glucan rich solid component. Lignin content reduction in organo-solv

pretreatment could result from solubilization and fragmentation that release lignin into the organic phase.[73a, 180] Though only reporting relative change in cell wall composition, compositional analysis seems to suggest organo-solv pretreatments may also degrade/remove cellulose. Similarly, hot water pretreatment after a 60 min residence time appears chemically comparable to biomass that underwent dilute acid pretreatment, partially removing xylan and increasing the relative Klason lignin content.

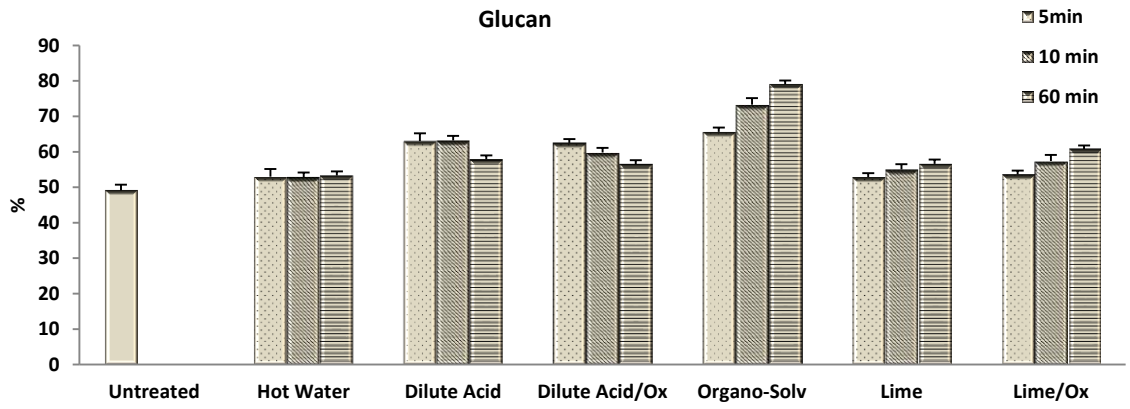

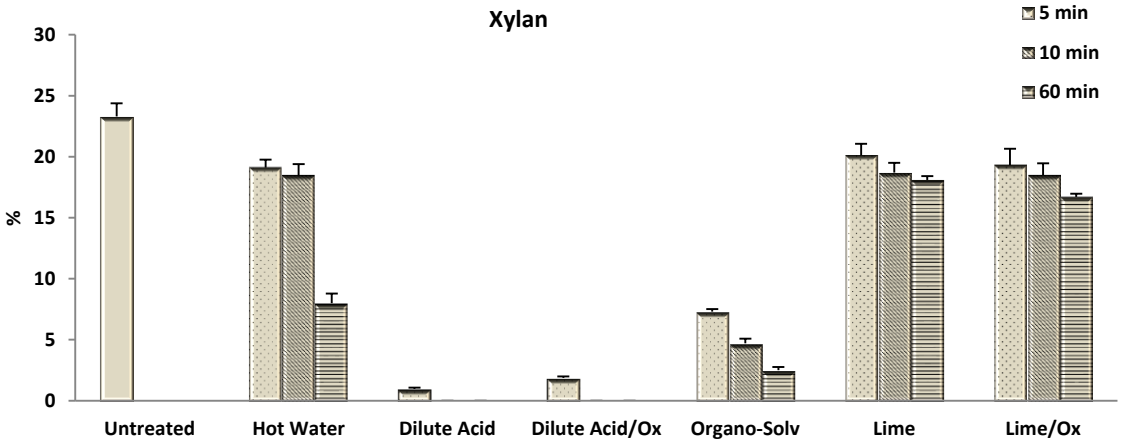

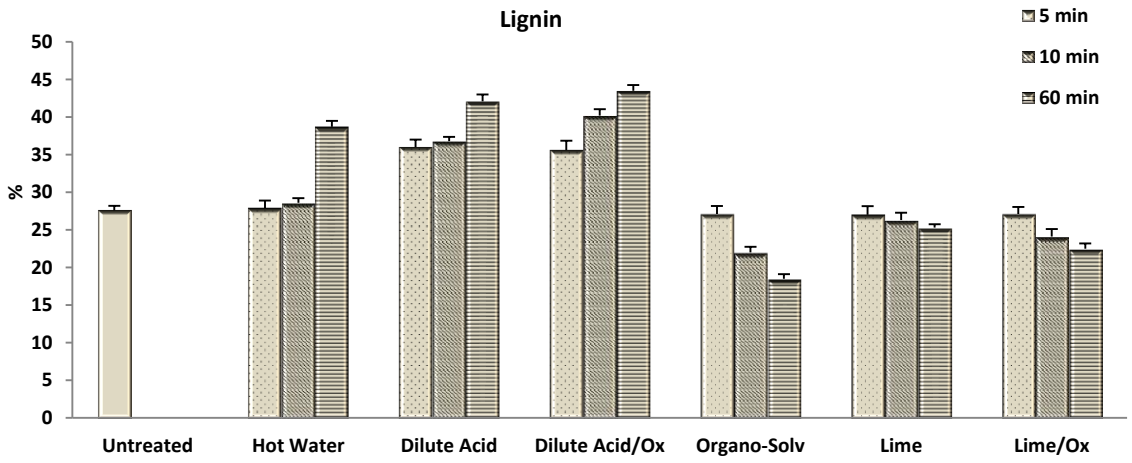

Figure 25 Relative glucan, xylan and lignin contents in the residual untreated and pretreated poplar solids.

4.3.2 Cellulose Crystallinity and Ultrastructure Analysis by NMR

The direct polarization magic-angle spinning (DP/MAS) with enough recycle delays that permit complete T1 relaxation of the observed nuclei magnetization can provide the most reliable method for obtaining quantitative solid state NMR spectra; however, it is usually time-consuming to achieve an acceptable signal-to-noise ratio with the long T1 in solid samples. Compared to DPMAS, CPMAS can enhance the signal intensity per measuring time by about an order of magnitude. While the difference in magnetization transfer from ^{1}H to carbons bonded to ^{1}H and to nonprotonated C or mobile segments with weaker H–C dipolar couplings can compromise the quantification of CP/MAS spectra, the quantitation of CPMAS ^{13}C NMR analysis can be achieved with the selected experimental conditions. The quantitative analysis of the particular cellulose C_4 peak at the selected chemical shift has been documented in literature with the choice of the

optimal contact time and applied experimental conditions that maximizes the signal intensity.[30, 36a]

The cellulose C_4-carbon region extends over a ^{13}C NMR chemical shift range of $\delta \sim 80 – 93$ ppm as shown in Figure 26. A commonly used probe for cellulose amorphous domains can be observed at a ^{13}C chemical shift range of $\delta \sim 80 – 85$ ppm, appearing as a series of fairly broad and overlapping resonances. ^{13}C CP/MAS NMR spectroscopy experiments were conducted to determine cellulose % crystallinity as shown in Figure 27. Cellulose % crystallinity is calculated by dividing the area of the crystalline peak by the total area assigned to the C_4-carbon region.

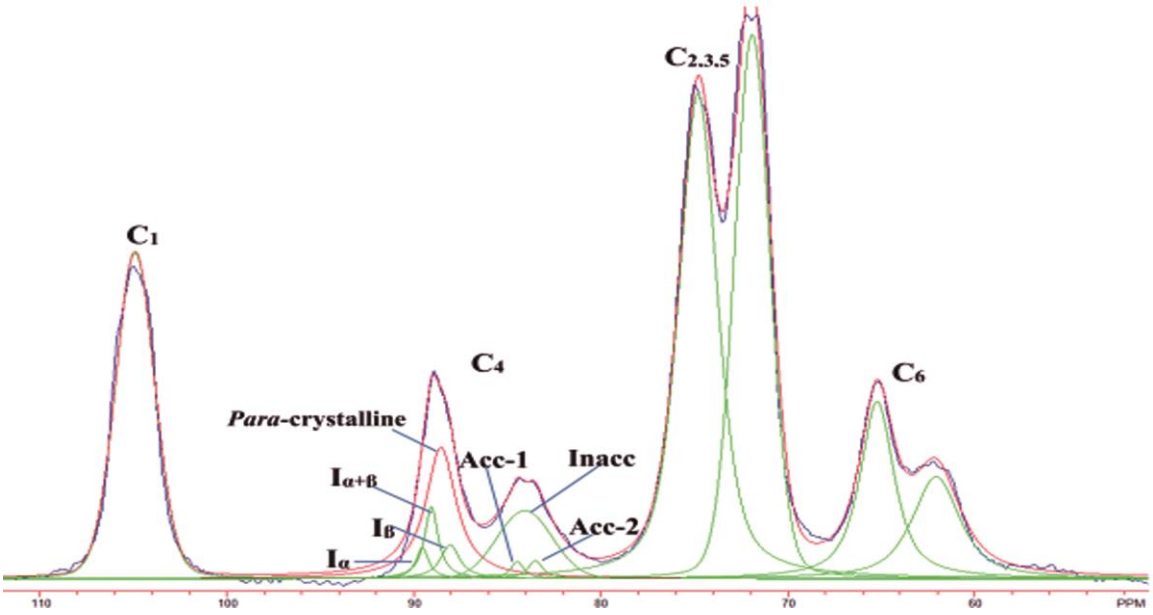

Figure 26 Non-linear least-squared line fitting of the C4 region of ^{13}C NMR spectrum of isolated cellulose samples.

The non-linear least-squared line fitting of the C_4 region for a ^{13}C CP/MAS spectra of isolated cellulose prepared from pretreated poplar are presented in Figure 26. The deconvolution was performed by fitting seven lines to the C_4 region with additional constraints for the areas of the three Lorentzian lines that originate from crystalline cellulose allomorphs I_α (90.2 – 89.7 ppm), I_β (88.1 –87.8 ppm) and $I_{\alpha+\beta}$ (89.0 – 88.6 ppm), and four Gaussian lines for non-crystalline cellulose accessible fibril surfaces (Acc-1: 84.9 – 84.2 and Acc-2: 83.6 – 83.2 ppm) and inaccessible fibril surface (Inacc: 83.9 – 83.4 ppm) as well as *para*-crystalline cellulose (88.6 – 88.4 ppm).[30, 44c, 45, 134c, 181] The relative intensity of the cellulosic ultrastructural components within cellulose fibrils and how those relative intensities change with pretreatment at the most severe conditions tested are shown in Table 18. In addition, the percentage of C_4-carbons detected at fibril surfaces and along a square cross-sectional cellulose microfibril model, can be used to estimate the cellulose microfibril (i.e., lateral fibril dimension (LFD) or cellulose crystallite dimension) and microfibril bundle (i.e., lateral fibril aggregate dimension (LFAD)) dimensions.

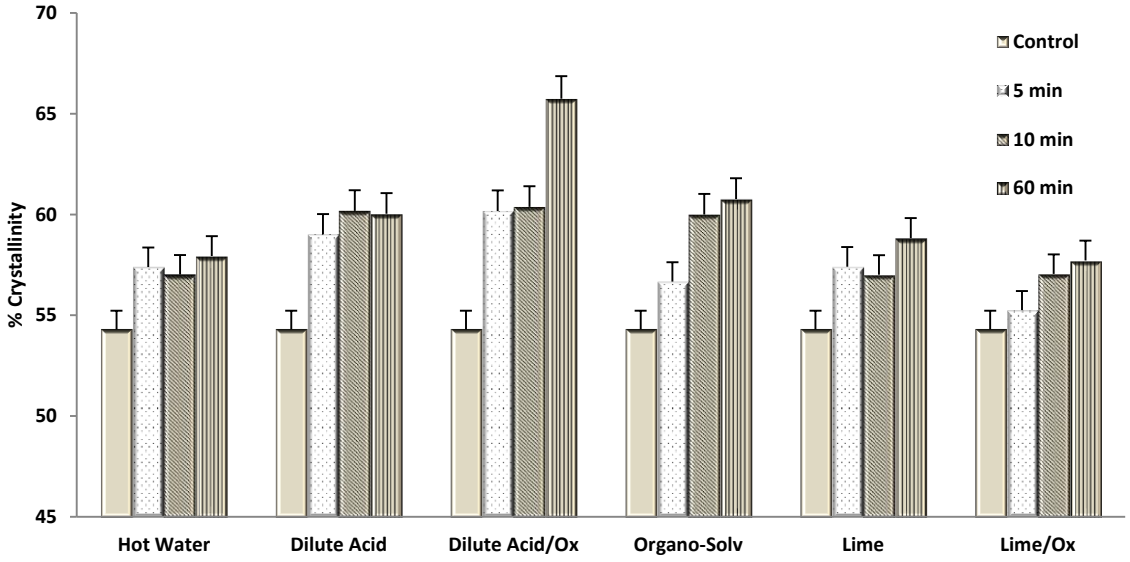

Figure 27 % Crystallinity of cellulose in the residual pretreated hybrid poplar solids as determined by acid isolated cellulose and ^{13}C CP/MAS NMR spectra.

The generalized major effects of the pretreatments on cellulose ultrastructure are: (1) increases in cellulose % crystallinity, (2) increases in the relative cellulose I_β and *para*-crystalline content, (3) increases in cellulose LFD and LFAD, and (4) decreases in the relative cellulose I_α content, cellulose accessible fibril surfaces, and cellulose inaccessible fibril surfaces. The observed increase in relative cellulose I_β content is accompanied by a reduction in resonances representing cellulose $I_{\alpha+\beta}$ and I_α content. This change most likely results from the thermal transformation of the cellulose I_α allomorph, which has a meta-stable triclinic one-chain crystal structure, to the cellulose I_β allomorph, a more thermodynamic favored monoclinic two-chain crystal structure.[30, 123a] Moreover, pretreatments result in the increase of *para*-crystalline cellulose content and a concurrent decrease in the relative proportion of amorphous (i.e., accessible and inaccessible fibril surfaces) cellulose. In conjunction with compositional analysis suggesting cellulosic

degradation occurs and previous study indicating hydrolysis of amorphous cellulose is kinetically favored over that of crystalline cellulose,[36a] increases in % crystallinity and even perhaps relative *para*-crystalline cellulose content could result from the preferential degradation/removal of amorphous cellulose during pretreatment.[30, 49b]

Table 18 The relative % cellulose crystalline allomorphs, para-crystalline cellulose and cellulose fibril surface in the residual hybrid poplar solids pretreated for 60 min.

Treatments	I_α ±0.3 (%)	$I_{\alpha+\beta}$ ±0.3 (%)	Para ±1.5 (%)	I_β ±0.3 (%)	Inacc ±1.6 (%)	Acc-1 ±0.3 (%)	Acc-2 ±0.3 (%)	LFD ±0.2 (nm)	LFAD ±3.0 (nm)
Untreated	4.0	8.6	37.5	4.2	39.4	4.2	2.1	4.2	34
Hot Water	3.1	7.5	40.5	6.9	37.4	2.9	1.7	4.6	47
Dilute Acid	3.6	5.7	43.0	7.8	35.8	2.5	1.7	4.9	52
Dilute Acid/Ox	1.7	8.9	45.9	9.3	30.3	3.3	0.6	5.8	55
Organo-Solv	3.6	6.0	44.8	6.4	35.5	2.1	1.6	5.0	59
Lime	2.6	7.9	40.7	7.7	35.1	3.4	2.6	4.7	36
Lime/Ox	3.1	4.6	45.1	4.9	37.0	3.1	2.2	4.6	41

Para: *para*-crystalline cellulose; Inacc: Inaccessible fibril surface; Acc-1 and Acc-2: Accessible fibril surface; LFD: Lateral fibril dimension; LFAD: Lateral fibril aggregate dimension

Various pretreatments increase cellulose % crystallinity to different extents. Acidic pretreatments increase the crystallinity significantly, while alkaline pretreatments including lime and lime/Ox have relatively less effect. This aligns with compositional analysis indicating amorphous cellulose is more susceptible to hydrolysis at acidic pretreatment conditions than at alkaline pretreatment conditions. The increase of cellulose % crystallinity in pretreated poplar could result from a combination of several factors. Aside from preferential removal of amorphous cellulose (see Table 18), a

hydrothermal "annealing"-like process that transforms cellulose I_α into cellulose I_β could also lead to ordering of amorphous cellulose into *para*-crystalline cellulose.[182]

Hornification describes the irreversible stiffening and shrinking of lignocellulosic materials upon drying or water removal. Hornification shrinks internal fiber volume, and upon re-suspension in water the original extent of water-swelling is not obtained. Interestingly, hornification is not only associated with decreases in water retention value, specific surface area, and pore size[183] but also with accompanying increases in crystallinity and crystallite size.[184] Several mechanisms have been proposed to explain hornification in lignocellulosic materials.[30, 185] One such proposed mechanism, co-crystallization of adjacent cellulose microfibrils,[184b, 186] may also be used here to explain the observed cellulose % crystallinity increases occurring as a result of severe pretreatment. However, if co-crystallization is indeed occurring, cellulose crystallite dimensions might be expected to increase as well.

Based on the LFD and LFAD results (see Table 18), cellulose isolated from acid, acid/Ox, and organo-solv pretreated poplar displayed significant increases in LFD and LFAD as compared to cellulose isolated from hot water, lime, and lime/Ox pretreated poplar. Previous pretreatment studies have attributed this increase in LFD to partially release in cellulose fibril distortion that (1) alters intra-chain hydrogen bonding and (2) then reduces the relative surface area to volume ratio of a cellulose fibril and subsequently increase the LFD.[30, 50b] Increases in LFAD, as a result of pretreatment, are attributed to thermal induced crystallization and aggregate growth.[30] The significant

LFAD increases in acidic and organo-solv pretreated samples could be attributed to the removal and disruption of hemicellulose and lignin that obstruct cellulose co-crystallization.[186]

In addition, chemical reagents employed in cellulose isolation process influence the cellulose structural feature to some extent.[187] However, the impact of isolation procedure on cellulose crystallinity and ultrastructure is minimal compared with those intensive hydrothermal pretreatments.[173, 188]

4.3.3 Crystallite Size Analysis by WAXD

A complementary technique to evaluate cellulose microfibril ultrastructure is wide-angle X-ray diffraction (WAXD). This method is sensitive to the regular or repetitive arrangement of the atoms which is more commonly used to extract crystallite dimension information in cellulose samples with high precision.[41b, 178] Therefore, crystallite size was used to monitor cellulose fibril dimension change as a result of various pretreatments in this study. A detailed description of the different backgrounds, including instrumental and cellulosic amorphous contributions (Figure 28), fitting approach highlighting the influence of the solvent (non-cellulosic) amorphous background that exists as two classes of contributions (Figure 29-30), and fits to pretreated poplar samples is presented as follows.

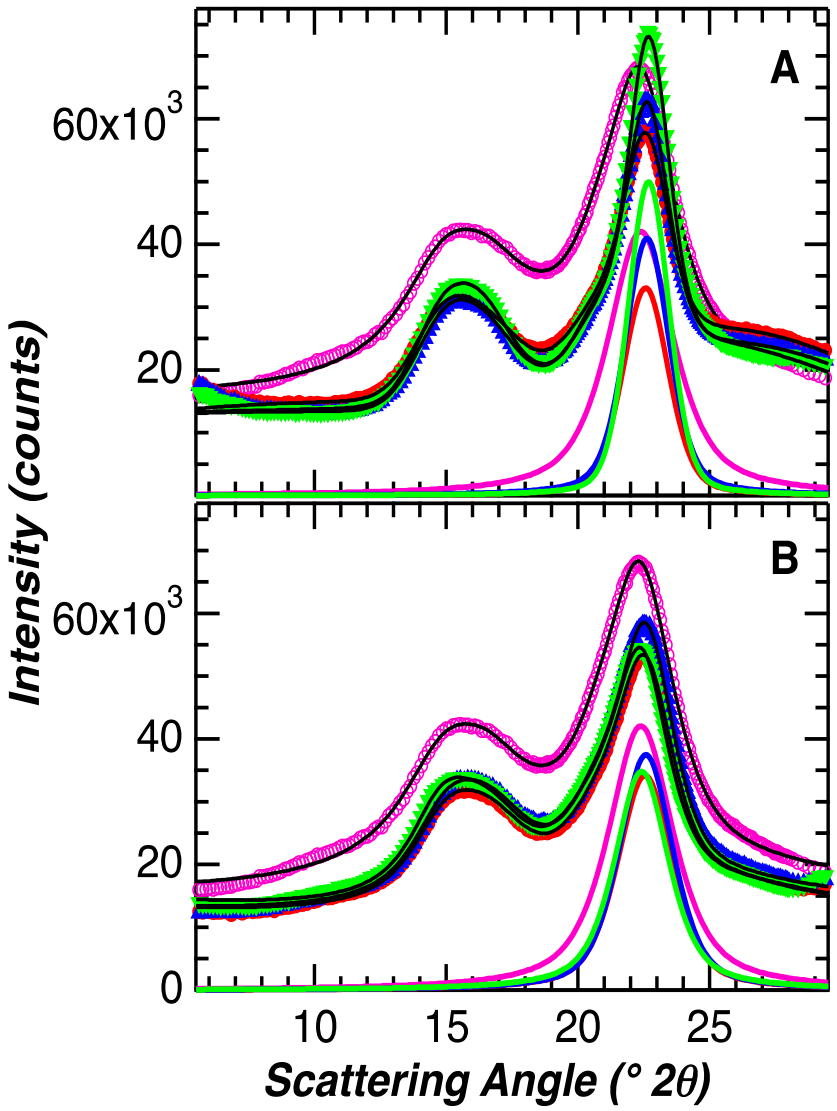

Figure 28 Powder X-ray diffraction data of native and pretreated poplar. Native poplar is in pink color. (A) Organo-solvent and (B) Lime Oxidant for increasing pretreatment resident time: 5 min (red); 10 min (blue) and 60 min (green). The black lines are fits to the experimental data.

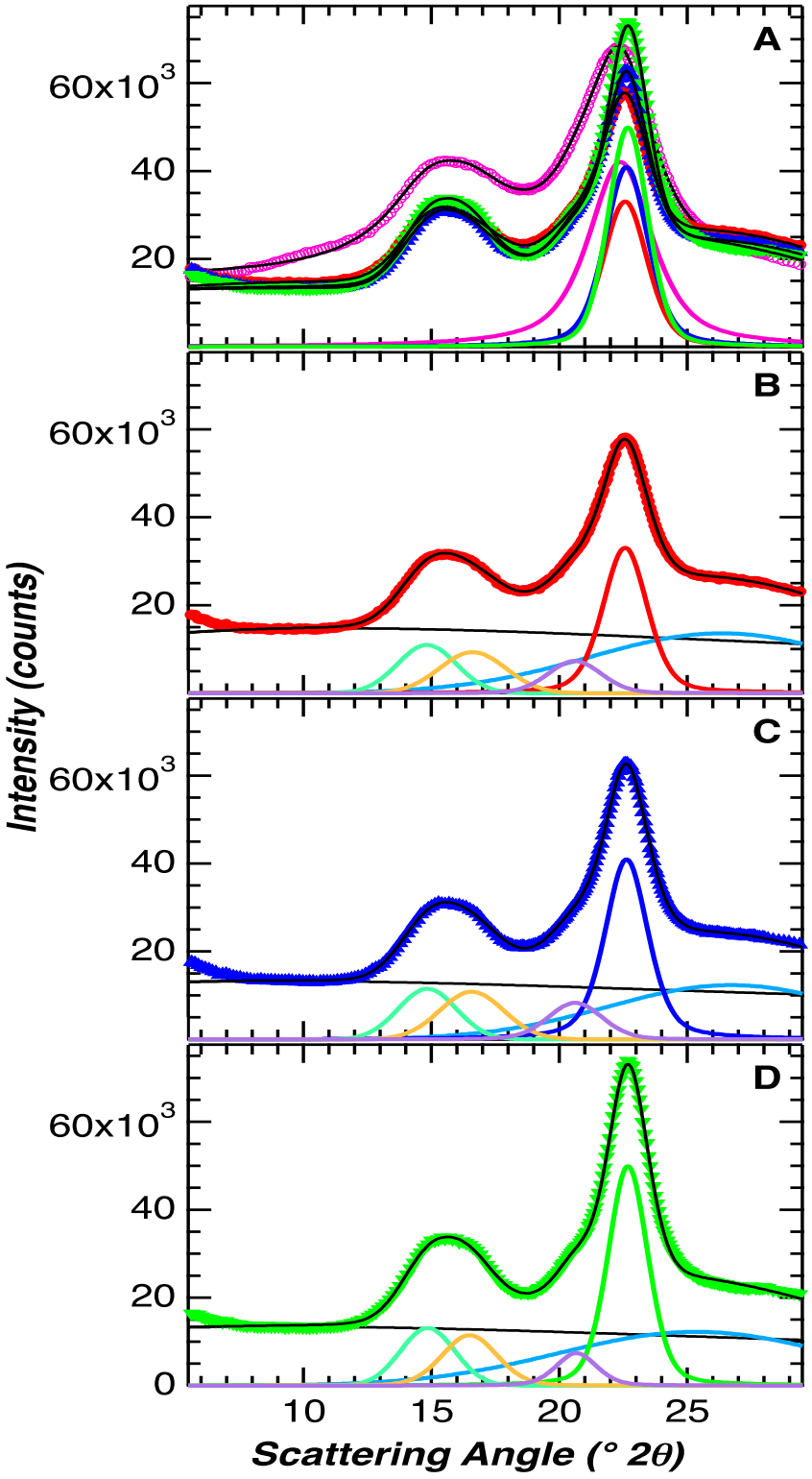

Figure 29 Powder X-ray diffraction data of organo-solv pretreated poplar.

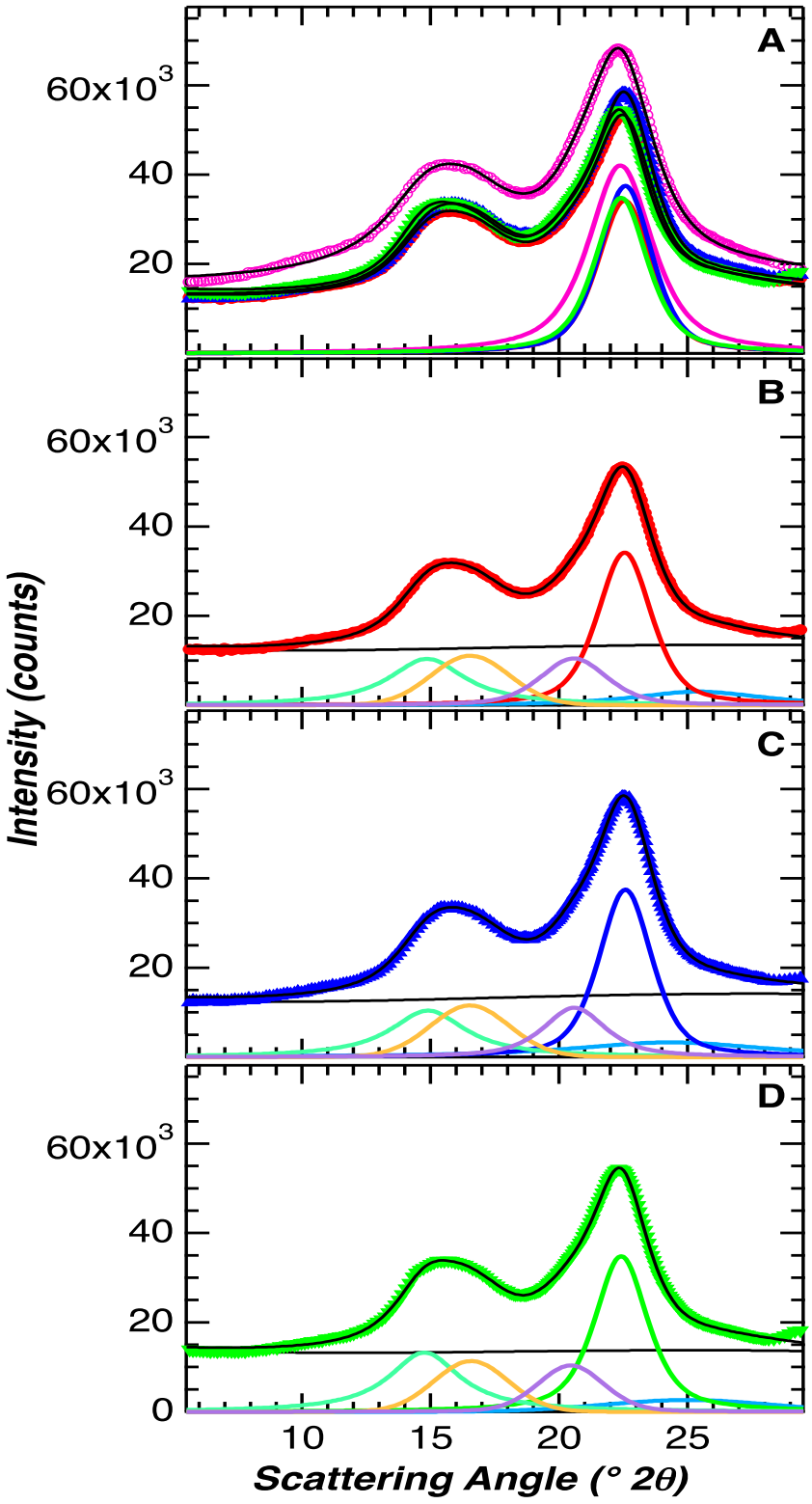

Figure 30 Powder X-ray diffraction data of lime/Ox pretreated poplar.

As shown in Table 19, all pretreatment methods increase the size of the cellulose crystallite and the degree of that increase seems to depend again on pretreatment severity (encompassing pretreatment temperature, residence time, and method employed). The WAXD cellulose crystallite results show a similar trend or ordering with NMR LFD results (Table 18). Among the pretreatments, all acidic treatments have a large influence on cellulose microfibril structure, displaying a large increase in the crystallite size.

Table 19 Crystallite size (L200) for different pretreatment methods.

Treatments	L200 ± 0.1 (nm)	L200 ± 0.1 (nm)	L200 ± 0.1 (nm)
	5 min	10 min	60 min
Untreated	2.7	2.7	2.7
Hot Water	3.0	3.3	4.0
Dilute Acid	3.8	4.3	5.0
Dilute Acid/Ox	4.1	4.1	4.5
Organo-Solv	4.0	4.1	4.4
Lime §	3.8	---	4.1
Lime/Ox	3.6	3.6	3.6

§ 10 min data not collected;

WAXD studies have shown that irrespective of the kind of pretreatment applied such as alkaline, organic or acidic, the crystalline dimension of cellulose microfibrils increase within 5 min of pretreatment time. Hot water pretreatment produces the least increase in the cellulose crystallite size from an untreated sample 2.7 nm to 3.0 nm while all the other pretreatments increase from 2.7 to ~ 4.0 nm. Beyond 5 min of pretreatment cellulose crystallite dimensions increase greater than 4.0 nm, with dilute acid producing the most increase to 5.0 nm. This is interesting because scattering studies of sliced intact poplar chips indicate cellulose fibril ― cellulose fibril distance is ~ 4.0 nm [188] and any

increase in the crystallite size beyond 4.0 nm implies neighboring fibril coalescence. Langan et al. suggest fibril coalescence is driven by expulsion of interstitial biopolymer or solvent.[188] This coalescing trend is however absent for the crystallite dimensions determined for cellulose in hot water, lime/Ox, and lime pretreated poplar. In summary, alkali pretreatments do not affect the cellulose crystallite dimension. This mostly likely is related to the fact alkali pretreatments were conducted at less severe conditions, and that not enough energy has been provided to overcome a kinetic barrier preventing cellulose microfibril coalescence.

4.3.4 Recalcitrance and Enzymatic Sugar Release

Figure 31 summarizes the relative increase in glucose yield after enzymatic hydrolysis for the different pretreatments with respect to the untreated sample. In order of performance, the hot-water pretreatment displayed the lowest increase in glucose yield after enzymatic hydrolysis, dilute acid and dilute acid-oxidant pretreatments, which displayed very similar sugar release profiles were next, with the lime and lime-oxidant pretreatments producing slightly higher increase, and lastly the organo-solv pretreatment generated the largest increase in sugar yield.

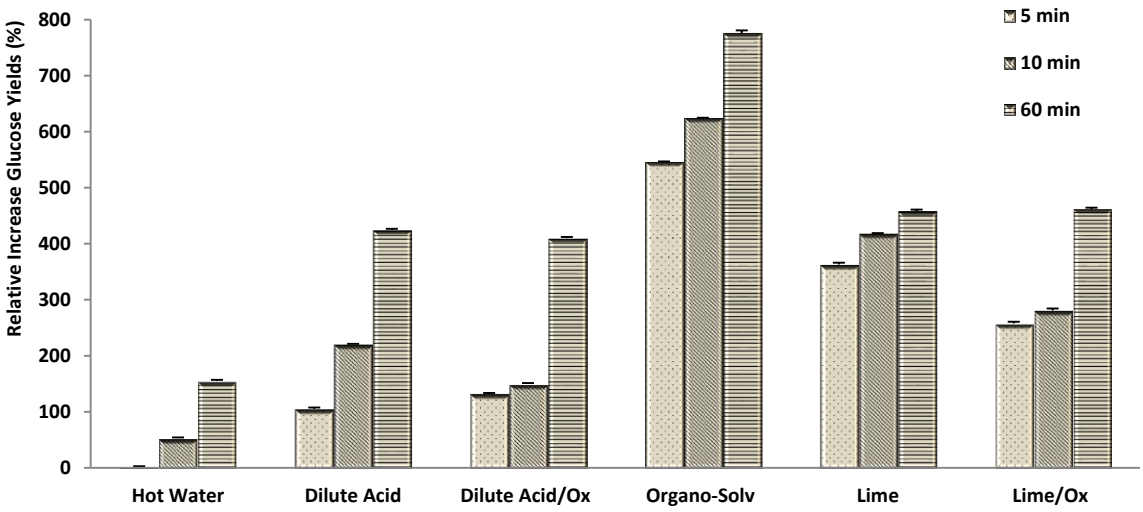

Figure 31 The relative increase in glucose yields due to enzymatic hydrolysis of pretreated hybrid poplar solids with respect to the sugar release profile of the untreated solids.

Enzymatic hydrolysis of cellulosic biomass depends on several comprehensive factors including cell wall biopolymer distribution and chemistry, cellulose degree of polymerization and crystallinity, microfibril crystallite size and morphology, cell wall pore size and enzyme accessibility.[19a, 30, 36a, 92a, 189] It has been postulated that crystalline regions reduce the resulting enzymatic degradation of cellulose,[86a] yet the cellulose crystallinity in most pretreated samples are greater than the untreated sample (Figure 27). Accordingly, the literature clearly shows enzymatic saccharification of biomass which has undergone many of the pretreatments in this study, increase sugar yields suggesting cellulose crystallinity alone may not be the global determinant in the enzymatic degradability of pretreated biomass as once thought.[190] Though true, when crystallinity is considered as a major factor, simple thermodynamic analysis suggests amorphous cellulose is more easily deconstructed than crystalline cellulose.[86a, 191] Therefore,

minimizing cellulose crystallinity increase during thermochemical pretreatment may display superior sugar release profiles. In addition, various cellulose crystalline allomorphic states may respond differently to enzymatic hydrolysis. The metastable triclinic cellulose I_α is more susceptible to enzymatic hydrolysis[36a, 192] and can be transformed into more stable monoclinic I_β by thermal treatment.[30, 123a] Large number of intra-chain hydrogen bonds in cellulose I_β with the increasing LFD is likely to present a thermodynamic barrier to the formation of a catalytically active complex with cellulases, which reduces enzymatic hydrolysis efficiency.[193] Moreover, since the *para*-crystalline cellulose is believed to be located on the surface of crystallites as thin mono-cellular layers, which weaken the crystallites, increase cellulose dissolution and accessibility to reagents, and lead to intra-lattice swelling,[194] therefore the increase of *para*-crystalline portion could also enhance the sugar yield in enzymatic hydrolysis.

4.4 Conclusion

In particular, key molecular features related to biomass recalcitrance, specifically cellulose ultrastructure, were studied. There is no a large influence of those pretreatments on cellulose crystallinity. However, compared with lime and lime/Ox pretreatments, acidic pretreatments relatively significantly alter cellulose ultrastructure, increasing cellulose % crystallinity and cellulose crystallite size significantly. The extent of these changes to cellulose ultrastructure seems to be related to pretreatment severity (time, temperature, and pH), suggesting the kinetics of (1) microfibril coalescence, (2) cellulose crystalline transformation, (3) xylan/lignin removal/redistribution, and (4) selective cellulose component degradation determine the type and the extent of changes that occurs

to cellulose ultrastructure during pretreatment. Lignin removal during alkaline and organo-solv pretreatments is a key factor in enhancing the sugar yield. Moreover, the large increase of LFD, crystallite size and *para*-crystalline cellulose in organo-solv pretreatment along with high sugar yield seems to suggest the increased proportion of *para*-crystalline cellulose could also be beneficial to enhance the sugar yield in enzymatic hydrolysis.

A direct correlation between these measured molecular features and reduced biomass recalcitrance cannot be made because of the numerous other inter-linked substrates characteristic which were modified during pretreatment. However, as shown in this study, clear changes in cellulose ultrastructure do occur, many of which could be tailored or optimized by choice of pretreatment and pretreatment conditions.

CHAPTER 5

THE EFFECT OF LIGNIN CONTENT ON CHANGES THAT OCCUR IN POPLAR CELLULOSE ULTRASTRUCTURE DURING DILUTE ACID PRETREATMENT[2]

5.1 Introduction

Grass and woody biomass is mainly composed of three biopolymers, namely cellulose, hemicelluloses, and lignin, which are largely located in secondary cell walls.[195] Cellulose (typically 40 to 50 wt% of the cell wall) is a linear polysaccharide that consists of repeating β-1,4-glycosidic units and that forms both crystalline and amorphous morphologies. These cellulosic morphologies are the basis for a framework of microfibrils further associated into bundles through strong intermolecular hydrogen bonds.[196] Hemicellulose (typically 15 to 25 wt% of the cell wall), another polysaccharide, is typically a shorter and highly branched heteropolymer composed of both 5- and 6-carbon monomeric sugars.[51a] Lignin (typically 10 to 30 wt% of the cell wall) is derived from hydroxycinnamyl monomers with various degrees of methoxylation forming a racemic, cross-linked, and highly heterogeneous aromatic macromolecule. Lignin and hemicellulose is embedded between and around cellulose microfibrils, providing rigidity

[2] This manuscript was accepted for publication in Biotechnology for Biofuels, 2014. It is entitled as — Effect of lignin content on changes occurring in poplar cellulose ultrastructure during dilute acid pretreatment. The other authors are Marcus Foston, Xianzhi Meng, Daisuke Sawada, Sai Venkatesh Pingali, Hugh M. O'Neill, Hongjia Li, Charles E. Wyman, Paul Langan, Art J. Ragauskas and Rajeev Kumar.

and structural support to the plant cell wall.[197] Lignin, considered as the essential 'glue' holding cellulose and hemicellulose together, is one of the most recalcitrant components of the major plant cell wall biopolymer. The plant cell wall is described as existing as a multi-component structure that is hierarchical, with order existing on multiple length-scales. This multi-component structure forms an encapsulating matrix of lignin and hemicellulose, confining cellulose and restricting the bioavailability of cellulose for biofuels generation.[198] Also, covalent cross-linking between carbohydrates and lignin, known as lignin carbohydrate complexes (LCCs), could act as additional sites confining cellulose and promoting cell wall recalcitrance.[19a, 199]

The biochemical conversion of biomass to biofuels involves three essential steps: pretreatment to reduce the inherent plant cell wall recalcitrance, enzymatic hydrolysis to deconstruct polysaccharides into fermentable sugars, and fermentation to convert those sugars into ethanol.[200] The main challenges related to large-scale biochemical conversion involve considerable cost and inefficiency related to enzymatic deconstruction of polysaccharides embedded in the complex structure of the plant cell wall,[201] which were designed over millions of years of evolution to resist enzymatic and chemical attack. As a result, effective enzymatic hydrolysis is closely related to plant cell wall physiochemical features including cell wall chemistry and composition, cellulose ultrastructure, enzymatic accessible surface area, and so forth.[27a, 202]

In particular, the literature has consistently cited cellulose ultrastructure, mainly crystallinity index (CrI) and degree of polymerization (DP), as a relevant performance

indicator of enzymatic hydrolysis.[19b] However, the exact role of cellulose CrI and DP on enzymatic hydrolysis is still not clearly defined due to the fact that biomass recalcitrance is a complex, multi-variant or scale phenomenon. For example, Del Rio *et al*. in a study on the enzymatic hydrolysis of organo-solv-pretreated softwood materials demonstrated single substrate characteristics such as fiber length, cellulose DP, and cellulose CrI have little effect on an enzymatic hydrolysis yield or rate.[203] However, a variety of studies show low cellulose CrI substrates have high enzymatic digestibility; one in particular by Hall *et al*. demonstrated this on microcrystalline cellulose.[204] However, a study by Foston and Ragauskas seems to indicate that despite increases in cellulose CrI, dilute acid pretreated poplar and switchgrass showed highly increased enzymatic yields.[30] Despite these differing conclusions on the effect of cellulose ultrastructure, it is quite clear that cellulose CrI and DP are altered during pretreatment and can affect biomass recalcitrance.[8, 19b]

The goal of pretreatment is therefore to modify plant cell wall physiochemical features such that the resulting biomass is more amenable to enzymatic deconstruction. The major effect of dilute acid pretreatment (DAP) on lignocellulose is the hydrolysis of hemicellulose and redistribution of lignin which, on average, causes beneficial (to enzymatic deconstruction) changes in cell wall chemistry and composition as well as enzymatic accessible surface area.[79c, 92a] However, it also causes changes in cellulose ultrastructure, which most likely are deleterious (to enzymatic deconstruction) including: increases in the relative cellulose I_β and *para*crystalline content, increases in cellulose CrI, and increases in cellulose crystallite dimension.[30] The increase in relative cellulose I_β

content during DAP is accompanied by a decrease in relative cellulose I_α content, which has been attributed to a thermal transformation of the cellulose I_α allomorph.[30, 205] Cellulose I_α has a meta-stable triclinic one-chain crystal structure, whereas cellulose I_β has a monoclinic two-chain crystal structure and is the more thermodynamic-favored crystal structure generated upon annealing at high temperatures.[123a, 206] DAP also produces characteristic increases in the content of *para*crystalline cellulose and simultaneous decreases in the relative proportion of amorphous cellulose. The above phenomena in conjunction with decreases that occur in cellulose DP during DAP (until a 'level-off' DP is reached) suggest that preferential degradation or removal of amorphous cellulose, and/or a hydrothermal annealing-like process, orders amorphous cellulose and expands cellulose crystallite dimensions.[207] Nuclear magnetic resonance (NMR)[30] and X-ray diffraction (XRD)[188, 208] results also show increases in cellulose crystallite dimension with DAP, which has been attributed to an irreversible process of cellulose co-crystallization and described as similar to hornification. In both cases, changes occurring in cellulose ultrastructure upon pretreatment require elevated temperatures and seem to be related to overcoming a kinetic barrier.

Lignin can act as a physical barrier, encapsulating and confining cellulose. This impacts enzymatic digestibility negatively.[187b, 209] However, if hydrothermal annealing of cellulose or cellulose co-crystallization processes are the major drivers for deleterious change in cellulose ultrastructure, the presence of lignin during pretreatment could retard those changes from occurring. This suggests, in the absence of an intact hemicelluloses and lignin matrix at pretreatment (elevated hydrothermal) conditions, that: removal of the

lignin barrier layers causes cellulose crystallites to have an increased propensity to co-crystallize and coalesce through irreversible hydrogen bonding; removal of the lignin barrier layers and lack of spatial confinement causes cellulose crystallites to have an increased propensity to expand through cellulose annealing and conversion of amorphous to crystalline cellulose; and/or removal of the lignin protecting layers causes the pretreatment severity experienced by the cellulose to be higher, not altering, but simply increasing the effect of pretreatment on cellulose ultrastructure. In combination with previous studies about the complete delignification resulting in the lower sugar release,[187b] this finding could have significant implications, for example, on how genetically modified low-lignin plants are pretreated for enzymatic hydrolysis. Also, establishing a correlation between lignin content and the changes that occur in cellulose ultrastructure during pretreatment could help elucidate the mechanisms that are responsible for cellulose CrI and crystallite size increase during DAP. In order to investigate the effect of lignin content within the presence of an intact lignin-carbohydrate complex has on changes occurring to cellulose ultrastructure during DAP, and consequently enzymatic hydrolysis, *Populus trichocarpa x Populus deltoides* substrates with controlled lignin contents were prepared and then pretreated.

5.2 Experimental Section

5.2.1 Materials

Poplar samples and chemicals were prepared as described in Chapter 3 (3.1.1 and 3.1.2). Baseline poplar (*P. trichocarpa x P. deltoides*) samples were harvested between 2007 and 2008 by the National Renewable Energy Laboratory (NREL) at area 0800 at Oak Ridge

National Laboratory, Tennessee, United States. Cellulase (Accellerase™ 1500, Lot number: 1681198062) and xylanase (Accellerase XY, Lot number: 4901131618) were generously provided by DuPont Industrial Biosciences (Palo Alto, California, United States).

5.2.2 Poplar Samples under Partial Delignification and Dilute Acid Pretreatment

Partial delignification and DAP were carried out following procedures described in Chapter 3 section 3.2.2.

5.2.3 Carbohydrates and Klason Lignin Analysis

The extractive-free biomass including native and treated samples were analyzed according to the NREL standard method for the determination of structural carbohydrates and lignin in biomass as described in Chapter 3 section 3.3.1.

5.2.4 ATR-FTIR Spectroscopy Analysis of Native and Pretreated Poplar

To investigate and quantify chemical changes in untreated and pretreated poplar samples with controlled lignin content, a PerkinElmer Spectrum 100 FTIR spectrometer with a universal attenuated total reflectance (ATR) sampling accessory (Perkin-Elmer Inc., Wellesley, MA, United States) was used, and detailed procedure is described in Chapter 3 section 3.3.2.

5.2.5 Cellulose Sample Preparation for CP/MAS ^{13}C NMR and GPC

Procedure is described in Chapter 3 section 3.2.4 and 3.2.5.

5.2.6 CP/MAS ^{13}C NMR and GPC Analysis of Cellulose

Cellulose isolated from native and treated poplar was measured by GPC and CP/MAS ^{13}C NMR as described in Chapter 3 section 3.3.4 and 3.3.9.1.

5.2.7 Wide-angle X-ray Diffraction Analysis of Native and Pretreated Poplar

Detailed procedure is described in Chapter 3 section 3.3.3.

5.2.8 Simons' Staining

Detailed procedure is described in Chapter 3 section 3.3.5.

5.2.9 Down-scaled Enzymatic Sugar Release Assay

Enzymatic hydrolysis of native and pretreated poplar samples was carried out based on procedure described in Chapter 3 section 3.3.6.

5.3 Results and Discussion

5.3.1 Cell Wall Compositional Analysis

Carbohydrate and Klason lignin (K-lignin) content for the untreated, delignified, and dilute acid pretreated poplar solids are reported in Figure 32. DAP as a cost-effective pretreatment method that significantly reduces lignocellulosic recalcitrance by removing hemicellulose, disrupting lignin-hemicellulose matrix, and redistributing lignin.[30] Delignification (holocellulose pulping) of the native poplar with starting K-lignin of

about 23 wt% (Table 14 PL23-t0; t indicates DAP time in minutes) for 15 minutes resulted in a K-lignin content of about 19 wt% (PL19-t0 sample) and increased the relative glucan and xylan contents in the residual solid from 49 to 56% and 22 to 23%, respectively. Further, delignification for an additional 15 minutes dropped lignin content to about 14 wt% (to produce the PL14-t0 sample), however, there was little change in the relative glucan and xylan contents. Based solely on this data, it seems reasonable to suggest that limited delignification had little effect on the cell wall carbohydrate components.

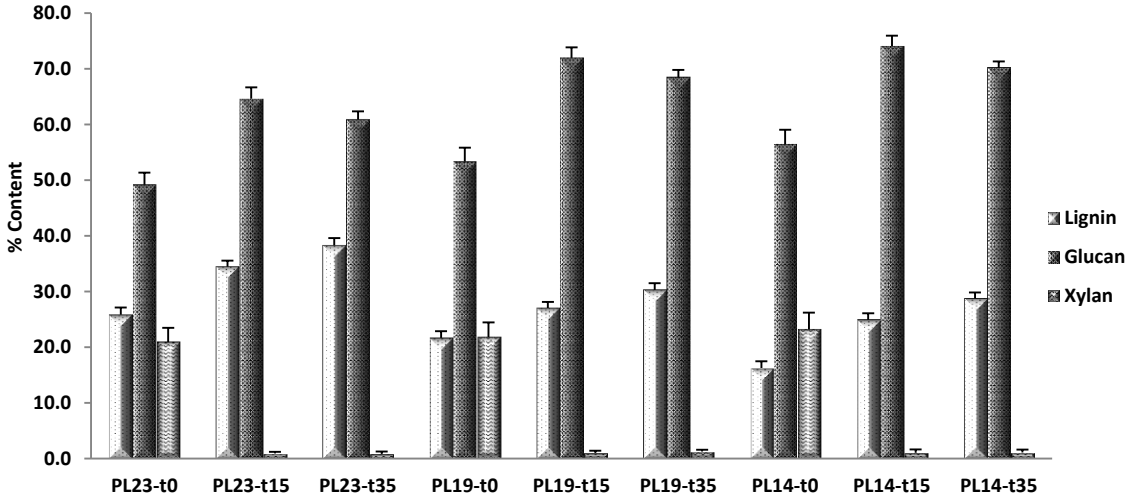

Figure 32 Klason lignin, glucan, and xylan contents from dilute acid pretreated poplar with reduced lignin contents. Sample code with definition is in Table 14.

When native poplar sample (PL23-t0) was subjected to DAP for 15 minutes (to produce sample PL23-t15), there was a significant reduction of xylan from 21 to 1% (PL23-t15), with a corresponding increase of the relative glucan and Klason lignin contents. When the

residence time of DAP was extended to 35 minutes, the residual solids had a slightly lower relative glucan and higher relative lignin content than the solids collected after 15-minutes pretreatment. This could be a result of hydrolytic degradation of cellulose but also, in part, result from the re-polymerization of polysaccharide degradation products forming pseudo-lignin.[115] Delignification of poplar followed by DAP resulted in a similar initial increase in relative glucan and Klason lignin contents, but a slight decrease in relative glucan content with increasing DAP residence time. Though delignification to a greater extent, followed by DAP, seems to correspond with greater magnitudes of change.

5.3.2 ATR-FTIR Spectroscopy Analysis

Relative changes in cell wall chemistry can be extracted from various absorption bands and presented in Table 20. The normalized Fourier transform infrared (FTIR) absorption spectra of lignocellulose at a band position of 1,424 cm^{-1} is primary due to the presence of cellulose, specifically the CH_2 scissor motion of cellulose.[31a, 210] A decrease in the spectral band at 1,424 cm^{-1}, as well as other cellulose specific spectral bands, can be used to determine possible degradation isolated to cellulose during sodium chlorite delignification followed by pretreatment. An increase in spectral intensity at 3,340 cm^{-1} represented an increase in cellulose-hydrogen bonding and indicated possible co-crystallization. Spectral intensity at 2,900 and 1,367 cm^{-1} was attributed to C-H bond stretching and relative decreases in those bands suggested general degradation to the biomass was occurring based on the removal of methyl and methylene groups. After DAP the reduction in the band intensity from around 1,740 cm^{-1} representing carbonyl groups

associated with lignin,[211] typically indicated possible cleavage of association of polysaccharide with lignin and the removal of acetylated hemicellulose. The presence of acetyl groups have long be thought to inhibit enzymatic hydrolysis, and the de-acetylation that occurred during DAP suggested hemicelluloses hydrolysis that would facilitate the cellulose hydrolysis to sugar conversion.[212] In all substrates after DAP, spectral intensity increased at 1,595 and 1,510 cm^{-1} representing aromatic rings,[31a, 213] indicated the increase in Klason lignin content after DAP. The reduction of spectral intensity at 1,240 cm^{-1} in all pretreated samples was tentatively attributed to the cleavage of acetyl groups. In addition, FTIR semi-quantitative analysis can examine the relative structural change in cellulose crystalline and amorphous components. The reduction of ratio I_{α}/I_{β} suggested the reduction of I_{α} and/or the increase of $I_{\beta,}$ and/or cellulose crystalline allomorph transformation from I_{α} to I_{β}. The increase of ratio 1,100/900 cm^{-1} plus a reduction in 900 cm^{-1} suggested that the cellulose amorphous components were degraded to some extent and that amorphous cellulose could be transformed into crystalline cellulose.

Table 20 Relative changes in poplar samples after dilute acid pretreatment by Fourier transform infrared spectroscopy. Sample code with definition is in Table 14.

Band position	Assignment[31a, 210-213]	Pretreatment conditions								
		PL23-t0	PL23-t15	PL23-t35	PL19-t0	PL19-t15	PL19-t35	PL14-t0	PL14-t15	PL14-t35
3340	O-H stretching, related to cellulose-hydrogen bonds	1.7	1.6	1.5	2.1	1.9	2.2	2.1	1.8	2.3
2900	C-H stretching, related to methyl/methylene	0.8	0.8	0.9	0.9	0.8	1.0	0.9	0.8	1.1

1740	Carbonyl bonds ascribed to hemicelluloses	1.3	--	--	1.6	--	--	1.5	--	--
1595	Lignin aromatic ring stretch	0.7	0.8	0.8	0.6	0.7	0.7	0.5	0.5	0.7
1510	Lignin aromatic ring stretch	0.6	0.9	1.0	0.5	0.8	0.8	0.4	0.7	0.7
1424	CH_2 scissor motion in cellulose	1.0	1.0	1.0	1.0	1.0	1.0	1.0	1.0	1.0
1367	Aliphatic C-H stretch in CH_3	1.1	0.9	0.8	1.3	1.1	1.1	1.4	1.2	1.1
1265	Ester absorption with uronic acid	--	1.1	1.2	--	1.2	1.1	--	1.3	1.2
1240	C-O absorption from acetyl group cleavage	1.6	1.3	1.2	2.2	1.1	1.0	2.0	1.2	1.1
1059	C-O stretch in secondary alcohol	5.0	3.6	3.4	--	4.0	4.3	--	5.3	4.9
1100/900	Crystalline to amorphous cellulose ration	3.0	4.4	4.5	2.9	3.7	4.5	2.7	4.1	4.4
750/710	I_α/I_β	0.9	0.6	0.4	0.3	0.3	0.2	0.3	0.3	0.2
900	Amorphous cellulose	1.1	0.6	0.6	1.2	0.8	0.8	1.2	0.9	0.7

5.3.3 Cellulose Degree of Polymerization

The cellulose average DP was determined following virtually complete lignin and hemicellulose removal and then using a published gel permeation chromatography (GPC) procedure.[30] The cellulose DP results were used to determine the ratio of terminal to interior β-glucosidic bonds that can be effectively used to analyze the relative change in cellulose chain length. Figure 33 shows the effect delignification and DAP had on poplar cellulose number-average DP (DP_n) and weight-average DP (DP_w). Delignification alone had a very limited effect on either DP_n or DP_w, displaying at most a 5% reduction. This result is in good agreement with a previous study analyzing the effect of holocellulose

pulping on cellulose molecular weight.[187c] However, DAP caused dramatic reductions in cellulose DP with increased residence time. The fact that a large portion of the cellulosic component had been hydrolytically degraded during DAP could have had large implication on concurrent changes in cellulose ultrastructure, specifically the change of cellulose crystallinity. However, significant differences between cellulose DP for the sample that was subjected to DAP only and samples that was delignified with sodium chlorite followed by DAP were not detected. This is most likely a result of the cellulose reaching its leveling-off DP.[30]

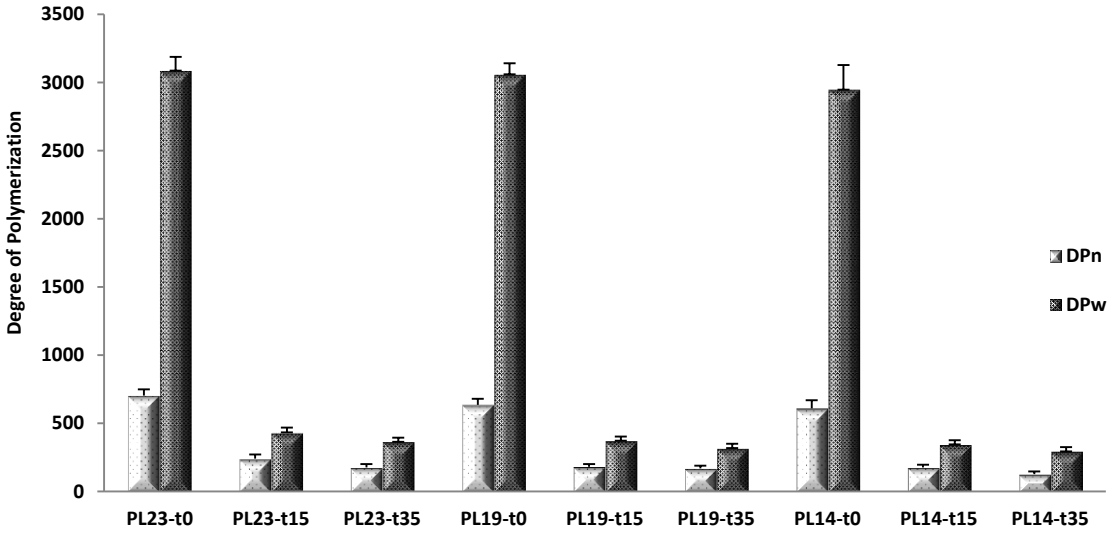

Figure 33 Number and weight average degree of polymerization of cellulose. DP_n: number-average degree of polymerization DP_w: weight-average degree of polymerization. Sample code with definition is in Table 14.

5.3.4 Cellulose Ultrastructure and Crystallinity by NMR

In an effort to better understand the detailed ultrastructural changes occurring within cellulose during partial delignification followed by DAP, ^{13}C cross-polarization (CP) magic-angle spinning (MAS) NMR spectroscopy experiments were applied to isolated cellulose to determine the relative intensity of crystalline and amorphous ultrastructural components of cellulose, following published procedures.[48, 184b] These results were then used to support observations made via FTIR analysis and to understand how crystalline and amorphous ultrastructural components of cellulose vary as a result of DAP and delignification followed by DAP.

Cellulose % crystallinity or CrI was obtained via two-peak integration of the ^{13}C CP/MAS spectrum of isolated cellulose. Cellulose CrI was calculated by taking the ratio of the integral of the cellulose C_4-crystalline carbon region (δ approximate to 85 to 92 ppm) over the integral of whole cellulose C_4-carbon region (δ approximate to 80 to 92 ppm), and the results are shown in Figure 34. Delignification alone had little effect on cellulose CrI, in contrast, DAP generated an increase from 57 to 65%, approximately. Extended DAP residence time caused a further increase in the cellulose crystallinity, and this trend continued for samples that were subjected to delignification followed by DAP. This increase in cellulose CrI with pretreatment, in part, resulted from the preferential hydrolysis and removal of amorphous cellulose, an inference supported by the FTIR results and cellulose DP data.

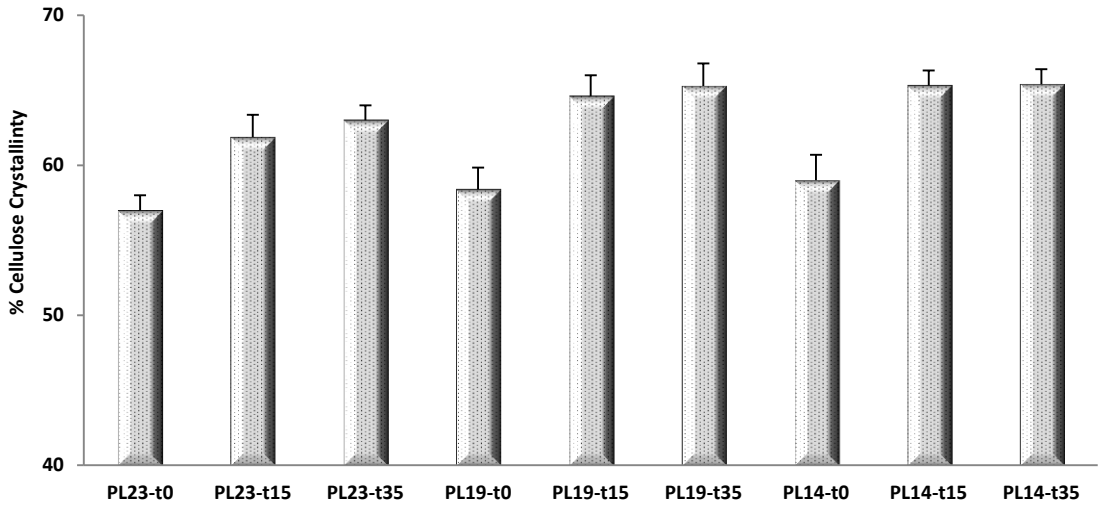

Figure 34 Percent crystallinity of cellulose from dilute acid pretreated poplar with reduced lignin contents. Sample code with definition is in Table 14.

The relative proportion of cellulose crystalline allomorphs, including I_α, I_β, and *para*crystalline and amorphous cellulose at accessible and inaccessible fibril surfaces can also be extracted from the same C_4-carbon region in the ^{13}C CP/MAS spectrum of isolated cellulose using a more complex seven-peak model and a least-squared non-linear fit. The results of this analysis are shown in Figure 35. Delignification seems not to have a significant effect on cellulose ultrastructure for both crystalline and amorphous components, which is in good agreement with a previous study analyzing the effect of acidified sodium chlorite treatment on pure cellulose.[187b] However, DAP caused an observed increase in relative cellulose I_β content, which was accompanied by a reduction in resonances representing cellulose $I_{\alpha+\beta}$ and I_α content, suggesting cellulose I_α was subject to preferential degradation and/or transformation into cellulose I_β during hydrothermal conditions. The latter would occur via H-bonding disruption and rearrangement under pretreatment conditions. This could be regarded as a cellulose

annealing.[123b] *Para*-crystalline cellulose is a form of cellulose that is less ordered than crystalline cellulose but more ordered than amorphous cellulose, and has been proposed to exist on the sub-surface of crystallites as a thin molecular layer.[214] Further ordering of amorphous cellulose into these *para*-crystalline layers could contribute to the observed increase in CrI and expansion of the crystalline lattice. All pretreated samples had a higher relative intensity for paracrystalline than the native or solely delignified samples.

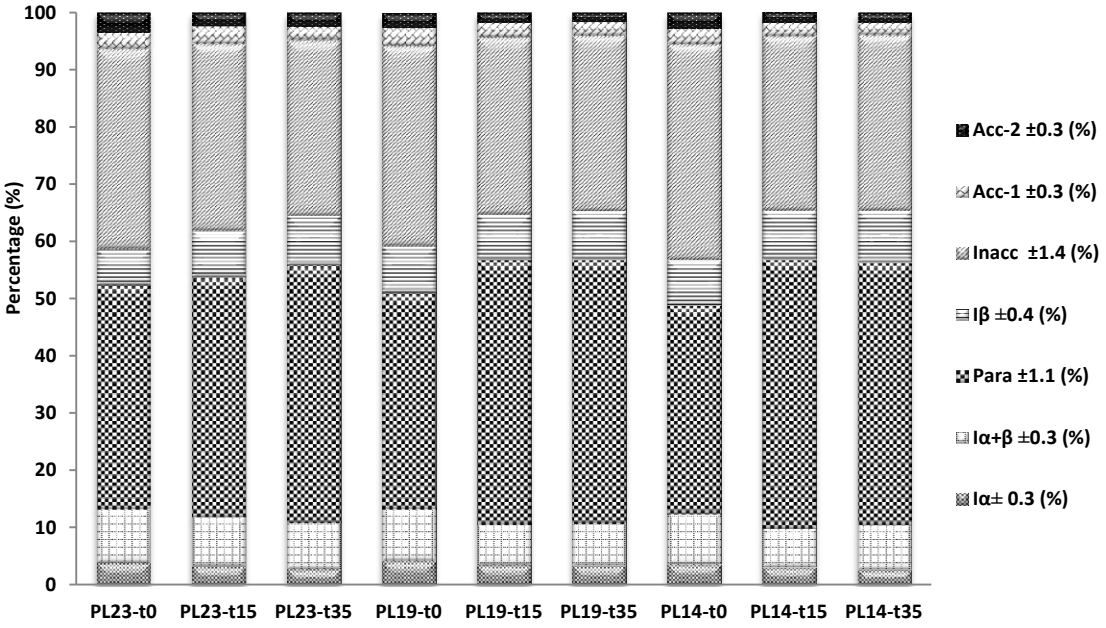

Figure 35 The relative % cellulose crystalline allomorphs, para-crystalline cellulose and cellulose fibril surface. Para: para-crystalline cellulose; Inacc: Inaccessible fibril surface; Acc-1, Acc-2: Accessible fibril surface. Sample code with definition is in Table 14.

Two forms of non-crystalline cellulose have been identified within the C_4-carbon region in a ^{13}C CP/MAS spectrum of isolated cellulose, amorphous cellulose at accessible and inaccessible (fibril-to-fibril contact) fibril surfaces. The relative proportion of cellulose at

accessible and inaccessible fibril surfaces is also shown in Figure 35. Delignification did not alter the inaccessible fibril surfaces but slightly decreased accessible surfaces, however, DAP generated obvious reduction in inaccessible and accessible surfaces. In conjunction with GPC and crystallinity results, it could suggest hydrolysis and degradation of amorphous cellulose is kinetically favored over that of crystalline cellulose during DAP, longer residence time could cause cellulose recrystallization into crystalline I_β, which proceeds with induced hydrogen bonding process in solvent of high polarity acidic system.

In addition to the relative proportion of cellulose crystalline allomorphs and amorphous cellulose at accessible and inaccessible fibril surfaces, the C_4-carbon region in a ^{13}C CP/MAS spectrum of isolated cellulose along with a simple geometric cellulose fibril model[215] can estimate the average lateral fibril dimension (LFD) and lateral fibril aggregate dimension (LFAD) of cellulose. The results of this analysis are shown in Figure 36. Delignification had little effect on LFD but generated an increase in LFAD from approximately 35 to 39 nm, which could be attributed to lignin removal.[50b, 216] DAP seems to cause an increase in LFD and LFAD, where the extent of increase was directly correlated to the increase in pretreatment residence time. The effect of DAP on the increase of LFD and LFAD was further enhanced by greater delignification.

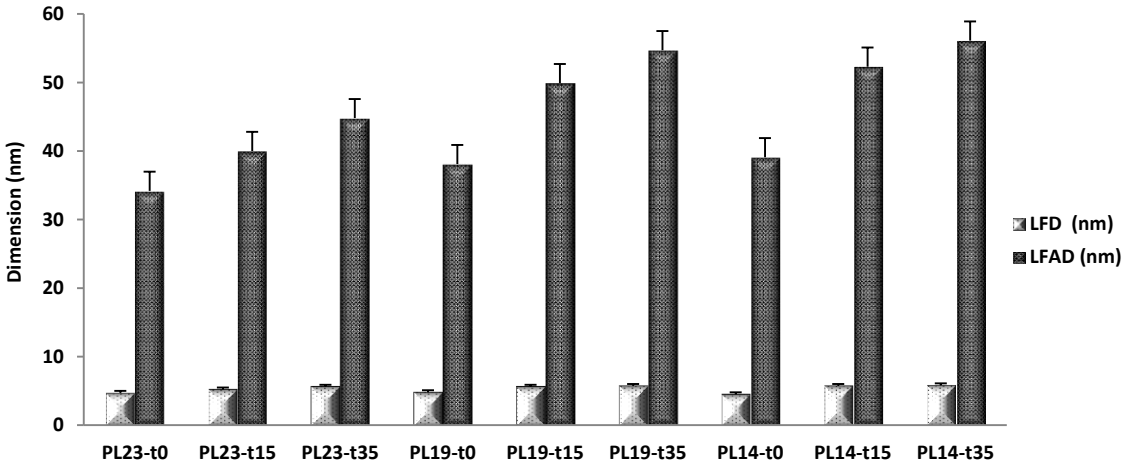

Figure 36 Lateral fibril dimension (LFD) and lateral fibril aggregate dimension (LFAD) of treated poplar cellulose. Sample code with definition is in Table 14.

5.3.5 Cellulose Crystallite Size Analysis

Wide-angle X-ray diffraction (WAXD), a more traditional but also complementary technique to NMR spectroscopy to extract information detailing cellulose ultrastructural features, is particularly sensitive to crystalline region due to their regular or repetitive arrangement of atoms. Two important measureable parameters are d_{hkl}, distance between atomic planes perpendicular to (*hkl*) direction and L_{hkl}, the distance or size of crystalline order in the (*hkl*) direction. As shown in Figure 37, delignification, DAP and delignification followed by DAP increased cellulose crystallite size to different extents. The increasing trend of cellulose crystallite size was in good qualitative agreement with the cellulose fibril dimensions extracted from NMR spectroscopy in Figure 36. DAP increased cellulose crystallite size of delignified substrates from 3.0 to 3.1 nm to 4.0 to 4.2 nm, which is interesting because scattering studies of sliced intact poplar samples indicate the cellulose fibril-fibril distance is approximately 4.0 nm,[188] and any increase in

the crystallite size beyond 4.0 nm implies neighboring microfibrils coalesce by expelling any interstitial biopolymer or solvent. Cellulose microfibril coalescence would be mainly reflected in a decrease of accessible cellulose surfaces, enlargement of LFADs, and the increase of cellulose% crystallinity. Moreover, the increase in the FTIR absorption bands ester linkages of covalent lactone bridges through esterification process could relate to occurred hornification,[188] and the change of hydrogen-bonded hydroxyl group in poplar samples subjected to severely delignification followed by DAP also supports the cellulose crystallites growth via co-crystallize and coalesce.

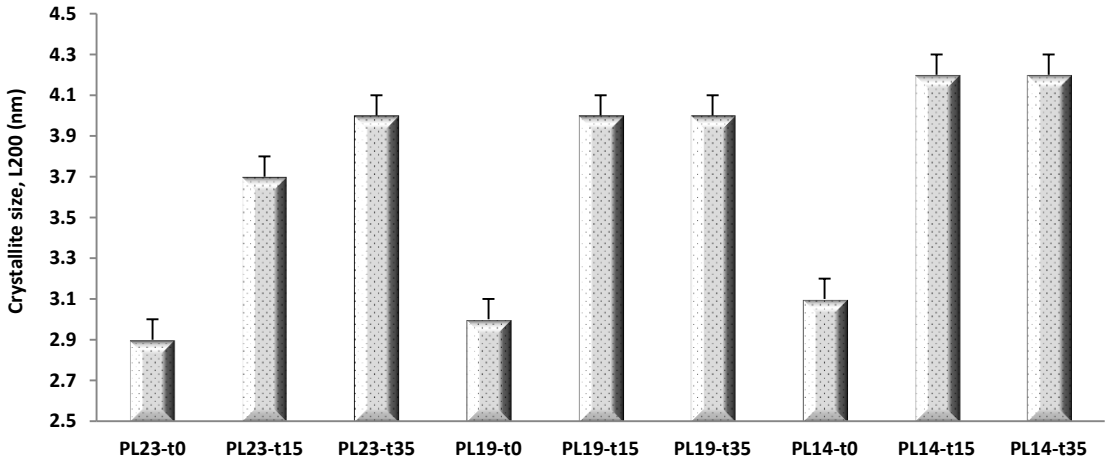

Figure 37 Crystallite size (L200) for different treated poplar samples. Sample code with definition is in Table 14.

5.3.6 Simons' Stain

The changes of cellulose accessibility to cellulase caused by DAP and delignification followed by DAP were also evaluated to further study lignin impact on the accessible surface area of cellulose for downstream enzymatic hydrolysis. Simons' stain testing has

been used to evaluate the accessibility of a lignocellulosic substrate by applying two dyes: Direct Blue (DB) 1 and Direct Orange (DO) 15.[217] DB 1 has a well-defined chemical formula with a molecular diameter of approximately 1 nm, whereas DO 15 is a poly-condensation product of 5-nito-*o*-toluenesulfonic acid with a molecular diameter in the range of approximately 5 to 36 nm. These two dyes absorb different wavelengths of light, have different molecular sizes, and most importantly, have different binding affinities for cellulosic surfaces. Therefore, the ratio of DO 15 and DB 1 dye (O/B) adsorbed into the biomass can be used to indicate the relative accessibility of cellulose in a lignocellulosic substrate. Arantes and Saddler[218] found that the higher the O/B ratio, the lower the protein loading required for efficient hydrolysis. However, it is also necessary to analyze the maximum amount of DO 15 adsorbed especially when large amounts of the smaller DB 1 dye are adsorbed by a substrate and cause a decrease in the overall O/B ratio. In this case, there may be a significant amount of large pore and cellulose accessibility, but analysis based solely on the low O/B ratio may skew the data interpretation.[92a]

As shown in Figure 38, the DO 15 adsorptions for samples which had not been subjected to DAP (PL23-t0, PL19-t0, and PL14-t0) were 21.8, 23.1, and 29.7 mg/g. This increase in DO 15 adsorption suggests delignification increases cellulose accessibility to some extent. For all samples under DAP for 35-minutes residence time, significant increases in the amount of DO 15 adsorbed were observed. The PL23-t0, PL19-t0, and PL14-t0 samples displayed an increase from 21.8 to 68.5 mg/g, 23.1 to 70.4 mg/g, and 28.7 to 72.5 mg/g, respectively after DAP for 35 minutes. This result indicated that DAP

significantly increased cellulose accessibility such that appreciable amounts of enzymes could have access to cellulose in spite of the fact that DAP actually increases the Klason lignin content. This suggested the increased cellulose accessibility was mainly due to the hemicellulose removal,[79c] lignin-hemicellulose phase separation,[188] and/or lignin redistribution caused by DAP.

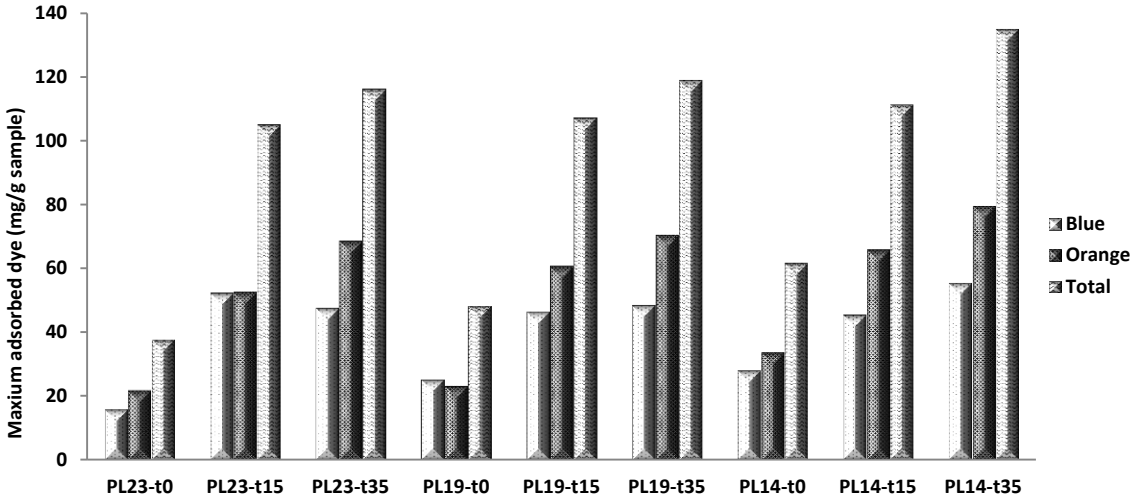

Figure 38 The maximum amount of direct orange 15 dye and direct blue 1 dye adsorbed by untreated and pretreated poplar. Sample code with definition is in Table 14.

5.3.7 Enzymatic Sugar Release

Cellulose ultrastructural changes, measured as a function of pretreatment severity, were evaluated using enzymatic sugar release assays. Sugar yields were calculated through dividing the glucose contents in enzymatic hydrolysis liquid from native, delignified, and dilute acid pretreated poplar samples by the glucan contents from carbohydrate analysis on those native and treated starting materials. Figure 39 summarizes the glucose yield after enzymatic hydrolysis for the delignified substrate after DAP with respect to the

unpretreated sample. DAP on undelignified substrate produced a 60% sugar yield (PL23-t35), and delignification without DAP also produced a 57.5% yield (PL14-t0). However, initial delignification followed by a second DAP step dramatically enhanced downstream enzymatic hydrolysis to facilitate sugar yields of approximately 80% for PL14-t35. In addition, P14-t0 with a lower cellulose accessibility (Figure 38) and higher sugar yield than P23-t15 suggests delignification could contribute more to the extent of enzymatic hydrolysis than DAP, as delignification enhances both enzymes macro-accessibility to cellulose and hemicelluloses, as well as enzymes effectiveness.[219]

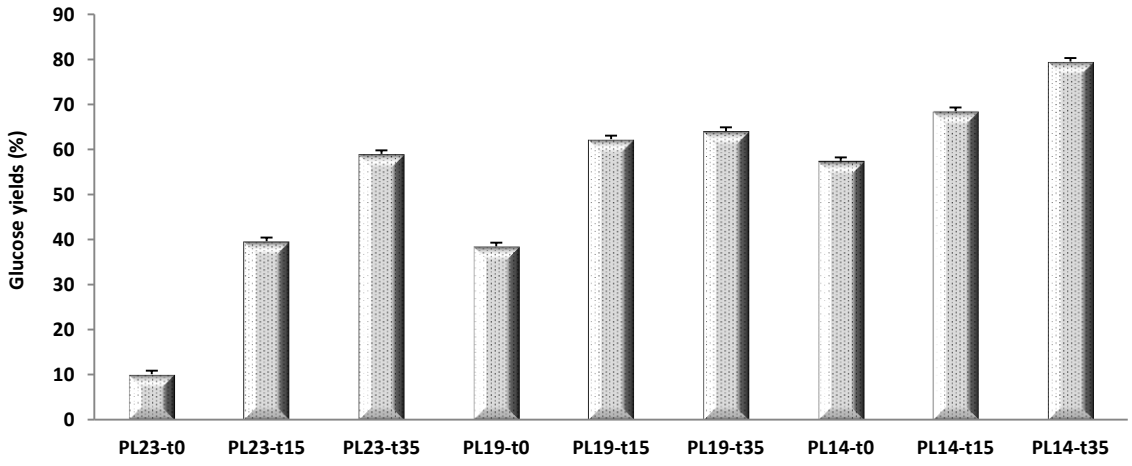

Figure 39 Glucose yields as a result of downscaled enzymatic hydrolysis. Sample code with definition is in Table 14.

Enzymatic hydrolysis of cellulosic biomass is restricted by substrate recalcitrant factors and influenced by treatment methods. In combination with the results above, reduction in poplar cellulose DP caused by DAP could increase cellulose chain-reducing ends,[86b] and short chains with a weak hydrogen-bonding network could make cellulose more

amenable to enzymatic deconstruction.[220] The increase of cellulose accessibility to cellulases caused by DAP is mainly due to the expansion of the pore size and volume, and the increase of a specific surface area, which thereby improve cellulases adsorption on cellulose surface.[91, 221] The inevitable increase of cellulose crystallinity and crystallite size with microfibril coalescence after DAP seems to have a negative effect on enzymatic hydrolysis since crystalline regions reduce the resulting enzymatic degradation of cellulose.[204] However, some changes on cellulose crystalline allomorphic states may be beneficial to enhance the sugar yield in enzymatic hydrolysis, such as the increased proportion of paracrystalline cellulose. It is believed to be located on the surface of crystallites as thin monocellular layers which weaken the crystallites, increase cellulose dissolution and accessibility to reagents, and cause intra-lattice swelling.[214] Furthermore, studies of acidified sodium chlorite treatment on Avicel cellulose with different crystallinities have proved that those minimal changes on crystalline and amorphous cellulose by sodium chlorite had no detectable effect on cellulose digestibility,[187b] which suggests the major role of sodium chlorite treatment on biomass is removing lignin with intact cellulose left, and thereby enhancing the cellulose digestibility.

Lignin content and distribution had a more pronounced effect on biomass recalcitrance and enzymatic digestibility, especially for poplar.[209] However, complete lignin removal on corn stover by sodium chlorite treatment following DAP has been found to reduce cellulose conversion,[187b] which was proposed to be attributed to cellulose microfibril aggregation in the absence of lignin and hemicellulose. This was confirmed by our NMR and WAXD analysis that indicated lignin presence played a key role in preventing

cellulose crystallites increased propensity to co-crystallize and coalesce during DAP, which therefore suggested partial delignification instead of complete lignin removal could better benefit the sugar yield. Furthermore, partial delignification with hemicelluloses removal during DAP retained cell wall spatial structure without elimination of all lignin spacer, increased specific surface area, reduced its irreversible adsorption to the enzyme,[95a, 222] and, to limited extent, caused the cellulose fibril coalescence to provide an optimal pretreated biomass for subsequent enzymatic deconstruction.

5.4 Conclusion

This study is another important step in providing the required data for a comprehensive analysis of biomass in an effort to optimize the integrated operations of pretreatment and enzymatic hydrolysis. In particular, key molecular features related to biomass recalcitrance, specifically cellulose ultrastructure and accessibility were, studied. In the absence of lignin spacer along with hemicellulose removal after DAP, changes occurred to cellulose ultrastructure include increases in cellulose% crystallinity, cellulose crystallite size, cellulose crystalline transformation, and cellulose accessibility accompanied by a decrease of cellulose DP. NMR and WAXD results indicated that lignin presence played a key role in preventing cellulose crystallite co-crystallization and coalescence during DAP. This indicates lignin acts as a barrier which restricts cellulose crystallinity increase and cellulose crystallite growth, and that partial delignification instead of complete lignin removal is better for enhanced sugar yield.

CHAPTER 6

INVESTIGATION OF STRUCTURAL TRANSFORMATION OF POPLAR AND SWITCHGRASS CELLULOLYTIC ENZYME LIGNINS DURING DILUTE ACID PRETREATMENT[3]

6.1 Introduction

Lignocellulosic biomass is one of the most abundantly sustainable resource for biofuels, biochemicals and biobased products production not only to meet the growing global demand for green energy and materials but also to decrease greenhouse gas emissions from fossil fuels.[223] To fully realize this potential, in-depth understanding of lignocellulosic recalcitrance which refers to plant cell wall's inherent resistance to deconstruction from microbes and enzymes needs to be advanced. Among numerous biomass features that contribute to the recalcitrance of biomass, lignin is considered as one of the most recalcitrant components in the plant cell wall[8, 72, 224] because of its structure, content, distribution and associations with plant polysaccharides within the cell wall.[104, 225] Lignin is derived from hydroxycinnamyl monomers with various degrees of methoxylation forming a racemic, cross-linked, and highly heterogeneous aromatic

[3] This manuscript was entitled as — Investigation of Structural Transformation of Isolated Poplar and Switchgrass Lignins from Dilute Acid Pretreatment. The other authors are Yunqiao Pu, Xianzhi Meng, Tyrone Wells, Jr. and Art J. Ragauskas from School of Chemistry and Biochemistry at Georgia Institute of Technology; Biosciences Division, Oak Ridge National Laboratory; and Department of Chemical and Biomolecular Engineering; Department of Forestry, Wildlife, and Fisheries, Center for Renewable Carbon, University of Tennessee.

macromolecule.[57] Lignin and hemicellulose are embedded between and around cellulose microfibrils, providing rigidity and structural support to plant cell walls, which were evolved over millions of years to resist biological and chemical attack. This native structural complexity and inhibition becomes a major barrier in biomass deconstruction and conversion to biofuels.[8]

To date, the biochemical conversion of lignocellulosic biomass to biofuels most often involves three essential steps: pretreatment to reduce the inherent plant cell wall recalcitrance, enzymatic hydrolysis to deconstruct polysaccharides into fermentable sugars, and fermentation to convert those sugars into ethanol. The goal of pretreatment is to modify physiochemical features of plant cell wall so that the resulting biomass is more amenable to enzymatic deconstruction. Dilute acid pretreatment (DAP) has been recognized to be one of the most effective pretreatment technologies that can enhance biomass sugar yield.[226] The important role of lignin morphological and structural change after DAP in enzymatic hydrolysis has been the target of several studies but is still under considerable debate. Study of morphology change has revealed that lignin tends to coalesce into larger aggregates accompanying with their relocalization and deposition as droplets on the surface of biomass cell walls during DAP as the reaction temperatures are above the melting point of lignin. This effect is proposed to open up the cell wall matrix structure and thereby improve the cellulose accessibility for enzymes.[103b] Recent studies have also revealed that the efficiency of downstream enzyme hydrolysis was impeded due to the blockage of the cellulose surface layer by lignin droplets, prevention of enzymes accessibility to inner layers,[227] and the formation of cellulase-lignin interactions

to deactivate the enzymes.[101] As a result, no clear picture was given up to date about lignin chemistry nature and how these structural changes limit efficient sugar release.

More recent work, which investigated the fate of cellulolytic enzyme lignin under autohydrolysis pretreatment conditions, reported a drastic decrease in the molecular weight [228] that is different from those research investigating the changes in structural characteristics of lignin isolated from pretreated biomass.[62b, 229] This difference in lignin fate during pretreatments is attributed to the partial protection of lignin by polysaccharides in the compact biomass matrix.[228] This suggests understanding lignin structural parameters relevant to plant cell wall recalcitrance and how those parameters individually and synergistically affect enzymatic saccharification are vital for improving current bioconversion process.

In order to provide fundamental information of lignin chemistry under dilute acid pretreatment at high severity with the least influence of plant cell wall polysaccharide biopolymers, cellulolytic enzyme lignin isolated from bioenergy crops, poplar and switchgrass, were pretreated with 0.1 M H_2SO_4 at 160 ℃ for 0-20 min residence time and were structurally analyzed by two dimensional (2D) ^{13}C-^{1}H heteronuclear single quantum coherence (HSQC) nuclear magnetic resonance (NMR) spectroscopy, phosphitylation followed by ^{31}P NMR and gel permeation chromatography (GPC) analysis (Sample code Poplar-0: indicates native lignin isolated from poplar; SWG-0: native lignin isolated from switchgrass; P-160-20: poplar lignin subjected to DAP at 160 ℃ for 20 min; SWG-160-20: switchgrass lignin subjected to DAP at 160 ℃ for 20 min).

6.2 Experimental Section

6.2.1 Materials

Poplar and switchgrass samples plus chemicals for biofuel study were prepared as described in Chapter 3 (3.1.1 and 3.1.2).

6.2.2 Enzymatic Isolation of Lignin

Cellulolytic enzyme lignin isolated from bioenergy crops, poplar and switchgrass was described in Chapter 3 section 3.2.6.

6.2.3 Dilute Acid Pretreatment of Cellulolytic Enzyme Lignins

DAP of lignin was described in Chapter 3 section 3.2.7.

6.2.4 GPC Analysis of Lignin

Analyzing procedure was described in Chapter 3 section 3.3.4.

6.2.5 NMR Analysis of Lignin

^{13}C-^{1}H HSQC and ^{31}P NMR spectroscopy analysis of lignin structural changed were described in Chapter 3 section 3.3.9.2 and 3.3.9.3.

6.3 Results and Discussion

6.3.1 Molecular Weight Analysis of Lignins

To determine the effect of DAP conditions on the molecular weight of lignin, untreated and pretreated lignin samples were acetylated and subsequently analyzed by GPC and these results are summarized in Figure 40. There was a drastic decrease in molecular weights of pretreated lignins within a short 5 min residence time (i.e., M_w of poplar lignin from 12,000 to 1560 g/mol; M_w of switchgrass lignin from 6800 to 1590 g/mol) followed by a leveling-off with increasing residence time. The GPC analysis also revealed that the most significant increase in PDI occurred after a 2 min DAP which is then accompanied by a decrease with longer residence time, which could be attributed to the behavior of M_n and M_w. Compared with previous studies reporting that M_w of lignin isolated from pretreated switchgrass and poplar was reduced by 16.8% and 3.2% respectively,[62b, 115, 229] it could be concluded that the protection of polysaccharides in plant cell walls offset this significant decrease in the molecular weight of lignin. This suggests in the absence of intact cellulose and hemicelluloses at elevated hydrothermal conditions, lignin is subjected to a significant de-polymerization in a very short residence time, which is consistent with previous study on lignin fate under autohydrolysis pretreatment.[228]

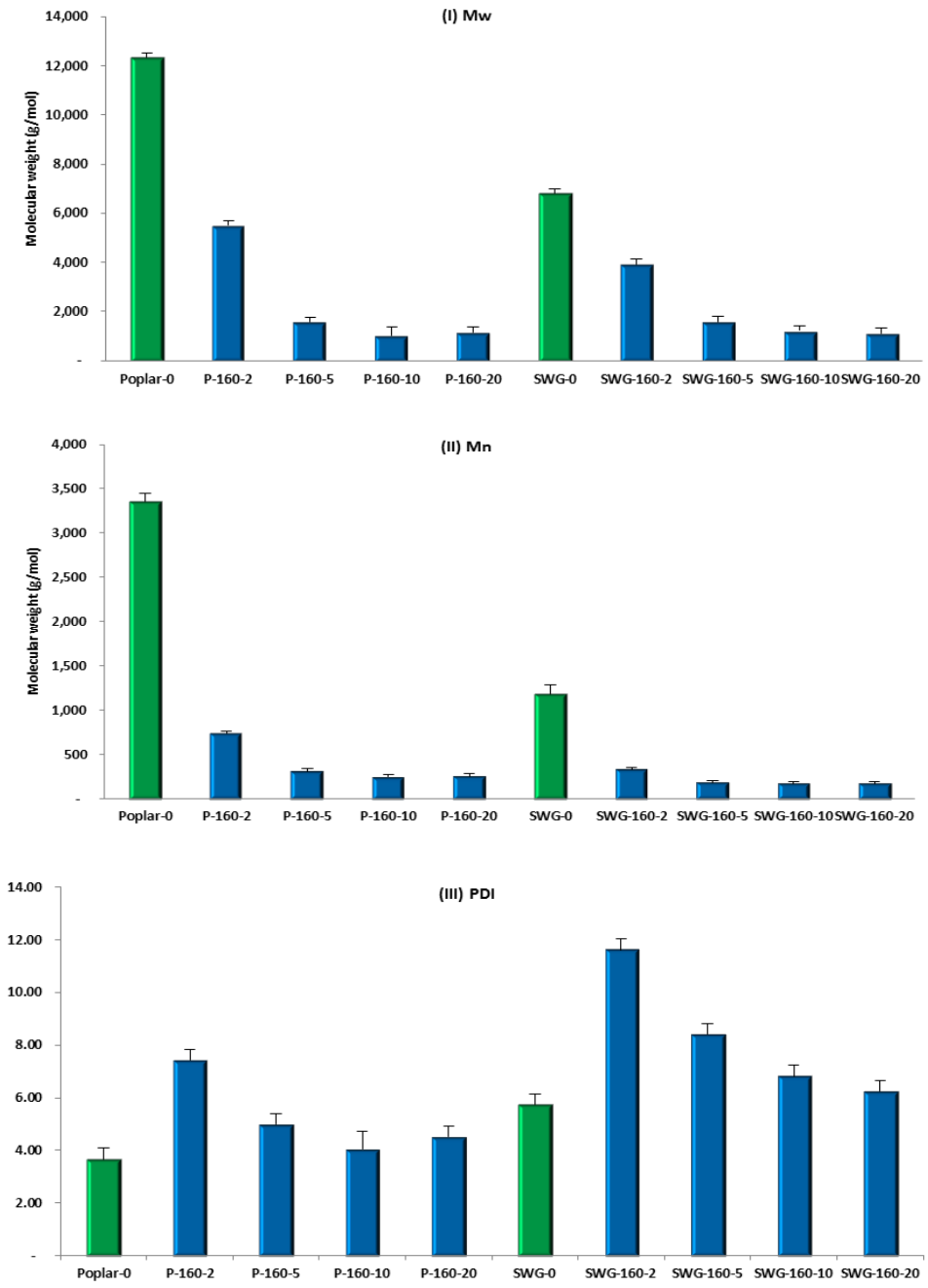

Figure 40 Molecular weight change of cellulolytic enzyme lignin after DAP at various residence time. (I) Weight average molar mass (M_w), (II) Number average molar mass (M_n), (III) polydispersity index (PDI).

6.3.2 Structural Analysis of Lignins by NMR

2D-HSQC NMR semi-quantitative analysis of untreated and pretreated lignin samples provided the evidence of structural changes in lignin side chain and aromatic regions during DAP. The cross peaks were assigned by comparing with literature data and summarized in Figure 41.[62b, 230] The major inter-units observed in untreated raw poplar and switchgrass lignins were the β-aryl ether linkages (A) with accompanying β-5/β-O-4 phenylcoumaran (B) and resinol (C) units. The presence of lignin syringyl (S), guaiacyl (G), p-hydroxybenzoate (PB), and cinnamaldehyde (E) units was confirmed in poplar lignin by the separate contour in the aromatic range, while syringyl, guaiacyl, p-hydroxyphenyl (H), and p-coumarate (E') units were observed in switchgrass lignin.

The assessment of cross-peak intensity qualitatively suggested a decrease in intensity of β-aryl ether linkages as well as phenylcoumaran and resinol units for both poplar and switchgrass lignins as DAP residence time extended from 2 to 20 min, which are typically correlated with the hydrolytic degradation and/or de-polymerization consistent with the observed molecular weight changes. Compared to switchgrass lignin, a more noticeable decrease in poplar lignin aromatic signal intensities of PB, and G units was observed under the same DAP conditions. In addition, the HSQC analysis revealed the signal intensity of E unit in untreated poplar lignin dramatically diminished after DAP for 2 min. Moreover, there were still traces in E' unit in switchgrass lignin after DAP for 20 min. Interestingly, HSQC NMR spectra indicated the presence of the polysaccharides (δ_C/δ_H 95.0-105.0/4.2-4.5) associated with lignin-carbohydrate linkages in untreated poplar and switchgrass cellulolytic enzyme lignins. The degradation of lignin-

carbohydrate linkages suggested those linkages in switchgrass were more resistant to DAP degradation than the comparable poplar lignin carbohydrate complexes. This could also suggest subsets of hemicelluloses might be the key recalcitrance-causing factors in switchgrass. [225a]

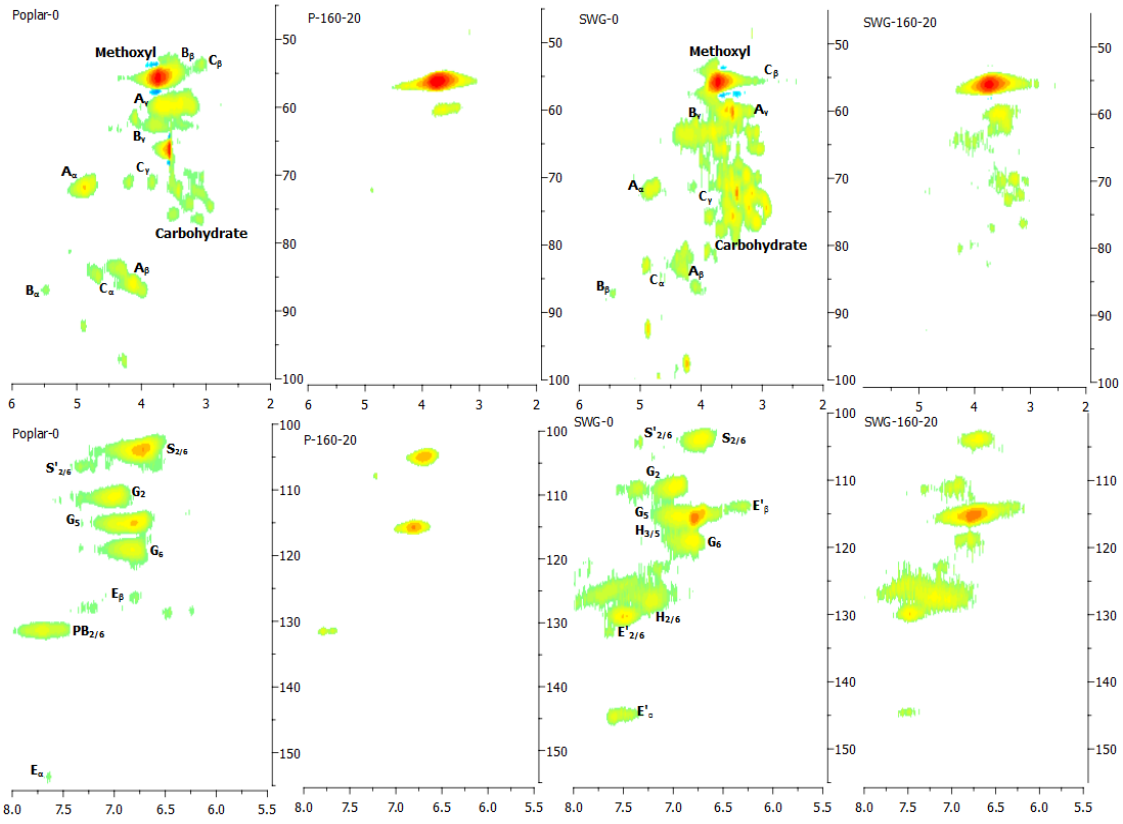

Figure 41 Selected 2D-HSQC spectra of poplar and switchgrass cellulolytic enzyme lignins before and after DAP. A: β-O-4 ether; B: phenylcoumaran; C: resinol; G: guaiacyl; S: syringyl; S': syringyl units with oxidized α–ketone; H: p-hydroxyphenyl; PB: p-hydroxybenzoate; E: cinnamaldehyde; E': p-coumarate unit (structure shown in Figure 43).

To further investigate the fundamental chemistry of lignin during the DAP during the pretreatment processes, quantitative ^{31}P NMR technique was applied to monitor the changes of aliphatic, phenolic hydroxylic and carboxylic functional groups in poplar and switchgrass lignins after DAP at different residence times and the results were shown in Figure 42. The relative increase of aliphatic and phenolic OH groups after 2 min DAP can be attributed to the cleavage of aryl ether linkages and a concomitant increase in free phenolics which could allow for lower molecular weight oligomers of lignin to be solubilized. This reaction pathway is supported by the observation of the increased PDI. Moreover, there is no noticeable change in the condensed lignin content for the 2 min pretreated samples which suggests that the de-polymerization reactions dominate the reaction pathways at the initial stage of DAP.

When residence time was extended beyond 2 min, a decrease in aliphatic OH, total phenols and G lignins along with an increase in S and condensed lignins and carboxylic acids were observed. The reduction in lignin side chain aliphatic hydroxyl contents resulted not only from the hydrolytic degradation of carbohydrate residue linked to lignin, but also from transformation of lignin α-OH, γ-OH groups into ketone, aldehyde and/or alkene structures like stilbene substructures.[229] The increase in phenolic S units content in both switchgrass and poplar lignin indicated that syringyl unit in lignin underwent a greater extent of ether linkage cleavage during the pretreatment. This could be attributed to the lacking of association and protection of lignin by cellulose and hemicelluloses in biomass matrix.[62b, 229] Furthermore, the larger values of carboxylic acid groups in pretreated switchgrass lignins were mainly attributed to the hydrolysis of *p*-

coumarate units, and partially from the cleavage of the ester bonds from lignin-carbohydrate linkages. This is proposed to improve enzymatic hydrolysis due to the decrease in lignin hydrophobicity and enzyme binding by electrostatic repulsion between enzymes and lignins.[108]

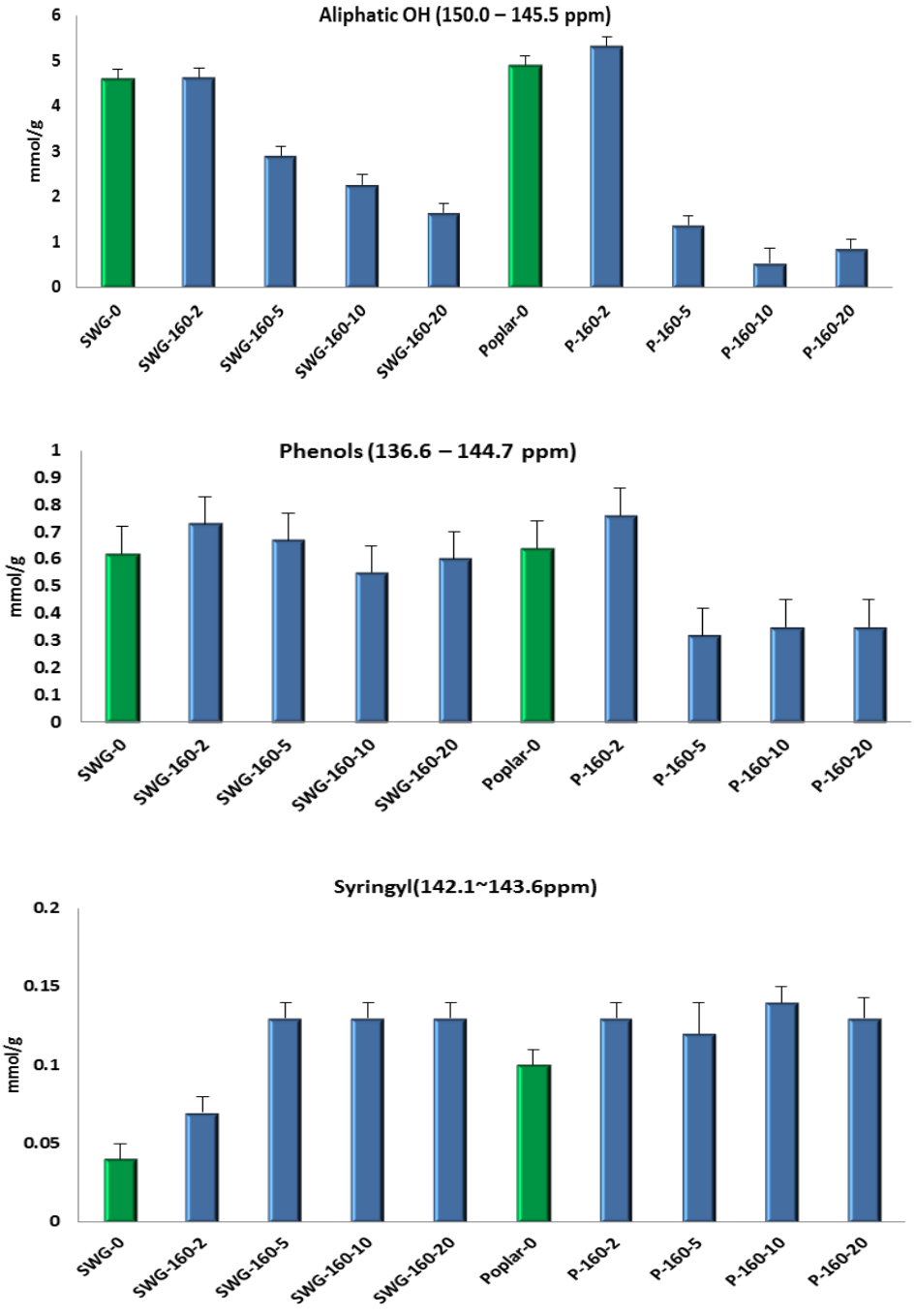

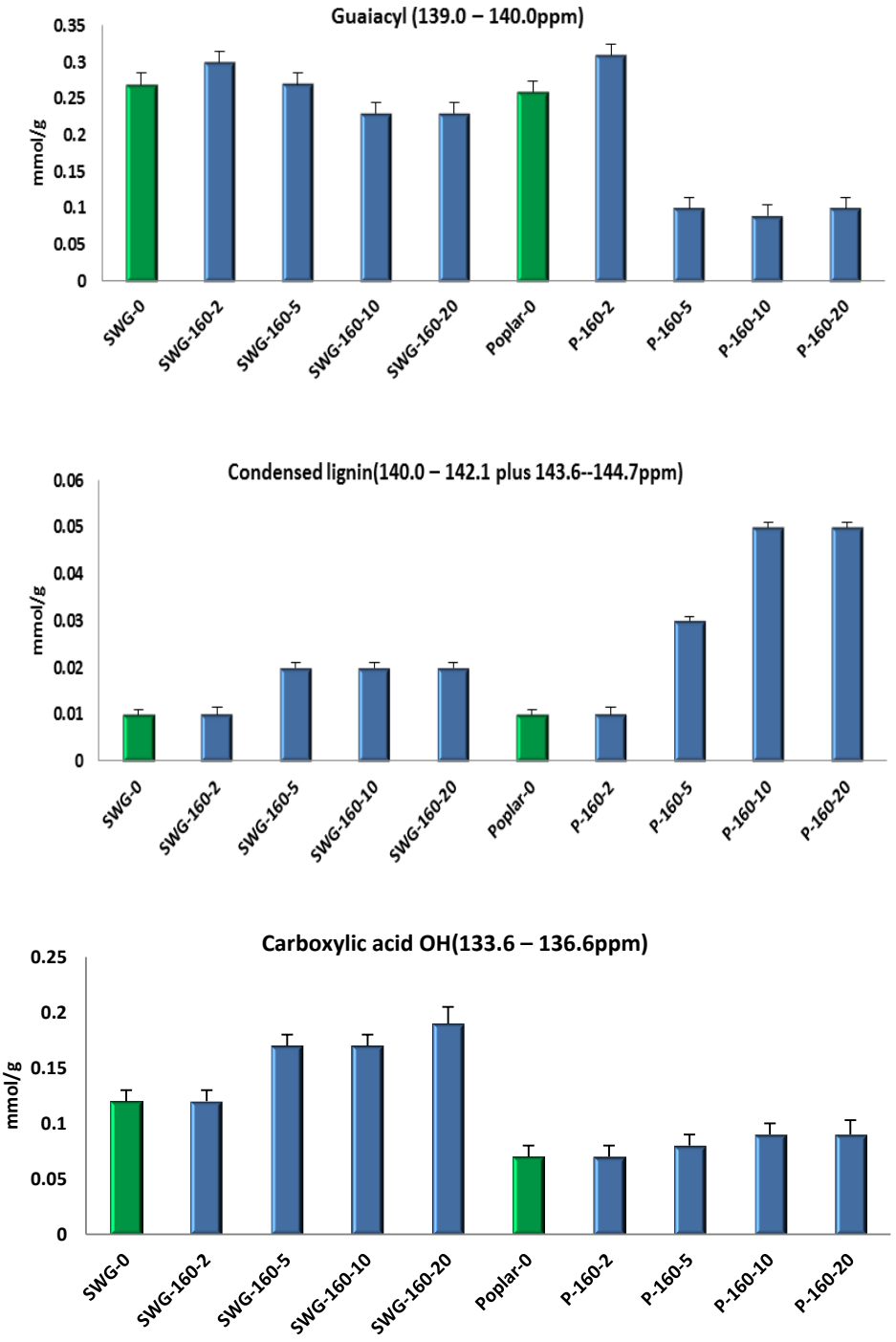

Figure 42 Hydroxyl group contents in poplar and switchgrass cellulolytic enzyme lignins before and after DAP calculated from quantitative ^{31}P NMR spectra.

In addition, the possible mechanistic pathways associated with these structural changes during DAP are proposed in Figure 43. Both switchgrass and poplar lignins are subjected to a de-polymerization reaction at the earlier stage of DAP followed by a competition between de-polymerization and re-polymerization reactions at a later pretreatment stage. The departure of a leaving group by an S_N1 process from a benzylic position (C_α of lignin side chain) leads to the formation of resonance-stabilized benzylic carbocation intermediate that could be involved into the key rate-determining step for a reaction and thereby direct the following lignin de-polymerization and re-polymerization under hydrothermal conditions. The resonance stabilized carbocation facilitates several potential condensed structures to formed, such as β-5 and α-5 linkages.

Given the results above and previous studies regarding higher severities favoring more condensation reactions,[231] in which higher temperature and longer residence time overcome the higher energy barrier and ultimately produce the equilibrium mixture of condensed lignins, the competition of lignin de-polymerization and re-polymerization could turn into the competition of kinetic and thermodynamic influence on lignin structural changes during DAP.

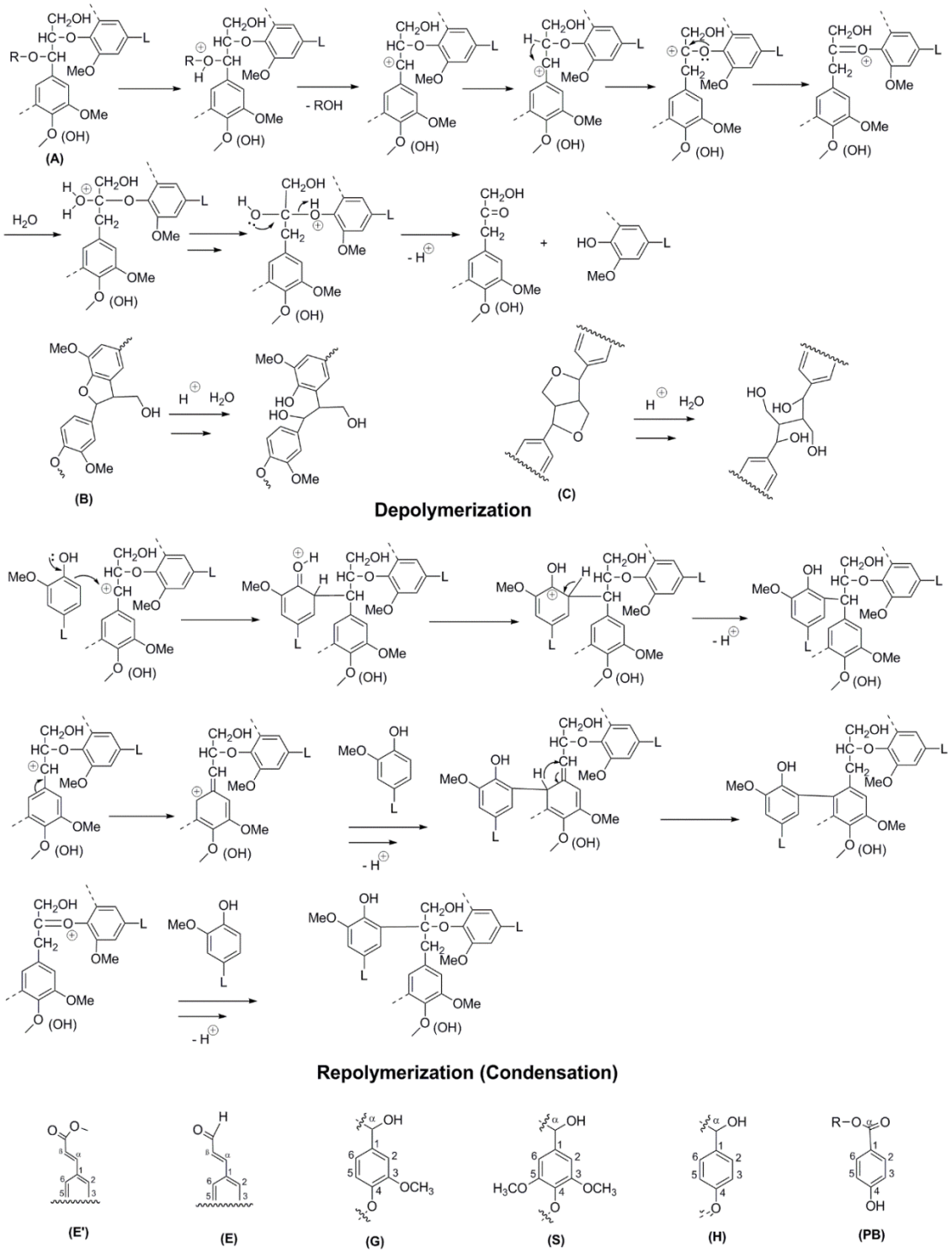

Figure 43 Proposed mechanistic pathway for cellulolytic enzyme lignin de-polymerization and re-polymerization during DAP.

6.4 Conclusion

Lignin was isolated from poplar and switchgrass using a cellulolytic enzyme system and then treated under DAP conditions in order to determine the intrinsic chemistry of lignin during dilute acid pretreatment (DAP). Our results highlights that lignin is subjected to de-polymerization within the 2 min of dilute acid pretreatment time at 160 ℃ and these changes are accompanied with increasing values for the aliphatic and phenolic hydroxyl groups of lignin. This is followed by a competing set of de-polymerization and re-polymerization reactions which lead to a decrease in the content of guaiacyl lignin units and an increase in condensed lignin units as the reaction residence time is extended beyond 5 min at 160 ℃. A detailed comparison of changes in functional groups and molecular weights of cellulolytic enzyme lignins demonstrated different structural parameters related to the recalcitrant properties of lignin are altered during the pretreatment conditions. A better and deeper understanding of the fundamental chemical structure of lignin in this study, the most recalcitrant component of biomass, during DAP is critical to the continued growth of renewable biofuel production.

CHAPTER 7

PHYSICOCHEMICAL PROPERTIES OF POPLAR LIGNIN CARBON PRECURSOR BEFORE AND AFTER MELT RHEOLOGY[4]

7.1 Introduction

Carbon fibers are one of the most important engineered materials for a variety of industrial applications due to its unique properties, including high stiffness and tensile strength, low thermal expansion and density, heat tolerance and reagent resistance. However, the main barriers to the large-scale production of commercial products are the high cost of petroleum-based precursors polyacrylonitrile (PAN) and associated processing costs.[232] In an effort to address these barriers, lignin as an alternative precursor with low cost draws significant attention to the future manufacturing of carbon fiber.[233] However, to date, lignin based carbon fibers do not offer mechanical properties required for many structural application. Several factors have been proposed to diminish physical properties of lignin carbon fiber, including structural heterogeneity, impurities

[4] This manuscript was entitled as — Physicochemical Characteristics of Poplar Lignin Carbon Precursors before and after Melt Rheology. The other authors are Ratayakorn Khunsupat, Sam K. Akato, Jingming Tao, Nicole Labbé, Nidia C. Gallego, Joseph J. Bozell, Timothy G. Rials, Gerald A. Tuskan, Timothy J. Tschaplinski, Amit K. Naskar, Yunqiao Pu and Art J. Ragauskas from School of Chemistry and Biochemistry, Renewable Bioproducts Institute, Georgia Institute of Technology; Carbon & Composites Group, Oak Ridge National Laboratory; Center for Renewable Carbon, University of Tennessee Institute of Agriculture; Biosciences Division, Oak Ridge National Laboratory; Department of Chemical and Biomolecular Engineering; Department of Forestry, Wildlife, and Fisheries, Center for Renewable Carbon, University of Tennessee.

and isolation methods.[233b] Our research focuses on exploring various lignin structures and the associated chemistry of lignin under thermal and mechanical deformation after a thermal melt treatment.

Lignin is one of the most abundant natural biopolymers that accounts for 10–30 wt% of the plant cell walls. It is a complex substituted polyphenol derived from typically hydroxycinnamyl monolignols (i.e., coniferyl alcohol, sinapyl alcohol, and para-coumaryl alcohol) with different degrees of methoxylation. The polymerization of these monolignols in native biomass yields a racemic, cross-linked, and highly heterogeneous aromatic macromolecule.[198, 234] Physical and chemical properties of lignin isolated from biomass depend to a large extent on its sources, syringyl (S), guaiacyl (G) and *p*-hydroxyphenol (H) monomer proportions, molecular weights, degree of branching, isolation methods, and purity. Of the chemical structures in biomass lignin, guaiacylic units show greater crosslinking reaction tendency than syringylic units,[156, 235] which result in more condensation reactions.[234, 236] Most of the lignin generated by the Kraft pulping process and the biofuel industry is currently utilized primarily as a low-cost fuel.[223] Therefore, significant attention has recently turned towards large-scale use of lignin in various applications, especially high value-added lignin-based high performance materials.

Current methods for the manufacturing of carbon fiber from lignin involve the preparation of lignin, fiber spinning, oxidative thermo-stabilization, carbonization, graphitization and surface treatment.[146] The complex and heterogeneous structure of

lignin has in the past restricted the application of lignin in biomaterial manufacturing. In an effort to increase the strength and maintain the integrity of lignin fiber during oxidative thermo-stabilization, keep the glass transition of lignin based material above the process temperature, and improve downstream processing and conversion methods, it is essential to understand changes in the thermo-rheological properties of lignin and its associated chemical structure. Such an understanding would facilitate the improvement of materials derived from lignin. The objective of this study is to build an understanding on the structural parameters relevant to lignin thermal behaviour and rheological properties and determine how those parameters individually and cooperatively affect melt processing of lignin for making value-added products.

The lignin syringyl/guaiacyl (S:G) ratio in biomass has been used in the past as good indicator of its response to pulping and biomass pretreatment.[237] In combination with previous studies concerning the correlation between lignin S:G and recalcitrance,[238] as well as the reported improved performance of engineered plastics with large amounts of guaiacyl groups,[239] this would suggest that the S:G may have significant implications on how to select suitable lignin for carbon fiber production. Moreover, establishing a correlation between lignin S:G values and lignin structural changes that occur during rheological testing could help elucidate the mechanisms that occur during carbon fiber melt spinning. This paper investigates the thermal behaviour and structural changes occurring to poplar (*Populus* sp.) lignin with various S:G properties as a result of thermal treatment at 170, 180 and 190 ℃ by nuclear magnetic resonance (NMR) spectroscopy (i.e. phosphitylation/^{31}P NMR, ^{13}C NMR), gel permeation chromatography (GPC), and

attenuated total reflectance Fourier transform infrared (ATR-FTIR) spectroscopy, in order to provide insight into the lignin cross-linking and/or scission mechanisms under thermo-rheological flow field.

7.2 Experimental Section

7.2.1 Materials

Three-year-old black cottonwood (*Populus trichocarpa*) clones harvested from a Genome-wide Association Study at Clatskanie, OR were harvested in December, 2012 as described in Chapter 3 section 3.1.2.

7.2.2 Lignin Isolation

Lignin isolation for carbon fiber study was described in Chapter 3 section 3.2.8.

7.2.3 Lignin Characterization and Thermal Analysis

Detailed procedure was described in Chapter 3 section 3.3.7.

7.2.4 Rheological Measurement

Melt viscosity values of the lignin samples (~ 400 mg) were measured using a strain-controlled ARES rheometer (TA Instruments) as described in Chapter 3 section 3.3.8.

7.2.5 Lignin Characterization after Rheological Test

To investigate and quantify chemical changes in lignin, a PerkinElmer Spectrum 100 FTIR spectrometer with a universal ATR sampling accessory was used as described in Chapter 3 section 3.3.2. Semi-quantitative analysis of chemical group change was carried out by normalizing the FTIR absorption spectra at a band position of 1506 cm^{-1} representing lignin aromatic skeletal vibration based on related studies.[240] For GPC test, the lignin samples (dried under vacuum at 40 ℃ overnight) were acetylated with acetic anhydride/pyridine (1/1, v/v) at room temperature for 24 h in a sealed flask under an inert atmosphere and prepared for molecular weight measurement, detailed procedure was described in Chapter 3 section 3.3.4. Phosphitylation and ^{31}P-NMR have been exploited to quantitatively determine hydroxyl functional groups in isolated lignin. Quantitative ^{31}P-NMR spectra were acquired after in situ derivatization of the lignin sample as described in Chapter 3 section 3.3.9.3. Further, HSQC experiments were carried out in a Bruker Avance/DMX 400 MHz NMR spectrometer as described in Chapter 3 section 3.3.9.2.

7.3 Results and Discussion

7.3.1 Lignin Purity and S/G Ratio

The values of original S/G ratios in the poplar samples used in this study are shown in Table 16. After solvent fractionation of lignin from the biomass, the S:G ratio in isolated lignin altered significantly, varying from 2.9 to 3.7. The chemical composition and S/G ratio of the lignin samples are summarized in Table 21. Lignins from TAG896 and

TAG99 which were fractionated at higher severity showed higher lignin purity at 95.30 and 94.80 wt%, respectively.

Table 21 Lignin chemical composition with syringyl, guaiacyl contents, and S/G ratio.

Biomass tag #	L (wt%)	Hm (wt%)	A (wt%)	S (%)	G (%)	S/ G
TAG750	92.58 ±0.37	1.56 ±0.01	0.20 ±0.00	39.8 ±0.2	13.1 ±0.2	3.0 ±0.0
TAG896	95.30 ±0.62	3.37 ±0.07	0.32 ±0.05	41.8 ±0.2	11.9 ±0.2	3.7 ±0.1
TAG1672	91.31 ±0.60	1.46 ±0.10	0.14 ±0.00	41.9 ±2.1	11.9 ±0.3	3.5 ±0.2
TAG562	91.43 ±0.40	1.64 ±0.34	0.21 ±0.05	44.4 ±0.1	14.2 ±0.2	3.11 ±0.0
TAG99	94.80 ±0.98	3.32 ±0.03	0.51 ±0.07	38.1 ±0.6	13.3 ±0.3	2.9 ±0.1

L: Lignin, Hm: Hemicellulose, A: Ash, S: syringyl, G: guaiacyl.

7.3.2 Thermal Analysis

The glass transition temperature (T_g) associated with all the lignin samples analyzed show a broad transition range (90–140 ℃). The differential scanning calorimetry (DSC) thermograms of the samples are shown in Figure 44. We hypothesized that G moieties in the poplar lignin are responsible for the crosslinked structure in lignin. It is expected that the sample with high S and low G content would exhibit low T_g.[241] On the other hand, lignin with high G content and least S component would exhibit high T_g.[241-242] lignin from TAG 896 exhibits a low T_g value and lignin from TAG 562 exhibits a high T_g value.

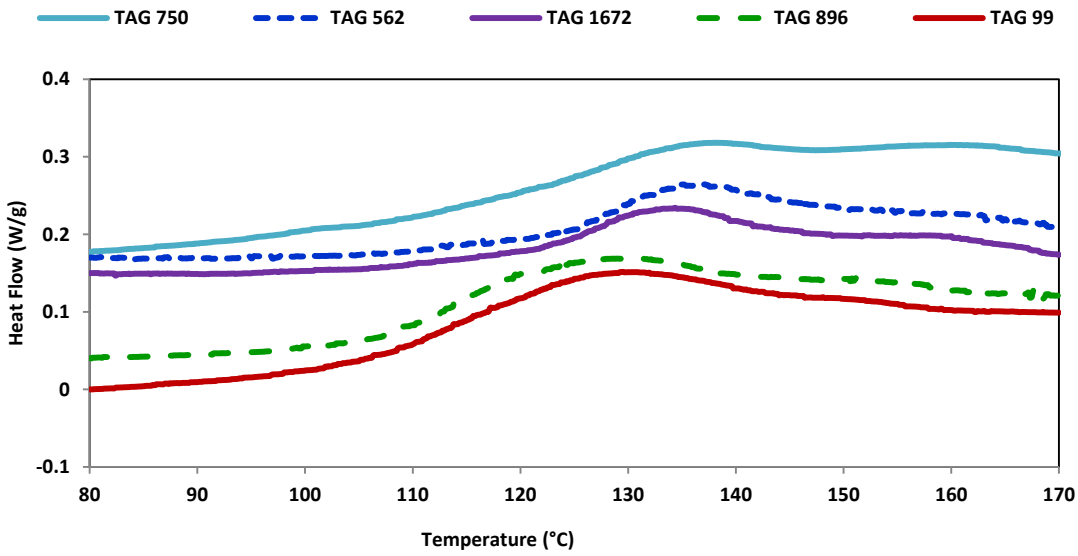

Figure 44 DSC thermograms of isolated lignin samples showing base line shift as glass transition temperature.

The results from thermogravemetric analysis (TGA) of the lignin samples (ran under nitrogen environment) are shown in Figure 45. The pyrolysis char residue at 1000 ℃ varies from 24–38 wt%. Lignin samples with high T_g offered high pyrolyzed char content and, likewise, low T_g lignin samples offered the least charred residue. The TGA runs were conducted on as-received samples without inducing any oxidative stabilization that is required for carbon fiber manufacturing. This trend suggests high yield carbon can be obtained from highly condensed lignin structure. However, such precursor is difficult to melt-spin into fiber form. Thus, an optimally crosslinked structure in lignin may not be necessary for initial fiber formation, but such crosslinking can be induced by thermal oxidation.

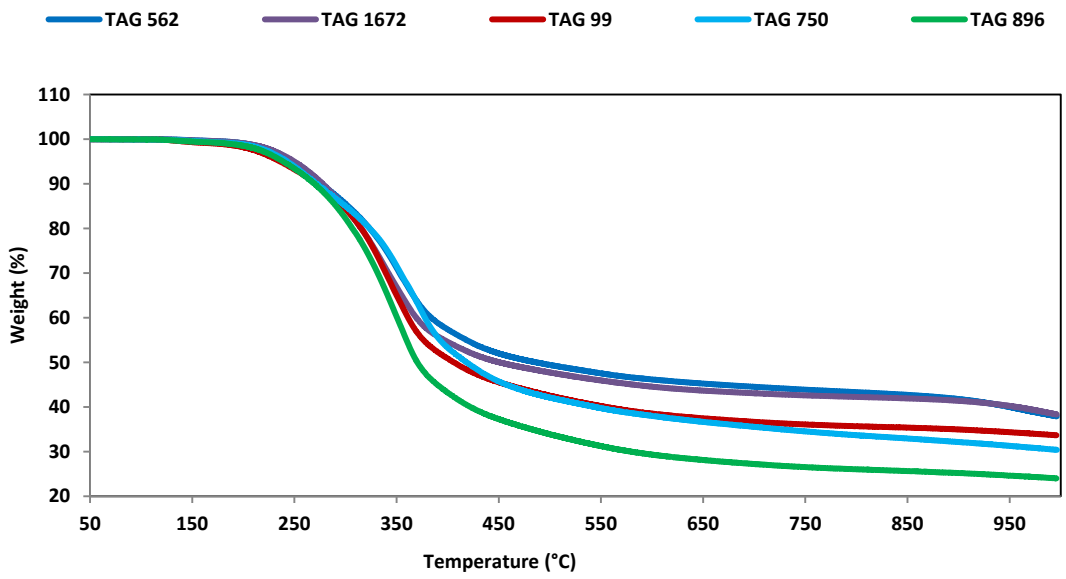

Figure 45 TGA thermogram of the isolated lignin samples.

7.3.3 Rheological Data Analysis

The rheological properties of lignin play an important role in optimizing the processing conditions during the melt spinning of lignin carbon fiber. The flow behaviors of poplar lignin samples were investigated at different temperatures of 170, 180, and 190 ℃. As shown in Figure 46, poplar lignin displayed differing time and temperature dependent transient viscosity profiles. At the lower temperature of 170 ℃, the low S:G poplar samples with high T_g exhibited higher viscosity values. Although lignin from TAG99 has A low S:G ratio, its molecular weight value is low (will be discussed later). Thus viscosity values are controlled by both chemical reactivity as well as degree of de-polymerization on the isolated lignin. Prolonged thermo-rheological shear exposure of lignin increased the melt viscosity suggesting thermal cross-linking of lignin segments.

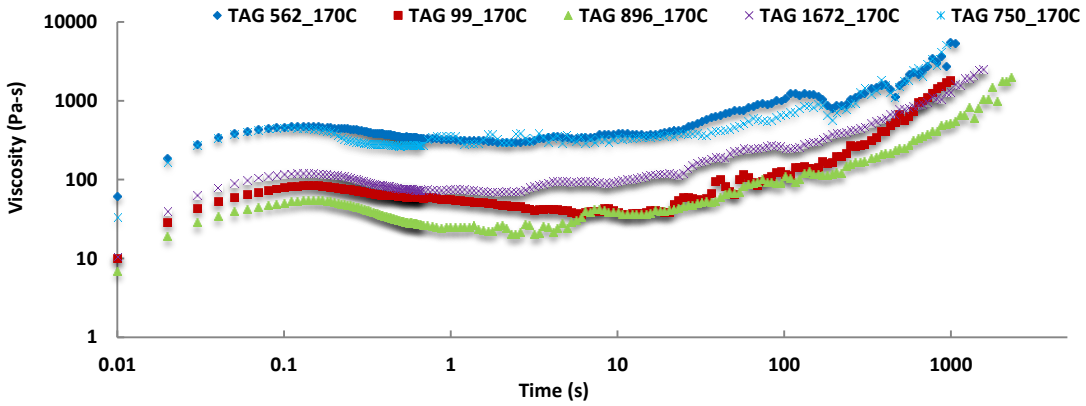
TAG 562_170C
TAG 99_170C
TAG 896_170C
TAG 1672_170C
TAG 750_170C
Viscosity (Pa-s)
10000
1000
100
10
1
0.01
0.1
1
10
100
1000
Time (s)

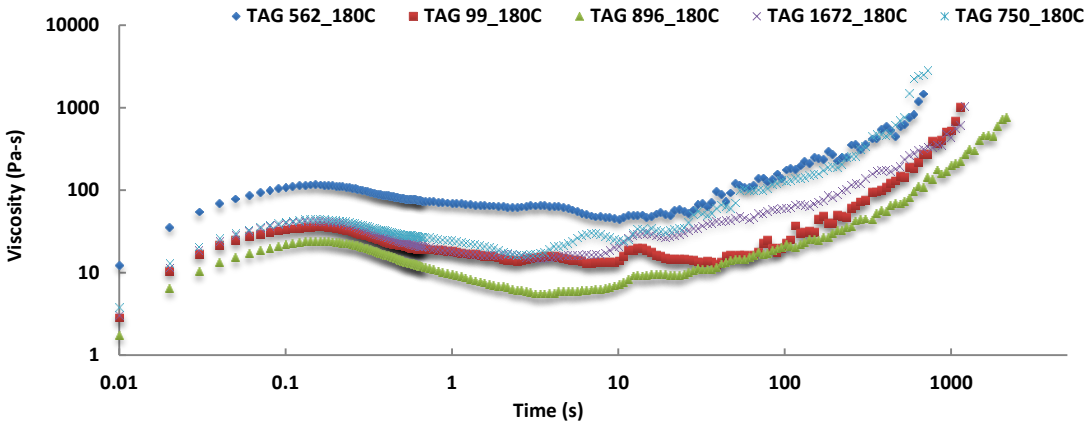
TAG 562_180C
TAG 99_180C
TAG 896_180C
TAG 1672_180C
TAG 750_180C
Viscosity (Pa-s)
10000
1000
100
10
1
0.01
0.1
1
10
100
1000
Time (s)

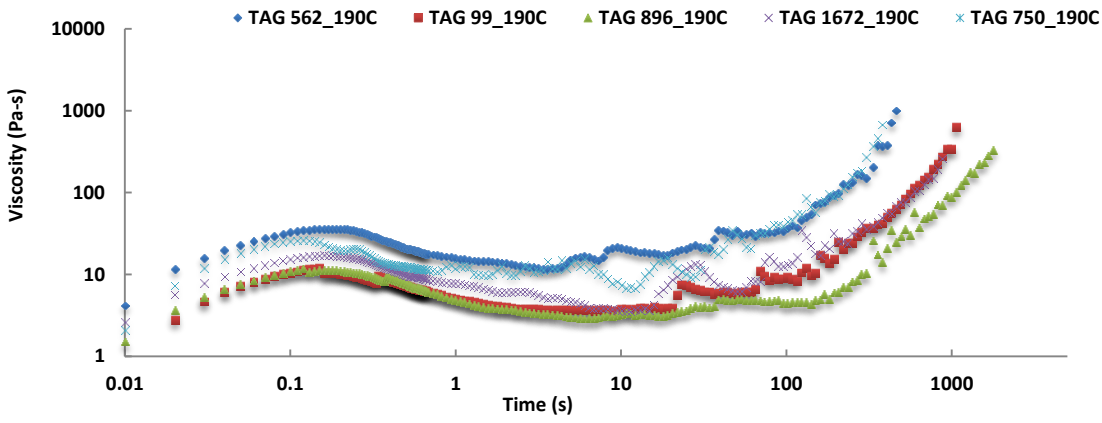
TAG 562_190C
TAG 99_190C
TAG 896_190C
TAG 1672_190C
TAG 750_190C
Viscosity (Pa-s)
10000
1000
100
10
1
0.01
0.1
1
10
100
1000
Time (s)

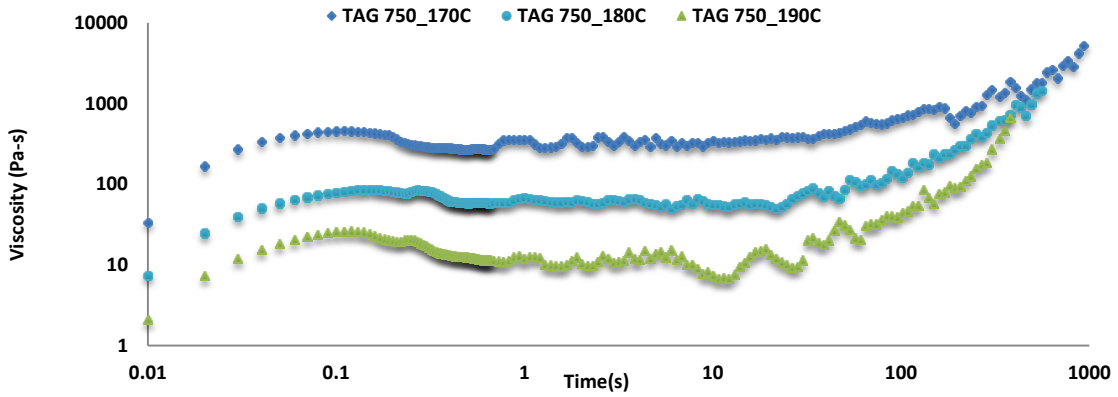

Figure 46 Relation between the shear viscosity and shear rate of poplar lignin at different temperatures (170, 180 and 190 ℃).

The melt viscosity of the lignin samples is reduced significantly with increased temperature ranging from 170 to 190 ℃. The rise in viscosity at high temperature at prolonged thermo-rheological treatment is very high for the lignin sample TAG562 in which the G content is high. As expected, the TAG896 sample in which S:G ratio is very high exhibits a low viscosity at all temperature range and slower rise in viscosity at longer time. The rheo-crosslinking kinetics or chemo-rheological data analyzed based on equations (I) – (III) are displayed in Table 22. The equilibrium rate constants (k_∞) for thermo-chemical reactions of lignins from TAG896 and TAG99 are significantly less than the other 3 samples. Both of these samples were obtained under high severity condition (high temperature) and have very low T_g compared to others. Although sample TAG99 has relatively lower S content than the other lignins, the high severity extraction conditions could be the reason for its anomalous reactivity. The activation energy for the thermal reactions ($\Delta E_k/R$) follows similar trend as that of the equilibrium rate constant

(k_∞). The activation energy for change in viscosity due to thermal effect ($\Delta E_\eta/R$) is low for lignins from TAG896, TAG562 and TAG99.

Table 22 Chemo-rheological characteristics of poplar lignin.

Sample ID	k_∞ (1/s)	η_∞ (Pa.s)	$\Delta E_k/R$ (K)	$\Delta E_\eta/R$(K)
TAG896	74	2.58×10^{-27}	-4709	29059
TAG99	43	4.19×10^{-27}	-4181	28865
TAG1672	4.5×10^{7}	1.14×10^{-31}	-10685	34028
TAG562	4.4×10^{8}	6.48×10^{-26}	-11472	28409
TAG750	1.9×10^{11}	1.48×10^{-34}	-14142	37244

7.3.4 Molecular Weight Analysis

GPC was employed to determine the molecular weight distribution of lignin after the rheology testing. Weight-average molecular weight (M_w), number-average molecular weight (M_n), and polydispersity index ($PDI=M_w/M_n$) values for the lignin samples are presented in Figure 47. Lignin molecular weights increased to different extents after rheological testing at various temperatures compared with their controlled samples. There was a relative decrease of molecular weight as the temperature during rheology testing increased from 170 to 190 ℃. This decrease corresponds to their viscosity properties and indicates that most of the re-polymerization reactions in lignin occur at lower processing temperature, since the de-polymerization of lignin dominate the whole reactions at higher temperature.[155b] The significant increase of molecular weight in TAG562 and TAG750 after the rheology test at 170 ℃ in conjunction with their higher viscosity values suggests lignin with lower S/G ratio could result in the condensing reaction to a higher extent. The isolated lignins TAG99 and TAG896 have lower molecular weight and smaller PDI

values than the other lignin samples. These two samples were isolated at higher temperature conditions which might have led to degradation of lignin molecules by hydrolysis of ether linkages. TAG99 lignin is significantly depolymerized (likely that is why it exhibits low T_g value) and thus it behaves differently in rheological response discussed earlier. Viscosity data typically depends on molecular weight and its change depends, in part, on chemical reactivity. These two combined effect gives TAG99 moderate viscosity behaviour and low chemo-rheologically determined rate constant value.

In addition, lignin samples cooled under air condition after the 190 ℃ rheology test exhibited higher molecular weight than those under nitrogen. This suggests that oxygen during cooling could affect lignin macromolecular structure and contribute more to the formation of re-polymerized structure in comparison to nitrogen.[243]

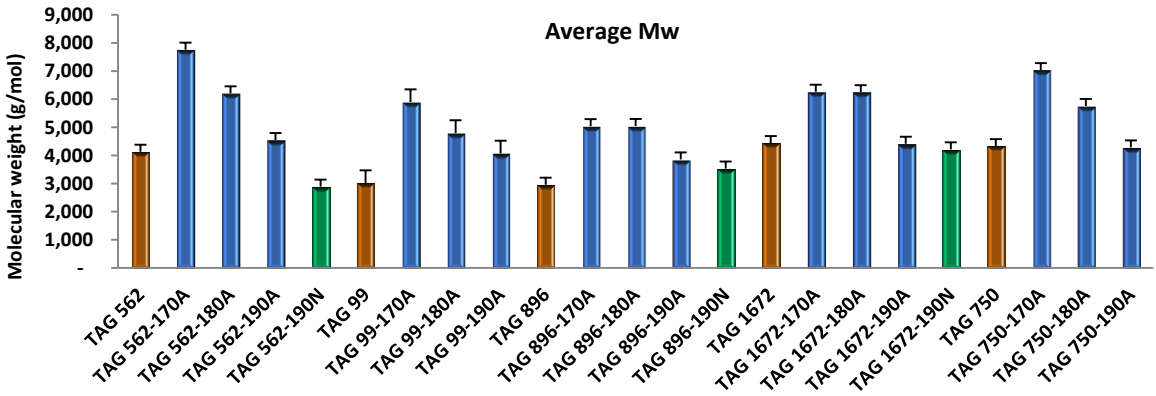

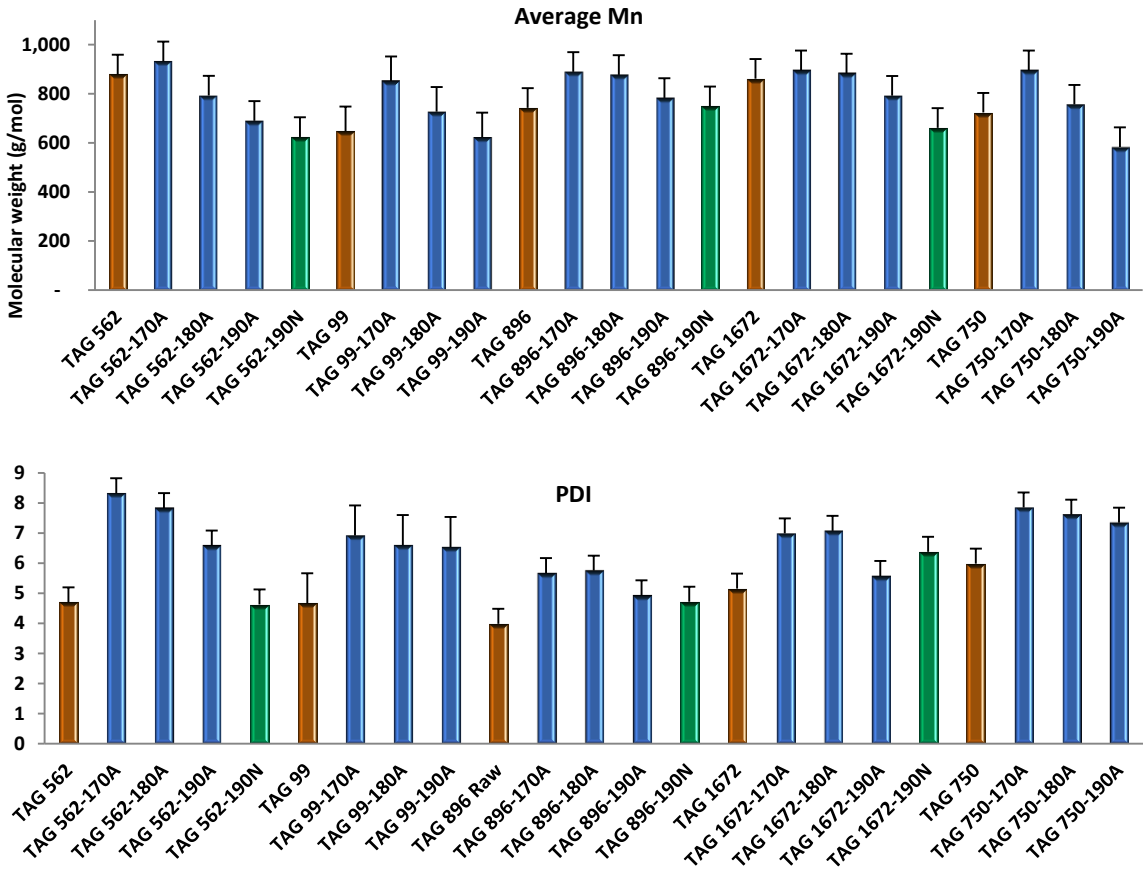

Figure 47 Molecular weights of lignin after rheology test.

7.3.5 NMR and FTIR Analysis

Structural changes occurring to poplar lignins as a result of the thermal rheology test were studied by solution NMR techniques, ^{31}P and ^{1}H-^{13}C HSQC experiment, and semi-quantitative ATR-FTIR analysis, in order to obtain details on chemical functionality. ^{31}P NMR quantitative analysis was carried out to analyze the amounts and distribution of various hydroxyl structures as summarized in Figure 48. Compared to controlled lignin samples, there is a reduction in lignin aliphatic hydroxyl and carboxyl acid groups as the rheology testing temperature is raised from 170 to 190 ℃. The decreased amounts of

these hydroxyl groups indicates that lignin side chain hydroxyl groups were eliminated the applied thermal condition, especially at higher temperature of 190 ℃. These cleavages of side chain hydroxyl groups could be attributed to the dehydration of aliphatic hydroxyl groups to water, sites of unsaturation and/or new formed cross-linkages bridging the aromatic rings. In contrast, the increased contents in guaiacyl, syringyl and catechol type hydroxyl groups after the rheology test at 170 ℃ could result from the cleavage of ether bonds, which was further confirmed by ATR-FTIR semi-analysis of main ether linkages as shown in Figure 50 The overall amount of phenols was also found to increase in the lignin sample after the rheology test at 170 ℃, which are attributed to a noticeable increase of syringyl and guaiacyl OH contents followed by ether linkage scission. However, higher temperature (190 ℃) favoring the cleavage of ether linkages, yielded lower amounts of phenolic OH, which could result from the intensive elimination reaction that transformed hydroxyl groups to water and/or double bonds of unsaturation. The noticeably increased amounts of terminal C5 condensed phenolic structures after 170 ℃ rheology test support the above results with respect to the increase of related molecular weights. This suggests rheology testing at 170 ℃ could lead to significant lignin re-polymerization, thereby resulting in modified lignin with higher viscosity and molecular weights. In contrast, the higher temperature of 190 ℃ tends to prevent the polymerization of lignin to a large degree, and thereby generating lignin with lower molecular weights and lower viscosity. During the rheology test, lignin with lower S;G generates more cross-linkages that could exist as a bridge between the aromatic rings and/or as a cyclic form attached to aromatic carbons. This could be attributed to the active C5 induced by the cross-linking reaction in a higher proportion of guaiacyl lignins.

Moreover, a large amount of aliphatic OH in controlled lignin sample TAG562 and TAG750 would be another key factor affecting their molecular weight and viscosity increase during rheology test, because the strength of hydrogen bonding for primary versus secondary alcohols is different. Previous study has shown the presence of γ-OH groups strongly reduced the thermal mobility of the β-O-4 model oligomers.[244] Therefore, lignin containing more aliphatic OH groups including both secondary α-OH and primary γ-OH groups would be shown to be more infusible during the rheology test. Moreover, lignin under nitrogen cooling after the rheology test at 190 ℃ yielded fewer amounts of various hydroxyl groups than lignin under air cooling, which indicates oxygen could oxidize parts of lignin hydroxyl groups to carboxylic acids and introduce more oxygenated compounds into the lignin macromolecules.

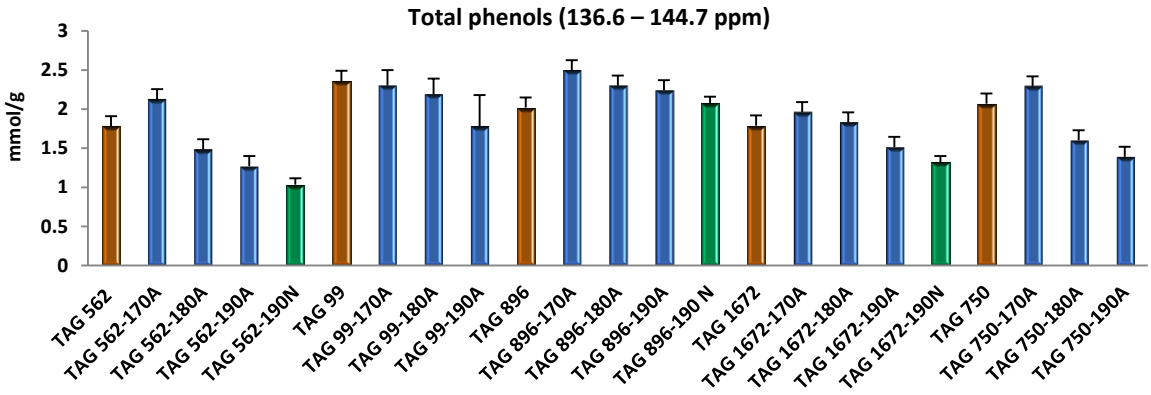

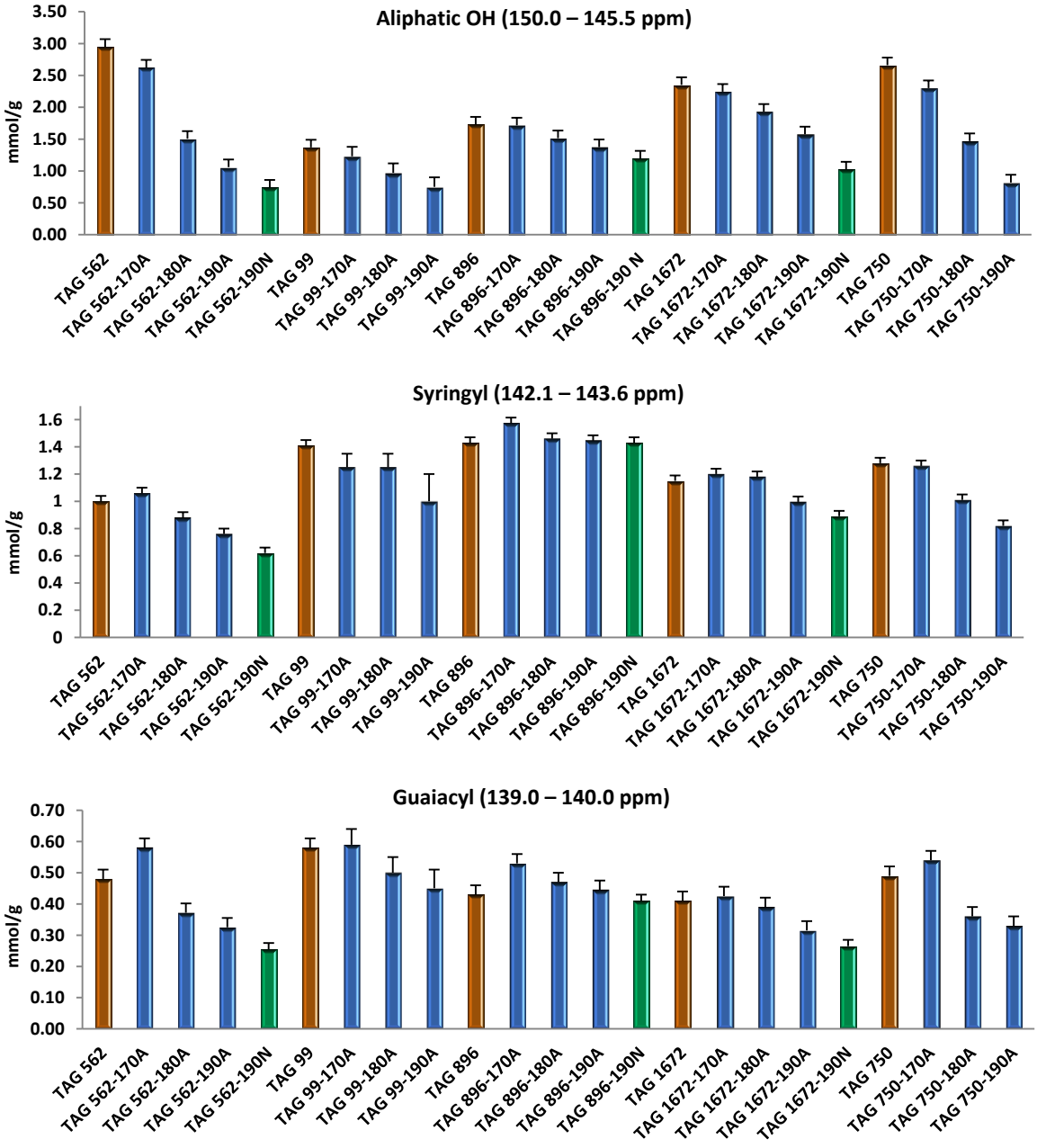
Aliphatic OH (150.0 – 145.5 ppm)
mmol/g
3.50
3.00
2.50
2.00
1.50
1.00
0.50
0.00
TAG 562
TAG 562-170A
TAG 562-180A
TAG 562-190A
TAG 562-190N
TAG 99
TAG 99-170A
TAG 99-180A
TAG 99-190A
TAG 896
TAG 896-170A
TAG 896-180A
TAG 896-190A
TAG 896-190 N
TAG 1672
TAG 1672-170A
TAG 1672-180A
TAG 1672-190A
TAG 1672-190N
TAG 750
TAG 750-170A
TAG 750-180A
TAG 750-190A
Syringyl (142.1 – 143.6 ppm)
mmol/g
1.6
1.4
1.2
1
0.8
0.6
0.4
0.2
0
TAG 562
TAG 562-170A
TAG 562-180A
TAG 562-190A
TAG 562-190N
TAG 99
TAG 99-170A
TAG 99-180A
TAG 99-190A
TAG 896
TAG 896-170A
TAG 896-180A
TAG 896-190A
TAG 896-190N
TAG 1672
TAG 1672-170A
TAG 1672-180A
TAG 1672-190A
TAG 1672-190N
TAG 750
TAG 750-170A
TAG 750-180A
TAG 750-190A
Guaiacyl (139.0 – 140.0 ppm)
mmol/g
0.70
0.60
0.50
0.40
0.30
0.20
0.10
0.00
TAG 562
TAG 562-170A
TAG 562-180A
TAG 562-190A
TAG 562-190N
TAG 99
TAG 99-170A
TAG 99-180A
TAG 99-190A
TAG 896
TAG 896-170A
TAG 896-180A
TAG 896-190A
TAG 896-190N
TAG 1672
TAG 1672-170A
TAG 1672-180A
TAG 1672-190A
TAG 1672-190N
TAG 750
TAG 750-170A
TAG 750-180A
TAG 750-190A

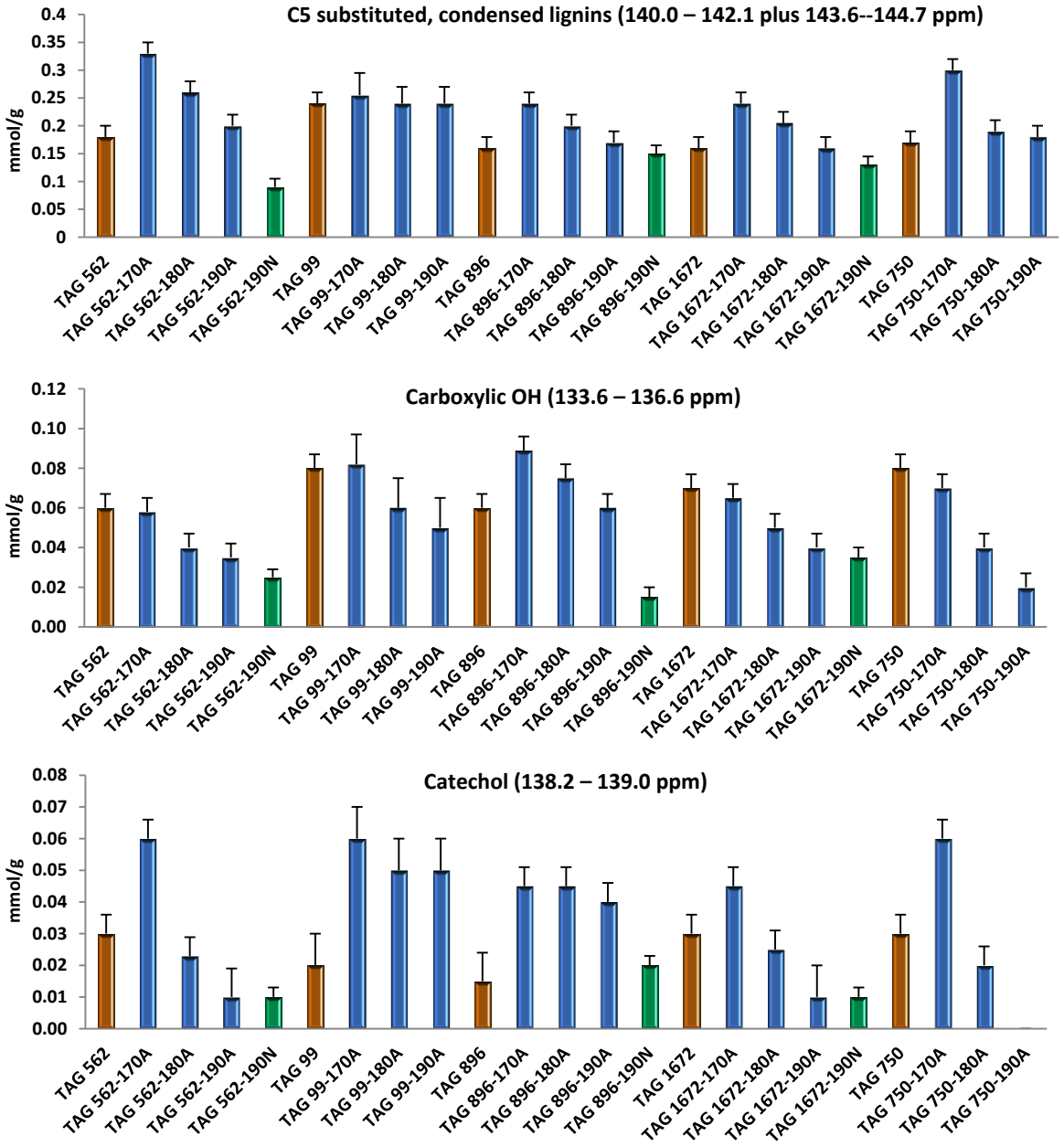

Figure 48 Integration regions and hydroxyl contents in lignin calculated from ^{31}P NMR data.

In addition, in an effort to investigate the lignin chemical structure changes under different cooling conditions at 190 ℃, HSQC NMR of three groups of lignin were carried out and the spectra are summarized in Figure 49. The cross peaks were assigned

by comparing with the literature data.[230a, 245] In aliphatic region, the reduction in signal intensity of A_γ, B_β and the signal loss in A_α, A_β, C_α, C_β, and C_γ indicate the decrease and/or loss of *β*-O-4 ether bonds, *β*-5/*α*-O-4 phenylcoumaran linkages, which suggest the scission of ether-aryl linkages during the rheology test. In the aromatic region, after the rheology test at 190 ℃, the considerable reduction in aromatic resonances including syringyl and guaiacyl lignin units is in good agreement with aliphatic region change indicating the change of lignin side chains and possible re-polymerization reaction of aromatic units. The change of side-chain signals from various *β*-O-4 linkages that constitute the main inter-monomeric linkage in lignin, is a good indicator of the characteristics of the lignin. The significant reduction of signal intensity in *β*-O-4 linkages after the rheology test at 190 ℃ was further confirmed by ATR-FTIR results in Figure 50, which indicated the re-polymerization of lignin. Interestingly, lignin under nitrogen cooling remained with relatively more *β*-O-4 ether linkages than lignin under air cooling. This could suggest nitrogen's inert properties protect the lignin and result in the less scission of ether linkages compared to oxygen at higher temperature 190 ℃. This in conjunction with molecular weight and ^{31}P NMR results indicate oxygen significantly contributes to the formation of cross-linkages among lignin molecules through a series of elimination, rearrangement and oxidative reactions of free radicals derived from homolysis of *β*-O-4 ether bonds in lignin.

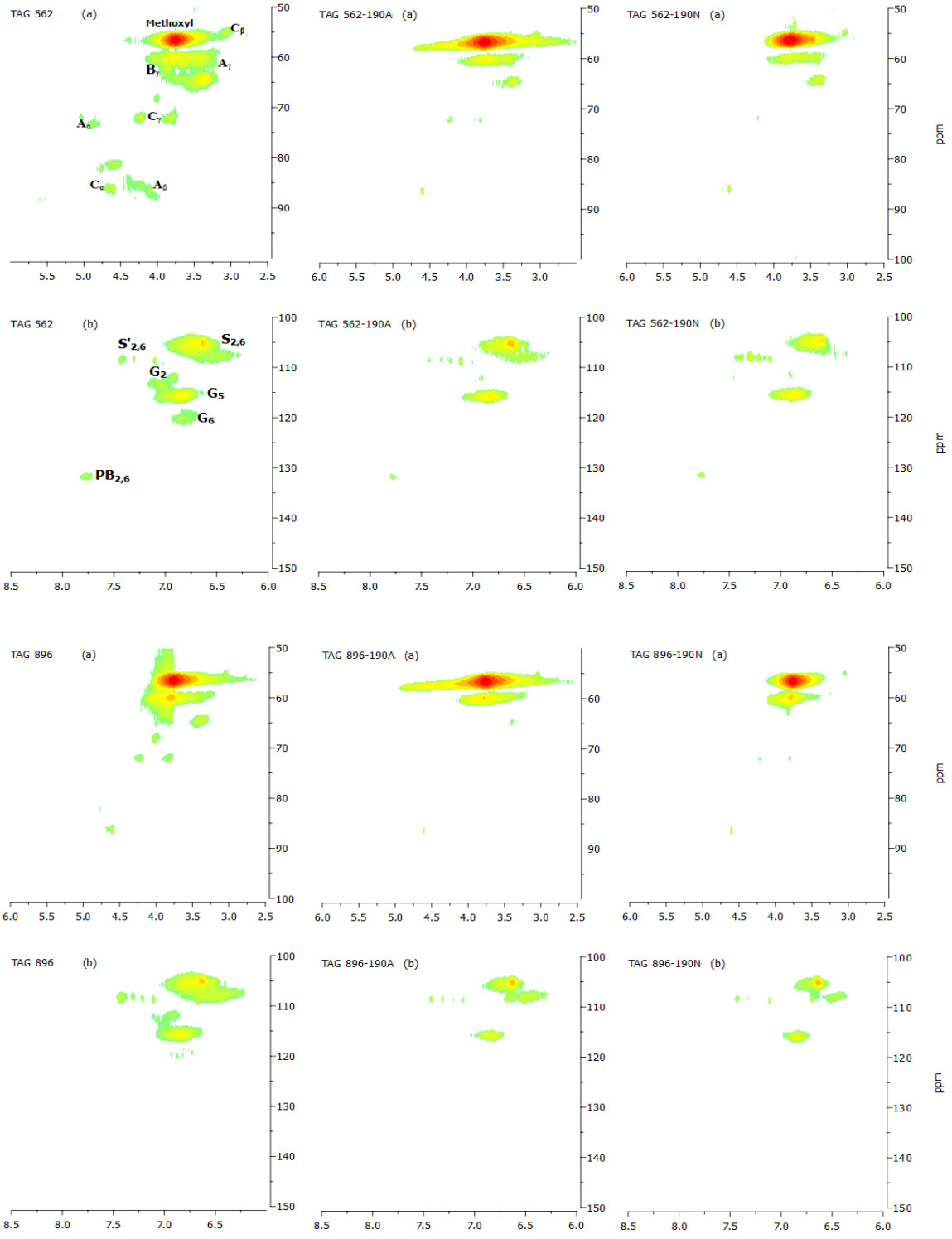
TAG 562 (a)
Methoxyl
Cβ
Bγ
Aγ
Cγ
Aα
Cα
Aβ
TAG 562-190A (a)
TAG 562-190N (a)
TAG 562 (b)
S'2,6
S2,6
G2
G5
G6
PB2,6
TAG 562-190A (b)
TAG 562-190N (b)
TAG 896 (a)
TAG 896-190A (a)
TAG 896-190N (a)
TAG 896 (b)
TAG 896-190A (b)
TAG 896-190N (b)
ppm

Figure 49 Selective HSQC spectra of lignin after rheology test. (a) aliphatic region; (b) aromatic region; A: β-O-4 ether; B: phenylcoumaran; C: resinol; G: guaiacyl; S: syringyl; S': syringyl units with oxidized α–ketone; PB: p-hydroxybenzoyl.

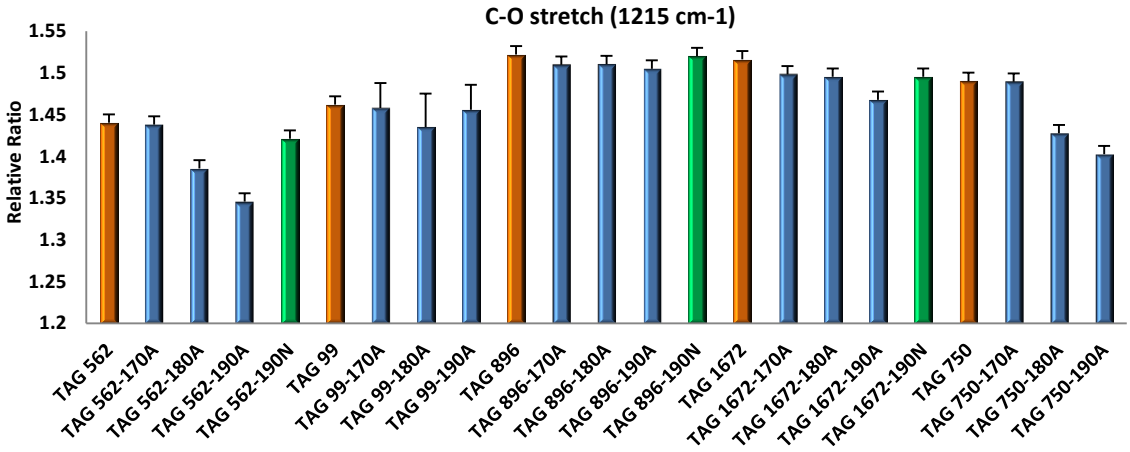

Figure 50 Ether linkages relative ratio calculated from ATR-FTIR absorption data.

Furthermore, the possible mechanistic pathways associated with these structural changes during the rheology test at different temperatures as a result of heat-induced association and dissociation behavior of lignin are proposed in Figure 51. At relatively low temperature, lignin samples could be mainly subjected to re-polymerization reactions starting from initial homolysis of C_α and/or C_β-ether linkages (A in Figure 51) generating a phenoxyl (C) and 1-phenyl-2-propyl (B) radical.[246] The formed phenoxyl radical will transform into their resonance mesomeric forms (C1) and thereby cause radical coupling reactions with C5 and/or C3 centered radicals to form new 4-O-5, 5-5', 3-3', 3-5' and 3-O-5 linkages along with increased molecular weight and condensed lignins. This suggests lignin with more guaiacyl (G) units could result in more cross-linkages due to less steric

hindrance in lignin C5 position that facilitates the formation of resonance structures. The increased amount of total phenols including G and S units, and catechols could also result from the release of phenoxyl radicals and homolysis of the methoxyl groups.

Relatively high temperature in the rheology test would lead to a competition of re-polymerization and de-polymerization reactions, and the de-polymerization reaction appears to dominate as evident by the apparent decrease in molecular weight and hydroxyl groups in lignin.[155b] Radical induced H-abstraction occurring at the C_{α}-H could form a benzyl radical that should have a lower unpaired spin density at the α-position with extensive electron delocalization analogous to the formed phenoxyl radicals[155b] that suggests the following different pathways for de-polymerization reaction in order to not only control molecular weight growth but also transform the reactive C-O bonds into C-C linkages. The 1-phenyl-2-propyl radical (B) formed at relatively low temperature is reported to be more exothermic than that of phenoxyl radical.[246a] Although intermediates generated by those radicals would be sterically hindered which further limited their participation in the chain propagating reaction, these radicals could be severely limited with regard to the sites that are capable of abstracting hydrogen from lignin to form more stable intermediates for the following de-polymerization reactions (possible pathways I and II in Figure 51) at relatively high temperature. Furthermore, cooling under air will lead to a series of highly reactive oxygen-based radicals, which further oxidizes the lignin structure introducing more carbonyl and carboxyl groups into lignin than that under nitrogen cooling condition.[155b]

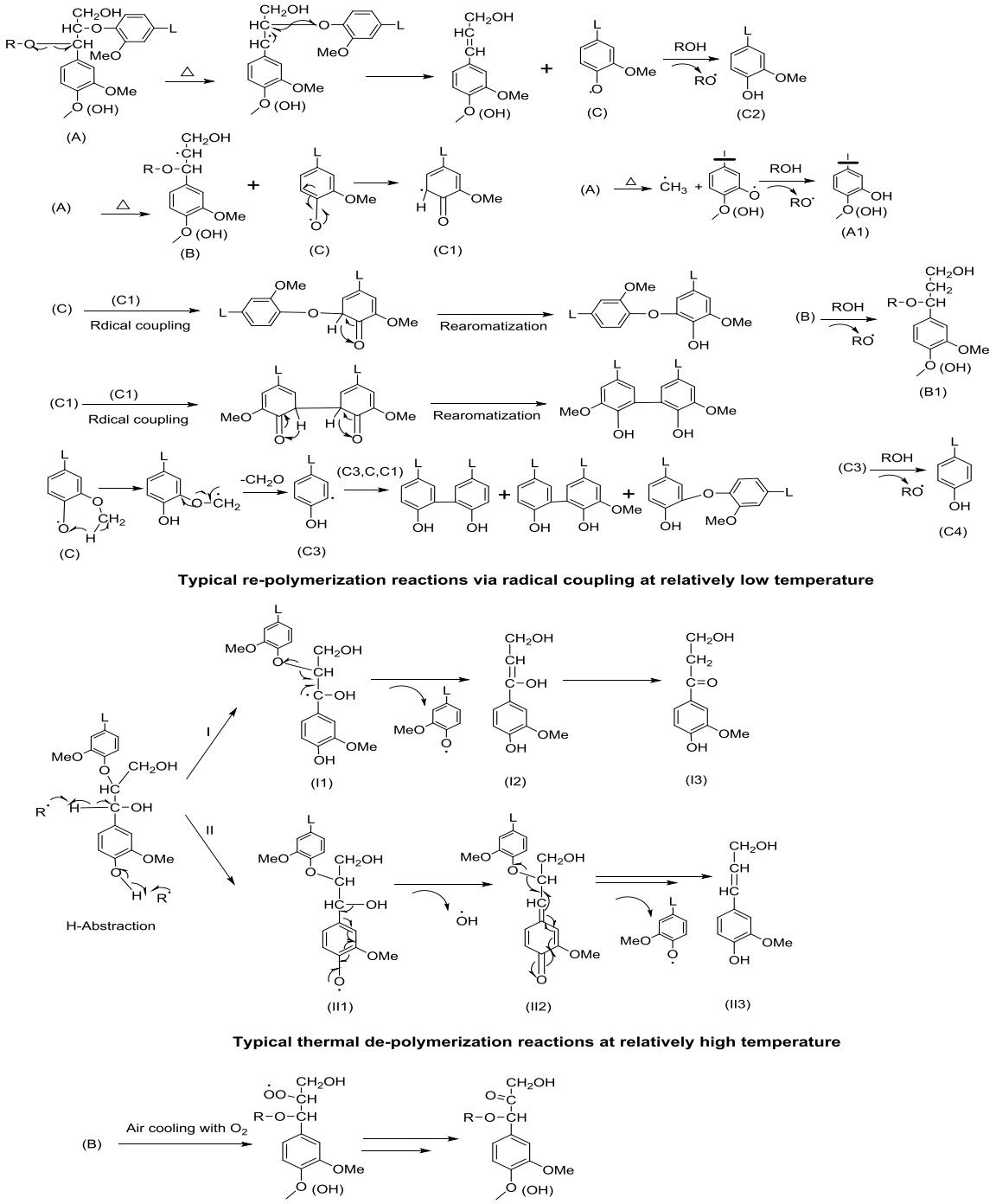

Figure 51 Proposed lignin re-polymerization and de-polymerization reaction mechanism during the melt rheology test.

7.4 Conclusion

Rheology test of lignins with different S/G ratios was accomplished at 170, 180, and 190 ℃ under different cooling conditions. 170 ℃ favors re-polymerization of lignin that displays an increase in guaiacyl, syringyl, catechol type hydroxyl groups, total phenols and condensed lignin structures, which resulted in the significant increase in molecular weights and viscosity values. In contrast, higher temperature 190 ℃ tends to prevent lignin polymerization to some extent in conjunction with considerable reduction of β-O-4 ether linkages, aliphatic, phenolic and carboxylic hydroxyls, and therefore yielded lignins with relatively lower molecular weights and lower viscosity values. Air cooling introduced more oxygenated hydroxyl, carboxylic compounds and condensed bonds into the lignin macromolecules but lower amounts of ether linkages than nitrogen cooling. Lignin with lower S/G ratio exhibited higher viscosity values, molecular weights with larger amounts of condensed structures after rheology test at relative lower temperature. Proper temperature and air cooling conditions could contribute to the crosslinking of lignin and the formation of condensed structures with more carbon-carbon linkages that improve the spinnability of organo-solv poplar lignins, which therefore facilitates the following rapid chemical transformation to infusible mass and formation of planar graphitic structure during pyrolysis. The detailed characterization of lignin physicochemical properties after rheology test by NMR, GPC, ATR-FTIR provides insight into the mechanisms of rheology of lignin and will be of high value in the production of novel lignin carbon fibers.

CHAPTER 8

OVERALL CONCLUSIONS

Lignocellulosic biomass as one of the most abundantly sustainable resource has been promoted instead of food-based materials for biofuels, biochemicals and biobased products production to meet the growing global demand for green energy and materials. The major challenge facing future lignocellulosic biofuel research is reducing the biomass recalcitrance through chemical and/or biological processes. Lignin is considered as one of the most recalcitrant components in the plant cell wall because of its structure, content, distribution and associations with plant polysaccharides within the cell wall, which not only affects the biomass substrate changes during pretreatment, particularly cellulose ultrastructure, but also influences the downstream enzymatic hydrolysis.

The primary goal of this thesis was to demonstrate the different effects of various leading pretreatment technologies on cellulose ultrastructure changes. To fulfill this, several pretreatment technologies were carried out to study their different effects on cellulose crystallinity, crystalline allomorph distribution, and cellulose ultrastructure. The observed changes in the cellulose ultrastructure of poplar were also related to changes in enzymatic hydrolysis, a measure of biomass recalcitrance. Hot-water, organo-solv, lime, lime-oxidant, dilute acid, and dilute acid-oxidant pretreatments were compared in terms of changes in enzymatic sugar release and then changes in cellulose ultrastructure measured by ^{13}C cross polarization magic angle spinning nuclear magnetic resonance (^{13}C CP/MAS NMR) and wide-angle X-ray diffraction (WAXD). Pretreatment severity and relative

chemical de-polymerization/degradation were assessed through compositional analysis and high-performance anion-exchange chromatography with pulsed amperometric detection (HPAEC-PAD). Results showed minimal cellulose ultrastructural changes occurred due to lime and lime-oxidant pretreatments, which however especially at short residence time displayed relatively high enzymatic glucose yield. Hot water pretreatment moderately changed cellulose crystallinity and crystalline allomorph distribution yet produced the lowest enzymatic glucose yield. Dilute acid and dilute acid-oxidant pretreatments resulted in the largest increase in cellulose crystallinity, *para*-crystalline, and cellulose-I_{β} allomorph content as well as the largest increase in cellulose microfibril or crystallite size. Perhaps related, compositional analysis and Klason lignin contents for samples that underwent dilute acid and dilute acid-oxidant pretreatments indicated the most significant polysaccharide de-polymerization/degradation also ensued. Organo-solv pretreatment generated the highest glucose yield, which was accompanied by the most significant increase in cellulose microfibril or crystallite size and decrease in relatively lignin contents. Hot-water, dilute acid, dilute acid-oxidant, and organo-solv pretreatments all showed evidence of cellulose microfibril coalescence.

Second study was designed to assess how the presence of lignin influences dilute acid pretreatment induced changes in cellulose ultrastructure, which ultimately have large implications with respect to enzymatic deconstruction efforts. Following extensive characterization, the partially delignified biomass displayed more significant changes in cellulose ultrastructure following DAP than the native untreated biomass. With respect to the native untreated poplar, delignified poplar followed by DAP (in which approximately

40% lignin removal occurred) experienced: increased cellulose accessibility indicated by increased Simons' stain (orange dye) adsorption from 21.8 to 72.5 mg/g, decreased cellulose weight-average degree of polymerization (DP_w) from 3087 to 294 units, and increased cellulose crystallite size from 2.9 to 4.2 nm. These changes following DAP ultimately increased enzymatic sugar yield from 10 to 80%.the results indicate a strong influence of lignin content on cellulose ultrastructural changes occurring during DAP. With the reduction of lignin content during DAP, the enlargement of cellulose microfibril dimensions and crystallite size becomes more apparent. Further, this enlargement of cellulose microfibril dimensions is attributed to specific processes, including the co-crystallization of crystalline cellulose driven by irreversible inter-chain hydrogen bonding (similar to hornification) and/or cellulose annealing that converts amorphous cellulose to *para*crystalline and crystalline cellulose. Essentially, lignin acts as a barrier to prevent cellulose crystallinity increase and cellulose fibril coalescence during DAP.

Third study regarding the lignin structural change caused by DAP demonstrated the detailed lignin chemistry during DAP and its following influence on the enzymatic hydrolysis. Results highlighted that lignin was subjected to de-polymerization within the 2 min of dilute acid pretreatment time and these changes were accompanied with increasing values for the aliphatic and phenolic hydroxyl groups of lignin. This was followed by a competing set of de-polymerization and re-polymerization reactions which lead to a decrease in the content of guaiacyl and *p*-hydroxyphenyl lignin units and an increase in condensed lignin units as the reaction residence time is extended beyond 5 min. A detailed comparison of changes in functional groups and molecular weights of

cellulolytic enzyme lignins demonstrated different structural parameters related to the recalcitrant properties of lignin are altered during the pretreatment conditions. A better and deeper understanding of the fundamental chemical structure of lignin in this study, the most recalcitrant component of biomass, during DAP is critical to the continued growth of renewable biofuel production.

In the last chapter in the thesis, lignins from poplar genotypes have been isolated for carbon precursor applications by an organo-solv extraction method. Physicochemical characterization of the lignin variants showed a broad distribution of glass transition temperatures (115–129 ℃), steady melt viscosity at 170 ℃ (20–320 Pa.s), and pyrolysis char residues (24–38 wt%). It has been hypothesized that the structure of lignin affects the physicochemical characteristics of the lignin, including their rheology and ability to form fiber structure. In this study we measured the structural changes occurring under different temperatures as a result of thermo-rheological processing history by solution nuclear magnetic resonance (NMR) spectroscopy techniques and gel permeation chromatography (GPC). Rheological measurement at 170 ℃ induced lignin re-polymerization reaction accompanied with an increase in the total phenols, condensed linkages, molecular weights, and viscosities. In contrast, rheology testing at 190 ℃ resulted in the decrease in lignin aliphatic and phenolic hydroxyl groups, β-O-4 ether linkages, molecular weights, and viscosity values. Air cooling generated lignin with more oxygenated and condensed compounds but lower amounts of ether linkages than nitrogen cooling did. During the rheology test, lignin with lower S/G (syringyl/guaiacyl) ratio

tends to form more cross-linkages along with higher viscosity values, higher molecular weight and larger amounts of condensed bonds compared to lignin with higher S/G ratio.

CHAPTER 9

RECOMMENDATIONS FOR FUTURE WORK

Lignin is a barrier to prevent cellulose crystallinity increase and cellulose fibril coalescence during DAP, which further affects the downstream enzymatic hydrolysis. In order to gain a deeper insight into the recalcitrant effect of lignin on biofuel production and its structural impact on biomaterial performance, several projects are worthy of further investigation.

These include the optimized partial delignification with hemicelluloses removal during DAP. This would remain cell wall spatial structure without elimination of all lignin spacer, increase specific area, reduce its irreversible adsorption to the enzyme, and result in the coalescence of cellulose fibril to limited extent and thereby to provide an optimal pretreated biomass for subsequent enzymatic deconstruction. These findings with optimized conditions could ultimately be applied to energy crop including woody and non-woody biomass, bamboo, soda pulp and even transgenic biomass in order to further boost the biofuel production.

In addition, efforts should be put to select suitable lignins with lower S/G ratio from various low-cost bio-resources and/or genetically engineered plants, and to investigate proper thermal treatment conditions that can improve the spinnability of lignin for commercial carbon fiber manufacturing.

REFERENCES

1. Ragauskas, A. J.; Williams, C. K.; Davison, B. H.; Britovsek, G.; Cairney, J.; Eckert, C. A.; Frederick, W. J.; Hallett, J. P.; Leak, D. J.; Liotta, C. L.; Mielenz, J. R.; Murphy, R.; Templer, R.; Tschaplinski, T., The path forward for biofuels and biomaterials. *Science* **2006,** *311* (5760), 484-489.
2. Mood, S. H.; Golfeshan, A. H.; Tabatabaei, M.; Jouzani, G. S.; Najafi, G. H.; Gholami, M.; Ardjmand, M., Lignocellulosic biomass to bioethanol, a comprehensive review with a focus on pretreatment. *Renew. Sust. Energ. Rev.* **2013,** *27*, 77-93.
3. Bayer, E. A.; Lamed, R.; Himmel, M. E., The potential of cellulases and cellulosomes for cellulosic waste management. *Curr. Opin. Biotechnol.* **2007,** *18* (3), 237-245.
4. The Renewable Fuel Standard: Issues for 2014 and Beyond (http://www.cbo.gov/publication/45477)
5. EPA Proposes 2014 Renewable Fuel Standards, 2015 Biomass-Based Diesel Volume (http://www.epa.gov/otaq/fuels/renewablefuels/documents/420f13048.pdf)
6. Demirbas, A., Biorefineries: current activities and future developments. *Energy Conv. Manag.* **2009,** *50* (11), 2782-2801.
7. Sun Q., Enzymatic Deconstruction of Lignocellulose to Fermentable Sugars. In Materials for Biofuels. World Scientific Publishing Co. 2014; pp 127-146.
8. Pu, Y.; Hu, F.; Huang, F.; Davison, B. H.; Ragauskas, A. J., Assessing the molecular structure basis for biomass recalcitrance during dilute acid and hydrothermal pretreatments. *Biotechnol. Biofuels* **2013,** *6* (1), 15.
9. Wyman, C. E.; Dale, B. E.; Elander, R. T.; Holtzapple, M.; Ladisch, M. R.; Lee, Y. Y., Coordinated development of leading biomass pretreatment technologies. *Bioresour. Technol.* **2005,** *96* (18), 1959-1966.
10. Drapcho, C. M.; Nhuan, N. P.; Walker, T. H., *Biofuels engineering process technology*. McGraw-Hill New York, NY, USA: 2008.
11. Munasinghe, P. C.; Khanal, S. K., Biomass-derived syngas fermentation into biofuels: Opportunities and challenges. *Bioresour. Technol.* **2010,** *101* (13), 5013-5022.
12. Brown, R., Biorenewable resources: engineering new products from agriculture. 2003. *Iowa: Blackwell*.
13. Gasparatos, A.; Stromberg, P.; Takeuchi, K., Sustainability impacts of first-generation biofuels. *Animal Frontiers* **2013,** *3* (2), 12-26.
14. International Energy Agency. From First- to Second-Generation Biofuel Technologies: An Overview of Current Industry and RD&D Activities. Paris: OECD/IEA.2008.(http://www.iea.org/publications/freepublications/publication/2nd_Biofuel_Gen_Exec_Sum.pdf)
15. (a) Association, R. F., *Accelerating industry innovation: 2012 ethanol industry outlook*. Renewable Fuels Association 2012; (b) Lichts, F., Industry statistics: 2010 world fuel ethanol production. *Renewable Fuels Association* **2010**.
16. Service, R., Renewable Energy. Cellulosic ethanol at last? *Science* **2014,** *345* (6201), 1111.
17. http://poet-dsm.com/

18. Luo, L.; van der Voet, E.; Huppes, G., Biorefining of lignocellulosic feedstock - Technical, economic and environmental considerations. *Bioresour. Technol.* **2010,** *101* (13), 5023-5032.
19. (a) Foston, M.; Ragauskas, A. J., Biomass Characterization: Recent Progress in Understanding Biomass Recalcitrance. *Ind. Biotechnol.* **2012,** *8* (4), 191-208; (b) Yang, B.; Dai, Z.; Ding, S.-Y.; Wyman, C. E., Enzymatic hydrolysis of cellulosic biomass. *Biofuels* **2011,** *2* (4), 421-450.
20. (a) Kumar, P.; Barrett, D. M.; Delwiche, M. J.; Stroeve, P., Methods for pretreatment of lignocellulosic biomass for efficient hydrolysis and biofuel production. *Ind. Eng. Chem. Res.* **2009,** *48* (8), 3713-3729; (b) Zhao, X. B.; Zhang, L. H.; Liu, D. H., Biomass recalcitrance. Part I: the chemical compositions and physical structures affecting the enzymatic hydrolysis of lignocellulose. *Biofuels Bioprod. Biorefining* **2012,** *6* (4), 465-482.
21. (a) Galbe, M.; Zacchi, G., Pretreatment of lignocellulosic materials for efficient bioethanol production. In *Biofuels*, Springer: 2007; pp 41-65; (b) Hamelinck, C. N.; Hooijdonk, G. v.; Faaij, A. P., Ethanol from lignocellulosic biomass: techno-economic performance in short-, middle-and long-term. *Biomass Bioenergy* **2005,** *28* (4), 384-410; (c) Kim, S. J.; Kim, M. Y.; Jeong, S. J.; Jang, M. S.; Chung, I. M., Analysis of the biomass content of various Miscanthus genotypes for biofuel production in Korea. *Industrial Crops and Products* **2012,** *38*, 46-49; (d) Ingram, T.; Wörmeyer, K.; Lima, J. C. I.; Bockemühl, V.; Antranikian, G.; Brunner, G.; Smirnova, I., Comparison of different pretreatment methods for lignocellulosic materials. Part I: conversion of rye straw to valuable products. *Bioresour. Technol.* **2011,** *102* (8), 5221-5228.
22. Gronowska, M.; Joshi, S.; MacLean, H. L., A review of US and Canadian biomass supply studies. *BioResources* **2008,** *4* (1), 341-369.
23. Klemm, D.; Heublein, B.; Fink, H. P.; Bohn, A., Cellulose: fascinating biopolymer and sustainable raw material. *Angew. Chem. Int. Ed.* **2005,** *44* (22), 3358-3393.
24. Zhang, Y. H. P.; Lynd, L. R., Toward an aggregated understanding of enzymatic hydrolysis of cellulose: noncomplexed cellulase systems. *Biotechnol. Bioeng.* **2004,** *88* (7), 797-824.
25. Sjöholm, E., Size exclusion chromatography of cellulose and cellulose derivatives. *Handbook Of Size Exclusion Chromatography And Related Techniques: Revised And Expanded* **2003,** *91*, 311.
26. (a) Dupont, A.-L.; Mortha, G., Comparative evaluation of size-exclusion chromatography and viscometry for the characterisation of cellulose. *Journal of Chromatography A* **2004,** *1026* (1), 129-141; (b) Hallac, B. B.; Ragauskas, A. J., Analyzing cellulose degree of polymerization and its relevancy to cellulosic ethanol. *Biofuels Bioprod. Biorefining* **2011,** *5* (2), 215-225.
27. (a) Puri, V. P., Effect of crystallinity and degree of polymerization of cellulose on enzymatic saccharification. *Biotechnol. Bioeng.* **1984,** *26* (10), 1219-1222; (b) Snyder, J.; Timell, T., Molecular properties of native balsam fir cellulose. *Sven papperstidn* **1955,** *58*, 851-859; (c) Timmel, T., Chain length distributions of native white spruce cellulose. *Pulp Paper Mag. Canada* **1955,** *10*, 104-117; (d) Timell, T., Molecular properties of seven native wood celluloses. *Tappi Journal* **1957,** *40* (1), 25; (e) Timell, T., Molecular weight and polymolecularity of white birch celluloses. *Sven papperstidn* **1956,** *59*, 1-11.

28. Blaschek, W.; Koehler, H.; Semler, U.; Franz, G., Molecular weight distribution of cellulose in primary cell walls. *Planta* **1982,** *154* (6), 550-555.
29. (a) Cohen, R.; Jensen, K. A.; Houtman, C. J.; Hammel, K. E., Significant levels of extracellular reactive oxygen species produced by brown rot basidiomycetes on cellulose. *FEBS Lett.* **2002,** *531* (3), 483-488; (b) KlemanLeyer, K. M.; SiikaAho, M.; Teeri, T. T.; Kirk, T. K., The cellulases endoglucanase I and cellobiohydrolase II of Trichoderma reesei act synergistically to solubilize native cotton cellulose but not to decrease its molecular size. *Appl. Environ. Microbiol.* **1996,** *62* (8), 2883-2887.
30. Foston, M.; Ragauskas, A. J., Changes in lignocellulosic supramolecular and ultrastructure during dilute acid pretreatment of Populus and switchgrass. *Biomass Bioenerg.* **2010,** *34* (12), 1885-1895.
31. (a) Kumar, R.; Mago, G.; Balan, V.; Wyman, C. E., Physical and chemical characterizations of corn stover and poplar solids resulting from leading pretreatment technologies. *Bioresour. Technol.* **2009,** *100* (17), 3948-3962; (b) Jahan, M. S.; Mun, S. P., Studies on the macromolecular components of nonwood available in Bangladesh. *Ind. Crops Prod.* **2009,** *30* (3), 344-350; (c) Sweet, M. S.; Winandy, J. E., Influence of degree of polymerization of cellulose and hemicellulose on strength loss in fire-retardant-treated southern pine. *Holzforschung* **1999,** *53* (3), 311-317; (d) Jahan, M. S.; Mun, S. P., Effect of tree age on the cellulose structure of Nalita wood (Trema orientalis). *Wood Sci. Technol.* **2005,** *39* (5), 367-373; (e) Xu, W.; Reddy, N.; Yang, Y., Extraction, characterization and potential applications of cellulose in corn kernels and Distillers' dried grains with solubles (DDGS). *Carbohydr. Polym.* **2009,** *76* (4), 521-527.
32. Klemm, D.; Schmauder, H.-P.; Heinze, T., Cellulose. In *Biopolymers Online*, Wiley-VCH Verlag GmbH & Co. KGaA: 2005.
33. Kroon-Batenburg, L.; Kroon, J., The crystal and molecular structures of cellulose I and II. *Glycoconj. J.* **1997,** *14* (5), 677-690.
34. Klemm, D.; Philipp, B.; Heinze, T.; Heinze, U.; Wagenknecht, W., Comprehensive Cellulose Chemistry: Fundamentals and Analytical Methods, Volume 1. Wiley-VCH Verlag GmbH & Co. KGaA: 2004.
35. (a) Chunilall, V.; Bush, T.; Larsson, P. T., Supra-Molecular Structure and Chemical Reactivity of Cellulose I Studied Using CP/MAS 13C-NMR. **2013** (http://dx.doi.org/10.5772/50673); (b) Sannigrahi, P.; Ragauskas, A. J.; Miller, S. J., Effects of Two-Stage Dilute Acid Pretreatment on the Structure and Composition of Lignin and Cellulose in Loblolly Pine. *BioEnergy Res.* **2008,** *1* (3-4), 205-214; (c) Wickholm, K.; Hult, E.-L.; Larsson, P. T.; Iversen, T.; Lennholm, H., Quantification of cellulose forms in complex cellulose materials: a chemometric model. *Cellulose* **2001,** *8* (2), 139-148.
36. (a) Pu, Y. Q.; Ziemer, C.; Ragauskas, A. J., CP/MAS C-13 NMR analysis of cellulase treated bleached softwood kraft pulp. *Carbohydr. Res.* **2006,** *341* (5), 591-597; (b) Nishiyama, Y.; Sugiyama, J.; Chanzy, H.; Langan, P., Crystal structure and hydrogen bonding system in cellulose Iα from synchrotron X-ray and neutron fiber diffraction. *J. Am. Chem. Soc.* **2003,** *125* (47), 14300-14306.
37. (a) Frey-Wyssling, A., The fine structure of cellulose microfibrils. *Science* **1954,** *119* (3081), 80-82; (b) NJ Heyn, A., The elementary fibril and supermolecular structure of cellulose in soft wood fiber. *J. Ultrastruct. Res.* **1969,** *26* (1), 52-68; (c) Brown, R. M.;

Saxena, I. M., Cellulose biosynthesis: A model for understanding the assembly of biopolymers. *Plant Physiol. Biochem.* **2000,** *38* (1-2), 57-67.
38. Imai, T.; Putaux, J.-L.; Sugiyama, J., Geometric phase analysis of lattice images from algal cellulose microfibrils. *Polymer* **2003,** *44* (6), 1871-1879.
39. (a) Mansikkamäki, P.; Lahtinen, M.; Rissanen, K., Structural changes of cellulose crystallites induced by mercerisation in different solvent systems; determined by powder X-ray diffraction method. *Cellulose* **2005,** *12* (3), 233-242; (b) Ciacco, G. T.; Morgado, D. L.; Frollini, E.; Possidonio, S.; El Seoud, O. A., Some aspects of acetylation of untreated and mercerized sisal cellulose. *J. Brazil. Chem. Soc.* **2010,** *21* (1), 71-77; (c) Dinand, E.; Vignon, M.; Chanzy, H.; Heux, L., Mercerization of primary wall cellulose and its implication for the conversion of cellulose I→ cellulose II. *Cellulose* **2002,** *9* (1), 7-18.
40. Langan, P.; Nishiyama, Y.; Chanzy, H., A revised structure and hydrogen-bonding system in cellulose II from a neutron fiber diffraction analysis. *J. Am. Chem. Soc.* **1999,** *121* (43), 9940-9946.
41. (a) Atalla, R. H.; Vanderhart, D. L., Native cellulose: a composite of two distinct crystalline forms. *Science* **1984,** *223* (4633), 283-285; (b) Park, S.; Baker, J. O.; Himmel, M. E.; Parilla, P. A.; Johnson, D. K., Cellulose crystallinity index: measurement techniques and their impact on interpreting cellulase performance. *Biotechnology for Biofuels* **2010,** *3*; (c) French, A. D.; Cintrón, M. S., Cellulose polymorphy, crystallite size, and the Segal crystallinity index. *Cellulose* **2013,** *20* (1), 583-588.
42. Beecher, J. F.; Hunt, C. G.; Zhu, J., Tools for the characterization of biomass at the nanometer scale. *The nanoscience and technology of renewable biomaterials, 1st edn. Singapore: Blackwell Publishing. p* **2009**, 61-80.
43. Nishiyama, Y.; Langan, P.; Chanzy, H., Crystal structure and hydrogen-bonding system in cellulose Iβ from synchrotron X-ray and neutron fiber diffraction. *J. Am. Chem. Soc.* **2002,** *124* (31), 9074-9082.
44. (a) Atalla, R. H.; Gast, J.; Sindorf, D.; Bartuska, V.; Maciel, G., Carbon-13 NMR spectra of cellulose polymorphs. *J. Am. Chem. Soc.* **1980,** *102* (9), 3249-3251; (b) Isogai, A.; Usuda, M.; Kato, T.; Uryu, T.; Atalla, R. H., Solid-state CP/MAS carbon-13 NMR study of cellulose polymorphs. *Macromolecules* **1989,** *22* (7), 3168-3172; (c) VanderHart, D. L.; Atalla, R., Studies of microstructure in native celluloses using solid-state carbon-13 NMR. *Macromolecules* **1984,** *17* (8), 1465-1472.
45. Wickholm, K.; Larsson, P. T.; Iversen, T., Assignment of non-crystalline forms in cellulose I by CP/MAS 13C NMR spectroscopy. *Carbohydr. Res.* **1998,** *312* (3), 123-129.
46. (a) Pu, Y.; Hallac, B.; Ragauskas, A. J., Plant Biomass Characterization: Application of Solution- and Solid-State NMR Spectroscopy. In *Aqueous Pretreatment of Plant Biomass for Biological and Chemical Conversion to Fuels and Chemicals*, John Wiley & Sons, Ltd: 2013; pp 369-390; (b) Hallac, B. B.; Sannigrahi, P.; Pu, Y.; Ray, M.; Murphy, R. J.; Ragauskas, A. J., Biomass characterization of Buddleja davidii: a potential feedstock for biofuel production. *J. Agric. Food Chem.* **2009,** *57* (4), 1275-1281.
47. Lennholm, H.; Larsson, T.; Iversen, T., Determination of cellulose Iα and Iβ in lignocellulosic materials. *Carbohydr. Res.* **1994,** *261* (1), 119-131.

48. Larsson, P. T.; Hult, E. L.; Wickholm, K.; Pettersson, E.; Iversen, T., CP/MAS C-13-NMR spectroscopy applied to structure and interaction studies on cellulose I. *Solid State Nucl. Magn. Reson.* **1999,** *15* (1), 31-40.
49. (a) Foston, M.; Hubbell, C. A.; Davis, M.; Ragauskas, A. J., Variations in Cellulosic Ultrastructure of Poplar. *Bioenerg. Res.* **2009,** *2* (4), 193-197; (b) Samuel, R.; Pu, Y.; Foston, M.; Ragauskas, A. J., Solid-state NMR characterization of switchgrass cellulose after dilute acid pretreatment. *Biofuels* **2010,** *1* (1), 85-90.
50. (a) Heux, L.; Dinand, E.; Vignon, M. R., Structural aspects in ultrathin cellulose microfibrils followed by 13C CP-MAS NMR. *Carbohydr. Polym.* **1999,** *40* (2), 115-124; (b) Hult, E. L.; Larsson, P. T.; Iversen, T., Cellulose fibril aggregation - an inherent property of kraft pulps. *Polymer* **2001,** *42* (8), 3309-3314; (c) Hult, E. L.; Iversen, T.; Sugiyama, J., Characterization of the supermolecular structure of cellulose in wood pulp fibres. *Cellulose* **2003,** *10* (2), 103-110; (d) Newman, R. H., Estimation of the lateral dimensions of cellulose crystallites using 13C NMR signal strengths. *Solid State Nucl. Magn. Reson.* **1999,** *15* (1), 21-29.
51. (a) Pu, Y. Q.; Zhang, D. C.; Singh, P. M.; Ragauskas, A. J., The new forestry biofuels sector. *Biofuels Bioprod. Biorefining* **2008,** *2* (1), 58-73; (b) Ebringerova, A.; Hromadkova, Z.; Heinze, T., Hemicellulose. In *Polysaccharides i*, Springer: 2005; pp 1-67.
52. (a) Jacobs, A.; Dahlman, O., Characterization of the molar masses of hemicelluloses from wood and pulps employing size exclusion chromatography and matrix-assisted laser desorption ionization time-of-flight mass spectrometry. *Biomacromolecules* **2001,** *2* (3), 894-905; (b) Sannigrahi, P.; Ragauskas, A. J.; Tuskan, G. A., Poplar as a feedstock for biofuels: a review of compositional characteristics. *Biofuels Bioprod. Biorefining* **2010,** *4* (2), 209-226; (c) Willfor, S.; Sundberg, A.; Pranovich, A.; Holmbom, B., Polysaccharides in some industrially important hardwood species. *Wood Sci. Technol.* **2005,** *39* (8), 601-617; (d) Gabrielii, I.; Gatenholm, P.; Glasser, W.; Jain, R.; Kenne, L., Separation, characterization and hydrogel-formation of hemicellulose from aspen wood. *Carbohyd. Polym.* **2000,** *43* (4), 367-374.
53. Saha, B. C., Hemicellulose bioconversion. *J. Ind. Microbiol. Biotechnol.* **2003,** *30* (5), 279-291.
54. Willför, S.; Sundberg, A.; Hemming, J.; Holmbom, B., Polysaccharides in some industrially important softwood species. *Wood Sci. and Technol.* **2005,** *39* (4), 245-257.
55. (a) Huang, F.; Singh, P. M.; Ragauskas, A. J., Characterization of Milled Wood Lignin (MWL) in Loblolly Pine Stem Wood, Residue, and Bark. *J. Agric. Food Chem.* **2011,** *59* (24), 12910-12916; (b) Hu, Z.; Sykes, R.; Davis, M. F.; Charles Brummer, E.; Ragauskas, A. J., Chemical profiles of switchgrass. *Bioresour. Technol.* **2010,** *101* (9), 3253-3257; (c) De Vrije, T.; De Haas, G.; Tan, G.; Keijsers, E.; Claassen, P., Pretreatment of Miscanthus for hydrogen production by Thermotoga elfii. *Int. J. Hydrogen Energy* **2002,** *27* (11), 1381-1390; (d) Templeton, D.; Sluiter, A.; Hayward, T.; Hames, B.; Thomas, S., Assessing corn stover composition and sources of variability via NIRS. *Cellulose* **2009,** *16* (4), 621-639; (e) Sun, J.; Mao, F.; Sun, X.; Sun, R., Comparative study of hemicelluloses isolated with alkaline peroxide from lignocellulosic materials. *J. Wood Chem. Technol.* **2005,** *24* (3), 239-262; (f) Silverstein, R. A.; Chen, Y.; Sharma-Shivappa, R. R.; Boyette, M. D.; Osborne, J., A comparison of chemical

pretreatment methods for improving saccharification of cotton stalks. *Bioresour. Technol.* **2007,** *98* (16), 3000-3011.
56. (a) Torget, R.; Werdene, P.; Himmel, M.; Grohmann, K., Dilute acid pretreatment of short rotation woody and herbaceous crops. *Appl. Biochem. Biotechnol.* **1990,** *24* (1), 115-126; (b) Sun, R.; Lawther, J. M.; Banks, W., Fractional and structural characterization of wheat straw hemicelluloses. *Carbohydr. polym.* **1996,** *29* (4), 325-331.
57. Ragauskas, A. J.; Beckham, G. T.; Biddy, M. J.; Chandra, R.; Chen, F.; Davis, M. F.; Davison, B. H.; Dixon, R. A.; Gilna, P.; Keller, M., Lignin Valorization: Improving Lignin Processing in the Biorefinery. *Science* **2014,** *344* (6185), 1246843.
58. Ralph, J.; Lundquist, K.; Brunow, G.; Lu, F.; Kim, H.; Schatz, P. F.; Marita, J. M.; Hatfield, R. D.; Ralph, S. A.; Christensen, J. H., Lignins: natural polymers from oxidative coupling of 4-hydroxyphenyl-propanoids. *Phytochem. Rev.* **2004,** *3* (1-2), 29-60.
59. Pu, Y. Q.; Hu, F.; Huang, F.; Davison, B. H.; Ragauskas, A. J., Assessing the molecular structure basis for biomass recalcitrance during dilute acid and hydrothermal pretreatments. *Biotechnol. Biofuels* **2013,** *6*.
60. (a) Walker, G. M., *Bioethanol: Science and technology of fuel alcohol*. Bookboon: 2010; (b) Hallac, B. B., Fundamental understanding of the biochemical conversion of Buddleja davidii to fermentable sugars. **2011**.
61. (a) Boerjan, W.; Ralph, J.; Baucher, M., Lignin biosynthesis. *Annual review of plant biology* **2003,** *54* (1), 519-546; (b) Baucher, M.; Monties, B.; Montagu, M. V.; Boerjan, W., Biosynthesis and Genetic Engineering of Lignin. *Crit. Rev.Plant Sci.* **1998,** *17* (2), 125-197.
62. (a) Ralph, J.; Akiyama, T.; Coleman, H. D.; Mansfield, S. D., Effects on lignin structure of coumarate 3-hydroxylase downregulation in Poplar. *BioEnergy Res.* **2012,** *5* (4), 1009-1019; (b) Samuel, R.; Pu, Y.; Raman, B.; Ragauskas, A. J., Structural characterization and comparison of switchgrass ball-milled lignin before and after dilute acid pretreatment. *Appl. Biochem. Biotechnol.* **2010,** *162* (1), 62-74; (c) Robinson, A. R.; Mansfield, S. D., Rapid analysis of poplar lignin monomer composition by a streamlined thioacidolysis procedure and near‐infrared reflectance‐based prediction modeling. *The Plant Journal* **2009,** *58* (4), 706-714; (d) El Hage, R.; Brosse, N.; Chrusciel, L.; Sanchez, C.; Sannigrahi, P.; Ragauskas, A., Characterization of milled wood lignin and ethanol organosolv lignin from miscanthus. *Polym. Degrad. Stab.* **2009,** *94* (10), 1632-1638; (e) Fox, S. C.; McDonald, A. G., Chemical and thermal characterization of three industrial lignins and their corresponding lignin esters. *BioResources* **2010,** *5* (2), 990-1009; (f) Buranov, A. U.; Mazza, G., Lignin in straw of herbaceous crops. *Ind. Crops Prod.* **2008,** *28* (3), 237-259; (g) Ramires, E. C.; Megiatto, J. D.; Gardrat, C.; Castellan, A.; Frollini, E., Valorization of an industrial organosolv–sugarcane bagasse lignin: Characterization and use as a matrix in biobased composites reinforced with sisal fibers. *Biotechnol. Bioeng.* **2010,** *107* (4), 612-621.
63. (a) Chakar, F. S.; Ragauskas, A. J., Review of current and future softwood kraft lignin process chemistry. *Ind. Crops and Prod.* **2004,** *20* (2), 131-141; (b) Zakzeski, J.; Bruijnincx, P. C.; Jongerius, A. L.; Weckhuysen, B. M., The catalytic valorization of lignin for the production of renewable chemicals. *Chem. Rev.* **2010,** *110* (6), 3552-3599.

64. Sjöström, E., *Wood chemistry: fundamentals and applications*. Gulf Professional Publishing: 1993.
65. (a) Baumberger, S.; Dole, P.; Lapierre, C., Using transgenic poplars to elucidate the relationship between the structure and the thermal properties of lignins. *J. Agric. Food Chem.* **2002,** *50* (8), 2450-2453; (b) Guerra, A.; Lucia, L. A.; Argyropoulos, D. S., Isolation and characterization of lignins from Eucalyptus grandis Hill ex Maiden and Eucalyptus globulus Labill. by enzymatic mild acidolysis (EMAL). *Holzforschung* **2008,** *62* (1), 24-30.
66. Lundquist, K., Proton (1H) NMR spectroscopy. In *Methods in lignin chemistry*, Springer: 1992; pp 242-249.
67. Gellerstedt, G.; Robert, D., Quantitative 13C NMR analysis of kraft lignins. *Acta Chem. Scand. B* **1987,** *41* (7).
68. Robert, D., Carbon-13 nuclear magnetic resonance spectrometry. In *Methods in lignin chemistry*, Springer: 1992; pp 250-273.
69. Heikkinen, S.; Toikka, M. M.; Karhunen, P. T.; Kilpeläinen, I. A., Quantitative 2D HSQC (Q-HSQC) via suppression of J-dependence of polarization transfer in NMR spectroscopy: application to wood lignin. *J. Am. Chem. Soc.* **2003,** *125* (14), 4362-4367.
70. (a) Balakshin, M. Y.; Capanema, E. A.; Chang, H.-m., MWL fraction with a high concentration of lignin-carbohydrate linkages: Isolation and 2D NMR spectroscopic analysis. *Holzforschung* **2007,** *61* (1), 1-7; (b) Zhang, L.; Gellerstedt, G.; Ralph, J.; Lu, F., NMR studies on the occurrence of spirodienone structures in lignins. *J. Wood Chem. Technol.* **2006,** *26* (1), 65-79.
71. (a) Rencoret, J.; Marques, G.; Gutierrez, A.; Ibarra, D.; Li, J.; Gellerstedt, G.; Santos, J. I.; Jimenez-Barbero, J.; Martinez, A. T.; del Rio, J. C., Structural characterization of milled wood lignins from different eucalypt species. *Holzforschung* **2008,** *62* (5), 514-526; (b) del Río, J. C.; Rencoret, J.; Marques, G.; Gutiérrez, A.; Ibarra, D.; Santos, J. I.; Jiménez-Barbero, J. s.; Zhang, L.; Martínez, A. n. T., Highly acylated (acetylated and/or p-coumaroylated) native lignins from diverse herbaceous plants. *J. Agric. Food Chem.* **2008,** *56* (20), 9525-9534; (c) Stewart, J. J.; Akiyama, T.; Chapple, C.; Ralph, J.; Mansfield, S. D., The effects on lignin structure of overexpression of ferulate 5-hydroxylase in hybrid poplar. *Plant Physiol.* **2009,** *150* (2), 621-635.
72. Pu, Y.; Cao, S.; Ragauskas, A. J., Application of quantitative 31P NMR in biomass lignin and biofuel precursors characterization. *Energy Environ. Sci.* **2011,** *4* (9), 3154-3166.
73. (a) Sannigrahi, P.; Ragauskas, A. J.; Miller, S. J., Lignin structural modifications resulting from ethanol organosolv treatment of loblolly pine. *Energy Fuels* **2010,** *24* (1), 683-689; (b) Hallac, B. B.; Pu, Y.; Ragauskas, A. J., Chemical transformations of Buddleja davidii lignin during ethanol organosolv pretreatment. *Energy Fuels* **2010,** *24* (4), 2723-2732.
74. (a) Yuan, T.-Q.; Sun, S.-N.; Xu, F.; Sun, R.-C., Characterization of lignin structures and lignin–carbohydrate complex (LCC) linkages by quantitative 13C and 2D HSQC NMR spectroscopy. *J. Agric. Food Chem.* **2011,** *59* (19), 10604-10614; (b) Lawoko, M.; Henriksson, G.; Gellerstedt, G., Structural differences between the lignin-carbohydrate complexes present in wood and in chemical pulps. *Biomacromolecules* **2005,** *6* (6), 3467-3473; (c) Lawoko, M.; Henriksson, G.; Gellerstedt, G.,

Characterisation of lignin-carbohydrate complexes (LCCs) of spruce wood (Picea abies L.) isolated with two methods. *Holzforschung* **2006,** *60* (2), 156-161.
75. (a) Azuma, J.; Takahashi, N.; Koshijima, T., ISOLATION AND CHARACTERIZATION OF LIGNIN-CARBOHYDRATE COMPLEXES FROM THE MILLED-WOOD LIGNIN FRACTION OF PINUS-DENSIFLORA SIEB ET ZUCC. *Carbohydr. Res.* **1981,** *93* (1), 91-104; (b) Mukoyoshi, S. I.; Azuma, J. I.; Koshijima, T., LIGNIN-CARBOHYDRATE COMPLEXES FROM COMPRESSION WOOD OF PINUS-DENSIFLORA SIEB ET ZUCC. *Holzforschung* **1981,** *35* (5), 233-240.
76. Balakshin, M.; Capanema, E.; Gracz, H.; Chang, H.-m.; Jameel, H., Quantification of lignin–carbohydrate linkages with high-resolution NMR spectroscopy. *Planta* **2011,** *233* (6), 1097-1110.
77. Himmel, M. E.; Ding, S.-Y.; Johnson, D. K.; Adney, W. S.; Nimlos, M. R.; Brady, J. W.; Foust, T. D., Biomass Recalcitrance: Engineering Plants and Enzymes for Biofuels Production. *Science* **2007,** *315* (5813), 804-807.
78. Ding, S. Y.; Himmel, M. E., The maize primary cell wall microfibril: A new model derived from direct visualization. *J. Agric. Food Chem.* **2006,** *54* (3), 597-606.
79. (a) Zhang, Y. H. P.; Lynd, L. R., Determination of the number-average degree of polymerization of cellodextrins and cellulose with application to enzymatic hydrolysis. *Biomacromolecules* **2005,** *6* (3), 1510-1515; (b) Pinto, R.; Carvalho, J.; Mota, M.; Gama, M., Large-scale production of cellulose-binding domains. Adsorption studies using CBD-FITC conjugates. *Cellulose* **2006,** *13* (5), 557-569; (c) Jeoh, T.; Ishizawa, C. I.; Davis, M. F.; Himmel, M. E.; Adney, W. S.; Johnson, D. K., Cellulase digestibility of pretreated biomass is limited by cellulose accessibility. *Biotechnol. Bioeng.* **2007,** *98* (1), 112-122.
80. Mittal, A.; Katahira, R.; Himmel, M. E.; Johnson, D. K., Effects of alkaline or liquid-ammonia treatment on crystalline cellulose: changes in crystalline structure and effects on enzymatic digestibility. *Biotechnol Biofuels* **2011,** *4* (1), 41.
81. Wada, M.; Ike, M.; Tokuyasu, K., Enzymatic hydrolysis of cellulose I is greatly accelerated via its conversion to the cellulose II hydrate form. *Polym. Degrad. Stabil.* **2010,** *95* (4), 543-548.
82. Weimer, P.; French, A.; Calamari, T., Differential fermentation of cellulose allomorphs by ruminal cellulolytic bacteria. *Appl. Environ. Microbiol.* **1991,** *57* (11), 3101-3106.
83. Igarashi, K.; Wada, M.; Samejima, M., Activation of crystalline cellulose to cellulose IIII results in efficient hydrolysis by cellobiohydrolase. *Febs Journal* **2007,** *274* (7), 1785-1792.
84. (a) Barnette, A. L.; Bradley, L. C.; Veres, B. D.; Schreiner, E. P.; Park, Y. B.; Park, J.; Park, S.; Kim, S. H., Selective detection of crystalline cellulose in plant cell walls with sum-frequency-generation (SFG) vibration spectroscopy. *Biomacromolecules* **2011,** *12* (7), 2434-2439; (b) Barnette, A. L.; Lee, C.; Bradley, L. C.; Schreiner, E. P.; Park, Y. B.; Shin, H.; Cosgrove, D. J.; Park, S.; Kim, S. H., Quantification of crystalline cellulose in lignocellulosic biomass using sum frequency generation (SFG) vibration spectroscopy and comparison with other analytical methods. *Carbohyd. polym.* **2012,** *89* (3), 802-809.
85. Väljamäe, P.; Pettersson, G.; Johansson, G., Mechanism of substrate inhibition in cellulose synergistic degradation. *Eur. J. Biochem.* **2001,** *268* (16), 4520-4526.

86. (a) Hall, M.; Bansal, P.; Lee, J. H.; Realff, M. J.; Bommarius, A. S., Cellulose crystallinity–a key predictor of the enzymatic hydrolysis rate. *FEBS journal* **2010,** *277* (6), 1571-1582; (b) Hallac, B. B.; Sannigrahi, P.; Pu, Y.; Ray, M.; Murphy, R. J.; Ragauskas, A. J., Effect of ethanol organosolv pretreatment on enzymatic hydrolysis of Buddleja davidii stem biomass. *Ind. Eng. Chem. Res.* **2010,** *49* (4), 1467-1472; (c) Pan, X.; Xie, D.; Kang, K.-Y.; Yoon, S.-L.; Saddler, J. N., Effect of organosolv ethanol pretreatment variables on physical characteristics of hybrid poplar substrates. In *Applied Biochemistry and Biotecnology*, Springer: 2007; pp 367-377.
87. Yang, B.; Wyman, C. E., BSA treatment to enhance enzymatic hydrolysis of cellulose in lignin containing substrates. *Biotechnol. Bioeng.* **2006,** *94* (4), 611-617.
88. (a) GOEL, S. C.; Ramachandran, K., Studies on the adsorption of cellulase on lignocellulosics. *J. Ferment. Technol.* **1983,** *61* (3), 281-286; (b) Peters, L.; Walker, L.; Wilson, D.; Irwin, D., The impact of initial particle size on the fragmentation of cellulose by the cellulase of thermomonospora fusca. *Bioresour. Technol.* **1991,** *35* (3), 313-319; (c) Goel, S. C.; Ramachandran, K., Comparison of the rates of enzymatic hydrolysis of pretreated rice straw and bagasse with celluloses. *Enzyme Microb. Technol.* **1983,** *5* (4), 281-284.
89. Meng, X.; Ragauskas, A. J., Recent advances in understanding the role of cellulose accessibility in enzymatic hydrolysis of lignocellulosic substrates. *Curr. Opin. Biotechnol.* **2014,** *27*, 150-158.
90. Liu, Y.-S.; Baker, J. O.; Zeng, Y.; Himmel, M. E.; Haas, T.; Ding, S.-Y., Cellobiohydrolase hydrolyzes crystalline cellulose on hydrophobic faces. *J. Biol. Chem.* **2011,** *286* (13), 11195-11201.
91. Chen, W.-H.; Tu, Y.-J.; Sheen, H.-K., Disruption of sugarcane bagasse lignocellulosic structure by means of dilute sulfuric acid pretreatment with microwave-assisted heating. *Appl. Energy* **2011,** *88* (8), 2726-2734.
92. (a) Meng, X.; Foston, M.; Leisen, J.; DeMartini, J.; Wyman, C. E.; Ragauskas, A. J., Determination of porosity of lignocellulosic biomass before and after pretreatment by using Simons' stain and NMR techniques. *Bioresour. Technol.* **2013,** *144*, 467-476; (b) Chandra, R.; Ewanick, S.; Hsieh, C.; Saddler, J. N., The characterization of pretreated lignocellulosic substrates prior to enzymatic hydrolysis, part 1: a modified Simons' staining technique. *Biotechnol. Prog.* **2008,** *24* (5), 1178-1185.
93. Y Lin, S., Accessibility of cellulose: A critical review. *Fibre Sci. Technol.* **1972,** *5* (4), 303-314.
94. (a) Chum, H.; Johnson, D.; Black, S.; Baker, J.; Grohmann, K.; Sarkanen, K.; Wallace, K.; Schroeder, H., Organosolv pretreatment for enzymatic hydrolysis of poplars: I. Enzyme hydrolysis of cellulosic residues. *Biotechnol. Bioeng.* **1988,** *31* (7), 643-649; (b) Yoshida, M.; Liu, Y.; Uchida, S.; Kawarada, K.; Ukagami, Y.; Ichinose, H.; Kaneko, S.; Fukuda, K., Effects of cellulose crystallinity, hemicellulose, and lignin on the enzymatic hydrolysis of Miscanthus sinensis to monosaccharides. *Biosci. Biotechnol. Biochem.* **2008,** *72* (3), 805-810.
95. (a) Öhgren, K.; Bura, R.; Saddler, J.; Zacchi, G., Effect of hemicellulose and lignin removal on enzymatic hydrolysis of steam pretreated corn stover. *Bioresour. Technol.* **2007,** *98* (13), 2503-2510; (b) Yang, B.; Wyman, C. E., Effect of xylan and lignin removal by batch and flowthrough pretreatment on the enzymatic digestibility of corn stover cellulose. *Biotechnol. Bioeng.* **2004,** *86* (1), 88-95.

96. Feng, P.; JunLi, R.; Feng, X.; RunCang, S.; Zhu, J.; Zhang, X.; Pan, X., Chemicals from hemicelluloses: a review. *Sustainable production of fuels, chemicals, and fibers from forest biomass* **2011**, 219-259.
97. Pan, X. J.; Gilkes, N.; Saddler, J. N., Effect of acetyl groups on enzymatic hydrolysis of cellulosic substrates. *Holzforschung* **2006,** *60* (4), 398-401.
98. Yu, Z.; Jameel, H.; Chang, H.-m.; Park, S., The effect of delignification of forest biomass on enzymatic hydrolysis. *Bioresour. Technol.* **2011,** *102* (19), 9083-9089.
99. Mooney, C. A.; Mansfield, S. D.; Touhy, M. G.; Saddler, J. N., The effect of initial pore volume and lignin content on the enzymatic hydrolysis of softwoods. *Bioresour. Technol.* **1998,** *64* (2), 113-119.
100. (a) Alvira, P.; Tomás-Pejó, E.; Ballesteros, M.; Negro, M., Pretreatment technologies for an efficient bioethanol production process based on enzymatic hydrolysis: a review. *Bioresour. Technol.* **2010,** *101* (13), 4851-4861; (b) Zheng, Y.; Pan, Z.; Zhang, R.; Wang, D.; Jenkins, B., Non-ionic surfactants and non-catalytic protein treatment on enzymatic hydrolysis of pretreated creeping wild ryegrass. In *Biotechnology for Fuels and Chemicals*, Springer: 2008; pp 351-368.
101. Yang, J.; Zhang, X.; Yong, Q.; Yu, S., Three-stage enzymatic hydrolysis of steam-exploded corn stover at high substrate concentration. *Bioresour. Technol.* **2011,** *102* (7), 4905-4908.
102. (a) Koo, B.-W.; Treasure, T. H.; Jameel, H.; Phillips, R. B.; Chang, H.-m.; Park, S., Reduction of enzyme dosage by oxygen delignification and mechanical refining for enzymatic hydrolysis of green liquor-pretreated hardwood. *Appl. Biochem. Biotechnol.* **2011,** *165* (3-4), 832-844; (b) Taherzadeh, M. J.; Karimi, K., Enzymatic-based hydrolysis processes for Ethanol. *BioResources* **2007,** *2* (4), 707-738.
103. (a) Palonen, H., *Role of lignin in the enzymatic hydrolysis of lignocellulose*. VTT Technical Research Centre of Finland: 2004; (b) Donohoe, B. S.; Decker, S. R.; Tucker, M. P.; Himmel, M. E.; Vinzant, T. B., Visualizing lignin coalescence and migration through maize cell walls following thermochemical pretreatment. *Biotechnol. Bioeng.* **2008,** *101* (5), 913-925.
104. Studer, M. H.; DeMartini, J. D.; Davis, M. F.; Sykes, R. W.; Davison, B.; Keller, M.; Tuskan, G. A.; Wyman, C. E., Lignin content in natural Populus variants affects sugar release. *Proc. Natl. Acad. Sci.* **2011,** *108* (15), 6300-6305.
105. Ramos, L.; Breuil, C.; Saddler, J., Comparison of steam pretreatment of eucalyptus, aspen, and spruce wood chips and their enzymatic hydrolysis. *Appl. Biochem. Biotechnol.* **1992,** *34* (1), 37-48.
106. Laureano-Perez, L.; Teymouri, F.; Alizadeh, H.; Dale, B. E., Understanding factors that limit enzymatic hydrolysis of biomass. *Appl. Biochem. Biotechnol.* **2005,** *121*, 1081-1099.
107. (a) Nakagame, S.; Chandra, R. P.; Saddler, J. N., The effect of isolated lignins, obtained from a range of pretreated lignocellulosic substrates, on enzymatic hydrolysis. *Biotechnol. Bioeng.* **2010,** *105* (5), 871-879; (b) Berlin, A.; Balakshin, M.; Gilkes, N.; Kadla, J.; Maximenko, V.; Kubo, S.; Saddler, J., Inhibition of cellulase, xylanase and beta-glucosidase activities by softwood lignin preparations. *J. Biotechnol.* **2006,** *125* (2), 198-209.

108. Nakagame, S.; Chandra, R. P.; Kadla, J. F.; Saddler, J. N., Enhancing the enzymatic hydrolysis of lignocellulosic biomass by increasing the carboxylic acid content of the associated lignin. *Biotechnol. Bioeng.* **2011,** *108* (3), 538-548.
109. Ximenes, E.; Kim, Y.; Mosier, N.; Dien, B.; Ladisch, M., Deactivation of cellulases by phenols. *Enzyme Microb. Technol.* **2011,** *48* (1), 54-60.
110. Morrison, D.; van Dyk, J. S.; Pletschke, B. I., The effect of alcohols, lignin and phenolic compounds on the enzyme activity of Clostridium cellulovorans XynA. *BioResources* **2011,** *6* (3), 3132-3141.
111. Kim, H. S.; Cho, D. H.; Won, K.; Kim, Y. H., Inactivation of Coprinus cinereus peroxidase during the oxidation of various phenolic compounds originated from lignin. *Enzyme Microb. Technol.* **2009,** *45* (2), 150-155.
112. (a) Hu, F.; Ragauskas, A., Pretreatment and lignocellulosic chemistry. *Bioenergy Res.* **2012,** *5* (4), 1043-1066; (b) Agbor, V. B.; Cicek, N.; Sparling, R.; Berlin, A.; Levin, D. B., Biomass pretreatment: fundamentals toward application. *Biotechnology advances* **2011,** *29* (6), 675-685; (c) Sanchez, C., Lignocellulosic residues: Biodegradation and bioconversion by fungi. *Biotechnol. Adv.* **2009,** *27* (2), 185-194.
113. (a) Wyman, C. E.; Dale, B. E.; Elander, R. T.; Holtzapple, M.; Ladisch, M. R.; Lee, Y. Y.; Mitchinson, C.; Saddler, J. N., Comparative Sugar Recovery and Fermentation Data Following Pretreatment of Poplar Wood by Leading Technologies. *Biotechnol. Prog.* **2009,** *25* (2), 333-339; (b) Kumar, R.; Wyman, C. E., Access of Cellulase to Cellulose and Lignin for Poplar Solids Produced by Leading Pretreatment Technologies. *Biotechnol. Prog.* **2009,** *25* (3), 807-819; (c) Li, C. L.; Knierim, B.; Manisseri, C.; Arora, R.; Scheller, H. V.; Auer, M.; Vogel, K. P.; Simmons, B. A.; Singh, S., Comparison of dilute acid and ionic liquid pretreatment of switchgrass: Biomass recalcitrance, delignification and enzymatic saccharification. *Bioresour. Technol.* **2010,** *101* (13), 4900-4906; (d) Shuai, L.; Yang, Q.; Zhu, J. Y.; Lu, F. C.; Weimer, P. J.; Ralph, J.; Pan, X. J., Comparative study of SPORL and dilute-acid pretreatments of spruce for cellulosic ethanol production. *Bioresour. Technol.* **2010,** *101* (9), 3106-3114; (e) Esteghlalian, A.; Hashimoto, A. G.; Fenske, J. J.; Penner, M. H., Modeling and optimization of the dilute-sulfuric-acid pretreatment of corn stover, poplar and switchgrass. *Bioresour. Technol.* **1997,** *59* (2), 129-136.
114. Hendriks, A. T. W. M.; Zeeman, G., Pretreatments to enhance the digestibility of lignocellulosic biomass. *Bioresour. Technol.* **2009,** *100* (1), 10-18.
115. Sannigrahi, P.; Kim, D. H.; Jung, S.; Ragauskas, A., Pseudo-lignin and pretreatment chemistry. *Energy Environ. Sci.* **2011,** *4* (4), 1306-1310.
116. (a) Um, B.-H.; Karim, M. N.; Henk, L. L., Effect of sulfuric and phosphoric acid pretreatments on enzymatic hydrolysis of corn stover. In *Biotechnology for Fuels and Chemicals*, Springer: 2003; pp 115-125; (b) Jensen, J. R.; Morinelly, J. E.; Gossen, K. R.; Brodeur-Campbell, M. J.; Shonnard, D. R., Effects of dilute acid pretreatment conditions on enzymatic hydrolysis monomer and oligomer sugar yields for aspen, balsam, and switchgrass. *Bioresour. Technol.* **2010,** *101* (7), 2317-2325; (c) Tian, S.; Zhu, W.; Gleisner, R.; Pan, X.; Zhu, J., Comparisons of SPORL and dilute acid pretreatments for sugar and ethanol productions from aspen. *Biotechnol. Prog.* **2011,** *27* (2), 419-427; (d) Wyman, C. E.; Balan, V.; Dale, B. E.; Elander, R. T.; Falls, M.; Hames, B.; Holtzapple, M. T.; Ladisch, M. R.; Lee, Y.; Mosier, N., Comparative data on effects of leading pretreatments and enzyme loadings and formulations on sugar yields from different

switchgrass sources. *Bioresour. Technol.* **2011,** *102* (24), 11052-11062; (e) Zhang, J.; Ma, X.; Yu, J.; Zhang, X.; Tan, T., The effects of four different pretreatments on enzymatic hydrolysis of sweet sorghum bagasse. *Bioresour. Technol.* **2011,** *102* (6), 4585-4589; (f) Zhao, X. B.; Wang, L.; Liu, D. H., Peracetic acid pretreatment of sugarcane bagasse for enzymatic hydrolysis: a continued work. *J. Chem. Technol. Biotechnol.* **2008,** *83* (6), 950-956.
117. (a) Lloyd, T.; Wyman, C. E., Application of a depolymerization model for predicting thermochemical hydrolysis of hemicellulose. In *Biotechnology for Fuels and Chemicals*, Springer: 2003; pp 53-67; (b) Kabel, M. A.; Bos, G.; Zeevalking, J.; Voragen, A. G.; Schols, H. A., Effect of pretreatment severity on xylan solubility and enzymatic breakdown of the remaining cellulose from wheat straw. *Bioresour. Technol.* **2007,** *98* (10), 2034-2042.
118. Selig, M. J.; Viamajala, S.; Decker, S. R.; Tucker, M. P.; Himmel, M. E.; Vinzant, T. B., Deposition of lignin droplets produced during dilute acid pretreatment of maize stems retards enzymatic hydrolysis of cellulose. *Biotechnol. Prog.* **2007,** *23* (6), 1333-1339.
119. (a) Hansen, M. A.; Kristensen, J. B.; Felby, C.; Jørgensen, H., Pretreatment and enzymatic hydrolysis of wheat straw (Triticum aestivum L.)–The impact of lignin relocation and plant tissues on enzymatic accessibility. *Bioresour. Technol.* **2011,** *102* (3), 2804-2811; (b) Holopainen-Mantila, U.; Marjamaa, K.; Merali, Z.; Käsper, A.; de Bot, P.; Jääskeläinen, A.-S.; Waldron, K.; Kruus, K.; Tamminen, T., Impact of hydrothermal pre-treatment to chemical composition, enzymatic digestibility and spatial distribution of cell wall polymers. *Bioresour. Technol.* **2013,** *138*, 156-162.
120. (a) Hu, F.; Jung, S.; Ragauskas, A., Pseudo-lignin formation and its impact on enzymatic hydrolysis. *Bioresour. Technol.* **2012,** *117*, 7-12; (b) Kumar, R.; Hu, F.; Sannigrahi, P.; Jung, S.; Ragauskas, A. J.; Wyman, C. E., Carbohydrate derived-pseudo-lignin can retard cellulose biological conversion. *Biotechnol. Bioeng.* **2013,** *110* (3), 737-753.
121. Stephens, C. H.; Whitmore, P. M.; Morris, H. R.; Bier, M. E., Hydrolysis of the amorphous cellulose in cotton-based paper. *Biomacromolecules* **2008,** *9* (4), 1093-1099.
122. Hsu, T.-C.; Guo, G.-L.; Chen, W.-H.; Hwang, W.-S., Effect of dilute acid pretreatment of rice straw on structural properties and enzymatic hydrolysis. *Bioresour. Technol.* **2010,** *101* (13), 4907-4913.
123. (a) Debzi, E.; Chanzy, H.; Sugiyama, J.; Tekely, P.; Excoffier, G., The $I\alpha \rightarrow I\beta$ transformation of highly crystalline cellulose by annealing in various mediums. *Macromolecules* **1991,** *24* (26), 6816-6822; (b) Lindgren, T.; Edlund, U.; Iversen, T., A multivariate characterization of crystal transformations of cellulose. *Cellulose* **1995,** *2* (4), 273-288.
124. Sierra, R.; Smith, A.; Granda, C.; Holtzapple, M. T., Producing fuels and chemicals from lignocellulosic biomass. *Chem. Eng. Prog.* **2008,** *104* (8), S10-S18.
125. (a) Pérez, J. A.; González, A.; Oliva, J. M.; Ballesteros, I.; Manzanares, P., Effect of process variables on liquid hot water pretreatment of wheat straw for bioconversion to fuel‐ethanol in a batch reactor. *J. Chem. Technol. Biotechnol.* **2007,** *82* (10), 929-938; (b) Pérez, J.; Ballesteros, I.; Ballesteros, M.; Sáez, F.; Negro, M.; Manzanares, P., Optimizing liquid hot water pretreatment conditions to enhance sugar recovery from wheat straw for fuel-ethanol production. *Fuel* **2008,** *87* (17), 3640-3647; (c) Hu, Z.;

Ragauskas, A. J., Hydrothermal pretreatment of switchgrass. *Ind. Eng. Chem. Res.* **2011,** *50* (8), 4225-4230.
126. Zheng, Y.; Pan, Z.; Zhang, R., Overview of biomass pretreatment for cellulosic ethanol production. *Int. J. Agric. Biol. Eng.* **2009,** *2* (3), 51-68.
127. Mosier, N.; Wyman, C.; Dale, B.; Elander, R.; Lee, Y. Y.; Holtzapple, M.; Ladisch, M., Features of promising technologies for pretreatment of lignocellulosic biomass. *Bioresour. Technol.* **2005,** *96* (6), 673-686.
128. (a) Chang, V. S.; Burr, B.; Holtzapple, M. T., Lime pretreatment of switchgrass. In *Biotechnology for Fuels and Chemicals*, Springer: 1997; pp 3-19; (b) Kim, S.; Holtzapple, M. T., Lime pretreatment and enzymatic hydrolysis of corn stover. *Bioresour. Technol.* **2005,** *96* (18), 1994-2006; (c) Liang, Y.; Siddaramu, T.; Yesuf, J.; Sarkany, N., Fermentable sugar release from Jatropha seed cakes following lime pretreatment and enzymatic hydrolysis. *Bioresour. Technol.* **2010,** *101* (16), 6417-6424; (d) Kaar, W. E.; Holtzapple, M. T., Using lime pretreatment to facilitate the enzymic hydrolysis of corn stover. *Biomass Bioenergy* **2000,** *18* (3), 189-199.
129. Kim, S.; Holtzapple, M. T., Effect of structural features on enzyme digestibility of corn stover. *Bioresour. Technol.* **2006,** *97* (4), 583-591.
130. Chang, V.; Holtzapple, M., Fundamental factors affecting biomass enzymatic reactivity. *Appl. Biochem. Biotechnol.* **2000,** *84-86* (1), 5-37.
131. (a) Botello, J.; Gilarranz, M.; Rodriguez, F.; Oliet, M., Preliminary study on products distribution in alcohol pulping of Eucalyptus globulus. *J. Chem. Technol. Biotechnol.* **1999,** *74* (2), 141-148; (b) Pan, X.; Arato, C.; Gilkes, N.; Gregg, D.; Mabee, W.; Pye, K.; Xiao, Z.; Zhang, X.; Saddler, J., Biorefining of softwoods using ethanol organosolv pulping: Preliminary evaluation of process streams for manufacture of fuel‐grade ethanol and co‐products. *Biotechnol. Bioeng.* **2005,** *90* (4), 473-481.
132. Zhao, X.; Cheng, K.; Liu, D., Organosolv pretreatment of lignocellulosic biomass for enzymatic hydrolysis. *Appl. Microbiol. Biotechnol.* **2009,** *82* (5), 815-827.
133. Cateto, C.; Hu, G.; Ragauskas, A., Enzymatic hydrolysis of organosolv Kanlow switchgrass and its impact on cellulose crystallinity and degree of polymerization. *Energ. Environ. Sci.* **2011,** *4* (4), 1516-1521.
134. (a) Pan, X.; Gilkes, N.; Kadla, J.; Pye, K.; Saka, S.; Gregg, D.; Ehara, K.; Xie, D.; Lam, D.; Saddler, J., Bioconversion of hybrid poplar to ethanol and co‐products using an organosolv fractionation process: Optimization of process yields. *Biotechnol. Bioeng.* **2006,** *94* (5), 851-861; (b) Brosse, N.; Sannigrahi, P.; Ragauskas, A., Pretreatment of Miscanthus x giganteus using the ethanol organosolv process for ethanol production. *Ind. Eng. Chem. Res.* **2009,** *48* (18), 8328-8334; (c) Sannigrahi, P.; Miller, S. J.; Ragauskas, A. J., Effects of organosolv pretreatment and enzymatic hydrolysis on cellulose structure and crystallinity in Loblolly pine. *Carbohydr. Res.* **2010,** *345* (7), 965-970; (d) Diaz, M. J.; Huijgen, W. J.; van der Laan, R. R.; Reith, J. H.; Cara, C.; Castro, E., Organosolv pretreatment of olive tree biomass for fermentable sugars. *Holzforschung* **2011,** *65* (2), 177-183.
135. (a) Habibi, Y.; Lucia, L. A.; Rojas, O. J., Cellulose nanocrystals: chemistry, self-assembly, and applications. *Chem. Rev.* **2010,** *110* (6), 3479-3500; (b) Eichhorn, S. J., Cellulose nanowhiskers: promising materials for advanced applications. *Soft Matter* **2011,** *7* (2), 303-315; (c) Hansen, N. M. L.; Plackett, D., Sustainable films and coatings from hemicelluloses: A review. *Biomacromolecules* **2008,** *9* (6), 1493-1505.

136. Kadla, J.; Kubo, S.; Venditti, R.; Gilbert, R.; Compere, A.; Griffith, W., Lignin-based carbon fibers for composite fiber applications. *Carbon* **2002,** *40* (15), 2913-2920.
137. Nagy, M.; Kosa, M.; Theliander, H.; Ragauskas, A. J., Characterization of CO 2 precipitated Kraft lignin to promote its utilization. *Green Chem.* **2010,** *12* (1), 31-34.
138. Holladay JE, JF White, JJ Bozell, and D Johnson. Top Value-Added Chemicals from Biomass - Volume II—Results of Screening for Potential Candidates from Biorefinery Lignin. PNNL-16983, Pacific Northwest National Laboratory, Richland, WA.2007.
139. (a) Lebo, S. E.; Gargulak, J. D.; McNally, T. J., Lignin. In *Kirk-Othmer Encyclopedia of Chemical Technology*, John Wiley & Sons, Inc.: 2000; (b) Silva, E.; Zabkova, M.; Araújo, J.; Cateto, C.; Barreiro, M.; Belgacem, M.; Rodrigues, A., An integrated process to produce vanillin and lignin-based polyurethanes from Kraft lignin. *Chem. Eng. Res. Des.* **2009,** *87* (9), 1276-1292.
140. Balakshin, M. Y.; Capanema, E. A.; Chen, C.-L.; Gracz, H. S., Elucidation of the structures of residual and dissolved pine kraft lignins using an HMQC NMR technique. *J. Agric. Food Chem.* **2003,** *51* (21), 6116-6127.
141. (a) Capanema, E. A.; Balakshin, M. Y.; Chen, C.-L.; Gratzl, J. S.; Gracz, H., Structural analysis of residual and technical lignins by 1H-13C correlation 2D NMR-spectroscopy. *Holzforschung* **2001,** *55* (3), 302-308; (b) Liitiä, T. M.; Maunu, S. L.; Hortling, B.; Toikka, M.; Kilpeläinen, I., Analysis of technical lignins by two-and three-dimensional NMR spectroscopy. *J. Agric. Food Chem.* **2003,** *51* (8), 2136-2143.
142. (a) Lora, J. H.; Glasser, W. G., Recent industrial applications of lignin: a sustainable alternative to nonrenewable materials. *J. Polym. Environ.* **2002,** *10* (1-2), 39-48; (b) Fenner, R. A.; Lephardt, J. O., Examination of the thermal decomposition of kraft pine lignin by Fourier transform infrared evolved gas analysis. *J. Agric. Food Chem.* **1981,** *29* (4), 846-849.
143. Pan, X.; Kadla, J. F.; Ehara, K.; Gilkes, N.; Saddler, J. N., Organosolv ethanol lignin from hybrid poplar as a radical scavenger: relationship between lignin structure, extraction conditions, and antioxidant activity. *J. Agric. Food Chem.* **2006,** *54* (16), 5806-5813.
144. (a) Sammons, R. J.; Harper, D. P.; Labbé, N.; Bozell, J. J.; Elder, T.; Rials, T. G., Characterization of Organosolv Lignins using Thermal and FT-IR Spectroscopic Analysis. *BioResources* **2013,** *8* (2), 2752-2767; (b) Glasser, W. G.; Barnett, C. A.; Muller, P. C.; Sarkanen, K. V., The chemistry of several novel bioconversion lignins. *J. Agric. Food Chem.* **1983,** *31* (5), 921-930; (c) Glasser, W. G.; Jain, R. K., Lignin derivatives. I. Alkanoates. *Holzforschung-International Journal of the Biology, Chemistry, Physics and Technology of Wood* **1993,** *47* (3), 225-233; (d) Glasser, W. G.; Davé, V.; Frazier, C. E., Molecular weight distribution of (semi-) commercial lignin derivatives. *J. Wood Chem. Technol.* **1993,** *13* (4), 545-559.
145. Tuck, C. O.; Pérez, E.; Horváth, I. T.; Sheldon, R. A.; Poliakoff, M., Valorization of biomass: deriving more value from waste. *Science* **2012,** *337* (6095), 695-699.
146. Baker, D. A.; Rials, T. G., Recent advances in low‐cost carbon fiber manufacture from lignin. *J. Appl. Polym. Sci.* **2013,** *130* (2), 713-728.
147. (a) Otani, S., Method for producing carbonized lignin fiber. US 3461082 A: 1969; (b) Sudo, K.; Okoshi, M.; Shimizu, K. In *Carbon-fiber from lignin--improvement of conversion process of lignin*, ABSTRACTS OF PAPERS OF THE AMERICAN

CHEMICAL SOCIETY, AMER CHEMICAL SOC 1155 16TH ST, NW, WASHINGTON, DC 20036: 1988; pp 107-CELL.
148. Kadla, J. F.; Gilbert, R. D.; Venditti, R. A.; Kubo, S., Porous fibers from natural/synthetic polymer blends. US20030212157 A1. US Patents: 2003.
149. Compere, A.; Griffith, W.; Leitten Jr, C.; Pickel, J., Evaluation of lignin from alkaline-pulped hardwood black liquor. *ORNL/TM-2005/88* **2005**.
150. Baker, D. A.; Baker, F. S.; Menchhofer, P. A., Carbon nanotube (cnt)-enhanced precursor for carbon fiber production and method of making a cnt-enhanced continuous lignin fiber. US20110285049 A1. Patents: 2010.
151. Eberle, C., Carbon Fiber From Lignin. http://www.cfcomposites.org/PDF/Breakout_Cliff.pdf. 2012.
152. (a) Ma, X.; Zhao, G., Variations in the microstructure of carbon fibers prepared from liquefied wood during carbonization. *J. Appl. Polym. Sci.* **2011,** *121* (6), 3525-3530; (b) Liu, W.; Zhao, G., Effect of temperature and time on microstructure and surface functional groups of activated carbon fibers prepared from liquefied wood. *BioResources* **2012,** *7* (4), 5552-5567; (c) Xiaojun, M.; Guangjie, Z., Preparation of carbon fibers from liquefied wood. *Wood Sci. Technol.* **2010,** *44* (1), 3-11.
153. (a) Seo, D. K.; Jeun, J. P.; Kim, H. B.; Kang, P. H., Preparation and characterization of the carbon nanofiber mat produced from electrospun PAN/lignin precursors by electron beam irradiation. *Rev. Adv. Mater. Sci.* **2011,** *28*, 31-34; (b) Lallave, M.; Bedia, J.; Ruiz‐Rosas, R.; Rodríguez‐Mirasol, J.; Cordero, T.; Otero, J. C.; Marquez, M.; Barrero, A.; Loscertales, I. G., Filled and hollow carbon nanofibers by coaxial electrospinning of alcell lignin without binder polymers. *Adv. Mater.* **2007,** *19* (23), 4292-4296; (c) Ruiz-Rosas, R.; Bedia, J.; Lallave, M.; Loscertales, I.; Barrero, A.; Rodríguez-Mirasol, J.; Cordero, T., The production of submicron diameter carbon fibers by the electrospinning of lignin. *Carbon* **2010,** *48* (3), 696-705; (d) Dallmeyer, I.; Ko, F.; Kadla, J. F., Electrospinning of technical lignins for the production of fibrous networks. *J. Wood Chem. Technol.* **2010,** *30* (4), 315-329.
154. Hosseinaei, O.; Baker, D. In *Electrospun carbon nanofibers from kraft lignin*, Extended abstract in Book of Abstracts of The Fiber Society 2012 Fall Conference, Boston Convention & Exhibition Center, Boston, Mass., USA, 2012.
155. (a) Prauchner, M. J.; Pasa, V.; Molhallem, N. D.; Otani, C.; Otani, S.; Pardini, L. C., Structural evolution of Eucalyptus tar pitch-based carbons during carbonization. *Biomass Bioenergy* **2005,** *28* (1), 53-61; (b) Braun, J.; Holtman, K.; Kadla, J., Lignin-based carbon fibers: Oxidative thermostabilization of kraft lignin. *Carbon* **2005,** *43* (2), 385-394.
156. Foston, M.; Nunnery, G. A.; Meng, X.; Sun, Q.; Baker, F. S.; Ragauskas, A., NMR a critical tool to study the production of carbon fiber from lignin. *Carbon* **2013,** *52*, 65-73.
157. (a) Hu, Z.; Yeh, T.-F.; Chang, H.-m.; Matsumoto, Y.; Kadla, J. F., Elucidation of the structure of cellulolytic enzyme lignin. *Holzforschung* **2006,** *60* (4), 389-397; (b) Rico, A.; Rencoret, J.; del Río, J. C.; Martínez, A. T.; Gutiérrez, A., Pretreatment with laccase and a phenolic mediator degrades lignin and enhances saccharification of Eucalyptus feedstock. *Biotechnol. Biofuels* **2014,** *7* (6).

158. Sun, Q.; Foston, M.; Sawada, D.; Pingali, S. V.; O'Neill, H. M.; Li, H.; Wyman, C. E.; Langan, P.; Pu, Y.; Ragauskas, A. J., Comparison of changes in cellulose ultrastructure during different pretreatments of poplar. *Cellulose*, **2014**, *21*, 2419-2431.
159. Bozell, J. J.; O'Lenick, C.; Warwick, S., Biomass fractionation for the biorefinery: Heteronuclear multiple quantum coherence–Nuclear magnetic resonance investigation of lignin isolated from solvent fractionation of switchgrass. *J. Agric. Food Chem.* **2011,** *59* (17), 9232-9242.
160. (a) Chum, H. L.; Johnson, D. K.; Black, S. K., Organosolv pretreatment for enzymic hydrolysis of poplars. 2. Catalyst effects and the combined severity parameter. *Ind. Eng. Chem. Res.* **1990,** *29* (2), 156-162; (b) Overend, R.; Chornet, E.; Gascoigne, J., Fractionation of lignocellulosics by steam-aqueous pretreatments [and discussion]. *Philosophical Transactions of the Royal Society of London. Series A, Mathematical and Physical Sciences* **1987,** *321* (1561), 523-536; (c) Pedersen, M.; Meyer, A. S., Lignocellulose pretreatment severity–relating pH to biomatrix opening. *New biotechnology* **2010,** *27* (6), 739-750.
161. Bozell, J. J.; Black, S. K.; Myers, M.; Cahill, D.; Miller, W. P.; Park, S., Solvent fractionation of renewable woody feedstocks: Organosolv generation of biorefinery process streams for the production of biobased chemicals. *Biomass Bioenergy* **2011,** *35* (10), 4197-4208.
162. Davis, M. W., A rapid modified method for compositional carbohydrate analysis of lignocellulosics by high pH anion-exchange chromatography with pulsed amperometric detection (HPAEC/PAD). *J. Wood Chem. Technol.* **1998,** *18* (2), 235-252.
163. (a) Cullity, B. D.; Stock, S. R., *Elements of X-ray Diffraction*. Prentice Hall, Upper Saddle River: 2001; (b) Klug, H. P.; Alexander, L. E., X-ray diffraction procedures: for polycrystalline and amorphous materials. *X-Ray Diffraction Procedures: For Polycrystalline and Amorphous Materials, 2nd Edition, by Harold P. Klug, Leroy E. Alexander, pp. 992. ISBN 0-471-49369-4. Wiley-VCH, May 1974.* **1974,** *1*.
164. Simons, F. L., A stain for use in the microscopy of beaten fibers. *Tappi* **1950,** *33* (7), 312-314.
165. Yu, X.; Atalla, R. H., A staining technique for evaluating the pore structure variations of microcrystalline cellulose powders. *Powder Technol.* **1998,** *98* (2), 135-138.
166. Esteghlalian, A. R.; Bilodeau, M.; Mansfield, S. D.; Saddler, J. N., Do enzymatic hydrolyzability and Simons' stain reflect the changes in the accessibility of lignocellulosic substrates to cellulase enzymes? *Biotechnol. Prog.* **2001,** *17* (6), 1049-1054.
167. Studer, M. H.; DeMartini, J. D.; Brethauer, S.; McKenzie, H. L.; Wyman, C. E., Engineering of a high ‐ throughput screening system to identify cellulosic biomass, pretreatments, and enzyme formulations that enhance sugar release. *Biotechnol. Bioeng.* **2010,** *105* (2), 231-238.
168. Sykes, R.; Yung, M.; Novaes, E.; Kirst, M.; Peter, G.; Davis, M., High-throughput screening of plant cell-wall composition using pyrolysis molecular beam mass spectroscopy. In *Biofuels*, Springer: 2009; pp 169-183.
169. Bortner, M. J.; Bhanu, V.; McGrath, J. E.; Baird, D. G., Shear rheological properties of acrylic copolymers and terpolymers suitable for potentially melt processable carbon fiber precursors. *J. Appl. Polym. Sci.* **2004,** *93* (6), 2856-2865.

170. Brunner, A. M.; Busov, V. B.; Strauss, S. H., Poplar genome sequence: functional genomics in an ecologically dominant plant species. *Trends Plant Sci.* **2004,** *9* (1), 49-56.
171. Chang, V.; Nagwani, M.; Kim, C.-H.; Holtzapple, M., Oxidative lime pretreatment of high-lignin biomass. *Appl. Biochem. Biotechnol.* **2001,** *94* (1), 1-28.
172. Lloyd, T. A.; Wyman, C. E., Combined sugar yields for dilute sulfuric acid pretreatment of corn stover followed by enzymatic hydrolysis of the remaining solids. *Bioresour. Technol.* **2005,** *96* (18), 1967-1977.
173. Kumar, R.; Hu, F.; Hubbell, C. A.; Ragauskas, A. J.; Wyman, C. E., Comparison of laboratory delignification methods, their selectivity, and impacts on physiochemical characteristics of cellulosic biomass. *Bioresour. Technol.* **2013,** *130*, 372-381.
174. Mosier, N.; Hendrickson, R.; Ho, N.; Sedlak, M.; Ladisch, M. R., Optimization of pH controlled liquid hot water pretreatment of corn stover. *Bioresour. Technol.* **2005,** *96* (18), 1986-1993.
175. Chang, V. S.; Nagwani, M.; Holtzapple, M. T., Lime pretreatment of crop residues bagasse and wheat straw. *Appl. Biochem. Biotechnol.* **1998,** *74* (3), 135-159.
176. Martin, C.; Klinke, H. B.; Thomsen, A. B., Wet oxidation as a pretreatment method for enhancing the enzymatic convertibility of sugarcane bagasse. *Enzyme Microb. Technol.* **2007,** *40* (3), 426-432.
177. (a) Bubner, P.; Plank, H.; Nidetzky, B., Visualizing cellulase activity. *Biotechnol. Bioeng.* **2013,** *110* (6), 1529-1549; (b) Zhao, H.; Kwak, J. H.; Wang, Y.; Franz, J. A.; White, J. M.; Holladay, J. E., Effects of crystallinity on dilute acid hydrolysis of cellulose by cellulose ball-milling study. *Energy Fuels* **2006,** *20* (2), 807-811.
178. Ibbett, R.; Gaddipati, S.; Hill, S.; Tucker, G., Structural reorganisation of cellulose fibrils in hydrothermally deconstructed lignocellulosic biomass and relationships with enzyme digestibility. *Biotechnol. Biofuels* **2013,** *6*, 33.
179. (a) Xu, J.; Cheng, J. J.; Sharma-Shivappa, R. R.; Burns, J. C., Lime pretreatment of switchgrass at mild temperatures for ethanol production. *Bioresour. Technol.* **2010,** *101* (8), 2900-2903; (b) Xu, J.; Cheng, J. J., Pretreatment of switchgrass for sugar production with the combination of sodium hydroxide and lime. *Bioresour. Technol.* **2011,** *102* (4), 3861-3868; (c) Wang, Z.; Cheng, J. J., Lime pretreatment of coastal bermudagrass for bioethanol production. *Energy Fuels* **2011,** *25* (4), 1830-1836.
180. Pan, X.; Xie, D.; Yu, R. W.; Saddler, J. N., The bioconversion of mountain pine beetle ‐ killed lodgepole pine to fuel ethanol using the organosolv process. *Biotechnol. Bioeng.* **2008,** *101* (1), 39-48.
181. Maciel, G. E.; Kolodziejski, W. L.; Bertran, M. S.; Dale, B. E., Carbon-13 NMR and order in cellulose. *Macromolecules* **1982,** *15* (2), 686-687.
182. Šturcová, A.; His, I.; Apperley, D. C.; Sugiyama, J.; Jarvis, M. C., Structural details of crystalline cellulose from higher plants. *Biomacromolecules* **2004,** *5* (4), 1333-1339.
183. Diniz, J. F.; Gil, M.; Castro, J., Hornification—its origin and interpretation in wood pulps. *Wood Sci Technol.* **2004,** *37* (6), 489-494.
184. (a) Chen, Y.; Wang, Y.; Wan, J.; Ma, Y., Crystal and pore structure of wheat straw cellulose fiber during recycling. *Cellulose* **2010,** *17* (2), 329-338; (b) Newman, R. H., Carbon-13 NMR evidence for cocrystallization of cellulose as a mechanism for hornification of bleached kraft pulp. *Cellulose* **2004,** *11* (1), 45-52.

185. Östlund, Å.; Köhnke, T.; Nordstierna, L.; Nydén, M., NMR cryoporometry to study the fiber wall structure and the effect of drying. *Cellulose* **2010,** *17* (2), 321-328.
186. Oksanen, T.; Buchert, J.; Viikari, L., The role of hemicelluloses in the hornification of bleached kraft pulps. *Holzforschung-International Journal of the Biology, Chemistry, Physics and Technology of Wood* **1997,** *51* (4), 355-360.
187. (a) Xu, F.; Ding, H.; Tejirian, A., Detrimental effect of cellulose oxidation on cellulose hydrolysis by cellulase. *Enzyme Microb. Technol.* **2009,** *45* (3), 203-209; (b) Ishizawa, C. I.; Jeoh, T.; Adney, W. S.; Himmel, M. E.; Johnson, D. K.; Davis, M. F., Can delignification decrease cellulose digestibility in acid pretreated corn stover? *Cellulose* **2009,** *16* (4), 677-686; (c) Hubbell, C. A.; Ragauskas, A. J., Effect of acid-chlorite delignification on cellulose degree of polymerization. *Bioresour. Technol.* **2010,** *101* (19), 7410-7415.
188. Langan, P.; Petridis, L.; O'Neill, H. M.; Pingali, S. V.; Foston, M.; Nishiyama, Y.; Schulz, R.; Lindner, B.; Hanson, B. L.; Harton, S., Common processes drive the thermochemical pretreatment of lignocellulosic biomass. *Green Chem.* **2014,** *16* (1), 63-68.
189. (a) Ding, S.-Y.; Liu, Y.-S.; Zeng, Y.; Himmel, M. E.; Baker, J. O.; Bayer, E. A., How does plant cell wall nanoscale architecture correlate with enzymatic digestibility? *Science* **2012,** *338* (6110), 1055-1060; (b) Arantes, V.; Saddler, J. N., Access to cellulose limits the efficiency of enzymatic hydrolysis: the role of amorphogenesis. *Biotechnol. Biofuels* **2010,** *3*, 4.
190. Foston, M.; Hubbell, C. A.; Samuel, R.; Jung, S.; Fan, H.; Ding, S.-Y.; Zeng, Y.; Jawdy, S.; Davis, M.; Sykes, R., Chemical, ultrastructural and supramolecular analysis of tension wood in Populus tremula x alba as a model substrate for reduced recalcitrance. *Energ. Environ. Sci.* **2011,** *4* (12), 4962-4971.
191. Beguin, P.; Aubert, J.-P., The biological degradation of cellulose. *FEMS Microbiol. Rev.* **1994,** *13* (1), 25-58.
192. Boisset, C.; Fraschini, C.; Schülein, M.; Henrissat, B.; Chanzy, H., Imaging the enzymatic digestion of bacterial cellulose ribbons reveals the endo character of the cellobiohydrolase Cel6A from Humicola insolens and its mode of synergy with cellobiohydrolase Cel7A. *Appl. Environ. Microbiol.* **2000,** *66* (4), 1444-1452.
193. Chundawat, S. P.; Bellesia, G.; Uppugundla, N.; da Costa Sousa, L.; Gao, D.; Cheh, A. M.; Agarwal, U. P.; Bianchetti, C. M.; Phillips Jr, G. N.; Langan, P., Restructuring the crystalline cellulose hydrogen bond network enhances its depolymerization rate. *J. Am. Chem. Soc.* **2011,** *133* (29), 11163-11174.
194. Ioelovich, M.; Leykin, A.; Figovsky, O., Study of cellulose paracrystallinity *BioResources* **2010,** *5* (3), 1393-1407.
195. Caffall, K. H.; Mohnen, D., The structure, function, and biosynthesis of plant cell wall pectic polysaccharides. *Carbohydr. Res.* **2009,** *344* (14), 1879-1900.
196. Klemm, D.; Heublein, B.; Fink, H. P.; Bohn, A., Cellulose: Fascinating biopolymer and sustainable raw material. *Angew. Chem. Int. Ed.* **2005,** *44* (22), 3358-3393.
197. Murphy, J. D.; McCarthy, K., Ethanol production from energy crops and wastes for use as a transport fuel in Ireland. *Appl. Energy* **2005,** *82* (2), 148-166.
198. Sannigrahi, P.; Pu, Y.; Ragauskas, A., Cellulosic biorefineries—unleashing lignin opportunities. *Curr. Opin Environ. Sustain.* **2010,** *2* (5), 383-393.

199. Himmel, M. E.; Ding, S. Y.; Johnson, D. K.; Adney, W. S.; Nimlos, M. R.; Brady, J. W.; Foust, T. D., Biomass recalcitrance: Engineering plants and enzymes for biofuels production. *Science* **2007,** *315* (5813), 804-807.
200. Hsu, T. A.; Ladisch, M. R.; Tsao, G. T., ALCOHOL FROM CELLULOSE. *Chemtech* **1980,** *10* (5), 315-319.
201. Lacayo, C. I.; Hwang, M. S.; Ding, S.-Y.; Thelen, M. P., Lignin Depletion Enhances the Digestibility of Cellulose in Cultured Xylem Cells. *PloS one* **2013,** *8* (7), e68266.
202. (a) Lee, S. B.; Kim, I. H.; Ryu, D. D. Y.; Taguchi, H., STRUCTURAL-PROPERTIES OF CELLULOSE AND CELLULASE REACTION-MECHANISM. *Biotechnol. Bioeng.* **1983,** *25* (1), 33-51; (b) Fan, L. T.; Lee, Y. H.; Beardmore, D. H., MECHANISM OF THE ENZYMATIC-HYDROLYSIS OF CELLULOSE - EFFECTS OF MAJOR STRUCTURAL FEATURES OF CELLULOSE ON ENZYMATIC-HYDROLYSIS. *Biotechnol. Bioeng.* **1980,** *22* (1), 177-199; (c) Mansfield, S. D.; Mooney, C.; Saddler, J. N., Substrate and enzyme characteristics that limit cellulose hydrolysis. *Biotechnol. Prog.* **1999,** *15* (5), 804-816.
203. Del Rio, L. F.; Chandra, R. P.; Saddler, J. N., Fibre size does not appear to influence the ease of enzymatic hydrolysis of organosolv-pretreated softwoods. *Bioresour. Technol.* **2012,** *107*, 235-242.
204. Hall, M.; Bansal, P.; Lee, J. H.; Realff, M. J.; Bommarius, A. S., Cellulose crystallinity - a key predictor of the enzymatic hydrolysis rate. *Febs J.* **2010,** *277* (6), 1571-1582.
205. O'SULLIVAN, A. C., Cellulose: the structure slowly unravels. *Cellulose* **1997,** *4* (3), 173-207.
206. (a) Yamamoto, H.; Horii, F., CPMAS carbon-13 NMR analysis of the crystal transformation induced for Valonia cellulose by annealing at high temperatures. *Macromolecules* **1993,** *26* (6), 1313-1317; (b) Yamamoto, H.; Horii, F.; Odani, H., Structural changes of native cellulose crystals induced by annealing in aqueous alkaline and acidic solutions at high temperatures. *Macromolecules* **1989,** *22* (10), 4130-4132; (c) Horii, F.; Yamamoto, H.; Kitamaru, R.; Tanahashi, M.; Higuchi, T., Transformation of native cellulose crystals induced by saturated steam at high temperatures. *Macromolecules* **1987,** *20* (11), 2946-2949.
207. Rinaldi, R.; Schuth, F., Acid Hydrolysis of Cellulose as the Entry Point into Biorefinery Schemes. *ChemSusChem* **2009,** *2* (12), 1096-1107.
208. Sun, Q.; Foston, M.; Sawada, D.; Pingali, S. V.; O'Neill, H. M.; Li, H.; Wyman, C. E.; Langan, P.; Pu, Y.; Ragauskas, A. J., Comparison of changes in cellulose ultrastructure during different pretreatments of poplar. *Cellulose*, 1-13.
209. DeMartini, J. D.; Pattathil, S.; Miller, J. S.; Li, H. J.; Hahn, M. G.; Wyman, C. E., Investigating plant cell wall components that affect biomass recalcitrance in poplar and switchgrass. *Energy Environ. Sci.* **2013,** *6* (3), 898-909.
210. (a) Marchessault, R. H., APPLICATIONS OF INFRARED SPECTROSCOPY TO THE STUDY OF WOOD POLYSACCHARIDES. *Spectrochim. Acta* **1962,** *18* (6), 876-876; (b) Yin, Y. F.; Berglund, L.; Salmen, L., Effect of Steam Treatment on the Properties of Wood Cell Walls. *Biomacromolecules* **2011,** *12* (1), 194-202.

211. He, J. X.; Cui, S. Z.; Wang, S. Y., Preparation and crystalline analysis of high-grade bamboo dissolving pulp for cellulose acetate. *J. Appl. Polym. Sci.* **2008,** *107* (2), 1029-1038.
212. (a) Zhang, J.; Siika-aho, M.; Tenkanen, M.; Viikari, L., The role of acetyl xylan esterase in the solubilization of xylan and enzymatic hydrolysis of wheat straw and giant reed. *Biotechnol. Biofuels* **2011,** *4* (1), 1-10; (b) Jonsson, L. J.; Alriksson, B.; Nilvebrant, N.-O., Bioconversion of lignocellulose: inhibitors and detoxification. *Biotechnol. Biofuels* **2013,** *6* (1), 16.
213. Sun, X. F.; Xu, F.; Sun, R. C.; Fowler, P.; Baird, M. S., Characteristics of degraded cellulose obtained from steam-exploded wheat straw. *Carbohydr. Res.* **2005,** *340* (1), 97-106.
214. Ioelovich, M.; Leykin, A.; Figovsky, O., STUDY OF CELLULOSE PARACRYSTALLINITY. *BioResources* **2010,** *5* (3), 1393-1407.
215. (a) Wickholm, K.; Hult, E. L.; Larsson, P. T.; Iversen, T.; Lennholm, H., Quantification of cellulose forms in complex cellulose materials: a chemometric model. *Cellulose* **2001,** *8* (2), 139-148; (b) Wickholm, K.; Larsson, P. T.; Iversen, T., Assignment of non-crystalline forms in cellulose I by CP/MAS C-13 NMR spectroscopy. *Carbohydr. Res.* **1998,** *312* (3), 123-129.
216. Sturcova, A.; His, I.; Apperley, D. C.; Sugiyama, J.; Jarvis, M. C., Structural details of crystalline cellulose from higher plants. *Biomacromolecules* **2004,** *5* (4), 1333-1339.
217. Simons, F. L., A stain for use in the microscopy of beaten fibers. *Tappi J.* **1950,** *33* (7), 312-314.
218. Arantes, V.; Saddler, J. N., Cellulose accessibility limits the effectiveness of minimum cellulase loading on the efficient hydrolysis of pretreated lignocellulosic substrates. *Biotechnol. Biofuels* **2011,** *4* (1), 1-17.
219. Kumar, R.; Wyman, C. E., Physical and Chemical Features of Pretreated Biomass that Influence Macro - /Micro - Accessibility and Biological Processing. *Aqueous Pretreatment of Plant Biomass for Biological and Chemical Conversion to Fuels and Chemicals* **2013**, 281-310.
220. Pan, X. J.; Xie, D.; Yu, R. W.; Saddler, J. N., The bioconversion of mountain pine beetle-killed lodgepole pine to fuel ethanol using the organosolv process. *Biotechnol. Bioeng.* **2008,** *101* (1), 39-48.
221. Foston, M.; Ragauskas, A. J., Changes in the Structure of the Cellulose Fiber Wall during Dilute Acid Pretreatment in Populus Studied by H-1 and H-2 NMR. *Energy Fuels* **2010,** *24*, 5677-5685.
222. Converse, A.; Ooshima, H.; Burns, D., Kinetics of enzymatic hydrolysis of lignocellulosic materials based on surface area of cellulose accessible to enzyme and enzyme adsorption on lignin and cellulose. *Appl. Biochem. Biotechnol.* **1990,** *24* (1), 67-73.
223. Ragauskas, A. J.; Williams, C. K.; Davison, B. H.; Britovsek, G.; Cairney, J.; Eckert, C. A.; Frederick, W. J.; Hallett, J. P.; Leak, D. J.; Liotta, C. L., The path forward for biofuels and biomaterials. *Science* **2006,** *311* (5760), 484-489.
224. Yu, Z.; Gwak, K. S.; Treasure, T.; Jameel, H.; Chang, H. m.; Park, S., Effect of Lignin Chemistry on the Enzymatic Hydrolysis of Woody Biomass. *ChemSusChem* **2014**.

225. (a) DeMartini, J. D.; Pattathil, S.; Miller, J. S.; Li, H.; Hahn, M. G.; Wyman, C. E., Investigating plant cell wall components that affect biomass recalcitrance in poplar and switchgrass. *Energy Environ. Sci.* **2013,** *6* (3), 898-909; (b) Zeng, Y.; Zhao, S.; Yang, S.; Ding, S.-Y., Lignin plays a negative role in the biochemical process for producing lignocellulosic biofuels. *Curr. Opin. Biotechnol.* **2014,** *27*, 38-45.
226. (a) Chandra, R. P.; Bura, R.; Mabee, W.; Berlin, d. A.; Pan, X.; Saddler, J., Substrate pretreatment: The key to effective enzymatic hydrolysis of lignocellulosics? In *Biofuels*, Springer: 2007; pp 67-93; (b) Wyman, C. E.; Dale, B. E.; Elander, R. T.; Holtzapple, M.; Ladisch, M. R.; Lee, Y.; Mitchinson, C.; Saddler, J. N., Comparative sugar recovery and fermentation data following pretreatment of poplar wood by leading technologies. *Biotechnol. Prog.* **2009,** *25* (2), 333-339.
227. Li, H.; Pu, Y.; Kumar, R.; Ragauskas, A. J.; Wyman, C. E., Investigation of lignin deposition on cellulose during hydrothermal pretreatment, its effect on cellulose hydrolysis, and underlying mechanisms. *Biotechnol. Bioeng.* **2014,** *111* (3), 485-492.
228. Samuel, R.; Cao, S.; Das, B. K.; Hu, F.; Pu, Y.; Ragauskas, A. J., Investigation of the fate of poplar lignin during autohydrolysis pretreatment to understand the biomass recalcitrance. *RSC Adv.* **2013,** *3* (16), 5305-5309.
229. Cao, S.; Pu, Y.; Studer, M.; Wyman, C.; Ragauskas, A. J., Chemical transformations of Populus trichocarpa during dilute acid pretreatment. *Rsc Adv.* **2012,** *2* (29), 10925-10936.
230. (a) Trajano, H. L.; Engle, N. L.; Foston, M.; Ragauskas, A. J.; Tschaplinski, T. J.; Wyman, C. E., The fate of lignin during hydrothermal pretreatment. *Biotechnol. Biofuels* **2013,** *6* (1), 110; (b) Samuel, R.; Foston, M.; Jiang, N.; Allison, L.; Ragauskas, A. J., Structural changes in switchgrass lignin and hemicelluloses during pretreatments by NMR analysis. *Polym. Degrad. Stabil.* **2011,** *96* (11), 2002-2009.
231. Moxley, G.; Gaspar, A. R.; Higgins, D.; Xu, H., Structural changes of corn stover lignin during acid pretreatment. *J. Ind. Microbiol. Biotechnol.* **2012,** *39* (9), 1289-1299.
232. Chand, S., Review carbon fibers for composites. *J. Mater. Sci.* **2000,** *35* (6), 1303-1313.
233. (a) Saito, T.; Brown, R. H.; Hunt, M. A.; Pickel, D. L.; Pickel, J. M.; Messman, J. M.; Baker, F. S.; Keller, M.; Naskar, A. K., Turning renewable resources into value-added polymer: development of lignin-based thermoplastic. *Green Chem.* **2012,** *14* (12), 3295-3303; (b) Awal, A.; Sain, M., Characterization of soda hardwood lignin and the formation of lignin fibers by melt spinning. *J. Appl. Polym. Sci.* **2013,** *129* (5), 2765-2771.
234. Ralph, J.; Lundquist, K.; Brunow, G.; Lu, F.; Kim, H.; Schatz, P. F.; Marita, J. M.; Hatfield, R. D.; Ralph, S. A.; Christensen, J. H., Lignins: natural polymers from oxidative coupling of 4-hydroxyphenyl-propanoids. *Phytochem. Rev.* **2004,** *3* (1-2), 29-60.
235. Norberg, I.; Nordström, Y.; Drougge, R.; Gellerstedt, G.; Sjöholm, E., A new method for stabilizing softwood kraft lignin fibers for carbon fiber production. *J. Appl. Polym. Sci.* **2013,** *128* (6), 3824-3830.
236. Sun, Q.-N.; Qin, T.-F.; Li, G.-Y., Chemical groups and structural characterization of brown-rotted Pinus massoniana lignin. *Int. J. Polym. Anal. Ch.* **2009,** *14* (1), 19-33.

237. Sannigrahi, P.; Ragauskas, A. J.; Tuskan, G. A., Poplar as a feedstock for biofuels: A review of compositional characteristics. *Biofuels Bioprod. Biorefining* **2010,** *4* (2), 209-226.
238. (a) Papa, G.; Varanasi, P.; Sun, L.; Cheng, G.; Stavila, V.; Holmes, B.; Simmons, B. A.; Adani, F.; Singh, S., Exploring the effect of different plant lignin content and composition on ionic liquid pretreatment efficiency and enzymatic saccharification of Eucalyptus globulus L. mutants. *Bioresour. Technol.* **2012,** *117*, 352-359; (b) Guo, F.; Shi, W.; Sun, W.; Li, X.; Wang, F.; Zhao, J.; Qu, Y., Differences in the adsorption of enzymes onto lignins from diverse types of lignocellulosic biomass and the underlying mechanism. *Biotechnol. Biofuels* **2014,** *7* (1), 38; (c) Davison, B. H.; Drescher, S. R.; Tuskan, G. A.; Davis, M. F.; Nghiem, N. P. In *Variation of S/G ratio and lignin content in a Populus family influences the release of xylose by dilute acid hydrolysis*, Twenty-Seventh Symposium on Biotechnology for Fuels and Chemicals, Springer: 2006; pp 427-435.
239. (a) Hatakeyama, H.; Hatakeyama, T., Lignin structure, properties, and applications. In *Biopolymers*, Springer: 2010; pp 1-63; (b) Kubo, S.; Kadla, J. F., Poly (ethylene oxide)/organosolv lignin blends: relationship between thermal properties, chemical structure, and blend behavior. *Macromolecules* **2004,** *37* (18), 6904-6911.
240. (a) Kubo, S.; Kadla, J. F., Hydrogen bonding in lignin: a Fourier transform infrared model compound study. *Biomacromolecules* **2005,** *6* (5), 2815-2821; (b) Hu, G.; Cateto, C.; Pu, Y.; Samuel, R.; Ragauskas, A. J., Structural characterization of switchgrass lignin after ethanol organosolv pretreatment. *Energy Fuels* **2011,** *26* (1), 740-745; (c) Sun, Q.; Foston, M.; Meng, X.; Sawada, D.; Pingali, S. V.; O'Neill, H. M.; Li, H.; Wyman, C. E.; Langan, P.; Ragauskas, A. J., Effect of lignin content on changes occurring in poplar cellulose ultrastructure during dilute acid pretreatment. *Biotechnol. Biofuels* **2014,** *7* (1), 150.
241. Olsson, A.; Salmén, L. In *Viscoelasticity of in situ lignin as affected by structure: softwood vs. hardwood*, ACS symposium series (USA) 1992, 489, 133-143.
242. (a) Tejado, A.; Pena, C.; Labidi, J.; Echeverria, J.; Mondragon, I., Physico-chemical characterization of lignins from different sources for use in phenol–formaldehyde resin synthesis. *Bioresour. Technol.* **2007,** *98* (8), 1655-1663; (b) El Mansouri, N. E.; Yuan, Q.; Huang, F., Characterization of alkaline lignins for use in phenol-formaldehyde and epoxy resins. *BioResources* **2011,** *6* (3), 2647-2662.
243. Sudo, K.; Shimizu, K., A new carbon fiber from lignin. *J. Appl. Polym. Sci.* **1992,** *44* (1), 127-134.
244. Uraki, Y.; Sugiyama, Y.; Koda, K.; Kubo, S.; Kishimoto, T.; Kadla, J. F., Thermal Mobility of β-O-4-Type Artificial Lignin. *Biomacromolecules* **2012,** *13* (3), 867-872.
245. Pu, Y.; Chen, F.; Ziebell, A.; Davison, B. H.; Ragauskas, A. J., NMR characterization of C3H and HCT down-regulated alfalfa lignin. *BioEnergy Res.* **2009,** *2* (4), 198-208.
246. (a) Elder, T., A computational study of pyrolysis reactions of lignin model compounds. *Holzforschung* **2010,** *64* (4), 435-440; (b) Cui, C.; Sadeghifar, H.; Sen, S.; Argyropoulos, D. S., Toward Thermoplastic Lignin Polymers; Part II: Thermal & Polymer Characteristics of Kraft Lignin & Derivatives. *BioResources* **2013,** *8* (1), 864-886; (c) Nakamura, T.; Kawamoto, H.; Saka, S., Pyrolysis behavior of Japanese cedar

wood lignin studied with various model dimers. *J. Anal. Appl. Pyrolysis* **2008,** *81* (2), 173-182; (d) Kawamoto, H.; Nakamura, T.; Saka, S., Pyrolytic cleavage mechanisms of lignin-ether linkages: A study on p-substituted dimers and trimers. *Holzforschung* **2008,** *62* (1), 50-56.